






Universitat Autònoma de Barcelona

**ADVERTIMENT.** L'accés als continguts d'aquesta tesi queda condicionat a l'acceptació de les condicions d'ús establertes per la següent llicència Creative Commons:  [http://cat.creativecommons.org/?page\\_id=184](http://cat.creativecommons.org/?page_id=184)

**ADVERTENCIA.** El acceso a los contenidos de esta tesis queda condicionado a la aceptación de las condiciones de uso establecidas por la siguiente licencia Creative Commons:  <http://es.creativecommons.org/blog/licencias/>

**WARNING.** The access to the contents of this doctoral thesis it is limited to the acceptance of the use conditions set by the following Creative Commons license:  <https://creativecommons.org/licenses/?lang=en>



**Universitat Autònoma  
de Barcelona**

ESCOLA D'ENGINYERIA

Departament d'Enginyeria Química, Biològica i Ambiental

Heterologous *Rhizopus oryzae* lipase expressed  
in *Komagataella phaffii*: improved production,  
biochemical characterization and industrial  
applications

Memoria para optar al Grado de Doctor por la Universitat Autònoma de Barcelona  
del Programa de Doctorado de Biotecnología bajo la dirección de los Doctores

Francisco Valero Barranco y Maria Dolors Benaiges Massa

**Josu López Fernández**

Bellaterra, 2022



Maria Dolors Benaiges Massa, Profesora Titular, y Francisco Valero Barranco, Catedrático, miembros del Departament d'Enginyeria Química, Biològica i Ambiental de la Universitat Autònoma de Barcelona,

CERTIFICAN:

que el biotecnólogo Josu López Fernández ha llevado a cabo, bajo su dirección en el Departament d'Enginyeria Química, Biològica i Ambiental de la Universitat Autònoma de Barcelona, el trabajo con el título “Heterologous *Rhizopus oryzae* lipase expressed in *Komagataella phaffii*: improved production, biochemical characterization and industrial applications” que se presenta en esta memoria, la cual constituye su Tesis para optar al Grado de Doctor por la citada universidad dentro del Programa de Doctorado en Biotecnología. Para su conocimiento y para que así conste, firmamos la presente certificación.

Bellaterra, marzo de 2022,

Dra. Maria Dolors Benaiges Massa

Dr. Francisco Valero Barranco



*En el punto de partida.*

*R.M.J.*

*Camins, somnis i promeses  
camins que ja són nous.*

*Sopa De Cabra*

*Gizakien lana jakintza dugu; ezagutuz aldatzea,*

*naturarekin bat izan eta harremanetan sartzea.*

*Eta indarrak ongi errotuz gure sustraiak lurrari lotuz,*

*bertatikan irautea: ezaren gudaz baietza sortuz,*

*ukazioa legetzat hartuz beti aurrera joatea.*

*Izarren hautsa, Mikel Laboa*

*Nothing ventured, nothing gained.*

*English saying*

الصبر مفتاح الفرج



## **Agradecimientos**

Agradecer a todas las instituciones públicas que han permitido realizar este trabajo: Universitat Autònoma de Barcelona, Ministerio de Ciencia, Unión Europea. También a los grupos y centros de investigación con los que hemos colaborado y en especial a Hausmann S.L y al Programa predoctoral de Formación de Personal Investigador No Doctor del Departamento de Educación del Gobierno Vasco del que he sido beneficiario estos años.

Acabadas las formalidades, mi primer agradecimiento quiero que sea para Dolors y Paco. Con vuestra guía científica y personal, estos cuatro años han sido infinitamente más llevaderos y fructíferos. Habéis sido y sois más que únicamente mis directores de tesis. Mi más sincero gracias por compartir tanto conmigo, a nivel científico y a nivel personal.

A los aseros, que han hecho que el día a día en el laboratorio fuera menos pozo de lo normal. A todos los chavales, que con su mofa continua de todo, sin duda habéis sacado risas de donde en su momento solo había cargo, sí, mucho cargo. Gracias a todos vosotros, incluso a Kírian, que supo venderme que en biocatálisis los horarios eran más sencillos que en fermentación (en realidad, muchas gracias por hacerlo). Javi, gracias por tu continuo buen humor e ironía. Miquel, infinita paciencia te ha dado el mundo. Gracias por escucharme y las risas en el despacho. Albert, el príncep, que siempre has puesto cordura entre todos, gracias por ser muchas veces mi confidente. A todos, incluso sin nombraros, gracias de verdad. No me quiero olvidar de las nuevas incorporaciones del grupo, Silvia, Kike y Núria, fuerza para la que se os viene. Y en especial gracias a ti Núria, por las risas y tu forma de ver el mundo. Que rápido crecen los minions ahora.

No me olvido de aquellos que sin estar ligados directamente al desarrollo de esta tesis, han estado involucrados. Las secretarias del departamento, siempre dispuestas a ayudarnos en todo. En especial a Rosa, que me ha ayudado hasta sacando billetes para el tren ¡Que



haríamos sin el Oráculo! A Manel, Pili y Rosi, por estar siempre dispuestos a ayudar. Pili, gracias por las risas y los cotilleos, has hecho que muchos días de cabreo/frustración pasaran a tener otro color. A Mariluz y Luisa, no podíais faltar. Aun recuerdo tus increíbles paellas y tartas Mariluz (y tus consejos de madre). Luisa, que siempre has estado dispuesta incluso a avisarnos si veías algo raro en las fermentaciones. Gracias por tener siempre una sonrisa, transmitirla y todo tu trabajo. A Xavi, Neus y Àngels, gracias por alegrar mi estancia en Hausmann, y a Xavi en concreto, por tu tiempo y risas. Era una promesa y aquí está, para el King Navas, que siempre ha estado, sin saberlo, cuando necesitaba un homenaje o levantarme el ánimo. Esos locos desconocidos.

No quiero perder la oportunidad de agradecer a mis padres y mi hermano el apoyo que me han dado y los fundamentos que me han enseñado en la vida que, en muchos momentos duros de la tesis, cogían más valor que el propio oro. El trabajo duro y bien hecho, la constancia. Son unos pocos de esos valores que más creo haber conseguido plasmar aquí. Gracias por apoyarme, aun sin entender qué es lo que hacía. Nunca os han faltado palabras de ánimo y felicitaciones para celebrar cada pequeño triunfo. Os quiero.

Y finalmente a ti, Javier. Porque lo has sido todo estos años. Porque hemos compartido todas las buenas y las malas juntos. Porque me has visto en todos los momentos y me has acompañado en cada uno de ellos, siendo más o menos difícil hacerlo. Uno ya sabe que es complicado de llevar. Siempre tendrás una gran parte de responsabilidad del logro personal que esta tesis supone, aunque te haya costado (y sigue haciéndolo) entender esas cosas abstractas que hago y que no se ven, pero que existen. Gracias y simplemente, te quiero.

Y a ti, que ya no lo verás, pero iré a contártelo. Ya lo he conseguido.

<b>Table of content.....</b>	<b>I</b>
<b>Abstract .....</b>	<b>III</b>
<b>Resumen .....</b>	<b>V</b>
<b>1. Introduction.....</b>	<b>1</b>
<b>2. Objectives.....</b>	<b>113</b>
<b>3. Materials and Methods.....</b>	<b>117</b>
<b>4. Results I: Biodiesel production.....</b>	<b>157</b>
<b>4.1. Second- and third-generation biodiesel production with immobilized recombinant <i>Rhizopus oryzae</i> lipase: influence of the support, substrate acidity and bioprocess scale up.....</b>	<b>157</b>
<b>4.2. Industrial enzymatic synthesis of biodiesel from waste cooking oil: Near Infrared Spectroscopy, a useful technique for inline monitoring of the biosynthesis.....</b>	<b>185</b>
<b>5. Results II: <i>Rhizopus oryzae</i> lipase production improvement and biocatalysts stability.....</b>	<b>211</b>
<b>5.1. Truncated prosequence of <i>Rhizopus oryzae</i> lipase: key factor for production improvement and biocatalyst stability.....</b>	<b>211</b>
<b>5.2. Mature <i>Rhizopus oryzae</i> lipase jointly with its truncated prosequence allows methanol independent heterologous production in <i>Komagataella phaffii</i> and improves biocatalyst operational stability.....</b>	<b>237</b>
<b>6. Results III: Biotransformations catalyzed with improved proROL biocatalyst.....</b>	<b>263</b>
<b>6.1. Natural flavors production with proROL from isoamyl alcohol and fusel oil.....</b>	<b>263</b>
<b>6.2. Polylactic acid production: Direct condensation and ring-opening polymerization.....</b>	<b>287</b>
<b>7. General conclusions.....</b>	<b>311</b>
<b>8. Abbreviations.....</b>	<b>319</b>
<b>9. Scientific contributions .....</b>	<b>325</b>
<b>10. Annex.....</b>	<b>329</b>



In this thesis, the *Rhizopus oryzae* 1,3-regiospecific lipase (ROL) has been studied, improving its operational stability and heterologous production, and it has been tested in different reactions of industrial interest.

Regarding the operational stability, the effect of the immobilization support and its functional groups on the performance of mature sequence ROL (rROL) during the synthesis of biodiesel in solvent-free reaction with olive pomace oil as a model substrate was assessed. Polymethacrylate supports with surface hydrocarbon chains improved the operational stability of the formed biocatalyst, allowing a longer half-life. The production of second- and third-generation biodiesel from non-edible vegetable oils and from microbial and used cooking oils (WCO), respectively, was also evaluated. In addition, the synthesis of biodiesel from WCO was inline monitored using a near infrared (NIR) spectroscopy probe into a laboratory scale reactor (50 mL), which proved to be a successful alternative to gas chromatography—the most commonly employed technique. The stability of the biocatalyst was also improved by means of adding the 28 amino acids from the C-terminal of the native prosequence of the enzyme—which have been described as acting as an intramolecular chaperone—to the N-terminal of rROL, obtaining proROL. The stability of proROL both free and immobilized was substantially improved compared to rROL against different conditions of pH, temperature and organic solvents. In addition, the former obtained 1.25 and 3 times more operational stability during the solvent-free synthesis of biodiesel and the esterification of ethyl butyrate (natural pineapple flavour), respectively.

The heterologous production of the enzyme was carried out in the methylotrophic yeast *Komagataella phaffii* (*Pichia pastoris*) under the methanol-inducible promoter of alcohol oxidase 1 ( $P_{AOX1}$ ). The production of proROL, instead of rROL, enabled the

obtention of a bioprocess with increased production and a volumetric productivity, 5.4 and 4.4 times, respectively, in the most extreme case. Likewise, proROL proved to reduce the harmful effects of its production in *K. phaffii* achieving, unlike with rROL, its constitutive expression under the methanol-independent promoter of glyceraldehyde 3-phosphate dehydrogenase ( $P_{GAP}$ ). The importance of the 28 amino acids of the prosequence in its role as an intramolecular chaperone by improving the stability of the biocatalyst and its heterologous production was thus confirmed. Besides, these amino acids were proved to alter the substrate specificity of proROL compared to rROL but they had no marked effect on the biochemical characterization of the enzyme.

Hence, a biocatalyst with improved characteristics was obtained which satisfactorily catalyzed the isoamyl acetate/butyrate esterification, regardless of the use of a branched alcohol and the potential steric hindrances. Isoamyl butyrate production — whose production exceeded the results obtained for isoamyl acetate— was optimized and scaled up to a 150 mL reactor. Fusel oil was also used as a low-cost alternative substrate to isoamyl alcohol and the specificity of proROL for the structural isomers 2- and 3-methylbutanol was assessed. Finally, proROL was also employed and compared with *Candida rugosa* lipase 1 (CRL1) in the production of polylactic acid (PLA) from lactic acid (direct condensation) and from lactide (ring-opening polymerization, ROP). proROL outperformed CRL1 in both reactions, although regardless of the enzyme, PLA was only detectable by nuclear magnetic resonance (NMR) in ROP.

In summary, the thorough study performed in this thesis, integrating various areas of knowledge, has led to an improvement in the enzyme under research, proROL, boosting its potential as industrial biocatalyst.

En la presente tesis, se ha estudiado la lipasa 1,3-regioespecífica de *Rhizopus oryzae* (ROL), mejorando su estabilidad operacional y su producción heteróloga, y se ha probado su capacidad biocatalítica en diferentes reacciones de interés industrial.

En lo relativo a la estabilidad operacional, se evaluó el efecto del soporte de inmovilización y sus grupos funcionales en la actividad de la secuencia madura de ROL (rROL) durante la síntesis de biodiesel en un medio de reacción sin solvente (*solvent-free*) con aceite de orujo como sustrato modelo. Los soportes de polimetacrilato con cadenas hidrocarbonadas mejoraron la estabilidad operacional del biocatalizador permitiendo una mayor vida media. Se estudió también la producción de biodiesel de segunda y tercera generación a partir de aceites vegetales no comestibles, de aceites microbianos y de aceites de fritura usados (*WCO*), respectivamente. Además, la síntesis de biodiesel a partir de *WCO* se monitoreó en línea mediante el uso de espectroscopia de infrarrojo cercano (*NIR*) en un reactor de escala de laboratorio (50 mL), obteniendo una alternativa exitosa a la cromatografía de gases —la técnica más comúnmente empleada. La estabilidad del biocatalizador también se mejoró mediante la adición de los 28 aminoácidos del extremo *C*-terminal de la prosequencia nativa del enzima —que han sido descritos que actúan como chaperona intramolecular— al extremo *N*-terminal de rROL obteniendo proROL. La estabilidad de proROL mejoró sustancialmente tanto libre como inmovilizada en comparación con rROL frente a distintas condiciones de pH, temperatura y solventes orgánicos. Además, se obtuvo 1.25 y 3 veces más estabilidad operacional durante la síntesis *solvent-free* de biodiesel y la esterificación de butirato de etilo (aroma natural de la piña), respectivamente.

La producción heteróloga del enzima se realizó en la levadura metilotrófica *Komagataella phaffii* (*Pichia pastoris*) bajo el promotor inducible por metanol de la

alcohol oxidasa 1 ( $P_{AOX1}$ ). La producción de proROL, en lugar de rROL, permitió conseguir un bioproceso con una producción y una productividad volumétrica 5.4 y 4.4 veces superiores, respectivamente, en el caso más extremo. Asimismo, proROL demostró reducir los efectos nocivos de su producción en *K. phaffii* consiguiendo, a diferencia de con rROL, la expresión de dicha lipasa bajo el promotor constitutivo e independiente de metanol de la gliceraldehído 3-fosfato deshidrogenasa ( $P_{GAP}$ ). Se confirmó así la importancia de los 28 aminoácidos de la prosequencia en su papel como chaperona intramolecular al mejorar la estabilidad del biocatalizador y su producción heteróloga. También se demostró que estos aminoácidos alteraban la especificidad de sustrato pero no tenían un efecto marcado en la caracterización bioquímica de proROL frente rROL.

Este biocatalizador con características mejoradas se probó con éxito en la esterificación de acetato/butirato de isoamilo, con independencia del empleo de un alcohol ramificado y sus potenciales impedimentos estéricos. La producción de butirato de isoamilo —que superó los resultados obtenidos con el acetato de isoamilo— se optimizó y se cambió de escala a un reactor de 150 mL. También se empleó aceite de fusel como sustrato de bajo coste alternativo al alcohol isoamílico y se estudió la especificidad de proROL por los isómeros estructurales 2- y 3-metilbutanol. Finalmente, proROL también se empleó y se comparó con la lipasa 1 de *Candida rugosa* (CRL1) en la producción de ácido poliláctico (PLA) a partir de ácido láctico (condensación directa) y a partir de lactida (polimerización por apertura de anillo, *ROP*). proROL superó a CRL1 en ambas reacciones, aunque con independencia de la enzima, únicamente se obtuvo PLA detectable a través de resonancia magnética nuclear (*NMR*) mediante *ROP*.

En resumen, el detallado estudio realizado en esta tesis, integrando diversas áreas de conocimiento, ha llevado a una mejora de la enzima en estudio (proROL) facilitando su potencial como biocatalizador en la industria





# Introduction

---

**Chapter accepted as review in Catalysts**

**López-Fernández J, Benaiges MD, Valero F.**

*Rhizopus oryzae* lipase, a promising industrial enzyme:  
biochemical characteristics, production and biocatalytic applications.

Catalysts 2020;10:1277. <https://doi.org/10.3390/catal10111277>



# 1. INTRODUCTION CONTENT

<b>1.1. Enzymes: a general overview</b> .....	5
<b>1.2. Enzymes in industry</b> .....	7
<b>1.3. <i>Rhizopus oryzae</i> fungus</b> .....	12
<b>1.4. <i>Rhizopus oryzae</i> lipase: biochemical properties</b> .....	14
<b>1.5. Production and bioprocess engineering of ROL</b> .....	25
1.5.1. <i>Komagataella phaffii</i> as a cell factory: ROL production.....	27
<b>1.6. Industrial uses of <i>Rhizopus oryzae</i> lipase</b> .....	29
1.6.1. Biodiesel production .....	30
1.6.2. Production of structured lipids.....	50
1.6.3. Production of flavor esters .....	56
1.6.4. Resolution of racemic mixtures .....	59
1.6.5. Polymerization reactions .....	61
<b>1.7. References</b> .....	65



## 1.1. Enzymes: a general overview

In 1836, Berzelius defined *catalysts* as chemical compounds that facilitate a reaction without undergoing any change themselves [1]. Subsequently, he hypothesized that enzymes could act as catalysts but failed to distinguish between chemical and biological catalysts; rather, he used the general term “contact substance” [2]. Catalysts operate by providing an alternative reaction mechanism involving a different transition state with a decreased activation energy. As a result, a greater number of molecular collisions will have enough energy to reach the transition state and eventually form the product. In this way, catalysts enable reactions that would otherwise be blocked or slowed down by a kinetic barrier; however, catalysts are not consumed in the process even though they can be altered as a result.

At the time Berzelius defined catalysts, the term “enzyme” had not yet been coined. In fact, the history of this concept is rather complex. Originally, the words “diastase” for enzymes involved in starch degradation to maltose, and “ferment” for both living yeasts and the action of their cellular content, were used to refer to what we now know were sets of reaction-catalyzing enzymes or microorganisms [3]. The subject was controversial, however, with some researchers claiming that a “life force” was needed to enact complex biotransformations and others that enzymes merely helped develop simple hydrolysis reactions [4]. The discussion focused on alcoholic fermentation, with those supporting the life force theory —Pasteur included— accepting that living yeasts were needed for a process such as this to develop. However, it was not until 1837, when Eduard Buchner found that alcoholic fermentation occurred without the need for living yeasts — but rather that it sufficed to use a substance he called “zymase”— that the term “enzyme”

was taken to represent biological catalysts and the life force theory was proved inaccurate [3]. Progress in the knowledge about enzymes in Buchner's time was impeded because their chemical nature was then completely unknown. It was not until in 1926, when James B. Sumner crystallized the first enzyme—a urease—that the protein nature of enzymes was confirmed [5]. Somewhat later, John H. Northrop succeeded in crystallizing several other proteins such as pepsin, trypsin, and chymotrypsin [2]. Currently, enzymes are known to essentially consist of a combination of 20 different amino acids—by exception, ribozymes consist of RNA [6]. Enzymes are thus polypeptides whose amino acid sequence (primary structure) is linked by peptide bonds to form the three-dimensional, secondary structure known as “ $\alpha$ -helix” or “ $\beta$ -sheet”. These 3D networks are established by hydrogen bonding between amino acids that need not to be close in the primary structure but are connected through loops and turns in the protein structure. Subsequently, this secondary structure rearranges itself through hydrophilic, hydrophobic or disulphide bonding interactions, among others, between side chains on the polypeptide backbone to form a tertiary structure that dictates the final shape of the protein and its catalytic activity. Some proteins additionally exhibit a quaternary structure resulting from side-chain interactions between two or more polypeptides [7].

The Enzyme Commission (EC) has classified enzymes into six large families according to activity (Table 1.1) and assigned a specific code (an EC number) to each. The first part of the EC number denotes the type of reaction the enzyme catalyzes (see Table 1.1) and the remaining digits represent the nature of the specific reaction. For instance, in the oxidoreductase category, the second digit in the EC number denotes the hydrogen donor, the third the acceptor and the fourth the number of categorized enzyme in its group.

**Table 1.1.** Enzyme families established by the Enzyme Commission.

<b>Class</b>	<b>Name</b>	<b>Reactions catalyzed</b>	<b>Example</b>
EC1	Oxidoreductases	Oxidation/reduction	Oxidase
EC2	Transferases	Transfer of functional groups between substances	Transaminase
EC3	Hydrolases	Formation of two products from one substrate	Lipase
EC4	Lyases	Nonhydrolytic addition or removal of groups from substrates	Decarboxylase
EC5	Isomerases	Intramolecular rearrangement	Isomerase
EC6	Ligases	Combination of two molecules by formation of new C–O, C–S, C–N or C–C bonds	Synthetase

Hence, lactate dehydrogenase has EC number 1.1.1.27 because it is an oxidoreductase (first digit), has the alcohol group of the lactate molecule as hydrogen donor (second digit) and  $\text{NAD}^+$  as acceptor (third digit), and is the 27th enzyme in its group (fourth digit) [8]. The number of reactions catalyzed by enzymes has grown in an exponential manner thanks to the development of increasingly powerful genetic modification tools allowing their aminoacid sequences to be altered. In fact, modifying the 3D structure or active site of enzymes has enabled catalytic reactions involving nonnatural substrates. Also, simply adjusting the reaction conditions has allowed such substrates to be catalyzed without the need to modify the enzymes, for instance, hydrolases have been widely used for this purpose [9–11].

## 1.2. Enzymes in industry

The wide variety of reactions enzymes can catalyze, and their high efficiency as biocatalysts, have made them suitable for a large number of current and future industrial uses. The process has been facilitated by their well-known advantages over chemical catalysts including outstanding selectivity and specificity, reduced environmental and



physiological toxicity, and the ability to operate under milder conditions [12–15]. Also, social concerns and public policies are forcing industries to increasingly shift from polluting manufacturing processes to more ecofriendly approaches where biocatalysis can play a major role [16–20]. As a result, the market value for industrially relevant enzymes is expected to reach \$16.9 billion by 2024 from \$8.2 billion in 2015 (Figure 1.1) at a remarkable compound annual growth rate (CAGR) of 6.6% for the period 2016–2024 [21].

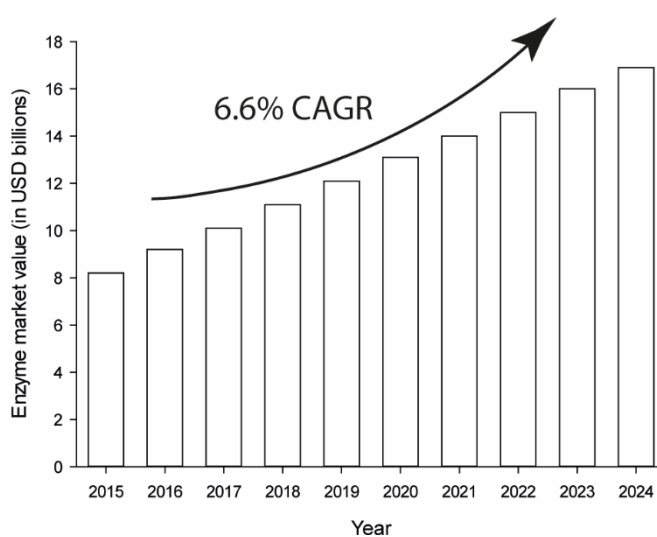


**Figure 1.1.** Global enzyme market value for the period 2015–2024 [21].

Hydrolytic enzymes currently dominate the market of industrial enzymes with more than 70% of all sales [22], and lipases (triacylglycerol hydrolases, E.C. 3.1.1.3) are the third largest group in this respect after proteases and amylases [23–25]. The main reason of the industrial importance of lipases is the wide variety of industrially relevant reactions they can enact (Figure 1.2). Thus, in aqueous media lipases catalyze the hydrolysis of fats at the water/lipid interface by cleaving ester bonds and concomitantly using water molecules to give the corresponding fatty acids and glycerol or a different alcohol. In addition, because they fulfill the principle of microreversibility, lipases can

catalyze the reverse process (i.e., a synthesis reaction) in nonaqueous media. These reactions can be of different types including esterification, which involves a double displacement between alcohols and carboxylic acids to give esters and water; transesterification, where an acyl group in an ester is exchanged with an alkyl group in an alcohol, acid or another ester to give an alcoholysis, acidolysis or interesterification product, respectively; and rarely, aminolysis, by which carboxylic esters are converted into amides [26–31]. Such a high flexibility makes lipases suitable for a number of uses including the production of flavors, detergents, pharmaceuticals, biopolymers, bioenergy and fine chemicals [25,32].

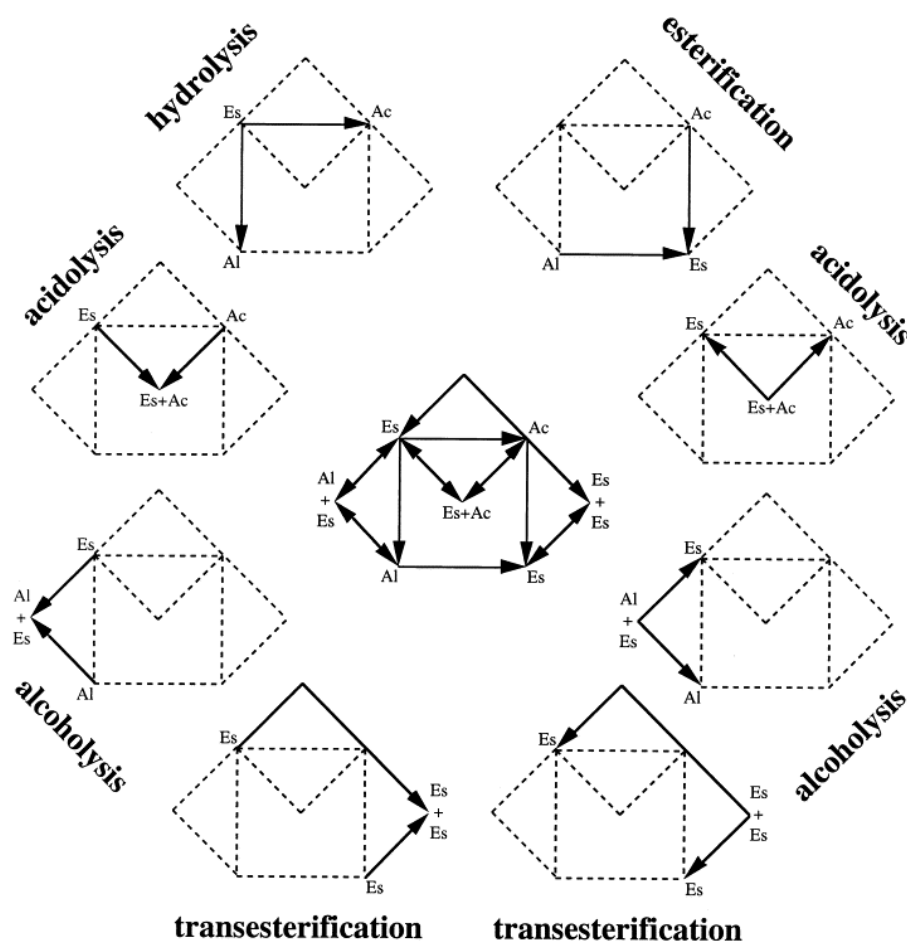


**Figure 1.2.** Wireframe of the lipase-catalyzed reaction domain. Es, Al and Ac denote esters, alcohols and acids respectively. Reactants are depicted in front of arrow starts and products behind arrow ends [30].

As can be seen in Figure 1.3, lipases are broadly classified according to two traits, namely: specificity and source [26,33]. As regards specificity, lipases can be (a) substrate-specific if they act selectively on a given substrate in a mixture of crude raw materials [34–37]; (b) enantioselective if they hydrolyze one isomer of a racemate preferentially over the other [38–41]; or (c) regioselective if their activity depends on their positional specificity [42–44].

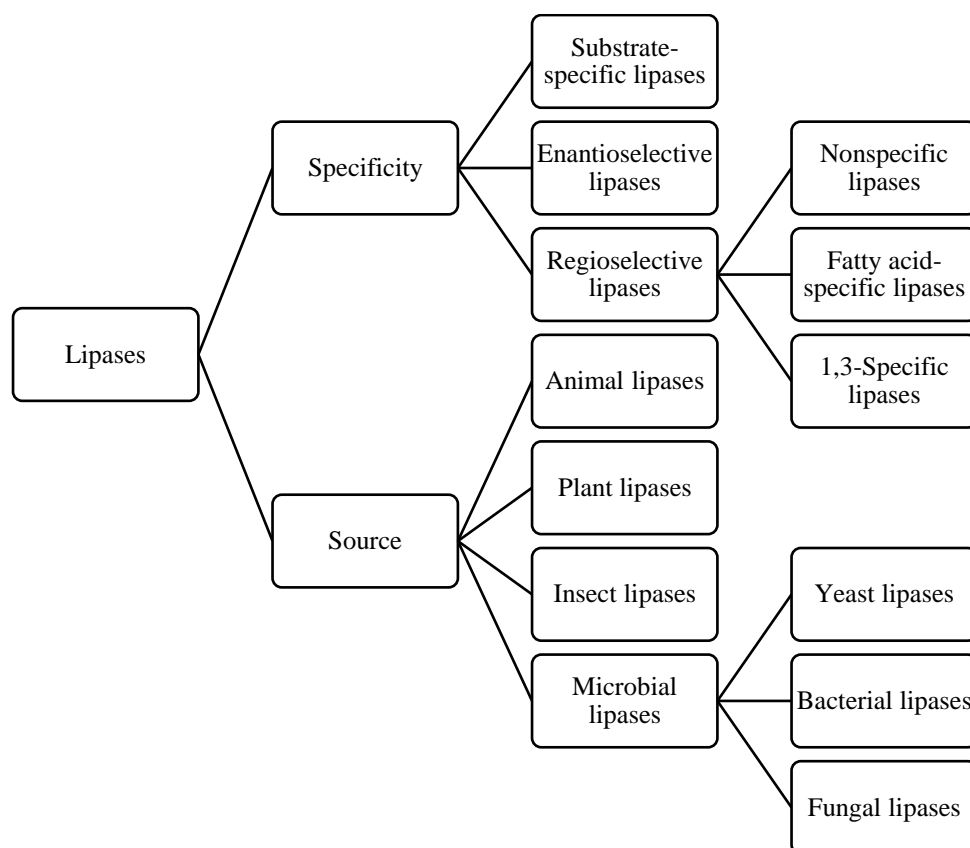


**Figure 1.3.** Classification of lipases according to specificity and source.

Regioselective lipases can in turn be of three different types. Nonspecific lipases catalyze the hydrolysis of triacylglycerols (TAG) into free fatty acids and glycerol with mono- and diglycerides as intermediates. These enzymes can act over all fatty acids from any position in the substrate. *Candida antarctica* lipase is one of the most widely used and researched nonspecific lipases [45,46]. Fatty acid-specific lipases are selective for

fatty acids and tend to hydrolyze esters containing long-chain fatty acids with double C9–C10 bonds. Such is the case with the lipases from *Geotrichum candidum* [47] and *Penicillium citrinum* [48]. 1,3-Specific lipases such as those from *Rhizopus oryzae* [49,50] and *Yarrowia lipolytica* [51] hydrolyze acylglycerols at positions *sn*-1 and *sn*-3 in TAG to give free fatty acids, 2-monoacylglycerols and 1,2- or 2,3-diacylglycerols, thereby avoiding the formation of glycerol. In this reaction, diacylglycerols form faster than monoacylglycerols [44]. In this process acyl migration might occur, which is a nonenzymatic process involving a spontaneous shift of an acyl group from a hydroxyl group to a neighboring one. As a result, acyl migration might cause 1,3-diacylglycerols and 1-monoacylglycerols to form from 1,2- or 2,3-diacylglycerols and 2-monoacylglycerols, respectively, thereby leading to glycerol formation with 1,3-specific lipases after an extended reaction time [43].

Lipase sources include animals, plants, insects and microbes [26,52]. Microbial lipases (Table 1.2) have been deemed desirable relative to animal and plant lipases; thus, microbial lipases tend to be more stable, chemoselective, enantioselective; also, they need no cofactor [27,33,42,53,54]. Specifically, fungal lipases have been broadly researched on the grounds of their being produced by native microorganisms in high amounts and possessing unique catalytic properties. The most widely used lipase-producing fungi belong to the genera of *Rhizopus* sp., *Aspergillus* sp., *Penicillium* sp., *Geotrichum* sp. and *Mucor* sp. [33,55,56].

**Table 1.2.** Most common lipases and their specificity.

Source	Organism	Specificity
Bacteria	<i>Burkholderia cepacia</i>	Nonspecific
	<i>Pseudomonas fluorescens</i>	Nonspecific
	<i>Chromobacterium viscosum</i>	Nonspecific
	<i>Pseudomonas stutzeri</i>	Nonspecific
Fungi	<i>Candida antarctica</i>	Nonspecific
	<i>Thermomyces lanuginosus</i>	1,3-Specific
	<i>Candida cylindracea</i>	Nonspecific
	<i>Candida rugosa</i>	Nonspecific
	<i>Mucor javanicus</i>	1,3-Specific
	<i>Rhizopus oryzae</i>	1,3-Specific
	<i>Aspergillus niger</i>	1,3-Specific
	<i>Penicillium cyclopium</i>	Nonspecific
	<i>Mucor miehei</i>	1,3-Specific
	<i>Candida deformans</i>	1,3-Specific
	<i>Geotrichum candidum</i>	Nonspecific or 1,3-specific
<i>Yarrowia lipolytica</i>	1,3-Specific	

Adapted from [57]

### 1.3. *Rhizopus oryzae* fungus

The industrial significance of the genus *Rhizopus* has led to careful classification of the species it encompasses and to examination of their essential differences. However, classification schemes have changed over time, which may have had an adverse impact on the accuracy of their enzymes notations. Traditionally, *Rhizopus* species have been distinguished according to morphological and physiological features [58]. For instance, Schipper [59] originally established three *Rhizopus* groups, namely: *R. microsporus*, *R. stolonifer*, and *R. arrhizus* (= *oryzae*). Lately, Abe *et al.* [60] conducted the first molecular phylogenetic study on *Rhizopus* and concurred with Schipper's classification. Subsequent studies, however, led to the genus being classified into ten [61] or eight [62] species until Abe *et al.* [63] finally confirmed the latter classification by using rDNA ITS, actin-1 and translation elongation factor 1 $\alpha$  sequences as differential traits. Notwithstanding these

classifications, most *Rhizopus* species in culture collections belong to only four species or complexes thereof, namely: *R. microsporus*, *R. stolonifer*, *R. arrhizus* (or *R. oryzae*, Figure 1.4) and *R. delemar* (or *R. arrhizus* var. *delemar*). According to GenBank records, *R. oryzae* or *arrhizus* (including *R. arrhizus* var. *delemar*) is the most significant, with more than 7000 identified isolates [58]; also, it is the most widely described specie of *Rhizopus* genus [64].

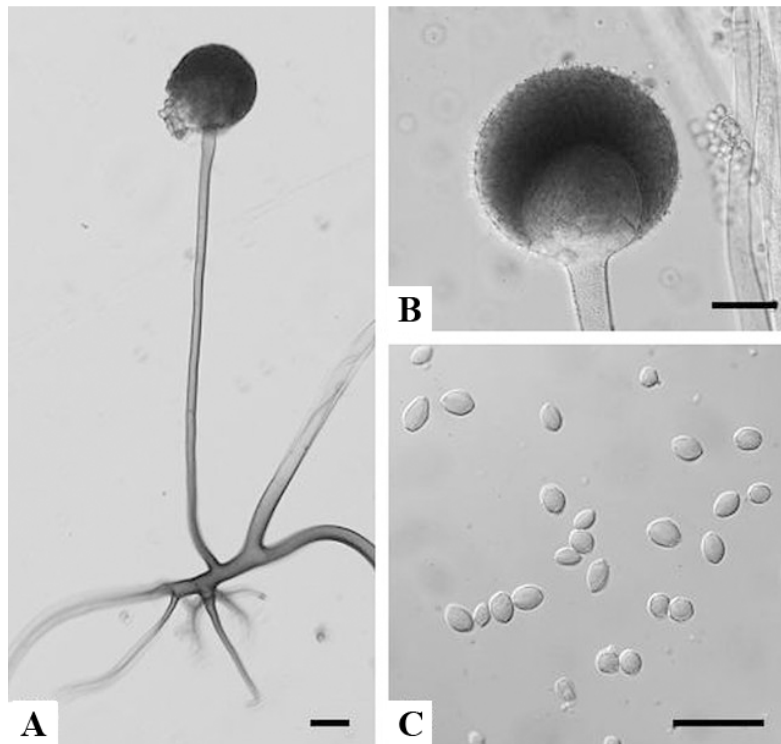


**Figure 1.4.** Micrographs of *Rhizopus oryzae* from Bioresource Collection and Research Center (BCRC 33888). (A) Rhizoid and sporangiophore (Bar = 55  $\mu\text{m}$ ). (B) Sporangium (Bar = 50  $\mu\text{m}$ ). (C) Sporangiospores (Bar = 20  $\mu\text{m}$ ). Reproduced from [65].

*Rhizopus oryzae* (Figure 1.4) is broadly used industrially to synthesize a great variety of products including organic acids (lactic and fumaric), volatile compounds and enzymes (cellulases, proteases, tannases, xylanases, pyruvate decarboxylases, lipases) [66–69]. Based on Web of Knowledge data, *R. oryzae* lipase (ROL) is one of the most broadly studied enzymes produced by this fungal species. In fact, ROL is commercially

available in five major formulations (Table 1.3); also, it has been the subject of more than 200 scientific papers in the last 5 years, which testifies to its great importance. Consequently, this Introduction provides a comprehensive overview of ROL in terms of biochemical properties, enzyme native and heterologous production, and industrial uses.

**Table 1.3.** Major commercial suppliers of *Rhizopus oryzae* lipase and selected lipase properties [27].

Supplier	Name	Use	Properties
Amano	Lipase DF “Amano” 15	Oil and fats	Optimum pH 6–7 Stable pH 4–7 Optimum <i>T</i> 35–40 °C
Sigma	Lipase from <i>R. oryzae</i> (no. 62305)	Oil and fats	Optimum pH 8 Optimum temperature 40 °C
Sigma	Lipase, immobilized on Immobead 150 from <i>R. oryzae</i> (no. 89445)	Pharmaceuticals and bioenergy	Optimum pH 7.5 Optimum temperature 40 °C
Creative Enzymes	NATE-0404	Resolution of chiral mixtures and bioenergy	Optimum pH 7.2 Highly active at pH 6.5–7.5
BIOCON	Lipase from <i>R. oryzae</i>	Baking, food processing and flavors	Optimum pH 3–9 Temperatures up to 50 °C

#### 1.4. *Rhizopus oryzae* lipase: biochemical properties

*Rhizopus oryzae* lipase (ROL) is a protein obtained as a precursor form that contains a presequence of 26 amino acids followed by a prosequence of 97 attached to the *N*-terminal of a mature sequence comprising 269 amino acids (Figure 1.5) [70]. All known lipases from the genus *Rhizopus* possess the same structure even though their primary sequences may differ in amino acid composition not only between species, but also between strain isolates of the same species (Figure 1.6). For instance, Ben Salah *et al.* [71] confirmed the presence of several substitutions in the sequences of *Rhizopus*

lipases reported by his group, Sayari *et al.* [72], Beer *et al.* [70], Derewenda *et al.* [73] and Khono *et al.* [74].

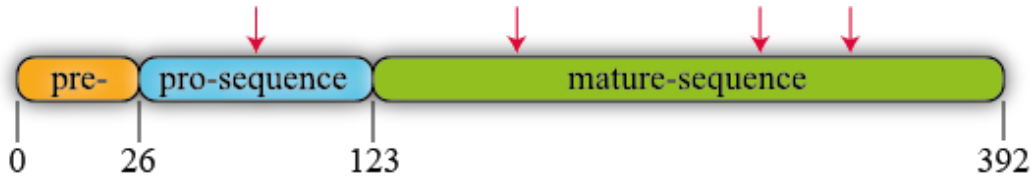


**Figure 1.5.** Schematic depiction of ROL. Arrows denote potential *N*-glycosylation points.

ROL has four potential *N*-glycosylation sites (Figure 1.5) that follow the consensus sequence Asn-X-Ser/Thr, where *X* can be any amino acid except proline. One of these putative sites occurs in the prosequence, where changes in glycosylation patterns have been found to affect protein secretion [75]. For instance, Yu *et al.* [76] included two additional *N*-glycosylation sites in ROL prosequence and expressed this mutant in *Komagataella phaffii* (*Pichia pastoris*). The resulting extracellular activity and total amount of protein were 218 and 6.25 times greater, respectively, in the strain harboring the additional sites than in the original strain, which testifies to the significance of glycosylation.

ROL prosequence has been reported to act as a signal peptide promoting enzyme secretion, and ROL prosequence to exhibit diverse functions that are still under research. Beer *et al.* [77] demonstrated the significance of the prosequence in reducing lipase toxicity during its synthesis and in acting as an intramolecular chaperone enabling appropriate folding of the enzyme. In fact, genetically modified *E.coli* strains producing heterologous ROL without the prosequence have been found to result in cell lysis. A large number of prosequences in various enzymes have also been found to function as



intramolecular chaperones and to assist in the folding of their respective proteins [78]. In addition, some authors have related ROL prosequence with protein translocation across the endoplasmic reticulum membrane, enhancement of free lipase stability and changes in substrate specificity. However, the underlying mechanisms remain unknown despite strong endeavors to establish them [79–84].

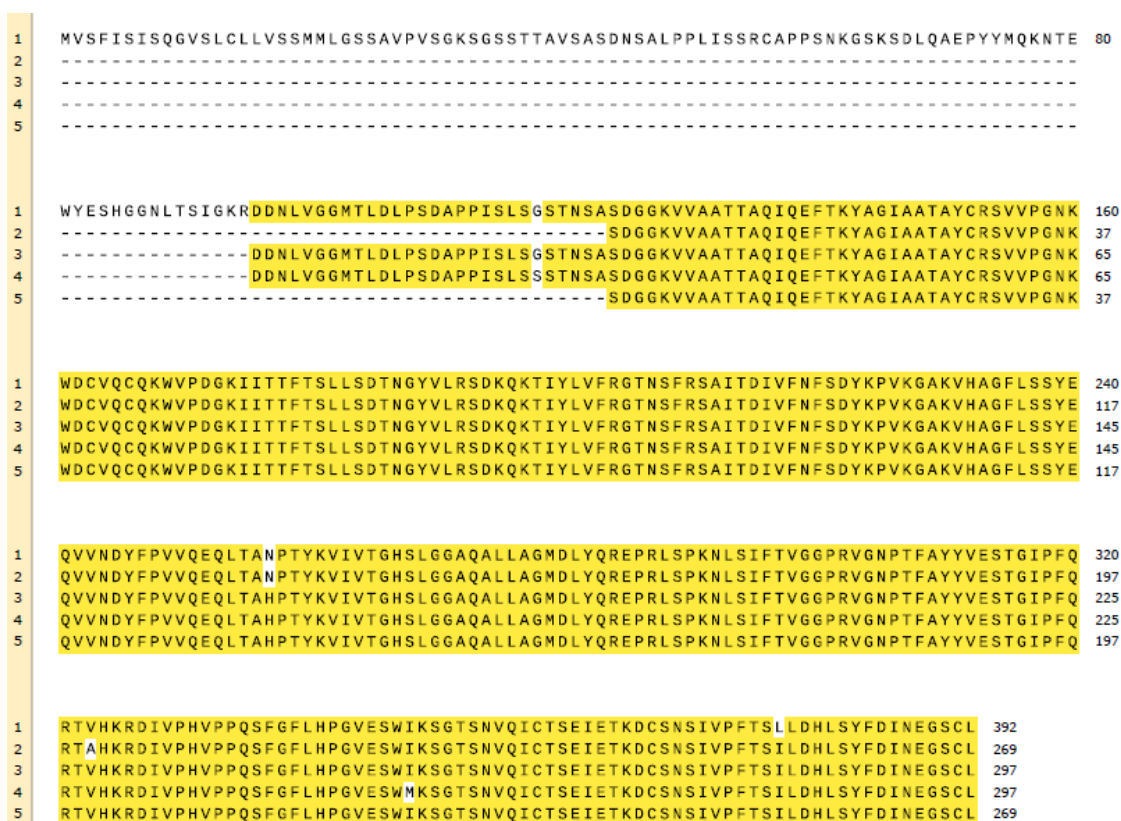


**Figure 1.6.** Multi-alignment of sequences reported by (1) Beer *et al.* (ROL) [70], (2) Ben Salah *et al.* (ROL) [71], (3) Sayari *et al.* (ROL) [72], (4) Khono *et al.* (*Rhizopus niveus* lipase) [74] and (5) Derewenda *et al.* (*Rhizopus delemar* lipase) [73]. Matching amino acids are highlighted in yellow and nonmatching amino acids are not. Data were obtained with the aid of BLAST (US National Library of Medicine) and Snapgene has been used for the creation of this figure.

In any case, both the presequence and the prosequence are expected to be proteolytically removed for mature lipase to form. In spite of which, the native microorganism secretes a lipase (native *Rhizopus oryzae* lipase “nROL”, also referred to as “proROL” in this thesis when heterologously produced, see Nomenclature Section)

which contains the 28 C-terminal amino acids of the prosequence attached to the *N*-terminal of the mature sequence that are subsequently cleaved by limited proteolysis in a process catalyzed by extracellular proteases [70,74,85]. However, some studies have shown that the presence of the 28 amino acids of the prosequence alongside the mature sequence suffices for some of the presumed features of the whole prosequence to occur. For instance, expression of the 28 amino acids of the prosequence together with the mature sequence in *K. phaffii* was found to increase free lipase stability and alter enzyme specificity (Section 5.1). Also, it reduced the toxicity of ROL production in *Escherichia coli* [77] and is believed to direct proteins to a secretory pathway in *Aspergillus oryzae* [86].

The mature sequence of *R. oryzae* lipase (rROL) consists of 269 amino acids forming a protein of molecular weight (MW) of 29.542 kDa and an isoelectric point (pI) of 8 as calculated on ExPASy Proteomics Server [71]. These results are consistent with reported experimental data (Table 1.4), namely MW about 29 kDa and pI around 8 [72,74,87,88]. However, the presence of the 28 amino acids of the prosequence has been found to increase MW to around 32 kDa and to decrease pI roughly to 7, thus highlighting the average acid nature of these amino acids [50,74,84,89,90]. Besides, production of a lipase including the whole prosequence (entire-proROL) and having MW close to 40 kDa has also been reported [70,79]

**Table 1.4.** Biochemical properties and substrate specificity of ROL used in various studies.

Lipase name <sup>1</sup>	MW (kDa)	Isoelectric point (pI)	Optimum pH	Optimum T (°C)	Substrate specificity	Ref.
rROL	29		8/7.25 <sup>2</sup>	30/40 <sup>2</sup>	C12 > C10 > C8 > C4 <sup>4</sup>	[50]
proROL	32		7.25	40	C8 > C12 > C10 > C4 <sup>4</sup>	[50]
rROL	30		8.5			[70]
Entire-proROL	40		8			[70]
Pre-entire-proROL <sup>3</sup>	42		8			[70]
rROL	29		8	37		[71]
rROL	29					[72]
proROL	32					[72]
proROL	34		6–6.5	35		[74]
rROL	30		6	40		[74]
proROL	35		9	40	C16 > C18 > C12 > C8 > C4 <sup>5</sup> C16 > C12 > C8 > C18 > C4 <sup>6</sup>	[82]
proROL	32	6.9				[84]
rROL	30	9.3	8.25	30	C8 > C10 > C6 > C4 > C12 > C16,C14 > C2 <sup>6</sup>	[87]
proROL	35		5.2	30	C12 > C10 > C8 > C6 > C16 > C5 > C4 > C3 > C2 <sup>4</sup>	[88]
proROL	32	7.6	7.5	35	C8 > C6 > C4 > C2 <sup>6</sup>	[89]
rROL	29				C12 > C10 > C8 > C6 > C4 > C3 > C2 <sup>4</sup> C8 > C10 > C18 > C4 > C6 <sup>6</sup>	[91]
proROL	34				C2 > C3 > C8 > C6 > C12 > C10 > C4 <sup>4</sup> C8 > C10 > C4 > C6 > C18 <sup>6</sup>	[91]
proROL			8	40		[92]
rROL	30.3	8.6	8–8.5	30		[93]
proROL			8.5	30		[94]
proROL	37		8.5	40		[95]
rROL	29		8			[96]

**Table 1.4.** Biochemical properties and substrate specificity of ROL used in various studies.

Lipase name <sup>1</sup>	MW (kDa)	Isoelectric point (pI)	Optimum pH	Optimum T (°C)	Substrate specificity	Ref.
ROL	17	4.2	7	40		[97]
ROL			7	40		[98]
ROL			6	45	C8 > C4 > C6 > C2 <sup>6</sup> C8 > C12 > C14 > C16 > C18 <sup>5</sup>	[99]
proROL	32		7	35		[100]
ROL			6	30	C7,C8,C12,C16 > C2,C3,C4,C18 <sup>5</sup>	[101]
ROL			7.5	50		[102]
proROL	32		7.5	30–40		[103]
ROL	14.45	6.5	9	30–40	C16 > C18 > C12 > C8 > C4 > C2 <sup>4</sup>	[104]
			8.3	35–37		[105]
proROL	35				C10 > C14 > C12 > C8 > C6 > C4 > C16 <sup>6</sup>	[79]
Entire-proROL	46					[79]

1 Names are based on the nomenclature used in this thesis, ROL indicating that the lipase cannot be exactly classified according to the criteria used here

2 Differences resulting from the use of 200 or 400 mM Tris-HCl buffer

3 Pre-entire-proROL includes the presequence and entire-proROL, in turn, includes the whole presequence

4 Specificity was assessed with *p*-nitrophenol esters

5 Specificity was assessed with methyl esters of variable chain length.

6 Specificity was assessed with homotriacylglycerols

Crystallographic resolution of the 3D structure of lipase from *R. oryzae* [73,74] (Figure 1.7) and various other microorganisms such as *Geotrichum candidum* [106], *Candida rugosa* [107], *Pseudomonas glumae* [108] and *Penicillium camemberti* [109] revealed that all lipases share an  $\alpha/\beta$  hydrolase fold structure also present in other hydrolases [56]. ROL contains nine  $\alpha$ -helices and eight  $\beta$ -strands forming a molecule that is stabilized by three disulphide bonds between residues 29–269, 40–43 and 235–244 [74]. In addition, this protein structure contains three key components that can also be found in most lipases besides ROL, namely: the lid, the active site and the oxyanion hole [26].

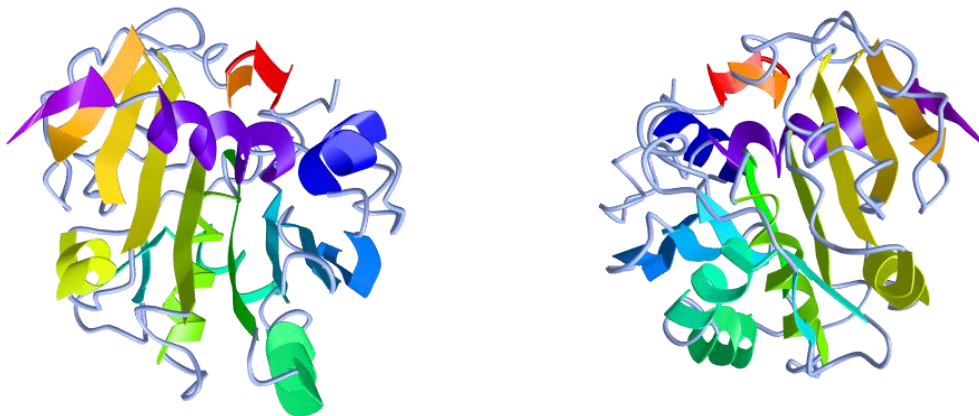


**Figure 1.7.** Three-dimensional structure of *R. delemar* (= *oryzae*) lipase from two different perspectives. PDB ID: 1TIC. Image obtained from iCn3D web-based 3D structure viewer.

The lid is an amphiphilic loop (a “flap”) that covers the active site to prevent access by the substrate while the enzyme is in aqueous medium [110]. The active site in turn enacts enzyme catalysis; in all  $\alpha/\beta$  hydrolases, the site consists of a highly conserved catalytic triad formed by a nucleophilic, a catalytic acidic and a histidine residue. In lipases, this triad consists of a nucleophilic serine residue and an aspartic or glutamic acid residue that it is bonded to a histidine residue; hence, lipases are classified as serine

hydrolases. In ROL, the lid domain is a short  $\alpha$ -helix structure comprising six amino acids (FRSAIT) and the active site consists of the following three: Ser<sup>145</sup>, Asp<sup>204</sup> and His<sup>257</sup> [73,74,111,112]. These two elements play a crucial role during catalysis; thus, the lipase binds to the water/lipid interface and lid opening occurs by a concomitant structural change that allows the substrate to bind to the active site —Derewenda *et al.* [73] described lid-closed and partially opened 3D structures in lipase from *Rhizopus delemar* (= *oryzae*). The resulting structural change, known as “interfacial activation”, is a unique trait of lipases that allows them to hydrolyze insoluble esters and be distinguished from esterases, which carry out the hydrolysis of water-soluble esters [26,113–115]. It should be noted that the 28 amino acids of the prosequence introduced above are believed to interfere with the catalytic process by effect of their being located next to the lid region and 50% of its residues being hydrophobic. Therefore, this sequence extends the hydrophobic patch created by the open lid in the lipase and the catalytic crevice, influencing interactions with the lipid substrate [72]. Although this role might explain some of the assumed properties of the 28 amino acids, the underlying mechanism remains unknown. Additionally, together with the catalytic triad and the lid, the oxyanion hole plays a major role; also, it is a highly conserved sequence which largely influences the catalytic efficiency of the enzyme. During hydrolysis, a negatively charged tetrahedral intermediate is produced that is stabilized by hydrogen bonding with the oxyanion hole [26,116,117]. This role has been ascribed to the hydroxyl and main-chain amide groups of Thr<sup>83</sup> in ROL [73,74,118].

Due to the relevance of the lipolytic activity of this enzyme, it has been widely researched in how it is affected by the reaction medium. Guillen *et al.* [91] found ionic strength to have a considerable impact. Thus, the relative activity of ROL in 200 mM

Tris-HCl buffer was twice that in 400 mM. Also, as with all enzymes, ROL activity is strongly influenced by pH and temperature. Although an optimum pH of 8 for ROL activity has been principally proposed [70,71,87,89,91–96,119], some authors have suggested more acid [88,97–103] and more basic values [82,104,105]. Similarly, the optimum temperature is believed to be between 30–45 °C, with 40 °C as the most widely agreed optimum [50,74,82,91,92,95,97,98,103,104] but lower [71,74,88,89,91,93,94,100,101] and higher levels [99,102] being also proposed (Table 1.4.). However, as can be seen in Table 1.4, the optimum pH and temperature depend on whether the 28 amino acids of the prosequence are present. Kohno *et al.* [74] encountered such differences and, later, other authors [50,77,91] reported similar results highlighting the significance of these amino acids to catalytic performance in ROL.

The influence of the presence of metal ions in the reaction medium has been extensively examined as it can affect enzymes structure and activity. In fact, metal ions can bind to some amino acid side chains in lipases and take part in the catalytic process, interfere with bonding in amino acid side chains and denature active sites or alter the activity of the enzymes by stabilizing or destabilising their conformation [100,120–122]. Although there have been contradictory reports in this respect, some metal ions have been found to enhance or worsen catalytic performance in ROL and other lipases. Thus, Wang *et al.* [82] and several other authors [97,100,104] found  $\text{Ca}^{2+}$  to increase ROL activity, possibly through electrostatic interactions masking repulsions either between the enzyme and its emulsified substrate or between the enzyme and produced free fatty acids [93]. On the other hand,  $\text{Hg}^{2+}$  has been reported to act as a ROL activity inhibitor, which suggests that thiol groups are required for the enzyme to perform its function [88]. Similar results have been reported for other lipases from *Pseudomonas aeruginosa* AAU2 [123],

*Galactomyces geotrichum* Y05 [124], *Yarrowia lipolytica* [125] and *Candida rugosa* [126]. By contrast, no substantial effects of the chelating agent EDTA have been observed, which confirms that ROL activity is metal-independent—and hence, that ROL is not a metalloprotein [88,104].

ROL activity has also been examined in the presence of amino acid-modifying agents in order to assess the significance of amino acids to catalytic performance. Thus, *N*-bromosuccinimide (NBS), which acts over tryptophan residues, has been reported to strongly inhibit enzyme activity. This suggests that the action of the protein might involve a tryptophan residue [88,97]. No conclusive results, however, were obtained with phenylmethylsulfonyl fluoride (PMSF), a serine protease inhibitor whose activity is related to changes in serine residues. Thus, Kantak *et al.* [97] found PMSF to have a substantial effect, whereas Hiol *et al.* [89] observed exactly the opposite. The discrepancy may have arisen from differences in the way the lipase lid was arranged during the assay (specifically, whether or not it was open, which would have enabled or prevented the interaction of PMSF with serine residue at the active site) [127].

As most lipases from the genus *Rhizopus*, ROL exhibits a strong 1,3-regiospecificity that makes it appealing for various industrial processes such as fat and oil modification for the production of structured lipids [27,69,89,99]. However, Li *et al.* [128] examined methanolysis performance in ROL and found it not to be regiospecific even though the enzyme exhibited a preference for 1,3-positions. These results were lately confirmed with *Rhizopus arrhizus* (= *oryzae*) lipase [129]. However, Okumura *et al.* and Song *et al.* [101,130] found lipase from *Rhizopus delemar* (= *oryzae*) not to hydrolyze the ester bond at position 2. Subsequently, Canet *et al.* and Cao *et al.* [131,132] showed mature ROL to have negligible activity on 2-monoolein, and hence that the lipase was



strongly 1,3-regioespecific. The previous discrepancies may have arisen from differences in reaction conditions—some favoring spontaneous acyl migration— or the presence of the 28 amino acids of the prosequence, which is known to affect lipase specificity [50,77].

Substrate specificity in ROL has also been widely studied (Table 1.4), largely by using *p*-nitrophenol esters of variable carbon chain length. For instance, ROL isolated and characterized by Adak *et al.* [104] was proved especially specific to *p*-nitrophenol esters of long carbon-chain such as *p*-nitrophenol palmitate (C16). Guillen *et al.* [91] reported a similar trend in rROL produced by *K. phaffii* and, although they found commercial proROL to be more specific to *p*-nitrophenol esters of short carbon chain, they ascribed their results to the presence of esterases in the commercial product they used. Tako *et al.* [88] found that the longer the carbon chain was, the higher was ROL specificity; however, specificity peaked with *p*-nitrophenol dodecanoate (C12) rather than with the palmitate (C16). ROL substrate specificity has been also assessed with homotriacylglycerols. ROL preferably hydrolyzes C8 and C10 homotriacylglycerols but barely acts over their C2 and C4 counterparts. In contrast to some studies, others have found no appreciable differences in the response of rROL and proROL to such substrates [79,87,89,91].

Lipases are widely known for their ability to enable syntheses in nonaqueous media. As noted earlier, this ability has fostered their use in a number of industrial processes involving synthetic reactions where the reactants or products are only soluble in organic solvents. Therefore, the higher the stability of the lipase in these solvents is, the more suitable the enzyme will be for industrial use [54]. ROL has been extensively reported to tolerate nonaqueous solvents (particularly alkanes and long-chain alcohols such as hexane and dodecanol) [82,89,94]. Its stability, however, is severely

compromised by polar solvents such as acetone and short-chain alcohols, which can strip off crucial bound water from the enzyme's surface [11]. In some cases, the enzyme can be rather differently stable in some alcohols such as methanol and ethanol when used as a solvent or as a substrate. Methanol has proved more detrimental than ethanol during biodiesel synthesis, but stability assays have shown exactly the opposite [50]. Thus, the operational stability of the enzyme when interacting with the solvent (as a substrate) at the open active site is more deleterious than when the solvent does not interact with the active site (lipase closed form).

### **1.5. Production and bioprocess engineering of *Rhizopus oryzae* lipase**

The earliest attempts at ROL production were made with the original fungi isolated from palm fruit [89,94,133]. As noted earlier, *R. oryzae* secretes a lipase form with MW close to 32 kDa whose mature sequence includes the 28 C-terminal amino acids of the prosequence. However, a second ROL form with MW around 29 kDa (viz., one containing the mature sequence alone by effect of the enzyme losing the 28 amino acids of its prosequence) was also detected after keeping the supernatant at 6 °C for a few days [72]. Consequently, reported *R. oryzae* lipase forms result from proteolysis rather than from the presence of different genes [70].

Although *R. oryzae* can be used as source of lipase, obtaining industrially useful ROL amounts requires heterologous expression in cell factories to maximize production, ease downstream work and bioprocess engineering, and consequently, minimize production costs [27]. ROL has so far been successfully produced in the three main cell factories, namely: *Escherichia coli*, *Saccharomyces cerevisiae* and *Komagataella phaffii*—the last is also known by its obsolete name *Pichia pastoris*.

In *E. coli*, the presence of disulphide bonds in ROL, and the absence of the enzymes needed to process fungal maturation signals, were found to lead to an enzymatically inactive protein in the form of insoluble aggregates [70]. However, active lipase was successfully produced on a laboratory scale by causing the aggregates to refold—no large-scale production was attempted, owing to the high cost of the procedure [77]. In any case, Di Lorenzo *et al.* [134] succeed in producing active, soluble rROL and proROL by using the *E. coli* Origami (DE3) strain and pET-11d expression system. Although the final specific activities of both enzymes were quite similar, the yield in proROL was higher than that in rROL as the likely result of proROL being less deleterious to host cells than was rROL because of the prosequence.

The eukaryotic cell factories *S. cerevisiae* and *K. phaffii* have been used to produce ROL extracellularly in order to circumvent the problems of prokaryotic cell factories in producing eukaryotic proteins (particularly those related to post-translational processing). Three different genes were used for this purpose, namely: one encoding the prosequence of 97 amino acids fused to the *N*-terminal of the mature lipase sequence of 269 amino acids (proROL-gene); another encoding a truncated prosequence of its 28 C-terminal amino acids fused to the *N*-terminal of the mature lipase region (28proROL-gene); and a third encoding mature lipase (rROL-gene). Whether proROL-gene or 28proROL-gene was expressed, a protein with only 28 amino acids of the prosequence in addition to mature lipase (proROL) was detected. Exceptionally, the whole prosequence and the mature lipase region (entire-proROL) were also observed with proROL-gene construction—on the contrary, only mature lipase (rROL) was obtained with rROL-gene construction.

ROL was first produced on eukaryotic platforms with the widely used *S. cerevisiae* cell factory. Takahasi *et al.* [79] found *S. cerevisiae* to secrete two active lipases upon transformation with the proROL-gene fused to the pre- $\alpha$ -factor, the entire-proROL and proROL, derived from the former by Kex2-like protease cleavage of the corresponding part of the prosequence. Almost no activity, however, was detected when *S. cerevisiae* strains were transformed with rROL-gene fused to the pre- $\alpha$  or prepro- $\alpha$  factor encoding gene, a result that highlights the above-mentioned significance of ROL prosequence to lipase production [80,83,85]. Consequently, although several works can be found in the literature regarding ROL heterologous production in *S. cerevisiae*, *K. phaffii* has emerged as successful alternative for this lipase production, obtaining promising results that will be specifically treated in the following Section.

### ***1.5.1. Komagataella phaffii as a cell factory: ROL production***

Because it is a methylotrophic yeast, *K. phaffii* can metabolize methanol as its sole source of carbon and energy. The first and main enzyme involved in this metabolic pathway is the alcohol oxidase, which is encoded by two genes in *K. phaffii*, namely: *AOX1* and *AOX2* [135]. The methanol inducible promoter of the former gene is very strong, which further increases the importance of *K. phaffii* as an expression host for producing recombinant proteins under that promoter. In addition, *AOX1* knockouts ( $Mut^S$  strains) result in strains with slow growth on methanol (in comparison to  $Mut^+$  strains, harbouring both *AOX* genes), but which have directed the force of the *AOX1* promoter mainly towards recombinant protein production. The high productivity of *K. phaffii* (no matter the  $Mut$  strain employed) has made it a major asset for the pharmaceutical and biotechnological industries. In addition, this cell factory has some salient advantages such as great thermo-

and osmotolerance, the ability to grow at high cell densities (ca. 100 g L<sup>-1</sup>) in defined media and to efficiently secrete proteins [136,137]

Unlike *S. cerevisiae*, proROL-gene expressed in *K. phaffii* only yielded proROL free lipase. This clearly indicates that Kex2-like protease activity is markedly higher in *K. phaffii* than it is in *S. cerevisiae* [81]. Moreover, rROL-gene was adequately expressed and the supernatant was found to contain the corresponding lipase [87]. Efficiently secreting proROL and rROL and the above-described outstanding properties of *K. phaffii* have made it the most suitable cell factory for heterologous production of ROL [138–141]. In addition, *K. phaffii* produces no endogenous extracellular lipases or esterases [142], which makes ROL downstream work less complex and expensive. On the other hand, using *K. phaffii* as a cell factory requires screening transformed clones and optimizing the operating conditions in order to maximize production, all of which is feasible with facilities like microbioreactors [143].

The inducible alcohol oxidase 1 promoter ( $P_{AOX1}$ ) remains the most widely used in its class for heterologous production of ROL in *K. phaffii* [27]. Ever since the functional expression of rROL under  $P_{AOX1}$  was first reported [87], there have been great endeavors at elucidating the effects of strain phenotypes ( $Mut^S$  or  $Mut^+$ ), gene dosage, coexpression of chaperones to reduce burden stress and certain operational bioprocess strategies [144]. Alternative promoters such as formaldehyde dehydrogenase 1 promoter ( $P_{FLD1}$ ), which can be induced by both methanol as sole carbon and energy source, and methylamine as nitrogen source, have also been used. The primary aim of using promoters other than  $P_{AOX1}$  (e.g.,  $P_{FLD1}$ ) is avoiding or minimizing the need for methanol in the bioprocess for greater safety—methylamine is less volatile and flammable than methanol [145,146]. In addition, though not extensively, the constitutive promoter of glyceraldehyde-3-

phosphate dehydrogenase ( $P_{GAP}$ ) has also been used in ROL production to completely dispense with methanol and methylamine. For instance, Yu *et al.* [76] obtained substantial proROL production levels after engineering the *N*-glycosylation pattern of the prosequence and produce the lipase under the constitutive  $P_{GAP}$ . In fact, production with modified proROL was 218 times greater than with the parent proROL, which demonstrates the ability of rational design of *N*-glycosylation sites to enhance proROL production under the constitutive promoter. The fact that no study appears to have focused on the constitutive expression of rROL (*viz.*, lipase mature sequence) highlights the importance of the ROL prosequence to alleviate the adverse effects of producing ROL mature sequence under  $P_{GAP}$  [76] —the resulting lipase form is harmful to the host cell [77]. In fact, rROL-gene expression has only been accomplished under the inducible  $P_{AOXI}$  [50,147] —inducible promoters are less troublesome than constitutive promoters as regards production of noxious proteins [148].

## 1.6. Industrial uses of *Rhizopus oryzae* lipase

The 1,3-regiospecificity and catalytic flexibility of ROL make it a suitable choice for improving sustainability in the food, pharmaceutical, biopolymer and energy industries [27,32,149]. Therefore, in the following sections, some successful studies in which ROL has been employed for the synthesis of several industrially relevant products will be treated.

### 1.6.1. Biodiesel production

Petroleum depletion and increasing environmental concerns over the last decade have led biodiesel, which essentially consists of monoalkyl esters of long-chain fatty acids, to gain importance as an alternative to fossil fuels by virtue of its being renewable, biodegradable, nontoxic, usable by existing engines, locally producible and carbon-neutral —carbon in biodiesel exhaust is recently fixed from the atmosphere [150,151]. Together with other alternative renewable energy sources, biodiesel can help limit the use of fossil fuels in order to alleviate the adverse impacts of combustion and meet the emission reduction plan established in the Paris Agreement of 2015. In fact, approximately 28% of all energy produced in the world is used for transportation (29% between the 27 countries of the European Union in 2018; Figure 1.8). Therefore, using biodiesel, which can be produced with existing technology, could undoubtedly help mitigate pollutant emissions in this sector [152].

2018 total: 3.8 Gt CO<sub>2</sub>e

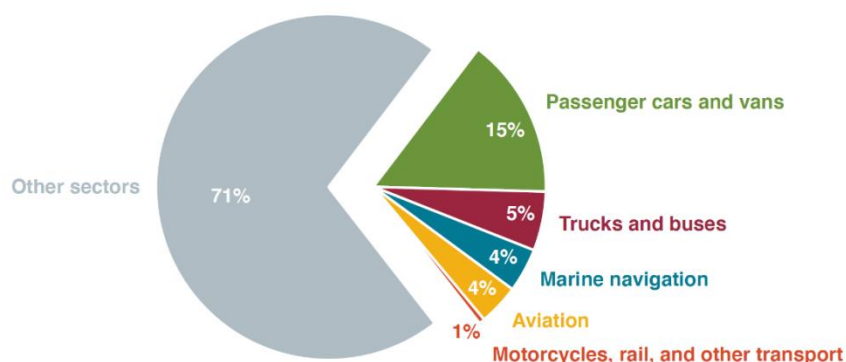


**Figure 1.8.** Greenhouse gas emissions in the EU-27 in 2018. Adapted from [153].

Biodiesel can be classified into three different generations according to source. First-generation biodiesel is produced from edible oils such as soybean or sunflower oils,

use of which may raise the food versus fuel debate (i.e., whether using agricultural land/food for nonnourishing purposes is ethical) [154]. Because first-generation biodiesel is currently the most widely produced and used one, alternative substrates have been sought which have led to the development of second- and third-generation biodiesel. These two are collectively designated “advanced biodiesel” in European Directive 2015/1513 and fostered by public institutions. Second-generation biodiesel is produced from nonedible oils, such as jatropha and makauba, obtained from crops typically grown on agriculturally useless land. Third-generation biodiesel completely avoids ethical issues because it is obtained by using microbial lipids and oily wastes such as oils from microalgae or oleaginous yeasts and waste cooking oils (WCO), respectively [155–158]. There is also fourth-generation biodiesel based on man-made biological tools (viz., genetically modified microorganisms), development of which is still at an incipient research stage [159,160]. Typically, the substrates yielding second- and third-generation biodiesel have increased contents in free fatty acids (FFA) which can make biodiesel production through chemical basic catalysis (i.e. the most commonly employed process at industrial scale) challenging by the need for pretreatments for FFA neutralization to avoid soap formation —the most frequent side-reaction [150,156,161]. In this sense, lipases have emerged as useful alternative catalysts for using milder reaction conditions and less water, simplifying downstream work and, especially, avoiding side reactions like soap formation —which enables the use of substrates with a high FFA content [162,163]. In fact, substrates containing large amounts of FFA are known to expedite enzymatic biodiesel production and to enhance operational stability of the biocatalyst [162,164,165]. A number of lipases from microorganisms such as *Candida rugosa* [166,167], *Aspergillus oryzae* [168,169] and *Burkholderia cepacia* [170,171] have been used for this purpose.



Regiospecificity is crucial trait with a view to making industrial enzyme-based biodiesel production feasible. Nonspecific enzymes produce monoalkyl esters and glycerol—which is an unwanted byproduct of the transesterification reaction that can hinder it or even detract from enzyme stability and complicate downstream work [172]. Conversely, 1,3-regioespecific lipases produce 2-monoacylglycerol—which has lubricating properties and enhances some characteristics of biodiesel— instead of glycerol [173–175]. In addition, monoacylglycerols can increase the cost-effectiveness of potential biodiesel biorefineries as they are more valuable products than is glycerol by virtue of their utility as emulsifiers in the pharmaceutical and food industries [176–178]. The 1,3-regioespecificity of ROL has promoted its exploration as a biocatalyst for biodiesel production.

Even if several studies have employed ROL with edible oils, boosting the ethical issue “food vs fuel”, such as olive [179], rapeseed [180,181], soybean [182–185] and sunflower [186,187] oils—commonly used as model substrates for research— most of the published works have focused on the use of alternative substrates (Table 1.5). Regarding second-generation biodiesel production, *Jatropha curcas* oil is one of the non-edible oils with high potential for the biofuel production, probably due to its easy cultivation process and because it can be found worldwide [188]. Rodrigues *et al.* [151] reported yields close to the theoretical 100%—a real yield of 66% considering ROL 1,3-regioespecificity— and high operational stability of the biocatalysts. In Table 1.5, other studies with promising results using this substrate as well as other non-edible oils yielding second-generation biodiesel like *Pistacia chinensis bge* oil [189], Tung oil [95], *Calophyllum inophyllum* oil [190] and *alperujo* oil (olive pomace oil) [175] can be found.

**Table 1.5.** Summary of biodiesel production methods using *Rhizopus oryzae* lipase as main biocatalyst.

Substrate	Lipase	Immobilization method	Reactor type	Stepwise addition	Biodiesel generation	Yield–Conversion/ Operational stability	Ref.
Olive oil + MeOH	rROL	IA onto ReliZyme™ OD 403M	PBR	Yes	First	Y: PBR 49.1% OS: second batch 44.8%	[179]
Olive oil + MeOH	rROL	IA onto ReliZyme™ OD 403M	STR	Yes	First	Y: STR 33.56% OS: second batch 7.7%	[179]
Rapeseed oil + MeOH	proROL	WCB over agar plate	SLLB	No	First	No biodiesel production	[180]
Rapeseed oil + EtOH	proROL	WCB over agar plate	SLLB	No	First	No biodiesel production	[180]
Rapeseed oil + MeOH	proROL	WCB over agar plate	SGLB	No	First	Y: 58%	[180]
Rapeseed oil + EtOH	proROL	WCB over agar plate	SGLB	No	First	Y: 72%	[180]
Crude canola oil + MeOH	proROL	Free enzymes	BR	Yes	First	Y: 68.56%	[181]
Crude canola oil + MeOH	proROL-CRL	Free enzymes	BR	Yes	First	Y: 84.25%	[181]
Crude canola oil + MeOH	proROL-CRL	CI onto functionalized silica gel	BR	Yes	First	Y: 88.9%	[181]
Soybean oil + MeOH	proROL	WCB immobilized into BSPs	BR	Yes	First	Y: 82.2% OS: nearly all activity lost after 6 cycles	[182]
Soybean oil + MeOH	proROL	CI WCB immobilized onto BSPs	BR	Yes	First	Y: 92.2% OS: no loss of activity after 6 cycles	[182]
Soybean oil + EtOH	proROL	IA onto microporous resin NKA (polystyrene)	BR	Yes	First	Y: 58.5%	[183]

**Table 1.5.** Summary of biodiesel production methods using *Rhizopus oryzae* lipase as main biocatalyst.

Substrate	Lipase	Immobilization method	Reactor type	Stepwise addition	Biodiesel generation	Yield–Conversion/ Operational stability	Ref.
Soybean oil + EtOH	proROL-CRL	IA onto microporous resin NKA (polystyrene)	BR	Yes	First	Y: 80.8%	[183]
Soybean oil + EtOH	proROL-Novozyme 435	proROL: IA onto microporous resin NKA (polystyrene). Novozyme 435: IA onto Lewatit VP OC 1600	BR	Yes	First	Y: 98.5% OS: Y decreased to 78.3% after 20 cycles	[183]
Soybean oil + EtOH	proROL-PFL	IA onto microporous resin NKA (polystyrene)	BR	Yes	First	Y: 55.8%	[183]
Soybean oil + MeOH	proROL	CI onto magnetic chitosan microspheres	MSFBR	Yes	First	Y: 91.3% OS: Y decreased to about 80% after 6 reaction cycles	[184]
Soybean oil + MeOH	proROL	WCB immobilized into BSPs	BR	Yes	First	Y: over 90% OS: Y decreased to 10% after 10 reaction cycles	[185]
Soybean oil + MeOH	proROL	WCB immobilized into BSPs	PBR	Yes	First	Y: over 90% OS: Y decreased to 80% after 10 reaction cycles	[185]
Sunflower oil + EtOH	proROL	CI onto modified sepiolite with <i>p</i> -hydroxybenzaldehyde linker	BR	No	First	C: 84.3% OS: C decreased to 21.4% after 9 cycles	[186]
Sunflower oil + EtOH	proROL	CI onto modified sepiolite with benzylamine–terephthalic aldehyde linker	BR	No	First		[186]

**Table 1.5.** Summary of biodiesel production methods using *Rhizopus oryzae* lipase as main biocatalyst.

Substrate	Lipase	Immobilization method	Reactor type	Stepwise addition	Biodiesel generation	Yield–Conversion/ Operational stability	Ref.
Sunflower oil + EtOH	proROL	IA onto demineralized sepiolite	BR	No	First	Y: 90.2% OS: proROL IA C decreased to 18.1% after 9 cycles	[186]
<i>Pistacia chinensis bge</i> seed oil + MeOH	rROL	CI onto Amberlite IRA-93	BR	Yes	Second	Y: 92% OS: Y decreased to 60% after 8 cycles	[189]
<i>Pistacia chinensis bge</i> seed oil + MeOH	rROL	IA microporous resin HPD-400	BR	Yes	Second	Y: 94% OS: Y decreased to 50% after 8 cycles	[189]
<i>Calophyllum inophyllum</i> linn oil + MeOH	proROL	WCB immobilized into BSPs	PBR	Yes	Second	Y: 92% OS: Y decreased a 4.9% after 6 cycles	[190]
Oil extracted from <i>Nannochloropsis gaditana</i> + MeOH	proROL	WCB	BR	Yes	Third	Y: 83% OS: Y decreased to 71% after 3 cycles	[191]
Oil extracted from <i>Nannochloropsis gaditana</i> + MeOH	proROL	WCB immobilized into BSPs	BR	Yes	Third	Y: 70% OS: Y decreased to 43% in the scond cycle	[191]
Oil extracted from <i>Nannochloropsis gaditana</i> + MeOH	proROL	WCB immobilized into BSPs	BR	Yes	Third	Y: 83% OS: Y decreased to 71% after 3 cycles	[192]
Oil extracted from <i>Nannochloropsis gaditana</i> + MeOH	proROL	WCB	TPB	No	Third	Y: 58%	[193]
Oil extracted from <i>Nannochloropsis gaditana</i> + EtOH	proROL	WCB	TPB	No	Third	Y: 92%	[193]

**Table 1.5.** Summary of biodiesel production methods using *Rhizopus oryzae* lipase as main biocatalyst.

Substrate	Lipase	Immobilization method	Reactor type	Stepwise addition	Biodiesel generation	Yield–Conversion/ Operational stability	Ref.
Oil extracted from <i>Botryococcus braunii</i> + MeOH	proROL	WCB	TPB	No	Third	Y: 58%	[193]
Oil extracted from <i>Botryococcus braunii</i> + EtOH	proROL	WCB	TPB	No	Third	Y: 68%	[193]
Oil extracted from <i>Chlorella vulgaris</i> + MeOH	proROL	Free enzyme	BR	Yes	Third	C: 75%	[194]
Oil extracted from <i>Chlorella vulgaris</i> + MeOH	proROL	IA onto MNP	BR	Yes	Third	C: 46% OS: decreased to 10% after 5 cycles	[194]
Oil extracted from <i>Chlorella vulgaris</i> + MeOH	proROL	CI onto AP modified MNP	BR	Yes	Third	C: 53% OS: C decreased to 25% after 5 cycles	[194]
Oil extracted from <i>Chlorella vulgaris</i> + MeOH	proROL	CI onto AP-GA modified MNP	BR	Yes	Third	C: 69.8% OS: C decreased to 45% after 5 cycles	[194]
Sludge palm oil + MeOH	proROL	IE into alginate-polyvinyl alcohol beads	BR	No	Third	Y: 91.30% OS: no activity loss after 15 cycles	[195]
Oil extracted from spent coffee ground + MeOH	<i>R. delemar</i> (= <i>oryzae</i> ) lipase	Free enzyme	BR	No	Third	Y: 18%	[196]
WCO + MeOH	proROL	Free enzyme	BR		Third	Y: 93%	[197]
WCO + iso-propanol	proROL	Free enzyme	BR		Third	Y: 86.8%	[197]

**Table 1.5.** Summary of biodiesel production methods using *Rhizopus oryzae* lipase as main biocatalyst.

Substrate	Lipase	Immobilization method	Reactor type	Stepwise addition	Biodiesel generation	Yield–Conversion/ Operational stability	Ref.
WCO + iso-butanol	proROL	Free enzyme	BR		Third	Y: 80.2%	[197]
WCO + iso-amyl alcohol	proROL	Free enzyme	BR		Third	Y: 64%	[197]
WCO + MeOH	proROL	WCB IE into calcium alginate beads	BR		Third	Y: 84%	[197]
WCO + iso-propanol	proROL	WCB IE into calcium alginate beads	BR		Third	Y: 71%	[197]
WCO + iso-butanol	proROL	WCB IE into calcium alginate beads	BR		Third	Y: 62%	[197]
WCO+ iso-amyl alcohol	proROL	WCB IE into calcium alginate beads	BR		Third	Y: 43%	[197]
Jatropha MeOH	oil + proROL	WCB IE into sodium alginate beads	BR	No	Second	Y: 80.5% OS: Y decreased to 61.5% after 6 cycles	[198]
Karanja MeOH	oil + proROL	WCB IE into sodium alginate beads	BR	No	Second	Y: 78.3% OS: Y decreased to 63.4% after 6 cycles	[198]
Soybean MeOH	oil + proROL	WCB	BR	Yes	First	Y: 80% OS: Y decreased to 18% after 3 cycles	[199]
Soybean MeOH	oil + proROL	WCB immobilized into BSPs	BR	Yes	First	Y: 82% OS: Y decreased to 10% after 10 cycles	[199]
Soybean MeOH	oil + proROL	CI WCB immobilized into BSPs	BR	Yes	First	Y: 74% OS: Y decreased to 65% after 35 cycles	[199]
Soybean MeOH	oil + proROL	WCB immobilized into BSPs	BR	Yes	First	Y: 82% OS: Y decreased to 48% after 6 cycles	[200]
Soybean MeOH	oil + proROL	CI WCB immobilized into BSPs	BR	Yes	First	Y: 80% OS: Y decreased to 70% after 6 cycles	[200]

**Table 1.5.** Summary of biodiesel production methods using *Rhizopus oryzae* lipase as main biocatalyst.

Substrate	Lipase	Immobilization method	Reactor type	Stepwise addition	Biodiesel generation	Yield–Conversion/ Operational stability	Ref.
Alperujo oil + MeOH	rROL	IA onto rice husk	BR	Yes	Second		[201]
Alperujo oil + MeOH	rROL	IA onto ReliZyme™ OD403	BR	Yes	Second	Y: 64.5% OS: Y decreased to 41.3% after 7 cycles	[201]
Crude microbial oil from <i>Candida</i> sp. LEB-M3 + MeOH	rROL	IA onto ReliZyme™ OD403	BR	Yes	Third	Y: 38% OS: Y decreased to 26.6% after 7 cycles	[202]
Neutralized microbial oil from <i>Candida</i> sp. LEB-M3 + MeOH	rROL	IA onto ReliZyme™ OD403	BR	Yes	Third	Y: 38%	[202]
Olive oil + MeOH	rROL	IA onto ReliZyme™ OD403	BR	Yes	First	Y: 54.3% OS: Y decreased to 40% after 7 cycles	[202]
Oleic fatty acid + MeOH	rROL	IA onto ReliZyme™ OD403	BR	Yes	First	Y: 68%	[202]
Rapeseed oil + EtOH	proROL	IA onto microporous resin NKA	BR	No	First	Y: above 98% OS: Y decreased to 60% after 10 cycles	[203]
Jatropha oil + MeOH	proROL-CRL	WCB (proROL) and free enzyme (CRL) IE into sodium alginate beads	PBR	No	Second	Y: 84.2%	[204]
Karanja oil + MeOH	proROL-CRL	WCB (proROL) and free enzyme (CRL) IE into sodium alginate beads	PBR	No	Second	Y: 81%	[204]
WCO + MeOH	proROL	WCB IE into sodium alginate beads	BR	No	Third	Y: 94.01%	[205]

**Table 1.5.** Summary of biodiesel production methods using *Rhizopus oryzae* lipase as main biocatalyst.

Substrate	Lipase	Immobilization method	Reactor type	Stepwise addition	Biodiesel generation	Yield–Conversion/ Operational stability	Ref.
WCO + Methyl acetate	proROL	WCB IE into sodium alginate beads	BR	No	Third	Y: 91.11%	[205]
WCO + Ethyl acetate	proROL	WCB IE into sodium alginate beads	BR	No	Third	Y: 90.06	[205]
WCO + MeOH	proROL	IE into sodium alginate beads	BR	No	Third	Y: 83%	[205]
WCO + Methyl acetate	proROL	IE into sodium alginate beads	BR	No	Third	Y: 80%	[205]
WCO + Ethyl acetate	proROL	IE into sodium alginate beads	BR	No	Third	Y: 78%	[205]
Oil extracted from <i>Chlorella vulgaris</i> + MeOH	proROL	IA into MNP	BR	Yes	Third	Y: 45% OS: Y decreased to 10% after 5 cycles	[206]
Oil extracted from <i>Chlorella vulgaris</i> + MeOH	proROL	IA into MGO	BR	Yes	Third	Y: 51% OS: Y decreased to 16% after 5 cycles	[206]
Oil extracted from <i>Chlorella vulgaris</i> + MeOH	proROL	IA into MGO-AP	BR	Yes	Third	Y: 54% OS: Y decreased to 25% after 5 cycles	[206]
Oil extracted from <i>Chlorella vulgaris</i> + MeOH	proROL	CI into MGO-AP-GA	BR	Yes	Third	Y: 68% OS: Y decreased to 58.77% after 5 cycles	[206]
Cottonseed oil + MeOH	proROL	WCB immobilized into BSPs	BR	Yes	First	Y: 27.9%	[207]
Rubber seed oil + MeOH	proROL	Free enzyme	BR	Yes	Second	Y: 31%	[208]



**Table 1.5.** Summary of biodiesel production methods using *Rhizopus oryzae* lipase as main biocatalyst.

Substrate	Lipase	Immobilization method	Reactor type	Stepwise addition	Biodiesel generation	Yield–Conversion/ Operational stability	Ref.
Rubber seed oil + Ethyl acetate	proROL	Free enzyme	BR	No	Second	Y: 33.3%	[208]
Soybean oil + MeOH	proROL-CRL	CI onto silica gel pretreated with AP and GA	BR	Yes	First	Y: 99.99% OS: Y decreased to 85% after 20 cycles	[209]
Rapeseed oil deodorizer distillate + MeOH	proROL	Free enzyme	BR	Yes	First	Y: 93.07%	[210]
Rapeseed oil deodorizer distillate + MeOH	proROL-CRL	Free enzyme	BR	Yes	First	Y: 98.16%	[210]
Alperujo oil + MeOH	rROL	CI onto ET, AP and GA pretreated ReliZyme™ HFA403	BR	Yes	Second	Yield: 57.16% OS: Y decreased a 12.31% after 5 cycles	[175]
Alperujo oil + EtOH	rROL	CI onto ET, AP and GA pretreated ReliZyme™ HFA403	BR	Yes	Second	Y: 60.25% OS: Y decreased a 11.89% after 7 cycles	[175]
Triolein + MeOH	rROL	Free enzyme	BR	No	First	Y: 71.2%	[131]
Triolein + EtOH	rROL	Free enzyme	BR	No	First	Y: 64.2%	[131]
Triolein + MeOH	rROL	IA onto RelyZyme™ OD403S	BR	No	First	Y: 82.6%	[131]
Triolein + EtOH	rROL	IA onto RelyZyme™ OD403S	BR	No	First	Y:100.7%	[131]
Jatropha oil + MeOH	rROL	IA onto Lewatit VP OC 1600	BR	Yes	Second	Y: 61% OS: Y decreased a 40% after 10 cycles	[211]
Jatropha oil + MeOH	rROL	IA onto Lifetech™ ECR1030M	BR	Yes	Second	Y: 63% OS: Y decreased a 40% after 10 cycles	[211]

**Table 1.5.** Summary of biodiesel production methods using *Rhizopus oryzae* lipase as main biocatalyst.

<b>Substrate</b>	<b>Lipase</b>	<b>Immobilization method</b>	<b>Reactor type</b>	<b>Stepwise addition</b>	<b>Biodiesel generation</b>	<b>Yield–Conversion/ Operational stability</b>	<b>Ref.</b>
Jatropha oil + MeOH	rROL	IA onto Lifetech™ AP1090M	BR	Yes	Second	Y: 55% OS: Y decreased a 25% after 10 cycles	[211]
Jatropha oil + MeOH	rROL	CI onto Lifetech™ ECR8285M	BR	Yes	Second	Y: 63% OS: Y decreased a 60% after 10 cycles	[211]
Jatropha oil + MeOH	rROL	CI onto Amberlita IRA 96	BR	Yes	Second	Y: 68% OS: Y decreased a 20% after 10 cycles	[211]
Olive oil + MeOH	prorROL	IA onto Amberlite XAD 761	BR	No	First	Y: 77%	[212]
Olive oil + EtOH	prorROL	IA onto Amberlite XAD 761	BR	No	First	Y: 62%	[212]
Olive oil + Propanol	prorROL	IA onto Amberlite XAD 761	BR	No	First	Y: 46%	[212]
Olive oil + Butanol	prorROL	IA onto Amberlite XAD 761	BR	No	First	Y: 18%	[212]
Soybean oil + MeOH	prorROL	IA onto Amberlite XAD 761	BR	No	First	Y: 50%	[212]
Soybean oil + EtOH	prorROL	IA onto Amberlite XAD 761	BR	No	First	Y: 46%	[212]
Soybean oil + Propanol	prorROL	IA onto Amberlite XAD 761	BR	No	First	Y: 35%	[212]
Soybean oil + Butanol	prorROL	IA onto Amberlite XAD 761	BR	No	First	Y: 10%	[212]
Canola oil + MeOH	prorROL	IA onto Amberlite XAD 761	BR	No	First	Y: 70%	[212]
Canola oil + EtOH	prorROL	IA onto Amberlite XAD 761	BR	No	First	Y: 56%	[212]

**Table 1.5.** Summary of biodiesel production methods using *Rhizopus oryzae* lipase as main biocatalyst.

<b>Substrate</b>	<b>Lipase</b>	<b>Immobilization method</b>	<b>Reactor type</b>	<b>Stepwise addition</b>	<b>Biodiesel generation</b>	<b>Yield–Conversion/ Operational stability</b>	<b>Ref.</b>
Canola oil + Propanol	prorROL	IA onto Amberlite XAD 761	BR	No	First	Y: 43%	[212]
Canola oil + Butanol	prorROL	IA onto Amberlite XAD 761	BR	No	First	Y: 16%	[212]
Sunflower oil + MeOH	prorROL	IA onto Amberlite XAD 761	BR	No	First	Y: 32%	[212]
Sunflower oil + EtOH	prorROL	IA onto Amberlite XAD 761	BR	No	First	Y: 28%	[212]
Sunflower oil + Propanol	prorROL	IA onto Amberlite XAD 761	BR	No	First	Y: 17%	[212]
Sunflower oil + Butanol	prorROL	IA onto Amberlite XAD 761	BR	No	First	Y: 7%	[212]
Algal oil + MeOH	prorROL	IA onto Amberlite XAD 761	BR	No	Third	Y: 63%	[212]
Algal oil + EtOH	prorROL	IA onto Amberlite XAD 761	BR	No	Third	Y: 55%	[212]
Algal oil + Propanol	prorROL	IA onto Amberlite XAD 761	BR	No	Third	Y: 40%	[212]
Algal oil + Butanol	prorROL	IA onto Amberlite XAD 761	BR	No	Third	Y: 13%	[212]
Alperujo MeOH	rROL	CI onto AP and GA treated ReliZyme™ HFA403	BR	Yes	Second	Yield: 28.62% Op. stability: Y decreased a 43% after 9 cycles	[164]
Jatropha oil + MeOH	proROL	WCB immobilized into BSPs	BR	Yes	Second	Y: 88.6% OS: Y decreased a 21% after 6 cycles	[213]
Oleic acid + MeOH	proROL	WCB immobilized into BSPs	BR	No	First	Y: 80% OS: nearly no activity loss after 8 cycles	[214]

**Table 1.5.** Summary of biodiesel production methods using *Rhizopus oryzae* lipase as main biocatalyst.

<b>Substrate</b>	<b>Lipase</b>	<b>Immobilization method</b>	<b>Reactor type</b>	<b>Stepwise addition</b>	<b>Biodiesel generation</b>	<b>Yield–Conversion/ Operational stability</b>	<b>Ref.</b>
Rice bran oil + MeOH	proROL	IA onto rod-like mesoporous silica	BR	No	First	Y: 81.7% OS: Y decreased to 67.7% after 3 cycles	[215]
Jatropha oil + MeOH	proROL	IE into polyvinyl alcohol – alginate matrix	BR	No	Second	Yield: 87.1%	[216]
Alperujo oil + MeOH	rROL	IA Octadecyl-Sepabeads	BR	Yes	Second	Yield: 58.31% OS: Y decreased to 54.67% after 2 cycles	[217]
Tung oil + MeOH	proROL	CI onto Amberlite IRA 93	BR	Yes	Second	Yield: 91.9% OS: Y decreased to 85.1% after 6 cycles	[95]
Babassu oil + EtOH	proROL	WCB immobilized into BSPs	BR	No	First	Yield: 74.15%	[218]

Third-generation biodiesel has so far been obtained from microalgal and waste oils mostly (Figure 1.9). The former makes biodiesel production more environmentally friendly as microalgae fixate atmospheric CO<sub>2</sub> during oil production and also, they can use domestic wastewater like growth substrate facilitating its posterior treatment. By contrast, using microalgal oil requires scaling-up photobioreactors and challenging processes of fat extraction [219,220]. In any case, ROL has been successfully used with this type of substrate, for instance, with oils extracted from *Nannochloropsis gaditana* [191–193], *Botryococcus braunii* [193] and *Chlorella vulgaris* [194]. In fact, with the latter ROL afforded conversions of fatty acid methyl esters (FAME) exceeding 70%, which testifies to its suitability for biodiesel production from microalgal oils. Additionally, oils extracted from oleaginous yeasts such as *Candida* sp. LEB-M3 have also been used for this purpose. Yeasts can in fact be highly useful for biodiesel refineries as they can successfully grow in glycerol formed in the biofuel production process (Figure 1.9) [202].

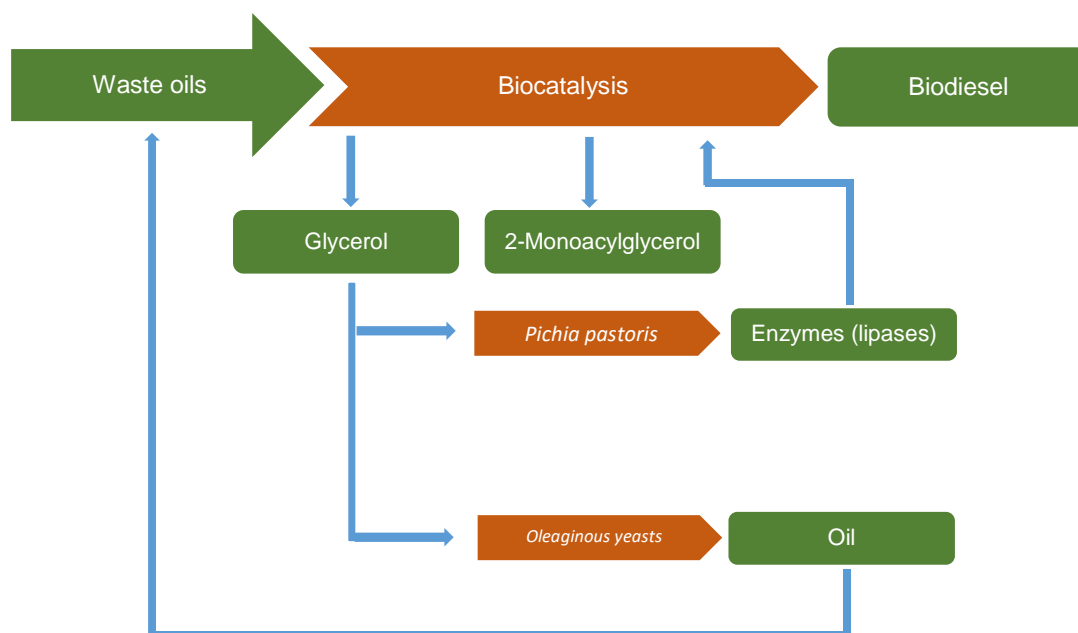


**Figure 1.9.** Flow chart for the use of waste oils to obtain third-generation biodiesel under the principles of circular economy.

Waste oils hold considerable potential for the biodiesel industry on account of their relevance to circular economy strategies, which aim at avoiding waste or finding new uses for it [221,222]. Also, tight economic competition between biodiesel and fossil fuels has raised the need for new, inexpensive raw materials. In fact, feedstocks account for more than the 70% of the total cost of producing biodiesel. Oily wastes can help reduce this proportion and make enzymatic biodiesel production feasible [223]. Sludge from palm oil [195] and spent coffee grounds [196] are amongst the oily wastes explored for biodiesel production with ROL. However, waste cooking oil (WCO) is the foremost substrate in this category, not only because it is inexpensive, but also because it dispenses with the need for costly disposal to public institutions [224,225]. In fact, WCO has provided revealing results in this context. Thus, Bharathiraja *et al.* [197] achieved triglyceride conversions up to 94%. However, few studies have so far examined the processing of WCO with ROL despite the high potential of the former as a substrate for the biodiesel industry—a likely research target for future projects.

The operational stability, reusability and cost of biocatalysts are mutually related; also, they are crucial traits to be considered for enzymatic biodiesel production owing to the typically high cost of enzymes and the tight economic competition of biodiesel with conventional diesel. Enzyme production costs can be reduced by using heterologous expression, as described in the previous section, but also by immobilization onto an appropriate support. This method allows enzymes to be reused and usually enhances their stability [17,226,227]. Below are described existing approaches to immobilizing ROL for biodiesel production.

Early attempts at using ROL in biodiesel syntheses involved whole-cell biocatalysts (WCB) mainly. Thus, the enzyme was confined in its natural cellular

environment to protect lipase from inactivation and degradation. This lowered costs considerably as no downstream work on the biocatalyst was needed [228]. Syed *et al.* [198] immobilized lipase-producing *R. oryzae* cells in alginate beads and used them to obtain biodiesel from jatropha and karanja oils. They used a response surface-based optimization strategy and obtained a biodiesel yield of 73.5% from jatropha oil, and one of 72.5% from karanja oil, under optimal conditions. Also, they assessed the biocatalyst for operational stability and found it to lose only 20% after 6 cycles. Even though they could have used free, unimmobilized cells, for biodiesel production, Sun *et al.* [199] used immobilization of cells to avoid enzyme leakage and denaturation. They immobilized *R. oryzae* fungal cells onto biomass support particles (BSP) and achieved a higher operational stability than with free cells. In order to further reduce enzyme leakage and deactivation, they used the crosslinking agent glutaraldehyde to treat previously immobilized cells. The crosslinked biocatalyst resulted in higher FAME yields and operational stability. Similarly, Ban *et al.* [200] succeeded in stabilizing WCB by treatment with glutaraldehyde —the so-called WCB stabilization. He *et al.* [182] followed the same approach to obtain a ROL based biocatalyst with increased operational stability capable of retaining more than 90% of its initial activity after 6 reaction cycles. However, WCB were more complicated to reuse and resulted in lower conversion rates than did free lipases immobilized onto acrylic resins [228]. For instance, Bharathiraja *et al.* [197] found WCB to exhibit poorer reaction rates than immobilized purified proROL owing to diffusional problems. The previous drawbacks, and progress in heterologous ROL production, have fostered the use of free and immobilized ROL for biodiesel synthesis.

Lipases have usually been immobilized by adsorption, especially onto hydrophobic supports (typically an acrylic resin with hydrophobic surface groups such as octadecyl or divinylbenzene) on the grounds of the presence of a large hydrophobic patch around the catalytic triad facilitating immobilization and hyperactivation of lipases [229,230]. However, the highly nonpolar reaction media used in enzyme-based biodiesel production can result in desorption or leakage of the enzyme, and hence in poor operational stability of the biocatalyst [113]. Nevertheless, some authors have obtained outstanding stability results by using this ROL immobilization method. For instance, Bonet-Ragel *et al.* [201] found biocatalysts to retain more than the 60% of their initial activity after 6 consecutive reaction cycles, and Duarte *et al.* [202] and Su *et al.* [203] subsequently obtained similar results. Some authors avoid enzyme leakage when using an adsorption technique by treating the biocatalyst with a crosslinking agent, such as glutaraldehyde, as previously described for WCB [189,231].

Notwithstanding the previous studies and others listed in Table 1.5, entrapment and covalent immobilization continue to be the most common methods for anchoring ROL to a support. As noted earlier, entrapment has been used not only with free ROL but also with WCB by virtue of the simplicity, expeditiousness and economy of the method [232]. The most common ROL entrapment methods use polyvinyl alcohol (PVA) and alginate [204,205,216,233]. Muanruksa *et al.* [195] obtained outstanding results with free proROL immobilized in alginate–PVA beads. Thus, esterification exceeded 90% and the biocatalyst lost virtually no activity after 15 reaction cycles.

Because the binding forces of lipase covalently immobilized onto a support are strong, the enzyme tends to exhibit a high stability in addition to high tolerance of extreme pH values and temperatures, and almost no leakage. However, the strong links between



enzyme and support, and the harsh conditions typically used for immobilization, can have an adverse impact on enzymatic activity [234–236]. In any case, some authors have successfully used this method to immobilize lipases for biodiesel production. Thus, Nematian *et al.* [206] immobilized proROL onto a superparamagnetic nanostructure to obtain three different biocatalysts. Two were based on lipase–support electrostatic interactions and the third on covalent bonding. Covalently immobilized proROL exhibited the highest conversions and operational stability. Bonet-Ragel *et al.* [175] immobilized rROL covalently onto glutaraldehyde pretreated epoxide polymethacrylate resins, and examined its performance and operational stability in biodiesel syntheses with methanol and ethanol as acyl acceptors. The optimum operational conditions provided yields close to the theoretical 100% after 360 min with methanol and 260 min with ethanol. Also, no significant loss of activity was observed after 5 consecutive reaction cycles with either alcohol. Luna *et al.* [186] obtained similar operational stability results with ethanol and sunflower oil as substrate. Covalent immobilization is therefore an effective choice for biodiesel synthesis with ROL.

Although ROL has proved an industrially suitable, solvent-tolerant enzyme, some biodiesel synthesis operational strategies have provided especially increased reaction yields and enzyme stability or allowed easier scaling-up of the bioprocess. One of the most commonly used approaches adds the alcohol stepwise to prevent it from deactivating the enzyme, as the interaction between the lipase and the alcohol is the main enzyme deactivating factor [237,238]. The alcohol stepwise addition strategy has been successfully used by some authors with ROL [175,207]; others, have sought the best acyl acceptor (*viz.*, that with the least adverse effects on the enzyme) from among different alcohols [197,233] —or even short esters of the alcohols performing in these cases

interesterification reaction [205,208]. In this sense, solvent-free systems have recently emerged as interesting operational choices to minimize biodiesel downstream work while avoiding the need for hazardous solvents, thus making the overall biotransformations more cost-effective and environmentally friendly [164,201,208,211].

Lately, 1,3-regiospecific and nonspecific lipases have been jointly used to increase biodiesel reaction rates and yields [181]. Thus, Lee *et al.* [209] obtained near-quantitative yields after 2 h reaction and very high operational stability by using proROL and *Candida rugosa* lipase (CRL) in combination. In fact, the conversion yield was still as high as 85% after 20 reaction cycles. In line with these results, Zeng *et al.* [210] obtained higher biodiesel yields and production rates with the proROL–CRL combination than with the two lipases separately.

Another important point to carry out an efficient and cost-effective production of biodiesel is the scale-up of the process. Canet *et al.* [179] compared the performance of a packed bed reactor (PBR) with that of a stirred tank reactor (STR) with a view to scaling-up biodiesel production with rROL immobilized by hydrophobic adsorption. Reaction rates were higher with the STR, but the enzyme operational stability was greater with the PBR. Other authors have used PBR [185,190,204] or even more genuine alternatives such as magnetically stabilized fluidized bed reactors [184] or three-phase bioreactors [180]. There have, however, been few attempts at scaling up biodiesel production with ROL for such a vast amount of research conducted on this biocatalyst.

### ***1.6.2. Production of structured lipids***

As major sources of energy, essential fatty acids, fats and oils are usual ingredients of daily diets. Their functional, nutritional and sensory properties depend on their composition in saturated and polyunsaturated fatty acids, the chain length of the acids and their distribution into the triacylglycerols (TAG) (position *sn*-1, *sn*-3 or *sn*-2). Therefore, modifying the composition of fatty acids or their profile can be useful to obtain lipids with improved properties (so-called “structured lipids”, SL). There are various types of commercially available SL, all with well-known properties (Table 1.6.), namely: (a) low-calorie and dietetic triacylglycerols including TAG with medium chains (MMM) and others with short- and medium-chain fatty acids in *sn*-1 and *sn*-3 positions and long-chain fatty acids in *sn*-2 (SLS and MLM, respectively); (b) human milk fat substitutes (HMFS); (c) cocoa butter equivalents (CBE); (d) *trans*-free plastic fats; (e) triacylglycerols rich in specific long-chain and polyunsaturated fatty acids (PUFA); and, more recently, (f) diacylglycerols (DAG) and monoacylglycerols (MAG) have been also considered as SLs [239,240].

**Table 1.6.** Definition and properties of the main commercially relevant structured lipids.

SL type	Definition	Properties	Ref.
Low-calorie and dietetic TAG	TAG with a lower caloric value than conventional oils and fats Include SLS, MLM and MMM type TAG	M and S fatty acids have lower caloric values than do their L counterparts M fatty acids are less prone to accumulate Released M fatty acids can be directly absorbed and provide ready energy in the liver	[239–242]
Human milk fat substitutes (HMFS)	Mimic the fatty acid profile of human milk Contain oleic (30–35%), palmitic (20–30%), linoleic (7–14%) and stearic acids (5.7–8%) Palmitic acid mainly at <i>sn</i> -2 position	Promote palmitic acid absorption as 2-monoacylpalmitate Promote calcium absorption	[239,240, 243–245]
Cocoa butter equivalents (CBE)	Mimic the scarce natural cocoa butter Mainly formed by saturated fatty acids at <i>sn</i> -1,3 (stearic and palmitic) and monounsaturated fatty acids (oleic) at <i>sn</i> -2	The desirable polymorph is the $\beta$ form Similar to cocoa butter in sensory properties	[239,240, 246,247]
<i>Trans</i> -free plastic fats	Mimic <i>trans</i> fatty acids contained in hydrogenated vegetable oils	Avoid potential cardiovascular diseases caused by <i>trans</i> fatty acids	[240,248, 249]
TAG rich in specific long-chain and polyunsaturated fatty acids (PUFA)	Modified TAG containing a combination of n-3 and n-6 PUFA to enhance nutritional values Eicosapentaenoic (EPA) and docosahexaenoic acid (DHA) mainly	EPA reduces blood viscosity and platelet aggregation, and promotes vasodilation. DHA promotes sensorial and neural maturation in infants	[239,250]
MAG and DAG	Modified lipids containing one or two fatty acids linked to a glycerol	Nonionic surfactants useful as emulsifiers for the food industry 1,3-DAG reduces serum TAG levels and suppresses accumulation of body fat	[176,178, 240,251]

Although structured lipids can be obtained under chemical or enzymatic catalysis, the latter choice has some advantages [252]. Thus, similarly to biodiesel syntheses, enzyme-catalyzed SL syntheses can be conducted under milder reaction conditions to reduce energy consumption; also, and specifically important in this case, they allow the original attributes of substrates and products, which are mainly temperature-sensitive, to be better preserved, and avoid the use of deleterious solvents, thereby enabling a more environmentally friendly and safer food production. In any case, the most salient advantage of using lipases to synthesize SL is their high specificity and selectivity [253,254]. Thus, 1,3-regiospecific lipases such as ROL, have aroused keen interest as they regiospecifically modify the *sn*-1 and *sn*-3 positions of TAG—even though non-enzymatic acyl migration phenomena might occur depending on reaction conditions.

Table 1.7 compiles recent reports of SL syntheses using ROL. As can be seen, Nunes *et al.* [255] obtained MLM-type SL by acidolysis of olive oil with capric and caprylic acids. They used rROL produced in *K. phaffii* and commercially available native ROL (proROL), both covalently immobilized onto either Eupergit<sup>®</sup> C or modified Sepiolite. Interestingly, rROL performed better than the native lipase as regards incorporation of capric or caprylic acid, and of operational stability. In spite of using pure or commercial substrates, oily wastes or even unprofitable oils are also useful to obtain MLM-type SL with ROL. For instance, Mota *et al.* [256] obtained low-calorie SL of the MLM-type by using oil extracted from spent coffee grounds and olive pomace in combination with proROL immobilized onto magnetic nanoparticles. Similarly, Costa *et al.* [257] synthesized MLM-type SL with oil from *Vitis vinifera* L. grapeseeds—a byproduct of the wine industry. Instead of oil waste, Nagao *et al.* [258] used oil from the oleaginous microorganism *Mortierella alpina* to obtain MLM rich in arachidonic acid, which is a precursor of various hormones.

**Table 1.7.** Summary of structured lipid production methods using *Rhizopus oryzae* lipase as main biotcatalyst.

Product	Substrates	Reaction type	Lipase	Immobilization method	ID/OS	Ref.
MLM	OO + CRA	Acidolysis	proROL/ rROL	CI onto Eupergit®C/Sepiolite (AlPO <sub>4</sub> -sepiolite)	ID: 21.6%. OS: half-life 159 h	[255]
MLM	OO + CA	Acidolysis	proROL/ rROL	CI onto Eupergit®C/Sepiolite (AlPO <sub>4</sub> -sepiolite)	ID: 34.82%. OS: half-life 136 h	[255]
MLM	SCG + CA	Acidolysis	proROL	CI onto GA treated MNP	ID: 50%	[256]
MLM	SCG + ethyl caprate	Interesterification	proROL	CI onto GA treated MNP	ID: 26%	[256]
MLM	OP + CA	Acidolysis	proROL	CI onto GA treated MNP	ID: 51% OS: 6.8 batches	[256]
MLM	OP + ethyl caprate	Interesterification	proROL	CI onto GA treated MNP	ID: 46%. OS: 9.1 batches	[256]
MLM	Grapeseed oil + CRA	Acidolysis	rROL	CI onto Amberlite IRA 96	ID: 54%. OS: half-life 166 h	[257]
MLM	Grapeseed oil + CA	Acidolysis	rROL	CI onto Amberlite IRA 96	ID: 69% OS: half-life 118 h	[257]
MLM	TGA58F + CA	Acidolysis	proROL	IA onto Dowex WBA	ID: 64.6%	[258]
MLM	TGA40 + CA	Acidolysis	proROL	IA onto Dowex WBA	ID: 62.8%	[258]
MLM	TGA55E + CA	Acidolysis	proROL	IA onto Dowex WBA	ID: 64.8% OS: 90 days in PBR <sup>1</sup> dropped 10%	[258]
MLM	OO + CRA	Acidolysis	rROL	CI onto Eupergit®/Lewatit VP OC 1600	OS: half time 2.4 batches (54.3 h) with Eupergit®C	[259]
MLM	OO + CA	Acidolysis	rROL	CI onto Eupergit® C/Lewatit VP OC 1600	OS: half time 10.2 batches (234 h) with Lewatit VP OC 1600	[259]
MLM	OO + CRA	Acidolysis	rROL	CI onto Eupergit® C	ID: 15.5%	[260]
MLM	OO + CA	Acidolysis	rROL	CI onto Eupergit® C	ID: 33.3%	[260]
MLM	OO + CRA	Acidolysis	rROL	CI onto Amberlite IRA 96	ID: 76.9	[261]
MLM	OO + CA	Acidolysis	rROL	CI onto Amberlite IRA 96	ID: 85.6%	[261]
HMFS	PA enriched TAG + OA enriched mixtures	Acidolysis	proROL	IA onto Accurel® MP-1000	ID: OA in <i>sn</i> -1,3 67.2% – PA in <i>sn</i> -2 67.8%. OS: no activity loss after 10 uses (190 h)	[262]
HMFS	Lard + FFA from EPAX 1050TG	Acidolysis	rROL	CI onto Accurel® MP-1000	ID: 24 mol%. OS: 55% of initial activity after 4 batches	[263]

**Table 1.7.** Summary of structured lipid production methods using *Rhizopus oryzae* lipase as main biotcatalyst.

Product	Substrates	Reaction type	Lipase	Immobilization method	ID/OS	Ref.
HMFS	Tripalmitin + FFA from camelina oil	Acidolysis	rROL	IA onto Relizyme™ OD403 CI onto Lewatit VP OC 1600	ID: 52%	[264]
HMFS	Tripalmitin + OA	Acidolysis	rROL	CI onto Accurel® MP-1000 / Lewatit VP OC 1600 / Eupergit® C	ID: 30% OS: 60% of initial activity after 8 cycles	[265]
TAG rich in PUFA	Cod liver + tuna oil + ethanol	Alcoholysis	proROL	IA onto Accurel® MP-1000	Alcoholysis ID: 72% OS: complete deactivation after 6 cycles	[266]
	2-MAG from alcoholysis + CRA	Esterification	proROL	IA onto Accurel® MP-1000	ID: 95%. OS: no activity loss after 5 cycles	[266]
TAG rich in PUFA	Tuna oil + CRA	Acidolysis	proROL	IA onto Accurel® MP-1000	OS: over one week	[267]
TAG rich in PUFA	Cod liver oil + 96% ethanol	Alcoholysis	proROL	IA onto Accurel® MP-1000	Alcoholysis Y: 78%. OS: 57% decrease after 3 cycles	[268]
	Cod liver oil + 1-butanol	Alcoholysis	proROL	IA onto Accurel® MP-1000	Alcoholysis Y: 78%. OS: no activity decrease after 3 cycles	[268]
	Esterification: 2-MAG from alcoholysis + CRA	Esterification	proROL	IA onto Accurel® MP-1000	Esterification Y: 71%.	[268]
TAG rich in PUFA	Fish oil + CRA	Acidolysis	proROL	Nonimmobilized	ID: 2.5%	[269]
HMFS	Milk fat + soybean oil	Interesterification	proROL	EI into polysiloxane-PVA	ID: 8.14%. OS: no activity loss after 10 batches	[270]
CBE	SO + SA-PA mixtures	Acidolysis	proROL	IA onto Accurel® MP-1000		[271]

Regarding HMFS, Esteban *et al.* [262] used various commercial lipases including proROL immobilized onto Accurel<sup>®</sup> MP-1000 to obtain a TAG rich in palmitic acid in *sn*-2 and oleic acid in *sn*-1,3; (viz., so-called “OPO”, which is the main TAG component of human milk). proROL proved the best choice as regards oleic acid incorporation and operational stability—it lost almost no activity after 10 reaction cycles. Simões *et al.* [263] also used various lipases for HMFS production and found rROL immobilized onto Accurel<sup>®</sup> MP-1000 to perform similarly to Novozymes 435 and Lipozyme RM IM in the acidolytic reaction between lard and an FFA mixture from fish oil rich in docosahexaenoic acid. Faustino *et al.* [264] used rROL from *K. phaffii* immobilized onto two different supports (Lewatit VP OC 1600 and Relizyme OD403/S) to obtain HMFS rich in polyunsaturated fatty acids (PUFA). The acidolysis reaction was performed in a solvent-free system consisting of tripalmitin and FFA (linoleic and linolenic acid, mainly) from camelina oil, which proved a good source of PUFA. The results obtained with rROL immobilized onto Lewatit VP OC 1600 were comparable with those provided by the widely used commercial lipase Lipozyme RM IM.

Triacylglycerols rich in long-chain and polyunsaturated fatty acids have also been produced with ROL, mostly in two steps in order to minimize acyl migration [272]. In the first step, an alcoholysis reaction is used to obtain 2-monoacylglycerols (2-MAG) from oils containing TAG rich in PUFA or long-chain fatty acids in the mentioned *sn*-2 position, usually fish oils. Then, the resulting 2-MAG are esterified with other relevant FFA to obtain nutritionally interesting PUFA-rich TAG. For instance, Muñoz *et al.* [266] assessed the performance of various commercial lipases including proROL immobilized onto Accurel<sup>®</sup> MP-1000 in the alcoholysis of tuna and cod oils to obtain 2-MAG for subsequent esterification with capric acid. The commercial lipase Novozyme 435



exhibited better operational stability than Lipase D (commercial proROL) in the alcoholysis reaction; however, the latter enzyme provided a higher reaction yield. In the esterification reaction, Lipase D led to the highest proportion of SL in the mixture (over 90%); also, there was no loss in proROL activity after 5 reaction cycles. Similarly, Hita *et al.* [267] and Rodriguez *et al.* [268] followed the previous two-step procedure and used immobilized proROL in the process.

ROL has scarcely been used to prepare cocoa butter equivalents (CBE). However, Ray *et al.* [271] examined the kinetics of acidolysis of high oleic sunflower oil with stearic–palmitic acid mixtures with a view to producing CBE formulations by further fractionating the ensuing product. Consequently, this subject might be a great research target for future projects with ROL, as well as DAG and MAG synthesis, which have so far been researched only tangentially in connection with the synthesis of other products such as biodiesel.

### ***1.6.3. Production of flavor esters***

Flavor and aroma esters, which have pleasant sensory attributes including fruity, floral, spicy, creamy and nutty aromas, occur widely in nature. These traits make them suitable ingredients for foods, beverages, cosmetics, pharmaceuticals, chemicals and personal care products including perfumes, body lotions, shampoos and other toiletries [273,274]. Most flavor and fragrance substances are obtained by extraction from their natural sources (usually fruits, plants or flowers). However, the fact that they occur at low concentrations naturally makes their extraction a costly process and one that cannot meet the growing demand for these substances. The increasing shortage of flavor esters has been met by devising effective chemical and enzymatic syntheses [275,276]. In addition to the above-

described advantages of enzymatic catalysis over chemical catalysis, the former allows the resulting products to be labeled as natural in accordance with European Legislation (EC 1334/2008, EC 32/2009) if the reactants used are also natural. In this way, enzymes help meet consumers' increasing demand for natural products and increase the value of the resulting flavor esters [273]. In fact, flavor esters have so far been obtained not only with ROL but also with other enzymes including commercial Novozym® 435 (*Candida antarctica* lipase B) [275,276], and lipase from *Candida rugosa* [277,278] and *Burkholderia cepacia* [279].

Ethyl butyrate is a major component of many fruit flavors including pineapple, passion fruit and strawberry [280]. This compound can be obtained by esterifying butyric acid with ethanol. Guillen *et al.* [281] used rROL immobilized onto three different supports (EP100, Eupergit®CM and Octadecyl-Sepabeads) for this esterification reaction. EP100-immobilized rROL proved the best performer in terms of reaction rate and yield, but rROL immobilized onto Octadecyl-Sepabeads exhibited the highest operational stability. As a result, the latter biocatalyst was chosen to examine the influence of the butyric acid and ethanol concentrations with a view to maximizing the reaction rate and final yield through a Design of Experiments (DoE) [282]. The best results were obtained with an acid:alcohol ratio of 1.45 and the reaction rate increased with increasing butyric acid concentration. However, as previously found by Grosso *et al.* [283], too high concentrations of butyric acid deactivated the enzyme.

Butyl acetate, which is one other ester with resembling organoleptic properties to pineapple, was successfully synthesized by Ben Salah *et al.* [284], who esterified acetic acid with butanol in the presence of proROL immobilized onto Celite 545—preliminary tests with the enzyme in free form gave poor yields and they were clearly exceeded by

the immobilized lipase. A solvent-free reaction was used for easier product purification and lower reaction toxicity and inflammability. In these conditions, the maximum yield was 60% and the biocatalyst remained stable for three consecutive runs with no loss of activity.

Flavor esters have also been obtained by ROL-catalyzed transesterification instead of esterification. Thus, Kumari *et al.* [285] succeeded in synthesizing isoamyl acetate—an ester with a pleasant banana flavor—by transesterifying isoamyl alcohol with vinyl acetate in the presence of immobilized proROL. This way, the inhibitory effect of the acid on the esterification reaction [286] was avoided by using transesterification instead of esterification. Under optimal conditions, conversion peaked at 95% after 8 h reaction; also, the enzyme exhibited a high operational stability and no loss of activity after 3 reaction cycles. Garlapati *et al.* [287] used proROL covalently immobilized onto activated silica to obtain methyl butyrate and octyl acetate—two esters with a pineapple and orange flavors, respectively—by transesterification. After an optimization process, the solvent-free system used afforded high reaction yields (*viz.*, 70.42% methyl butyrate in 14 h and 92.35% octyl acetate in 12 h). Also, the biocatalyst retained more than 95% of its initial relative activity after 5 reaction cycles. A transesterification reaction was also used to obtain citronellol esters with proROL immobilized onto a copolymer of hydroxypropyl methyl cellulose (HPMC) and polyvinyl alcohol (PVA) in a supercritical carbon dioxide reaction medium [288]. The yields in the three target flavor esters (citronellol acetate, citronellol butyrate and citronellol laurate) exceeded 90%, which testifies to the suitability of the biocatalyst and the operational approaches followed in the biotransformations.

As per legislation currently in force in Europe, the substrates for esterification or transesterification reactions giving flavor esters must be natural if the products are to be labelled “natural” as well. Because most of the esters used in transesterification reactions are in general nonnatural, the resulting products cannot be legally deemed natural, so esterification reactions are to be preferred (especially when the natural flavor market is targeted). Further research is therefore needed to improve ROL activity and operational stability in esterification reactions yielding natural flavors.

#### ***1.6.4. Resolution of racemic mixtures***

Enantiomerically pure compounds are very attractive for preparing a wide range of products. This is particularly so in the food and pharmaceutical industries, where the desired organoleptic properties or medical effects might be present in only one isomer. As a result, racemic resolution has become increasingly important and made lipases even more interesting by virtue of their enantioselectivity and specificity [289,290].

Palomo *et al.* [291] used proROL to resolve (*R*)-glycidyl butyrate isomers. This compound is an essential substrate for obtaining linezolid, a product currently used to treat multidrug-resistant Gram-positive infections. A “conformational engineering” approach was used to prepare proROL in various immobilized forms in order to alter the rigidity of the enzyme structure and its microenvironment so as to change the shape of the open form of the lipase and its catalytic performance as a result. Of the three different biocatalysts tested, proROL immobilized by adsorption onto dextran sulfate-coated Sepabeads provided 55% conversion and the highest enantiomeric excess (ee = 99%).

Benzoin is an important  $\alpha$ -hydroxy ketone and a potential building block for some organic syntheses. Songür *et al.* [292] achieved its enantioselective production from benzoin acetate in the presence of *R. oryzae* cell homogenates (Figure 1.10) to combine enantioselective hydrolysis by proROL with the racemization by native racemase from *R. oryzae* for increased ee and conversion levels. The resulting (*S*)-benzoin conversion was close to 100% and ee = 96%.

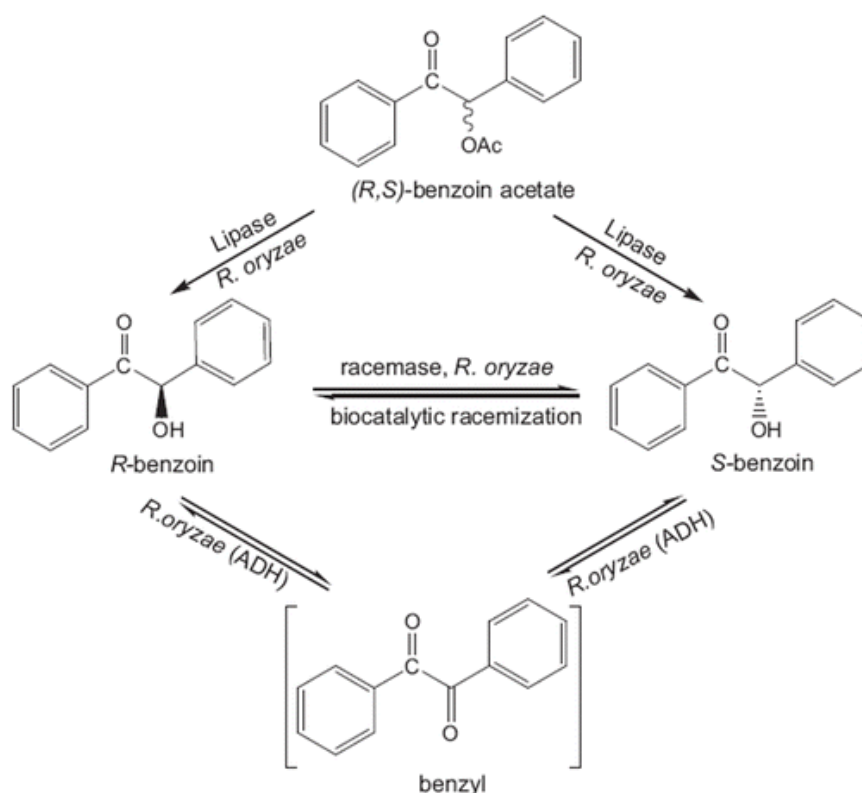


**Figure 1.10.** Schematic representation of enantioselective benzoin acetate hydrolysis and deracemization of benzoin using *R. oryzae* cells [292].

proROL covalently immobilized onto a Lewatit-aldehyde support proved an effective biocatalyst for asymmetric hydrolysis of dimethyl 3-phenylglutarate [293]. Under the best conditions, (*R*)-methyl-3-phenylglutarate was obtained with ee = 92% and a monoester yield of 97%.

The (*S*)-enantiomer of ibuprofen is 160 times more active than its (*R*)-counterpart—also, the latter can have unwanted side effects on the gastrointestinal tract. Using the right enantiomer of each drug is in fact crucial. Yousefi *et al.* [294] succeeded in resolving racemic ibuprofen esters by using proROL immobilized onto octadecyl sepharose (Figure 1.11).

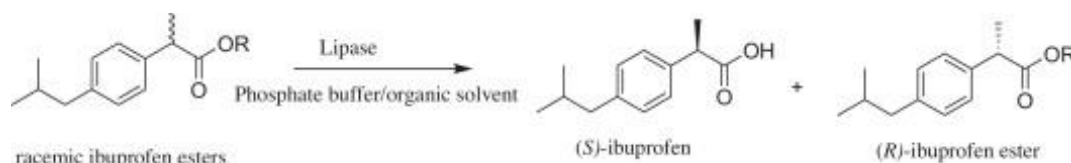


**Figure 1.11.** Lipase-catalyzed enantioselective hydrolysis of racemic ibuprofen esters [294].

A proROL-displaying yeast whole-cell biocatalyst (*viz.*, one obtained by genetically modifying a *S. cerevisiae* strain to exhibit proROL on its cell surfaces) allowed the racemic resolution of (*R,S*)-1-phenylethanol to obtain (*S*)-1-phenylethanol, a chiral building block. A yield of 97.3% and ee = 93.3% were obtained after 36 h of reaction [295]. The same biocatalyst was used to accomplish the optical resolution of the pharmaceutical precursor (*R,S*)-1-benzyloxy-3-chloro-2-propyl monosuccinate. The enzyme remained operationally stable over at least 8 reaction cycles [296].

### 1.6.5. Polymerization reactions

Current consumption patterns in developed countries are heavily reliant on plastics, whose excellent properties have led to their becoming essential for all of the products we use in daily life [297]. Because they are most often derived from fossil fuels, however, their overuse has worsened some problems such as petroleum depletion, the dependence on oil-producing countries, and the worldwide environmental crisis sparked by the

massive use of nonbiodegradable plastics and careless disposal of plastic wastes. In fact, tonnes of plastics are buried in landfills, burnt in incinerators or simply thrown into rivers and seas each year, thereby polluting all land, air and water [298,299]. All of this has turned the environmental crisis into a health emergency also, as the ubiquity of plastics in nature is leading to their reaching the food chain with still largely unknown effects on fauna and human health [300].

In this context, bio-based and biodegradable biopolymers (so-called “bioplastics”) are emerging as a much needed transition to plastics with less adverse impacts [301]. The European Commission has lately established some policies in this direction including the Plastic Strategy (COM/2018/028). However, the new terms used in connection with the polymers can raise confusion. For example, the word “biopolymer” encompasses all plastics that are bio-based and/or biodegradable but “bio-based” does not equal “biodegradable”. In fact, the former term refers to origin (renewable resources) whereas the latter is connected with degradability upon exposure to certain conditions or microorganisms [301–303]. Thus, biopolyethylene is a bio-based but not biodegradable biopolymer, whereas polycaprolactone is a biodegradable but not bio-based biopolymer, and polylactic acid (PLA) is both bio-based and biodegradable [304]. In fact PLA is arousing increasing interest by virtue of the technological advances focused on improving its productivity and functionality, its being an effective alternative to polystyrene and polypropylene for packaging, and its affording other challenging uses such as biomedical products —PLA is a biocompatible and bioabsorbable polyester [301,305,306].

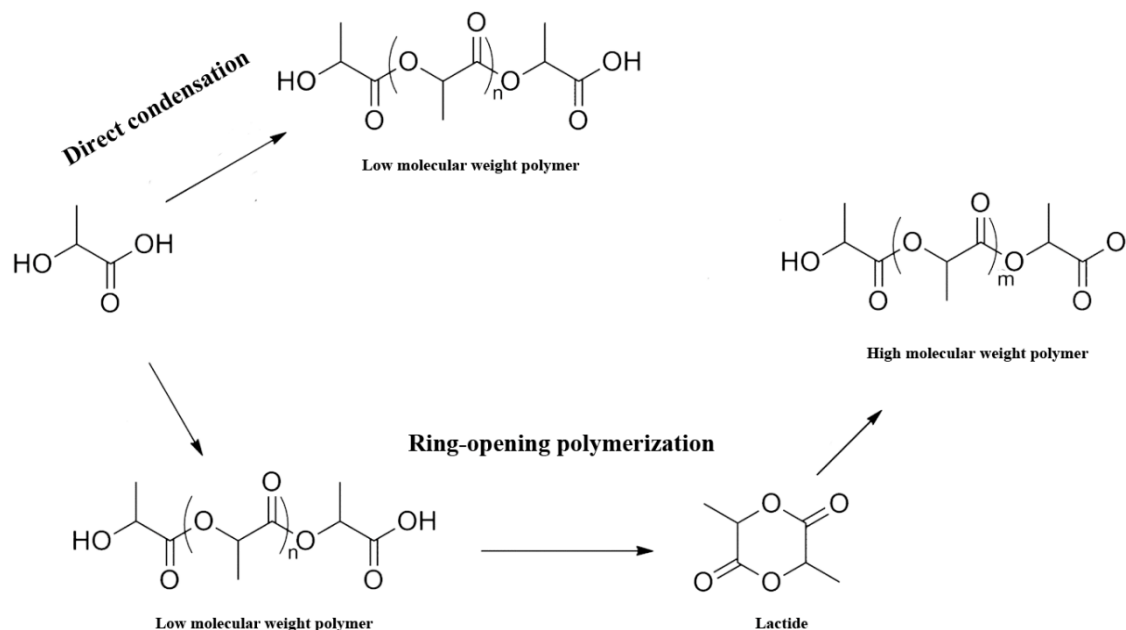


**Figure 1.12** – Polylactic acid (PLA) synthesis by direct lactic acid condensation or ring-opening polymerization. Image adapted from [307].

There are two main ways of synthesizing polyesters (PLA included) with lipases (Figure 1.12), namely: by ring-opening polymerization (ROP) of lactones and by polycondensation or direct condensation [308,309]. The latter process involves esterification of a carboxyl group with a hydroxyl group to form an ester bond. On the other hand, ROP is a chain-growth polymerization process where one end of the polymer chain carries a reactive site for addition of cyclic monomers [310,311]. ROP allows polyesters with an increased molecular weight relative to direct condensation but requires using a lactone—and hence a preliminary step to synthesize it [309,311]. ROP has scarcely been used in polymerization reactions of this type [312]. Among the few relevant reports is one by Uyama *et al.* [313], who back in 1995 used *Rhizopus japonicus* and *Rhizopus delemar* lipases (currently deemed ROL) for ROP of macrolides (macrocylic esters) consisting of 11-membered lactones. However, no conversion was obtained with lipases from *Rhizopus sp.* Nevertheless, many other microbial lipases have obtained



significant results in these reactions. For instance, Kondabagil *et al.* [314] obtained a PLA of 1423 Da by using porcine pancreatic lipase (PPL) through direct lactic acid condensation while Chuensangjun *et al.* [306], by utilizing the commercial Lipozyme TL IM, a PLA of 4515 Da. Regarding ROP, various lipases have been also employed, such as PPL, *Pseudomonas cepacia* lipase, CALB and CRL. The former has been successfully employed reporting values over 10000 Da [315] while the latter have also exhibited extraordinary results forming a PLA around 5500 Da [316]. Consequently, there is still room for improvement for the use of ROL in ROP and direct lactic acid condensation reactions.

## 1.7. References

- [1] Berzelius JJ. Quelques idées sur une nouvelle force agissant dans les combinaisons des corps organiques. *Anal Chim Phys* 1836;61:146–51.
- [2] Heckmann CM, Paradisi F. Looking back: a short history of the discovery of enzymes and how they became powerful chemical tools. *ChemCatChem* 2020;12:6082–102. <https://doi.org/10.1002/CCTC.202001107>.
- [3] Punekar NS. Enzymes: historical aspects. *Enzym Catal Kinet Mech* 2018;5–13. [https://doi.org/10.1007/978-981-13-0785-0\\_2](https://doi.org/10.1007/978-981-13-0785-0_2).
- [4] McGovern PE, Zhang J, Tang J, Zhang Z, Hall GR, Moreau RA, et al. Fermented beverages of pre- and proto-historic China. *Proc Natl Acad Sci U S A* 2004;101:17593–8. <https://doi.org/10.1073/pnas.0407921102>.
- [5] Summer JB. *The chemical nature of enzymes*. Oxford Academic; 1933;6 <https://doi.org/10.1093/jn/6.1.103>.
- [6] Park S V., Yang JS, Jo H, Kang B, Oh SS, Jung GY. Catalytic RNA, ribozyme, and its applications in synthetic biology. *Biotechnol Adv* 2019;37:107452. <https://doi.org/10.1016/j.biotechadv.2019.107452>.
- [7] Sun PD, Foster CE, Boyington JC. Overview of protein structural and functional folds. *Curr Protoc Protein Sci* 2004;35:1711. <https://doi.org/10.1002/0471140864.PS1701S35>.
- [8] Robinson PK. *Enzymes: principles and biotechnological applications*. Essays

- Biochem 2015;59:1. <https://doi.org/10.1042/BSE0590001>.
- [9] Singh RK, Tiwari MK, Singh R, Lee JK. From protein engineering to immobilization: promising strategies for the upgrade of industrial enzymes. *Int J Mol Sci* 2013;14:1232–77. <https://doi.org/10.3390/ijms14011232>.
- [10] Budnik LT, Scheer E, Burge PS, Baur X. Sensitising effects of genetically modified enzymes used in flavour, fragrance, detergent and pharmaceutical production: Cross-sectional study. *Occup Environ Med* 2017;74:39–45. <https://doi.org/10.1136/oemed-2015-103442>.
- [11] Zaks A, Klibanov AM. Enzymatic catalysis in nonaqueous solvents. *J Biol Chem* 1988;263:3194–201.
- [12] Chapman J, Ismail A, Dinu C. Industrial applications of enzymes: recent advances, techniques, and outlooks. *Catalysts* 2018;8:238–64. <https://doi.org/10.3390/catal8060238>.
- [13] Singh R, Kumar M, Mittal A, Mehta PK. Microbial enzymes: industrial progress in 21<sup>st</sup> century. *3 Biotech* 2016;6:174–89. <https://doi.org/10.1007/s13205-016-0485-8>.
- [14] Bilal M, Cui J, Iqbal HMN. Tailoring enzyme microenvironment: state-of-the-art strategy to fulfill the quest for efficient bio-catalysis. *Int J Biol Macromol* 2019;130:186–96. <https://doi.org/10.1016/j.ijbiomac.2019.02.141>.
- [15] Girelli AM, Astolfi ML, Scuto FR. Agro-industrial wastes as potential carriers for enzyme immobilization: A review. *Chemosphere* 2020;244:1–12. <https://doi.org/10.1016/j.chemosphere.2019.125368>.

- [16] Raveendran S, Parameswaran B, Ummalyma SB, Abraham A, Mathew AK, Madhavan A, et al. Applications of microbial enzymes in food industry. *Food Technol Biotechnol* 2018;56:16–30. <https://doi.org/10.17113/ftb.56.01.18.5491>.
- [17] Basso A, Serban S. Industrial applications of immobilized enzymes—A review. *Mol Catal* 2019;479:1–20. <https://doi.org/10.1016/j.mcat.2019.110607>.
- [18] Ravindran R, Hassan SS, Williams GA, Jaiswal AK. A review on bioconversion of agro-industrial wastes to industrially important enzymes. *Bioengineering* 2018;5:93–113. <https://doi.org/10.3390/bioengineering5040093>.
- [19] Woodley JM. Accelerating the implementation of biocatalysis in industry. *Appl Microbiol Biotechnol* 2019;103:4733–4739. <https://doi.org/10.1007/s00253-019-09796-x>.
- [20] Singh G, Arya SK. Utility of laccase in pulp and paper industry: a progressive step towards the green technology. *Int J Biol Macromol* 2019;134:1071–84. <https://doi.org/10.1016/j.ijbiomac.2019.05.168>.
- [21] Ameri research Inc. Global Enzymes Market Size, Analysis | Industry Research Report 2024. Ameri Res Inc 2017. <https://www.ameriresearch.com/product/global-enzymes-market-size/> (accessed January 8, 2022).
- [22] Li S, Yang X, Yang S, Zhu M, Wang X. Technology prospecting on enzymes: application, marketing and engineering. *Comput Struct Biotechnol J* 2012;2:1–11. <https://doi.org/10.5936/csbj.201209017>.
- [23] Haki GD, Rakshit SK. Developments in industrially important thermostable

- enzymes: A review. *Bioresour Technol* 2003;89:17–34.  
[https://doi.org/10.1016/S0960-8524\(03\)00033-6](https://doi.org/10.1016/S0960-8524(03)00033-6).
- [24] Dalla-Vecchia R, Sebrão D, Nascimento MDG, Soldi V. Carboxymethylcellulose and poly(vinyl alcohol) used as a film support for lipases immobilization. *Process Biochem* 2005;40:2677–82. <https://doi.org/10.1016/j.procbio.2004.12.004>.
- [25] Hasan F, Shah AA, Hameed A. Industrial applications of microbial lipases. *Enzyme Microb Technol* 2006;39:235–51.  
<https://doi.org/10.1016/j.enzmictec.2005.10.016>.
- [26] Sarmah N, Revathi D, Sheelu G, Yamuna Rani K, Sridhar S, Mehtab V, et al. Recent advances on sources and industrial applications of lipases. *Biotechnol Prog* 2018;34:5–28. <https://doi.org/10.1002/btpr.2581>.
- [27] Yu XW, Xu Y, Xiao R. Lipases from the genus *Rhizopus*: characteristics, expression, protein engineering and application. *Prog Lipid Res* 2016;64:57–68.  
<https://doi.org/10.1016/j.plipres.2016.08.001>.
- [28] Melani NB, Tambourgi EB, Silveira E. Lipases: from production to applications. *Sep Purif Rev* 2020;49:143–58. <https://doi.org/10.1080/15422119.2018.1564328>.
- [29] Lima RN, Porto ALM. Biocatalytic aminolysis of ethyl (S)-mandelate by lipase from *Candida antarctica*. *Catal Commun* 2017;100:157–63.  
<https://doi.org/10.1016/j.catcom.2017.06.020>.
- [30] Paiva AL, Balcão VM, Malcata FX. Kinetics and mechanisms of reactions catalyzed by immobilized lipases. *Enzyme Microb Technol* 2000;27:187–204.  
[https://doi.org/10.1016/S0141-0229\(00\)00206-4](https://doi.org/10.1016/S0141-0229(00)00206-4).

- [31] Zeng S, Liu J, Anankanbil S, Chen M, Guo Z, Adams JP, et al. Amide synthesis via aminolysis of ester or acid with an intracellular lipase. *ACS Catal* 2018;8:8856–8865. <https://doi.org/10.1021/acscatal.8b02713>.
- [32] Ken Ugo A, Vivian Amara A, CN I, Kenechuwku U. Microbial lipases: a prospect for biotechnological industrial catalysis for green products: a review. *Ferment Technol* 2017;6:144–56. <https://doi.org/10.4172/2167-7972.1000144>.
- [33] Bharathi D, Rajalakshmi G. Microbial lipases: An overview of screening, production and purification. *Biocatal Agric Biotechnol* 2019;22:101368–75. <https://doi.org/10.1016/j.bcab.2019.101368>.
- [34] Borza P, Peter F, Paul C. Improved enantioselectivity of *Candida antarctica* A lipase through sol-gel entrapment. *Chem Bull “POLITEHNICA” Univ (Timisoara)* 2015;60:49–54.
- [35] Fernandez-Lafuente R. Lipase from *Thermomyces lanuginosus*: uses and prospects as an industrial biocatalyst. *J Mol Catal B Enzym* 2010;62:197–212. <https://doi.org/10.1016/j.molcatb.2009.11.010>.
- [36] Guncheva M, Zhiryakova D. Catalytic properties and potential applications of *Bacillus* lipases. *J Mol Catal B Enzym* 2011;68:1–21. <https://doi.org/10.1016/j.molcatb.2010.09.002>.
- [37] Jachmanián I, Schulte E, Mukherjee KD. Substrate selectivity in esterification of less common fatty acids catalysed by lipases from different sources. *Appl Microbiol Biotechnol* 1996;44:563–7. <https://doi.org/10.1007/BF00172486>.
- [38] Barros M, Fleuri LF, MacEdo GA. Seed lipases: sources, applications and

- properties - A review. *Brazilian J Chem Eng* 2010;27:15–29. <https://doi.org/10.1590/S0104-66322010000100002>.
- [39] Dhake KP, Thakare DD, Bhanage BM. Lipase: A potential biocatalyst for the synthesis of valuable flavour and fragrance ester compounds. *Flavour Fragr J* 2013;28:71–83. <https://doi.org/10.1002/ffj.3140>.
- [40] Su E, Xu J, You P. Functional expression of *Serratia marcescens* H30 lipase in *Escherichia coli* for efficient kinetic resolution of racemic alcohols in organic solvents. *J Mol Catal B Enzym* 2014;106:11–6. <https://doi.org/10.1016/j.molcatb.2014.04.012>.
- [41] Pomeisl K, Lamatová N, Šolínová V, Pohl R, Brabcová J, Kašička V, et al. Enantioselective resolution of side-chain modified gem-difluorinated alcohols catalysed by *Candida antarctica* lipase B and monitored by capillary electrophoresis. *Bioorganic Med Chem* 2019;27:1246–53. <https://doi.org/10.1016/j.bmc.2019.02.022>.
- [42] Javed S, Azeem F, Hussain S, Rasul I, Siddique MH, Riaz M, et al. Bacterial lipases: A review on purification and characterization. *Prog Biophys Mol Biol* 2018;132:23–34. <https://doi.org/10.1016/j.pbiomolbio.2017.07.014>.
- [43] Kapoor M, Gupta MN. Lipase promiscuity and its biochemical applications. *Process Biochem* 2012;57:555–69. <https://doi.org/10.1016/j.procbio.2012.01.011>.
- [44] Ribeiro BD, De Castro AM, Coelho MAZ, Freire DMG. Production and use of lipases in bioenergy: A review from the feedstocks to biodiesel production. *Enzyme Res* 2011;1–16. <https://doi.org/10.4061/2011/615803>.

- [45] Savaghebi D, Safari M, Rezaei K, Ashtari P, Farmani J. Structured lipids produced through lipase-catalyzed acidolysis of canola oil. *J Agric Sci Technol* 2012;14:1297–310.
- [46] Nandi S, Misra G. Functional Foods from soybean oil deodorizer distillate using *Candida Rugosa* and *Candida Antarctica* lipases. *Chem Sci Trans* 2019;8:268–72. <https://doi.org/10.7598/cst2019.1567>.
- [47] Jensen RG. Characteristics of the lipase from the mold, *Geotrichum candidum*: a review. *Lipids* 1974;9:149–57. <https://doi.org/10.1007/BF02532686>.
- [48] Miettinen H, Nyssölä A, Rokka S, Kontkanen H, Kruus K. Screening of microbes for lipases specific for saturated medium and long-chain fatty acids of milk fat. *Int Dairy J* 2013;32:61–7. <https://doi.org/10.1016/j.idairyj.2013.05.007>.
- [49] Zhao J feng, Lin J ping, Yang L rong, Wu M bin. Enhanced performance of *Rhizopus oryzae* lipase by reasonable immobilization on magnetic nanoparticles and its application in synthesis 1,3-diacylglycerol. *Appl Biochem Biotechnol* 2019;188:677–89. <https://doi.org/10.1007/s12010-018-02947-2>.
- [50] López-Fernández J, Barrero JJ, Benaiges MD, Valero F. Truncated prosequence of *Rhizopus oryzae* lipase: key factor for production improvement and biocatalyst stability. *Catalysts* 2019;9:961. <https://doi.org/10.3390/catal9110961>.
- [51] da S. Pereira A, Fontes-Sant’Ana GC, Amaral PFF. Mango agro-industrial wastes for lipase production from *Yarrowia lipolytica* and the potential of the fermented solid as a biocatalyst. *Food Bioprod Process* 2019;115:68–77. <https://doi.org/10.1016/j.fbp.2019.02.002>.



- [52] Filho DG, Silva AG, Guidini CZ. Lipases: sources, immobilization methods, and industrial applications. *Appl Microbiol Biotechnol* 2019;103:7399–423. <https://doi.org/10.1007/s00253-019-10027-6>.
- [53] Thapa S, Li H, OHair J, Bhatti S, Chen FC, Nasr K Al, et al. Biochemical characteristics of microbial enzymes and their significance from industrial perspectives. *Mol Biotechnol* 2019;61:579–601. <https://doi.org/10.1007/s12033-019-00187-1>.
- [54] Kumar A, Dhar K, Kanwar SS, Arora PK. Lipase catalysis in organic solvents: advantages and applications. *Biol Proced Online* 2016;18:1–11. <https://doi.org/10.1186/s12575-016-0033-2>.
- [55] Pandey N, Dhakar K, Jain R, Pandey A. Temperature dependent lipase production from cold and pH tolerant species of *Penicillium*. *Mycosphere* 2016;7:1533–45. <https://doi.org/10.5943/mycosphere/si/3b/5>.
- [56] Mehta A, Bodh U, Gupta R. Fungal lipases: a review. *J Biotech Res* 2017;8:58–77.
- [57] Truong, Tuyen; Lopez, Christelle; Bhandari, Bhesh; Prakash S. Dairy fat products and functionality. Springer International Publishing; 2020. <https://doi.org/10.1007/978-3-030-41661-4>.
- [58] Gryganskyi AP, Golan J, Dolatabadi S, Mondo S, Robb S, Idnurm A, et al. Phylogenetic and phylogenomic definition of *Rhizopus* species. *G3 Genes, Genomes, Genet* 2018;8:2007–18. <https://doi.org/10.1534/g3.118.200235>.
- [59] MAA Schipper. A revision of the genus *Rhizopus*. I. The *Rhizopus stolonifer*-group

- and *Rhizopus oryzae*. *Stud Mycol* 1984;25:1–19.
- [60] Abe A, Oda Y, Asano K, Sone T. The molecular phylogeny of the genus *Rhizopus* based on rDNA sequences. *Biosci Biotechnol Biochem* 2006;70:2387–93. <https://doi.org/10.1271/bbb.60101>.
- [61] Liu X-Y, Huang H, Zheng R-Y. Molecular phylogenetic relationships within *Rhizopus* based on combined analyses of ITS rDNA and pyrG gene sequences. *Sydowia* 2007;59:235–53.
- [62] Zheng RY, Chen GQ, Huang H, Liu XY. A monograph of *Rhizopus*. *Sydowia* 2007;59:273–372.
- [63] Abe A, Asano K, Sone T. A molecular phylogeny-based taxonomy of the genus *Rhizopus*. *Biosci Biotechnol Biochem* 2010;74:1325–31. <https://doi.org/10.1271/bbb.90718>.
- [64] Lennartsson PR, Taherzadeh MJ, Edebo L. *Rhizopus*. *Encycl. Food Microbiol.* Second Ed., Academic Press; 2014, p.284–90. <https://doi.org/10.1016/B978-0-12-384730-0.00391-8>.
- [65] Chen C-C, Liou G-Y, Lee F-L. *Rhizopus* and related species from peka in Taiwan. *Fung Sci* 2007;22:51–7.
- [66] Londoño-Hernández L, Ramírez-Toro C, Ruiz HA, Ascacio-Valdés JA, Aguilar-Gonzalez MA, Rodríguez-Herrera R, et al. *Rhizopus oryzae* – Ancient microbial resource with importance in modern food industry. *Int J Food Microbiol* 2017;257:110–27. <https://doi.org/10.1016/j.ijfoodmicro.2017.06.012>.
- [67] Sebastian J, Hegde K, Kumar P, Rouissi T, Brar SK. Bioproduction of fumaric

- acid: an insight into microbial strain improvement strategies. *Crit Rev Biotechnol* 2019;39:817–34. <https://doi.org/10.1080/07388551.2019.1620677>.
- [68] Benabda O, M’Hir S, Kasmi M, Mnif W, Hamdi M. Optimization of protease and amylase production by *Rhizopus oryzae* cultivated on bread waste using solid-state fermentation. *J Chem* 2019;2019:1–9. <https://doi.org/10.1155/2019/3738181>.
- [69] Ghosh B, Ray RR. Current commercial perspective of *Rhizopus oryzae*: a review. *J Appl Sci* 2011;11:2470–86. <https://doi.org/10.3923/jas.2011.2470.2486>.
- [70] Beer HD, McCarthy JEG, Bornscheuer UT, Schmid RD. Cloning, expression, characterization and role of the leader sequence of a lipase from *Rhizopus oryzae*. *Biochim Biophys Acta - Gene Struct Expr* 1998;1399:173–80. [https://doi.org/10.1016/S0167-4781\(98\)00104-3](https://doi.org/10.1016/S0167-4781(98)00104-3).
- [71] Salah R Ben, Mosbah H, Fendri A, Gargouri A, Gargouri Y, Mejdoub H. Biochemical and molecular characterization of a lipase produced by *Rhizopus oryzae*. *FEMS Microbiol Lett* 2006;260:241–8. <https://doi.org/10.1111/j.1574-6968.2006.00323.x>.
- [72] Sayari A, Frikha F, Miled N, Mtibaa H, Ali Y Ben, Verger R, et al. N-terminal peptide of *Rhizopus oryzae* lipase is important for its catalytic properties. *FEBS Lett* 2005;579:976–82. <https://doi.org/10.1016/j.febslet.2004.12.068>.
- [73] Derewenda U, Swenson L, Wei Y, Green R, Kobos PM, Joerger R, et al. Conformational lability of lipases observed in the absence of an oil- water interface: crystallographic studies of enzymes from the fungi *Humicola lanuginosa* and *Rhizopus delemar*. *J Lipid Res* 1994;35:524–34. <https://doi.org/10.2210/pdb1tib/pdb>.

- [74] Kohno M, Kugimiya W, Hashimoto Y, Morita Y. Purification, characterization, and crystallization of two types of lipase from *Rhizopus niveus*. *Biosci Biotechnol Biochem* 1994;58:1007–12. <https://doi.org/10.1271/bbb.58.1007>.
- [75] Yang M, Yu XW, Zheng H, Sha C, Zhao C, Qian M, et al. Role of N-linked glycosylation in the secretion and enzymatic properties of *Rhizopus chinensis* lipase expressed in *Pichia pastoris*. *Microb Cell Fact* 2015;14:40–54. <https://doi.org/10.1186/s12934-015-0225-5>.
- [76] Yu XW, Yang M, Jiang C, Zhang X, Xu Y. N-glycosylation engineering to improve the constitutive expression of *Rhizopus oryzae* lipase in *Komagataella phaffii*. *J Agric Food Chem* 2017;65:6009–15. <https://doi.org/10.1021/acs.jafc.7b01884>.
- [77] Beer HD, Wohlfahrt G, Schmid RD, McCarthy JE. The folding and activity of the extracellular lipase of *Rhizopus oryzae* are modulated by a prosequence. *Biochem J* 1996;319:351–9. <https://doi.org/10.1042/bj3190351>.
- [78] Chen YJ, Inouye M. The intramolecular chaperone-mediated protein folding. *Curr Opin Struct Biol* 2008;18:765–70. <https://doi.org/10.1016/j.sbi.2008.10.005>.
- [79] Takahashi S, Ueda M, Atomi H, Beer HD, Bornscheuer UT, Schmid RD, et al. Extracellular production of active *Rhizopus oryzae* lipase by *Saccharomyces cerevisiae*. *J Ferment Bioeng* 1998;86:164–8. [https://doi.org/10.1016/S0922-338X\(98\)80055-X](https://doi.org/10.1016/S0922-338X(98)80055-X).
- [80] Ueda M, Takahashi S, Washida M, Shiraga S, Tanaka A. Expression of *Rhizopus oryzae* lipase gene in *Saccharomyces cerevisiae*. *J Mol Catal - B Enzym* 2002;17:113–24. [https://doi.org/10.1016/S1381-1177\(02\)00018-8](https://doi.org/10.1016/S1381-1177(02)00018-8).

- [81] Niu W, Li Z, Tan T. Secretion of pro- and mature *Rhizopus arrhizus* lipases by *Pichia pastoris* and properties of the proteins. *Mol Biotechnol* 2006;32:73–81. <https://doi.org/10.1385/MB:32:1:073>.
- [82] Wang JR, Li YY, Xu S De, Li P, Liu JS, Liu DN. High-level expression of pro-form lipase from *Rhizopus oryzae* in *Pichia pastoris* and its purification and characterization. *Int J Mol Sci* 2014;15:203–17. <https://doi.org/10.3390/ijms15010203>.
- [83] Takahashi S, Ueda M, Tanaka A. Function of the prosequence for in vivo folding and secretion of active *Rhizopus oryzae* lipase in *Saccharomyces cerevisiae*. *Appl Microbiol Biotechnol* 2001;55:454–62. <https://doi.org/10.1007/s002530000537>.
- [84] Ben Salah A, Sayari A, Verger R, Gargouri Y. Kinetic studies of *Rhizopus oryzae* lipase using monomolecular film technique. *Biochimie* 2001;83:463–9. [https://doi.org/10.1016/S0300-9084\(01\)01283-4](https://doi.org/10.1016/S0300-9084(01)01283-4).
- [85] Takahashi S, Ueda M, Tanaka A. Independent production of two molecular forms of a recombinant *Rhizopus oryzae* lipase by KEX2-engineered strains of *Saccharomyces cerevisiae*. *Appl Microbiol Biotechnol* 1999;52:534–40. <https://doi.org/10.1007/s002530051556>.
- [86] Hama S, Tamalampudi S, Shindo N, Numata T, Yamaji H, Fukuda H, et al. Role of N-terminal 28-amino-acid region of *Rhizopus oryzae* lipase in directing proteins to secretory pathway of *Aspergillus oryzae*. *Appl Microbiol Biotechnol* 2008;79:1009–18. <https://doi.org/10.1007/s00253-008-1502-6>.
- [87] Minning S, Schmidt-Dannert C, Schmid RD. Functional expression of *Rhizopus oryzae* lipase in *Pichia pastoris*: high-level production and some properties. *J*

- Biotechnol 1998;66:147–56. [https://doi.org/10.1016/S0168-1656\(98\)00142-4](https://doi.org/10.1016/S0168-1656(98)00142-4).
- [88] Takó M, Kotogán A, Papp T, Kadaikunnan S, Alharbi NS, Vágvölgyi C. Purification and properties of extracellular lipases with transesterification activity and 1,3-regioselectivity from *Rhizomucor miehei* and *Rhizopus oryzae*. J Microbiol Biotechnol 2017;27:277–88. <https://doi.org/10.4014/jmb.1608.08005>.
- [89] Hiol A, Jonzo MD, Rugani N, Druet D, Sarda L, Comeau LC. Purification and characterization of an extracellular lipase from a thermophilic *Rhizopus oryzae* strain isolated from palm fruit. Enzyme Microb Technol 2000;26:421–30. [https://doi.org/10.1016/S0141-0229\(99\)00173-8](https://doi.org/10.1016/S0141-0229(99)00173-8).
- [90] Shimada Y, Iwai M, Tsujisaka Y. Reversibility of the modification of *Rhizopus delemar* lipase by phosphatidylcholine. J Biochem 1981;89:937–42. <https://doi.org/10.1093/oxfordjournals.jbchem.a133277>.
- [91] Guillén M, Benaiges MD, Valero F. Comparison of the biochemical properties of a recombinant lipase extract from *Rhizopus oryzae* expressed in *Pichia pastoris* with a native extract. Biochem Eng J 2011;54:117–23. <https://doi.org/10.1016/j.bej.2011.02.008>.
- [92] Pashangeh K, Akhond M, Karbalaeei-Heidari HR, Absalan G. Biochemical characterization and stability assessment of *Rhizopus oryzae* lipase covalently immobilized on amino-functionalized magnetic nanoparticles. Int J Biol Macromol 2017;105:300–7. <https://doi.org/10.1016/j.ijbiomac.2017.07.035>.
- [93] Haas MJ, Cichowicz DJ, Bailey DG. Purification and characterization of an extracellular lipase from the fungus *Rhizopus delemar*. Lipids 1992;27:571–6. <https://doi.org/10.1007/BF02536112>.

- [94] Essamri M, Deyris V, Comeau L. Optimization of lipase production by *Rhizopus oryzae* and study on the stability of lipase activity in organic solvents. *J Biotechnol* 1998;60:97–103. [https://doi.org/10.1016/S0168-1656\(97\)00193-4](https://doi.org/10.1016/S0168-1656(97)00193-4).
- [95] Yu XW, Sha C, Guo YL, Xiao R, Xu Y. High-level expression and characterization of a chimeric lipase from *Rhizopus oryzae* for biodiesel production. *Biotechnol Biofuels* 2013;6:29–41. <https://doi.org/10.1186/1754-6834-6-29>.
- [96] Ben Salah R, Gargouri A, Verger R, Gargouri Y, Mejdoub H. Expression in *Pichia pastoris* X33 of his-tagged lipase from a novel strain of *Rhizopus oryzae* and its mutant Asn 134 His: purification and characterization. *World J Microbiol Biotechnol* 2009;25:1375–84. <https://doi.org/10.1007/s11274-009-0024-4>.
- [97] Kantak JB, Prabhune AA. Characterization of smallest active monomeric lipase from novel *Rhizopus* strain: application in transesterification. *Appl Biochem Biotechnol* 2012;166:1769–80. <https://doi.org/10.1007/s12010-012-9584-0>.
- [98] Li C, Zhang G, Liu N, Liu L. Preparation and properties of *Rhizopus oryzae* lipase immobilized using an adsorption-crosslinking method. *Int J Food Prop* 2015;19:1776–85. <https://doi.org/10.1080/10942912.2015.1107732>.
- [99] Razak CNA, Salleh AB, Musani R, Samad MY, Basri M. Some characteristics of lipases from thermophilic fungi isolated from palm oil mill effluent. *J Mol Catal - B Enzym* 1997;3:153–9. [https://doi.org/10.1016/S1381-1177\(96\)00035-5](https://doi.org/10.1016/S1381-1177(96)00035-5).
- [100] Li Z, Li X, Wang Y, Wang Y, Wang F, Jiang J. Expression and characterization of recombinant *Rhizopus oryzae* lipase for enzymatic biodiesel production. *Bioresour Technol* 2011;10:9810–3. <https://doi.org/10.1016/j.biortech.2011.07.070>.

- [101] Song X, Qi X, Hao B, Qu Y. Studies of substrate specificities of lipases from different sources. *Eur J Lipid Sci Technol* 2008;110:1095–101. <https://doi.org/10.1002/ejlt.200800073>.
- [102] Pereira RM, Andrade GSS, De Castro HF, Campos MGN. Performance of chitosan/glycerol phosphate hydrogel as a support for lipase immobilization. *Mater Res* 2017;20:190–201. <https://doi.org/10.1590/1980-5373-mr-2017-0091>.
- [103] Yuzbashev T V., Yuzbasheva EY, Vibornaya T V., Sobolevskaya TI, Laptev IA, Gavrikov A V., et al. Production of recombinant *Rhizopus oryzae* lipase by the yeast *Yarrowia lipolytica* results in increased enzymatic thermostability. *Protein Expr Purif* 2012;82:83–9. <https://doi.org/10.1016/j.pep.2011.11.014>.
- [104] Adak S, Banerjee R. Biochemical characterisation of a newly isolated low molecular weight lipase from *Rhizopus oryzae* NRRL 3562. *Enzym Eng* 2013;2:118–25. <https://doi.org/10.4172/2329-6674.1000118>.
- [105] Karra-Châabouni M, Bouaziz I, Boufi S, Botelho do Rego AM, Gargouri Y. Physical immobilization of *Rhizopus oryzae* lipase onto cellulose substrate: activity and stability studies. *Colloids Surfaces B Biointerfaces* 2008;66:168–77. <https://doi.org/10.1016/j.colsurfb.2008.06.010>.
- [106] Schrag JD, Cygler M. 1.8 Å refined structure of the lipase from *Geotrichum candidum*. *J Mol Biol* 1993;230:575–91. <https://doi.org/10.1006/jmbi.1993.1171>.
- [107] Grochulski P, Li Y, Schrag JD, Bouthillier F, Smith P, Harrison D, et al. Insights into interfacial activation from an open structure of *Candida rugosa* lipase. *J Biol Chem* 1993;268:12843–7. <https://doi.org/10.2210/pdb1crl/pdb>.



- [108] Noble MEM, Cleasby A, Johnson LN, Egmond MR, Frenken LGJ. The crystal structure of triacylglycerol lipase from *Pseudomonas glumae* reveals a partially redundant catalytic aspartate. FEBS Lett 1993;331:123–8. [https://doi.org/10.1016/0014-5793\(93\)80310-Q](https://doi.org/10.1016/0014-5793(93)80310-Q).
- [109] Derewenda U, Swenson L, Green R, Wei Y, Dodson GG, Yamaguchi S, et al. An unusual buried polar cluster in a family of fungal lipases. Nat Struct Biol 1994;1:36–47. <https://doi.org/10.1038/nsb0194-36>.
- [110] Khan FI, Lan D, Durrani R, Huan W, Zhao Z, Wang Y. The lid domain in lipases: structural and functional determinant of enzymatic properties. Front Bioeng Biotechnol 2017;5:1–13. <https://doi.org/10.3389/fbioe.2017.00016>.
- [111] Satomura A, Kuroda K, Ueda M. Generation of a functionally distinct *Rhizopus oryzae* lipase through protein folding memory. PLoS One 2015;10:1–13. <https://doi.org/10.1371/journal.pone.0124545>.
- [112] Shiraga S, Ueda M, Takahashi S, Tanaka A. Construction of the combinatorial library of *Rhizopus oryzae* lipase mutated in the lid domain by displaying on yeast cell surface. J Mol Catal - B Enzym 2002;17:167–73. [https://doi.org/10.1016/S1381-1177\(02\)00024-3](https://doi.org/10.1016/S1381-1177(02)00024-3).
- [113] Adlercreutz P. Immobilisation and application of lipases in organic media. Chem Soc Rev 2013;7:6406–36. <https://doi.org/10.1039/c3cs35446f>.
- [114] Verger R. “Interfacial activation” of lipases: facts and artifacts. Trends Biotechnol 1997;15:32–8. [https://doi.org/10.1016/S0167-7799\(96\)10064-0](https://doi.org/10.1016/S0167-7799(96)10064-0).
- [115] Reis P, Holmberg K, Watzke H, Leser ME, Miller R. Lipases at interfaces: a

- review. *Adv Colloid Interface Sci* 2009;147–148:237–50.  
<https://doi.org/10.1016/j.cis.2008.06.001>.
- [116] Kourist R, Brundiek H, Bornscheuer UT. Protein engineering and discovery of lipases. *Eur J Lipid Sci Technol* 2010;112:64–74.  
<https://doi.org/10.1002/ejlt.200900143>.
- [117] Zhang Y, Zhao Y, Gao X, Jiang W, Li Z, Yao Q, et al. Kinetic model of the enzymatic Michael addition for synthesis of mitomycin analogs catalyzed by immobilized lipase from *T. laibacchii*. *Mol Catal* 2019;466:146–56.  
<https://doi.org/10.1016/j.mcat.2019.01.017>.
- [118] Shiraga S, Ishiguro M, Fukami H, Nakao M, Ueda M. Creation of *Rhizopus oryzae* lipase having a unique oxyanion hole by combinatorial mutagenesis in the lid domain. *Appl Microbiol Biotechnol* 2005;68:779–85.  
<https://doi.org/10.1007/s00253-005-1935-0>.
- [119] Hermanová S, Zarevúcká M, Bouša D, Pumera M, Sofer Z. Graphene oxide immobilized enzymes show high thermal and solvent stability. *Nanoscale* 2015;7:5852–8. <https://doi.org/10.1039/c5nr00438a>.
- [120] Ebrahimpour A, Rahman RNZRA, Basri M, Salleh AB. High level expression and characterization of a novel thermostable, organic solvent tolerant, 1,3-regioselective lipase from *Geobacillus* sp. strain ARM. *Bioresour Technol* 2011;102:6972–81. <https://doi.org/10.1016/j.biortech.2011.03.083>.
- [121] Lin SF. Production and stabilization of a solvent-tolerant alkaline lipase from *Pseudomonas pseudoalcaligenes* F-111. *J Ferment Bioeng* 1996;82:448–51.  
[https://doi.org/10.1016/S0922-338X\(97\)86981-4](https://doi.org/10.1016/S0922-338X(97)86981-4).

- [122] Lesuisse E, Schanck K, Colson C. Purification and preliminary characterization of the extracellular lipase of *Bacillus subtilis* 168, an extremely basic pH-tolerant enzyme. *Eur J Biochem* 1993;216:155–60. <https://doi.org/10.1111/j.1432-1033.1993.tb18127.x>.
- [123] Bose A, Keharia H. Production, characterization and applications of organic solvent tolerant lipase by *Pseudomonas aeruginosa* AAU2. *Biocatal Agric Biotechnol* 2013;2:255–66. <https://doi.org/10.1016/j.bcab.2013.03.009>.
- [124] Yan J, Yang J, Xu L, Yan Y. Gene cloning, overexpression and characterization of a novel organic solvent tolerant and thermostable lipase from *Galactomyces geotrichum* Y05. *J Mol Catal B Enzym* 2007;49:28–35. <https://doi.org/10.1016/j.molcatb.2007.07.006>.
- [125] Zhao H, Zheng L, Wang X, Liu Y, Xu L, Yan Y. Cloning, expression and characterization of a new lipase from *Yarrowia lipolytica*. *Biotechnol Lett* 2011;33:2445–52. <https://doi.org/10.1007/s10529-011-0711-8>.
- [126] Katiyar M, Ali A. Effect of metal ions on the hydrolytic and transesterification activities of *Candida rugosa* Lipase. *J Oleo Sci* 2013;62:912–24. <https://doi.org/10.5650/jos.62.919>.
- [127] Ateşlier ZBB, Metin K. Production and partial characterization of a novel thermostable esterase from a thermophilic *Bacillus* sp. *Enzyme Microb Technol* 2006;38:628–35. <https://doi.org/10.1016/j.enzmictec.2005.07.015>.
- [128] Li W, Li RW, Li Q, Du W, Liu D. Acyl migration and kinetics study of 1(3)-positional specific lipase of *Rhizopus oryzae*-catalyzed methanolysis of triglyceride for biodiesel production. *Process Biochem* 2010;45:1888–93.

- <https://doi.org/10.1016/j.procbio.2010.03.034>.
- [129] Šinkuniene D, Adlercreutz P. Effects of regioselectivity and lipid class specificity of lipases on transesterification, exemplified by biodiesel production. *JAACS, J Am Oil Chem Soc* 2014;91:1283–90. <https://doi.org/10.1007/s11746-014-2465-7>.
- [130] Okumura S, Iwai M, Tsujisaka Y. Positional specificities of four kinds of microbial lipases. *Agric Biol Chem* 1976;40:655–60. <https://doi.org/10.1080/00021369.1976.10862109>.
- [131] Canet A, Benaiges MD, Valero F, Adlercreutz P. Exploring substrate specificities of a recombinant *Rhizopus oryzae* lipase in biodiesel synthesis. *N Biotechnol* 2017;39:59–67. <https://doi.org/10.1016/j.nbt.2017.07.003>.
- [132] Cao X, Mangas-Sánchez J, Feng F, Adlercreutz P. Acyl migration in enzymatic interesterification of triacylglycerols: effects of lipases from *Thermomyces lanuginosus* and *Rhizopus oryzae*, support material, and water activity. *Eur J Lipid Sci Technol* 2016;118:1579–87. <https://doi.org/10.1002/ejlt.201500485>.
- [133] Ben Salah A, Fendri K, Gargoury Y. The enzyme of *Rhizopus oryzae* - Production, Purification and Biochemical Characteristics. *Rev Fr Des Corps Gras* 1994.
- [134] Di Lorenzo M, Hidalgo A, Haas M, Bornscheuer UT. Heterologous production of functional forms of *Rhizopus oryzae* lipase in *Escherichia coli*. *Appl Environ Microbiol* 2005;71:8974–7. <https://doi.org/10.1128/AEM.71.12.8974-8977.2005>.
- [135] Cregg JM, Madden KR, Barringer KJ, Thill GP, Stillman CA. Functional characterization of the two alcohol oxidase genes from the yeast *Pichia pastoris*. *Mol Cell Biol* 1989;9:1316. <https://doi.org/10.1128/MCB.9.3.1316>.

- [136] Sturmberger L, Chappell T, Geier M, Krainer F, Day KJ, Vide U, et al. Refined *Pichia pastoris* reference genome sequence. *J Biotechnol* 2016;235:121–31. <https://doi.org/10.1016/j.jbiotec.2016.04.023>.
- [137] Bernauer L, Radkohl A, Lehmayr LGK, Emmerstorfer-Augustin A. *Komagataella phaffii* as emerging model organism in fundamental research. *Front Microbiol* 2021;0:3462. <https://doi.org/10.3389/FMICB.2020.607028>.
- [138] Çelik E, Çalik P. Production of recombinant proteins by yeast cells. *Biotechnol Adv* 2012;30:1108–18. <https://doi.org/10.1016/j.biotechadv.2011.09.011>.
- [139] Juturu V, Wu JC. Heterologous protein expression in *Pichia pastoris*: latest research progress and applications. *ChemBioChem* 2018;19:7–21. <https://doi.org/10.1002/cbic.201700460>.
- [140] Ahmad M, Hirz M, Pichler H, Schwab H. Protein expression in *Pichia pastoris*: recent achievements and perspectives for heterologous protein production. *Appl Microbiol Biotechnol* 2014;98:5301–17. <https://doi.org/10.1007/s00253-014-5732-5>.
- [141] García-Ortega X, Cámara E, Ferrer P, Albiol J, Montesinos-Seguí JL, Valero F. Rational development of bioprocess engineering strategies for recombinant protein production in *Pichia pastoris* (*Komagataella phaffii*) using the methanol-free GAP promoter. Where do we stand? *N Biotechnol* 2019;53:24–34. <https://doi.org/10.1016/j.nbt.2019.06.002>.
- [142] Mattanovich D, Graf A, Stadlmann J, Dragosits M, Redl A, Maurer M, et al. Genome, secretome and glucose transport highlight unique features of the protein production host *Pichia pastoris*. *Microb Cell Fact* 2009;8:29.

- <https://doi.org/10.1186/1475-2859-8-29>.
- [143] Hemmerich J, Adelantado N, Barrigón JM, Ponte X, Hörmann A, Ferrer P, et al. Comprehensive clone screening and evaluation of fed-batch strategies in a microbioreactor and lab scale stirred tank bioreactor system: application on *Pichia pastoris* producing *Rhizopus oryzae* lipase. *Microb Cell Fact* 2014;13:36–52. <https://doi.org/10.1186/1475-2859-13-36>.
- [144] López-Fernández J, Benaiges MD, Valero F. *Rhizopus oryzae* lipase, a promising industrial enzyme: biochemical characteristics, production and biocatalytic applications. *Catalysts* 2020;10:1277. <https://doi.org/10.3390/catal10111277>.
- [145] Resina D, Serrano A, Valero F, Ferrer P. Expression of a *Rhizopus oryzae* lipase in *Pichia pastoris* under control of the nitrogen source-regulated formaldehyde dehydrogenase promoter. *J Biotechnol* 2004;109:103–13. <https://doi.org/10.1016/j.jbiotec.2003.10.029>.
- [146] Cos O, Resina D, Ferrer P, Montesinos JL, Valero F. Heterologous production of *Rhizopus oryzae* lipase in *Pichia pastoris* using the alcohol oxidase and formaldehyde dehydrogenase promoters in batch and fed-batch cultures. *Biochem Eng J* 2005;26:86–94. <https://doi.org/10.1016/j.bej.2005.04.005>.
- [147] Ponte X, Barrigón JM, Maurer M, Mattanovich D, Valero F, Montesinos-Seguí JL. Towards optimal substrate feeding for heterologous protein production in *Pichia pastoris* (*Komagataella* spp) fed-batch processes under  $P_{AOXI}$  control: a modeling aided approach. *J Chem Technol Biotechnol* 2018;93:3208–18. <https://doi.org/10.1002/jctb.5677>.
- [148] Kluge J, Terfehr D, Kück U. Inducible promoters and functional genomic

- approaches for the genetic engineering of filamentous fungi. *Appl Microbiol Biotechnol* 2018;102:6357–72. <https://doi.org/10.1007/s00253-018-9115-1>.
- [149] Thomas SM, DiCosimo R, Nagarajan V. Biocatalysis: Applications and potentials for the chemical industry. *Trends Biotechnol* 2002;20:238–42. [https://doi.org/10.1016/S0167-7799\(02\)01935-2](https://doi.org/10.1016/S0167-7799(02)01935-2).
- [150] Ranganathan SV, Narasimhan SL, Muthukumar K. An overview of enzymatic production of biodiesel. *Bioresour Technol* 2008;99:3975–81. <https://doi.org/10.1016/j.biortech.2007.04.060>.
- [151] Rodrigues J, Perrier V, Lecomte J, Dubreucq E, Ferreira-Dias S. Biodiesel production from crude jatropha oil catalyzed by immobilized lipase/acyltransferase from *Candida parapsilosis* in aqueous medium. *Bioresour Technol* 2016;218:1224–9. <https://doi.org/10.1016/j.biortech.2016.07.090>.
- [152] Mathew GM, Raina D, Narisetty V, Kumar V, Saran S, Pugazhendi A, et al. Recent advances in biodiesel production: challenges and solutions. *Sci Total Environ* 2021;794:148751. <https://doi.org/10.1016/J.SCITOTENV.2021.148751>.
- [153] Buysse C, Miller J. Transport could burn up the EU's entire carbon budget - International Council on Clean Transportation 2021. <https://theicct.org/transport-could-burn-up-the-eus-entire-carbon-budget/> (accessed January 16, 2022).
- [154] Tenenbaum DJ. Food vs. fuel diversion of crops could cause more hunger. *Environ Health Perspect* 2008;116:A254–7. <https://doi.org/10.1289/ehp.116-a254>.
- [155] Amin A. Review of diesel production from renewable resources: catalysis, process kinetics and technologies. *Ain Shams Eng J* 2019;201:112155–70.

- <https://doi.org/10.1016/j.asej.2019.08.001>.
- [156] Singh D, Sharma D, Soni SL, Sharma S, Kumar Sharma P, Jhalani A. A review on feedstocks, production processes, and yield for different generations of biodiesel. *Fuel* 2020;262:116553–68. <https://doi.org/10.1016/j.fuel.2019.116553>.
- [157] Yew GY, Lee SY, Show PL, Tao Y, Law CL, Nguyen TTC, et al. Recent advances in algae biodiesel production: from upstream cultivation to downstream processing. *Bioresour Technol Reports* 2019;7:100227. <https://doi.org/10.1016/j.biteb.2019.100227>.
- [158] Sitepu IR, Garay LA, Sestric R, Levin D, Block DE, German JB, et al. Oleaginous yeasts for biodiesel: current and future trends in biology and production. *Biotechnol Adv* 2014;32:1336–60. <https://doi.org/10.1016/j.biotechadv.2014.08.003>.
- [159] Singh D, Sharma D, Soni SL, Sharma S, Kumari D. Chemical compositions, properties, and standards for different generation biodiesels: A review. *Fuel* 2019;253:60–71. <https://doi.org/10.1016/j.fuel.2019.04.174>.
- [160] Ambat I, Srivastava V, Sillanpää M. Recent advancement in biodiesel production methodologies using various feedstock: a review. *Renew Sustain Energy Rev* 2018;90:356–69. <https://doi.org/10.1016/j.rser.2018.03.069>.
- [161] Guldhe A, Singh B, Mutanda T, Permaul K, Bux F. Advances in synthesis of biodiesel via enzyme catalysis: novel and sustainable approaches. *Renew Sustain Energy Rev* 2015. <https://doi.org/10.1016/j.rser.2014.09.035>.
- [162] Christopher LP, Hemanathan Kumar, Zambare VP. Enzymatic biodiesel:



- challenges and opportunities. *Appl Energy* 2014;119:497–520.  
<https://doi.org/10.1016/j.apenergy.2014.01.017>.
- [163] Santos S, Puna J, Gomes J. A review on bio-based catalysts (immobilized enzymes) used for biodiesel production. *Energies* 2020;13:3013–32.  
<https://doi.org/10.3390/en13113013>.
- [164] Bonet-Ragel K, Canet A, Benaiges MD, Valero F. Synthesis of biodiesel from high FFA *alperujo* oil catalysed by immobilised lipase. *Fuel* 2015;161:12–7.  
<https://doi.org/10.1016/j.fuel.2015.08.032>.
- [165] Lin YH, Luo JJ, John Hwang SC, Liao PR, Lu WJ, Lee HT. The influence of free fatty acid intermediate on biodiesel production from soybean oil by whole cell biocatalyst. *Biomass and Bioenergy* 2011;35:2217–23.  
<https://doi.org/10.1016/j.biombioe.2011.02.039>.
- [166] Aghababaie M, Beheshti M, Razmjou A, Bordbar AK. Enzymatic biodiesel production from crude *Eruca sativa* oil using *Candida rugosa* lipase in a solvent-free system using response surface methodology. *Biofuels* 2020;11:93–9.  
<https://doi.org/10.1080/17597269.2017.1345359>.
- [167] Guldhe A, Singh P, Renuka N, Bux F. Biodiesel synthesis from wastewater grown microalgal feedstock using enzymatic conversion: a greener approach. *Fuel* 2019;237:1112–8. <https://doi.org/10.1016/j.fuel.2018.10.033>.
- [168] Remonato D, de Oliveira JV, Manuel Guisan J, de Oliveira D, Ninow J, Fernandez-Lorente G. Production of FAME and FAEE via alcoholysis of sunflower oil by Eversa lipases immobilized on hydrophobic supports. *Appl Biochem Biotechnol* 2018;185:705–16. <https://doi.org/10.1007/S12010-017->

2683-1/FIGURES/6.

- [169] Martínez-Sánchez JA, Arana-Peña S, Carballares D, Yates M, Otero C, Fernandez-Lafuente R. Immobilized biocatalysts of Eversa® Transform 2.0 and lipase from *Thermomyces Lanuginosus*: comparison of some properties and performance in biodiesel production. *Catalysts* 2020;10:738. <https://doi.org/10.3390/CATAL10070738>.
- [170] Liu LH, Shih YH, Liu WL, Lin CH, Huang HY. Enzyme immobilized on nanoporous carbon derived from metal–organic framework: a new support for biodiesel synthesis. *ChemSusChem* 2017;10:1364–9. <https://doi.org/10.1002/cssc.201700142>.
- [171] Shah S, Gupta MN. The effect of ultrasonic pre-treatment on the catalytic activity of lipases in aqueous and non-aqueous media. *Chem Cent J* 2008;2. <https://doi.org/10.1186/1752-153X-2-1>.
- [172] Estevez R, Aguado-Deblas L, Bautista FM, Luna D, Luna C, Calero J, et al. Biodiesel at the crossroads: a critical review. *Catalysts* 2019;9:1033–71. <https://doi.org/10.3390/catal9121033>.
- [173] Dunn RO. Effects of monoacylglycerols on the cold flow properties of biodiesel. *JAACS, J Am Oil Chem Soc* 2012;89:1509–20. <https://doi.org/10.1007/s11746-012-2045-7>.
- [174] Calero J, Verdugo C, Luna D, Sancho ED, Luna C, Posadillo A, et al. Selective ethanolysis of sunflower oil with Lipozyme RM IM, an immobilized *Rhizomucor miehei* lipase, to obtain a biodiesel-like biofuel, which avoids glycerol production through the monoglyceride formation. *N Biotechnol* 2014;31:596–601.

- <https://doi.org/10.1016/j.nbt.2014.02.008>.
- [175] Bonet-Ragel K, Canet A, Benaiges MD, Valero F. Effect of acyl-acceptor stepwise addition strategy using *alperujo* oil as a substrate in enzymatic biodiesel synthesis. *J Chem Technol Biotechnol* 2018;93:541–7. <https://doi.org/10.1002/jctb.5399>.
- [176] Fredrick E, Moens K, Heyman B, Fischer S, Van der Meeren P, Dewettinck K. Monoacylglycerols in dairy recombined cream: I. The effect on milk fat crystallization. *Food Res Int* 2013;51:892–8. <https://doi.org/10.1016/j.foodres.2013.02.007>.
- [177] Itabaiiana I, Gonçalves KM, Cordeiro YML, Zoumpanioti M, Leal ICR, Miranda LSM, et al. Kinetics and mechanism of lipase catalyzed monoacylglycerols synthesis. *J Mol Catal B Enzym* 2013;96:34–9. <https://doi.org/10.1016/j.molcatb.2013.06.008>.
- [178] Feltes MMC, de Oliveira D, Block JM, Ninow JL. The production, benefits, and applications of monoacylglycerols and diacylglycerols of nutritional interest. *Food Bioprocess Technol* 2013;6:17–35. <https://doi.org/10.1007/s11947-012-0836-3>.
- [179] Canet A, Bonet-Ragel K, Benaiges MD, Valero F. Biodiesel synthesis in a solvent-free system by recombinant *Rhizopus oryzae*: comparative study between a stirred tank and a packed-bed batch reactor. *Biocatal Biotransformation* 2017;35:35–40. <https://doi.org/10.1080/10242422.2016.1278211>.
- [180] Ciudad G, Reyes I, Jorquera MA, Azócar L, Wick LY, Navia R. Novel three-phase bioreactor concept for fatty acid alkyl ester production using *R. oryzae* as whole cell catalyst. *World J Microbiol Biotechnol* 2011;27:2505–12. <https://doi.org/10.1007/s11274-011-0719-1>.

- [181] Jang MG, Kim DK, Park SC, Lee JS, Kim SW. Biodiesel production from crude canola oil by two-step enzymatic processes. *Renew Energy* 2012;42:99–104. <https://doi.org/10.1016/j.renene.2011.09.009>.
- [182] He Q, Shi H, Gu H, Naka G, Ding H, Li X, et al. Immobilization of *Rhizopus oryzae* ly6 onto loofah sponge as a whole-cell biocatalyst for biodiesel production. *BioResources* 2016;11:850–60. <https://doi.org/10.15376/biores.11.1.850-860>.
- [183] Su F, Li GL, Fan YL, Yan YJ. Enhancing biodiesel production via a synergic effect between immobilized *Rhizopus oryzae* lipase and Novozym 435. *Fuel Process Technol* 2015;137:298–304. <https://doi.org/10.1016/j.fuproc.2015.03.013>.
- [184] Zhou G xiong, Chen G yi, Yan B bei. Biodiesel production in a magnetically-stabilized, fluidized bed reactor with an immobilized lipase in magnetic chitosan microspheres. *Biotechnol Lett* 2014;36:63–8. <https://doi.org/10.1007/s10529-013-1336-x>.
- [185] Hama S, Yamaji H, Fukumizu T, Numata T, Tamalampudi S, Kondo A, et al. Biodiesel-fuel production in a packed-bed reactor using lipase-producing *Rhizopus oryzae* cells immobilized within biomass support particles. *Biochem Eng J* 2007;34:273–8. <https://doi.org/10.1016/j.bej.2006.12.013>.
- [186] Luna C, Verdugo C, Sancho ED, Luna D, Calero J, Posadillo A, et al. Biocatalytic behaviour of immobilized *Rhizopus oryzae* lipase in the 1,3-selective ethanolysis of sunflower oil to obtain a biofuel similar to biodiesel. *Molecules* 2014;19:11419–39. <https://doi.org/10.3390/molecules190811419>.
- [187] Luna C, Verdugo C, Sancho ED, Luna D, Calero J, Posadillo A, et al. A biofuel similar to biodiesel obtained by using a lipase from *Rhizopus oryzae*, optimized by

- response surface methodology. *Energies* 2014;7:3383–99.  
<https://doi.org/10.3390/en7053383>.
- [188] Meher LC, Churamani CP, Ahmed Z, Naik SN. *Jatropha curcas* as a renewable source for bio-fuels — A review. *Renew Sustain Energy Rev* 2013;26:397–407.  
<https://doi.org/10.1016/j.rser.2013.05.065>.
- [189] Li X, He XY, Li ZL, Wang YD, Wang CY, Shi H, et al. Enzymatic production of biodiesel from *Pistacia chinensis* bge seed oil using immobilized lipase. *Fuel* 2012;92:89–93. <https://doi.org/10.1016/j.fuel.2011.06.048>.
- [190] Arumugam A, Ponnusami V. Biodiesel production from *Calophyllum inophyllum* oil using lipase producing *Rhizopus oryzae* cells immobilized within reticulated foams. *Renew Energy* 2014;64:276–82.  
<https://doi.org/10.1016/j.renene.2013.11.016>.
- [191] Navarro López E, Robles Medina A, González Moreno PA, Esteban Cerdán L, Martín Valverde L, Molina Grima E. Biodiesel production from *Nannochloropsis gaditana* lipids through transesterification catalyzed by *Rhizopus oryzae* lipase. *Bioresour Technol* 2016;203:233–44.  
<https://doi.org/10.1016/j.biortech.2015.12.036>.
- [192] Navarro López E, Robles Medina A, González Moreno PA, Esteban Cerdán L, Molina Grima E. Extraction of microalgal lipids and the influence of polar lipids on biodiesel production by lipase-catalyzed transesterification. *Bioresour Technol* 2016;216:904–13. <https://doi.org/10.1016/j.biortech.2016.06.035>.
- [193] Araya K, Ugarte A, Azócar L, Valerio O, Wick LY, Ciudad G. Whole cell three phase bioreactors allow for effective production of fatty acid alkyl esters derived

- from microalgae lipids. Fuel 2015;144:25–32.  
<https://doi.org/10.1016/j.fuel.2014.12.014>.
- [194] Nematian T, Salehi Z, Shakeri A. Conversion of bio-oil extracted from *Chlorella vulgaris* micro algae to biodiesel via modified superparamagnetic nano-biocatalyst. Renew Energy 2020;146:1796–804.  
<https://doi.org/10.1016/j.renene.2019.08.048>.
- [195] Muanruksa P, Kaewkannetra P. Combination of fatty acids extraction and enzymatic esterification for biodiesel production using sludge palm oil as a low-cost substrate. Renew Energy 2020;146:901–6.  
<https://doi.org/10.1016/j.renene.2019.07.027>.
- [196] Karmee SK, Swanepoel W, Marx S. Biofuel production from spent coffee grounds via lipase catalysis. Energy Sources, Part A Recover Util Environ Eff 2018;40:294–300. <https://doi.org/10.1080/15567036.2017.1415394>.
- [197] Bharathiraja B, Ranjithkumar R, Chakravarthy M, Yogendran D, Vivek P, Yuvaraj D, et al. Kinetic analysis of fatty acid alkyl esters using whole cell biocatalyst and lipase catalyzed transesterification from waste cooking oil. Asian J Microbiol Biotechnol Environ Sci 2014;16:745–52.
- [198] Syed MB, Ali MY, Ishaq M, Bakkiyaraj S, Devanesan MG, Tangavelu V. Response surface optimization of biodiesel production using immobilized *Rhizopus oryzae* cells. Biofuels 2016;7:1–8.  
<https://doi.org/10.1080/17597269.2016.1153364>.
- [199] Sun T, Du W, Liu D. Comparative study on stability of whole cells during biodiesel production in solvent-free system. Process Biochem 2011;46:661–4.

- <https://doi.org/10.1016/j.procbio.2010.11.006>.
- [200] Ban K, Hama S, Nishizuka K, Kaieda M, Matsumoto T, Kondo A, et al. Repeated use of whole-cell biocatalysts immobilized within biomass support particles for biodiesel fuel production. *J Mol Catal - B Enzym* 2002;17:157–65. [https://doi.org/10.1016/S1381-1177\(02\)00023-1](https://doi.org/10.1016/S1381-1177(02)00023-1).
- [201] Bonet-Ragel K, López-Pou L, Tutusaus G, Benaiges MD, Valero F. Rice husk ash as a potential carrier for the immobilization of lipases applied in the enzymatic production of biodiesel. *Biocatal Biotransformation* 2018;36:151–8. <https://doi.org/10.1080/10242422.2017.1308498>.
- [202] Duarte SH, del Peso Hernández GL, Canet A, Benaiges MD, Maugeri F, Valero F. Enzymatic biodiesel synthesis from yeast oil using immobilized recombinant *Rhizopus oryzae* lipase. *Bioresour Technol* 2015;183:175–80. <https://doi.org/10.1016/j.biortech.2015.01.133>.
- [203] Su F, Li G, Zhang H, Yan Y. Enhanced performance of *Rhizopus oryzae* lipase immobilized on hydrophobic carriers and its application in biorefinery of rapeseed oil deodorizer distillate. *Bioenergy Res* 2014;7:935–45. <https://doi.org/10.1007/s12155-014-9415-y>.
- [204] Bakkiyaraj S, Syed MB, Devanesan MG, Thangavelu V. Production and optimization of biodiesel using mixed immobilized biocatalysts in packed bed reactor. *Environ Sci Pollut Res* 2016;23:9276–83. <https://doi.org/10.1007/s11356-015-4583-7>.
- [205] Balasubramanian B, Ramanujam PK, Ravi Kumar R, Muninathan C, Dhinakaran Y. Optimization of biological transesterification of waste cooking oil in different

- solvents using response surface methodology. *Manag Environ Qual An Int J* 2016;27:537–50. <https://doi.org/10.1108/MEQ-06-2015-0118>.
- [206] Nematian T, Shakeri A, Salehi Z, Saboury AA. Lipase immobilized on functionalized superparamagnetic few-layer graphene oxide as an efficient nanobiocatalyst for biodiesel production from *Chlorella vulgaris* bio-oil. *Biotechnol Biofuels* 2020;13. <https://doi.org/10.1186/s13068-020-01688-x>.
- [207] Athalye S, Sharma-Shivappa R, Peretti S, Kolar P, Davis JP. Producing biodiesel from cottonseed oil using *Rhizopus oryzae* ATCC #34612 whole cell biocatalysts: culture media and cultivation period optimization. *Energy Sustain Dev* 2013;17:331–6. <https://doi.org/10.1016/j.esd.2013.03.009>.
- [208] Vipin VC, Sebastian J, Muraleedharan C, Santhiagu A. Enzymatic transesterification of rubber seed oil using *Rhizopus Oryzae* lipase. *Procedia Technol* 2016;25:1014–21. <https://doi.org/10.1016/j.protcy.2016.08.201>.
- [209] Lee JH, Kim SB, Kang SW, Song YS, Park C, Han SO, et al. Biodiesel production by a mixture of *Candida rugosa* and *Rhizopus oryzae* lipases using a supercritical carbon dioxide process. *Bioresour Technol* 2011;102:2105–8. <https://doi.org/10.1016/j.biortech.2010.08.034>.
- [210] Zeng L, He Y, Jiao L, Li K, Yan Y. Preparation of biodiesel with liquid synergetic lipases from rapeseed oil deodorizer distillate. *Appl Biochem Biotechnol* 2017;183:778–91. <https://doi.org/10.1007/s12010-017-2463-y>.
- [211] Rodrigues J, Canet A, Rivera I, Osório NM, Sandoval G, Valero F, et al. Biodiesel production from crude *Jatropha* oil catalyzed by non-commercial immobilized heterologous *Rhizopus oryzae* and *Carica papaya* lipases. *Bioresour Technol*



- 2016;213:88–95. <https://doi.org/10.1016/j.biortech.2016.03.011>.
- [212] Mukhtar H, Khursheed S, Ikram-ul-Haq, Mumtaz MW, Rashid U, Al-Resayes SI. Optimization of lipase biosynthesis from *Rhizopus oryzae* for biodiesel production using multiple oils. Chem Eng Technol 2016;39:1–10. <https://doi.org/10.1002/ceat.201500584>.
- [213] Zhou G xiong, Chen G yi, Yan B bei. Two-step biocatalytic process using lipase and whole cell catalysts for biodiesel production from unrefined jatropha oil. Biotechnol Lett 2015;37:1959–63. <https://doi.org/10.1007/s10529-015-1883-4>.
- [214] Sattari S, Vahabzadeh F, Aghtaei HK. Performance of loofa-immobilized *Rhizopus oryzae* in the enzymatic production of biodiesel with use of oleic acid in n-hexane medium. Brazilian J Chem Eng 2015;32:367–76. <https://doi.org/10.1590/0104-6632.20150322s00003525>.
- [215] Ramachandran P, Narayanan GK, Gandhi S, Sethuraman S, Krishnan UM. *Rhizopus oryzae* lipase immobilized on hierarchical mesoporous silica supports for transesterification of rice bran oil. Appl Biochem Biotechnol 2015;175:2332–46. <https://doi.org/10.1007/s12010-014-1432-y>.
- [216] Zarei A, Amin NAS, Talebian-Kiakalaieh A, Zain NAM. Immobilized lipase-catalyzed transesterification of *Jatropha curcas* oil: optimization and modeling. J Taiwan Inst Chem Eng 2014;45:444–51. <https://doi.org/10.1016/j.jtice.2013.05.015>.
- [217] Canet A, Dolors Benaiges M, Valero F. Biodiesel synthesis in a solvent-free system by recombinant *Rhizopus oryzae* lipase. Study of the catalytic reaction progress. JAOCS, J Am Oil Chem Soc 2014;91:1499–506.

- <https://doi.org/10.1007/s11746-014-2498-y>.
- [218] Andrade GSS, Freitas L, Oliveira PC, De Castro HF. Screening, immobilization and utilization of whole cell biocatalysts to mediate the ethanolysis of babassu oil. *J Mol Catal B Enzym* 2012;84:183–8. <https://doi.org/10.1016/j.molcatb.2012.02.011>.
- [219] Deshmukh S, Kumar R, Bala K. Microalgae biodiesel: a review on oil extraction, fatty acid composition, properties and effect on engine performance and emissions. *Fuel Process Technol* 2019;191:232–47. <https://doi.org/10.1016/j.fuproc.2019.03.013>.
- [220] Yin Z, Zhu L, Li S, Hu T, Chu R, Mo F, et al. A comprehensive review on cultivation and harvesting of microalgae for biodiesel production: environmental pollution control and future directions. *Bioresour Technol* 2020;301:122804–23. <https://doi.org/10.1016/j.biortech.2020.122804>.
- [221] Lisboa P, Rodrigues AR, Martín JL, Simões P, Barreiros S, Paiva A. Economic analysis of a plant for biodiesel production from waste cooking oil via enzymatic transesterification using supercritical carbon dioxide. *J Supercrit Fluids* 2014;85:31–40. <https://doi.org/10.1016/j.supflu.2013.10.018>.
- [222] Tsoutsos T, Tournaki S, Gkouskos Z, Paraíba O, Giglio F, García PQ, et al. Quality characteristics of biodiesel produced from used cooking oil in Southern Europe. *ChemEngineering* 2019;3:19–32. <https://doi.org/10.3390/chemengineering3010019>.
- [223] Yaakob Z, Mohammad M, Alherbawi M, Alam Z, Sopian K. Overview of the production of biodiesel from waste cooking oil. *Renew Sustain Energy Rev*

- 2013;18:184–93. <https://doi.org/10.1016/j.rser.2012.10.016>.
- [224] Mandolesi De Araújo CD, De Andrade CC, De Souza E Silva E, Dupas FA. Biodiesel production from used cooking oil: a review. *Renew Sustain Energy Rev* 2013;27:445–52. <https://doi.org/10.1016/j.rser.2013.06.014>.
- [225] Zhang Y, Dubé MA, McLean DD, Kates M. Biodiesel production from waste cooking oil: 2. Economic assessment and sensitivity analysis. *Bioresour Technol* 2003;90:229–40. [https://doi.org/10.1016/S0960-8524\(03\)00150-0](https://doi.org/10.1016/S0960-8524(03)00150-0).
- [226] Wahab RA, Elias N, Abdullah F, Ghoshal SK. On the taught new tricks of enzymes immobilization: an all-inclusive overview. *React Funct Polym* 2020;152:104613. <https://doi.org/10.1016/j.reactfunctpolym.2020.104613>.
- [227] Sheldon RA, Woodley JM. Role of biocatalysis in sustainable chemistry. *Chem Rev* 2018;118:801–38. <https://doi.org/10.1021/acs.chemrev.7b00203>.
- [228] Fukuda H, Hama S, Tamalampudi S, Noda H. Whole-cell biocatalysts for biodiesel fuel production. *Trends Biotechnol* 2008;26:668–73. <https://doi.org/10.1016/j.tibtech.2008.08.001>.
- [229] Fernandez-Lafuente R, Armisén P, Sabuquillo P, Fernández-Lorente G, Guisán JM. Immobilization of lipases by selective adsorption on hydrophobic supports. *Chem Phys Lipids* 1998;93:185–97. [https://doi.org/10.1016/S0009-3084\(98\)00042-5](https://doi.org/10.1016/S0009-3084(98)00042-5).
- [230] Fernandez-Lorente G, Rocha-Martín J, Guisan JM. Immobilization of lipases by adsorption on hydrophobic supports: modulation of enzyme properties in biotransformations in anhydrous media. *Methods Mol Biol* 2020;21000:143–58.

- [https://doi.org/10.1007/978-1-0716-0215-7\\_9](https://doi.org/10.1007/978-1-0716-0215-7_9).
- [231] Wang YD, Shen XY, Li ZL, Li X, Wang F, Nie XA, et al. Immobilized recombinant *Rhizopus oryzae* lipase for the production of biodiesel in solvent free system. *J Mol Catal B Enzym* 2010;67:45–51. <https://doi.org/10.1016/j.molcatb.2010.07.004>.
- [232] Tan T, Lu J, Nie K, Deng L, Wang F. Biodiesel production with immobilized lipase: a review. *Biotechnol Adv* 2010;28:628–34. <https://doi.org/10.1016/j.biotechadv.2010.05.012>.
- [233] Balasubramaniam B, Sudalaiyadum Perumal A, Jayaraman J, Mani J, Ramanujam P. Comparative analysis for the production of fatty acid alkyl esterase using whole cell biocatalyst and purified enzyme from *Rhizopus oryzae* on waste cooking oil (sunflower oil). *Waste Manag* 2012;32:1539–47. <https://doi.org/10.1016/j.wasman.2012.03.011>.
- [234] Zhao X, Qi F, Yuan C, Du W, Liu D. Lipase-catalyzed process for biodiesel production: enzyme immobilization, process simulation and optimization. *Renew Sustain Energy Rev* 2015;44:182–97. <https://doi.org/10.1016/j.rser.2014.12.021>.
- [235] Mendes AA, Freitas L, De Carvalho AKF, De Oliveira PC, De Castro HF. Immobilization of a commercial lipase from *Penicillium camembertii* (Lipase G) by different strategies. *Enzyme Res* 2011;2011. <https://doi.org/10.4061/2011/967239>.
- [236] Illanes A. Enzyme biocatalysis: principles and applications. *Enzym. Biocatal. Princ. Appl.*, 2008, p. 172–3. <https://doi.org/10.1007/978-1-4020-8361-7>.

- [237] Norjannah B, Ong HC, Masjuki HH, Juan JC, Chong WT. Enzymatic transesterification for biodiesel production: a comprehensive review. *RSC Adv* 2016;6:60034–55. <https://doi.org/10.1039/c6ra08062f>.
- [238] Lotti M, Pleiss J, Valero F, Ferrer P. Effects of methanol on lipases: molecular, kinetic and process issues in the production of biodiesel. *Biotechnol J* 2015;10:22–30. <https://doi.org/10.1002/biot.201400158>.
- [239] Ferreira-Dias S, Sandoval G, Plou F, Valero F. The potential use of lipases in the production of fatty acid derivatives for the food and nutraceutical industries. *Electron J Biotechnol* 2013;16. <https://doi.org/10.2225/vol16-issue3-fulltext-5>.
- [240] Guo Y, Cai Z, Xie Y, Ma A, Zhang H, Rao P, et al. Synthesis, physicochemical properties, and health aspects of structured lipids: A review. *Compr Rev Food Sci Food Saf* 2020;19:759–800. <https://doi.org/10.1111/1541-4337.12537>.
- [241] Smith RE, Finley JW, Leveille GA. Overview of SALATRIM, a Family of low-calorie fats. *J Agric Food Chem* 1994;42:432–4. <https://doi.org/10.1021/jf00038a036>.
- [242] Osborn HT, Akoh CC. Structured lipids-novel fats with medical, nutraceutical, and food applications. *Compr Rev Food Sci Food Saf* 2002;1:110–20. <https://doi.org/10.1111/j.1541-4337.2002.tb00010.x>.
- [243] López-López A, Castellote-Bargalló AI, Campoy-Folgozo C, Rivero-Urgel M, Tormo-Carnicé R, Infante-Pina D, et al. The influence of dietary palmitic acid triacylglyceride position on the fatty acid, calcium and magnesium contents of at term newborn faeces. *Early Hum Dev* 2001;65:S83–94. [https://doi.org/10.1016/S0378-3782\(01\)00210-9](https://doi.org/10.1016/S0378-3782(01)00210-9).

- [244] Şahin N, Akoh CC, Karaalı A. Human milk fat substitutes containing omega-3 fatty acids. *J Agric Food Chem* 2006;54:3717–22. <https://doi.org/10.1021/jf053103f>.
- [245] Tecelão C, Silva J, Dubreucq E, Ribeiro MH, Ferreira-Dias S. Production of human milk fat substitutes enriched in omega-3 polyunsaturated fatty acids using immobilized commercial lipases and *Candida parapsilosis* lipase/acyltransferase. *J Mol Catal B Enzym* 2010;65:122–7. <https://doi.org/10.1016/J.MOLCATB.2010.01.026>.
- [246] Biswas N, Cheow YL, Tan CP, Siow LF. Physicochemical properties of enzymatically produced palm-oil-based Cocoa Butter Substitute (CBS) with cocoa butter mixture. *Eur J Lipid Sci Technol* 2018;120:1700205. <https://doi.org/10.1002/ejlt.201700205>.
- [247] Yamoneka J, Malumba P, Lognay G, Béra F, Blecker C, Danthine S. Enzymatic inter-esterification of binary blends containing *Irvingia gabonensis* seed fat to produce cocoa butter substitute. *Eur J Lipid Sci Technol* 2018;120:1700423. <https://doi.org/10.1002/ejlt.201700423>.
- [248] Lakum R, Sonwai S. Production of trans-free margarine fat by enzymatic interesterification of soy bean oil, palm stearin and coconut stearin blend. *Int J Food Sci Technol* 2018;53:2761–9. <https://doi.org/10.1111/ijfs.13888>.
- [249] Li Y, Zhao J, Xie X, Zhang Z, Zhang N, Wang Y. A low trans margarine fat analog to beef tallow for healthier formulations: optimization of enzymatic interesterification using soybean oil and fully hydrogenated palm oil. *Food Chem* 2018;255:405–13. <https://doi.org/10.1016/j.foodchem.2018.02.086>.

- [250] Kawashima A, Shimada Y, Yamamoto M, Sugihara A, Nagao T, Komemushi S, et al. Enzymatic synthesis of high-purity structured lipids with caprylic acid at 1, 3-positions and polyunsaturated fatty acid at 2-position. *JAOCS, J Am Oil Chem Soc* 2001;78:611–6. <https://doi.org/10.1007/s11746-001-0313-0>.
- [251] Lo SK, Tan CP, Long K, Yusoff MSA, Lai OM. Diacylglycerol oil-properties, processes and products: a review. *Food Bioprocess Technol* 2008;1:223–33. <https://doi.org/10.1007/s11947-007-0049-3>.
- [252] Iwasaki Y, Yamane T. Enzymatic synthesis of structured lipids. *Adv Biochem Eng Biotechnol* 2004;10:129–40. <https://doi.org/10.1201/9780203908198.ch21>.
- [253] Kim BH, Akoh CC. Recent research trends on the enzymatic synthesis of structured lipids. *J Food Sci* 2015;80:C1713–24. <https://doi.org/10.1111/1750-3841.12953>.
- [254] Utama QD, Sitanggang AB, Adawiyah DR, Hariyadi P. Lipase-catalyzed interesterification for the synthesis of medium-long-medium (MLM) structured lipids - A review. *Food Technol Biotechnol* 2019;57:305–18. <https://doi.org/10.17113/ftb.57.03.19.6025>.
- [255] Nunes PA, Pires-Cabral P, Guillén M, Valero F, Luna D, Ferreira-Dias S. Production of MLM-type structured lipids catalyzed by immobilized heterologous *Rhizopus oryzae* lipase. *JAOCS, J Am Oil Chem Soc* 2011;64:57–68. <https://doi.org/10.1007/s11746-010-1702-y>.
- [256] Mota DA, Rajan D, Heinzl GC, Osório NM, Gominho J, Krause LC, et al. Production of low-calorie structured lipids from spent coffee grounds or olive pomace crude oils catalyzed by immobilized lipase in magnetic nanoparticles.

- Bioresour Technol 2020;307:123223–32.  
<https://doi.org/10.1016/j.biortech.2020.123223>.
- [257] Costa CM, Osório NM, Canet A, Rivera I, Sandoval G, Valero F, et al. Production of MLM type structured lipids from grapeseed oil catalyzed by non-commercial lipases. Eur J Lipid Sci Technol 2018;120:1700320–8.  
<https://doi.org/10.1002/ejlt.201700320>.
- [258] Nagao T, Kawashima A, Sumida M, Watanabe Y, Akimoto K, Fukami H, et al. Production of structured TAG rich in 1,3-capryloyl-2-arachidonoyl glycerol from *Mortierella* single-cell oil. JAOCS, J Am Oil Chem Soc 2003;80:867–72.  
<https://doi.org/10.1007/s11746-003-0787-9>.
- [259] Nunes PA, Pires-Cabral P, Guillén M, Valero F, Ferreira-Dias S. Batch operational stability of immobilized heterologous *Rhizopus oryzae* lipase during acidolysis of virgin olive oil with medium-chain fatty acids. Biochem Eng J 2012;67:265–8.  
<https://doi.org/10.1016/j.bej.2012.06.004>.
- [260] Nunes PA, Pires-Cabral P, Guillén M, Valero F, Ferreira-Dias S. Optimized production of MLM triacylglycerols catalyzed by immobilized heterologous *Rhizopus oryzae* lipase. JAOCS, J Am Oil Chem Soc 2012;89:1287–95.  
<https://doi.org/10.1007/s11746-012-2027-9>.
- [261] Balieiro AL, Osório NM, Lima ÁS, Soares CMF, Valero F, Ferreira-Dias S. Production of dietetic triacylglycerols from olive oil catalyzed by immobilized heterologous *Rhizopus oryzae* lipase. Chem Eng Trans 2018;64.  
<https://doi.org/10.3303/CET1864065>.
- [262] Esteban L, Jiménez MJ, Hita E, González PA, Martín L, Robles A. Production of



- structured triacylglycerols rich in palmitic acid at *sn*-2 position and oleic acid at *sn*-1,3 positions as human milk fat substitutes by enzymatic acidolysis. *Biochem Eng J* 2011;54:62–9. <https://doi.org/10.1016/j.bej.2011.01.009>.
- [263] Simões T, Valero F, Tecelão C, Ferreira-Dias S. Production of human milk fat substitutes catalyzed by a heterologous *Rhizopus oryzae* lipase and commercial lipases. *JAOCS, J Am Oil Chem Soc* 2014;91:411–9. <https://doi.org/10.1007/s11746-013-2379-9>.
- [264] Faustino AR, Osório NM, Tecelão C, Canet A, Valero F, Ferreira-Dias S. Camelina oil as a source of polyunsaturated fatty acids for the production of human milk fat substitutes catalyzed by a heterologous *Rhizopus oryzae* lipase. *Eur J Lipid Sci Technol* 2016;118:532–44. <https://doi.org/10.1002/ejlt.201500003>.
- [265] Tecelão C, Guillén M, Valero F, Ferreira-Dias S. Immobilized heterologous *Rhizopus oryzae* lipase: a feasible biocatalyst for the production of human milk fat substitutes. *Biochem Eng J* 2012;67:104–10. <https://doi.org/10.1016/J.BEJ.2012.06.001>.
- [266] Muñío M del M, Robles A, Esteban L, González PA, Molina E. Synthesis of structured lipids by two enzymatic steps: ethanolysis of fish oils and esterification of 2-monoacylglycerols. *Process Biochem* 2009;44:723–30. <https://doi.org/10.1016/j.procbio.2009.03.002>.
- [267] Hita E, Robles A, Camacho B, Ramírez A, Esteban L, Jiménez MJ, et al. Production of structured triacylglycerols (STAG) rich in docosahexaenoic acid (DHA) in position 2 by acidolysis of tuna oil catalyzed by lipases. *Process Biochem* 2007;42:415–22. <https://doi.org/10.1016/j.procbio.2006.09.023>.

- [268] Rodríguez A, Esteban L, Martín L, Jiménez MJ, Hita E, Castillo B, et al. Synthesis of 2-monoacylglycerols and structured triacylglycerols rich in polyunsaturated fatty acids by enzyme catalyzed reactions. *Enzyme Microb Technol* 2012;51:148–55. <https://doi.org/10.1016/j.enzmictec.2012.05.006>.
- [269] Zhou D, Xu X, Mu H, HØY CE, Adler-Nissen J. Lipase-catalyzed production of structured lipids via acidolysis of fish oil with caprylic acid. *J Food Lipids* 2000;7:263–74. <https://doi.org/10.1111/j.1745-4522.2000.tb00177.x>.
- [270] Paula A V., Nunes GFM, De Castro HF, Santos JC. Synthesis of structured lipids by enzymatic interesterification of milkfat and soybean oil in a basket-type stirred tank reactor. *Ind Eng Chem Res* 2015;54:1731–7. <https://doi.org/10.1021/ie503189e>.
- [271] Ray J, Nagy ZK, Smith KW, Bhaggan K, Stapley AGF. Kinetic study of the acidolysis of high oleic sunflower oil with stearic-palmitic acid mixtures catalysed by immobilised *Rhizopus oryzae* lipase. *Biochem Eng J* 2013;73:17–28. <https://doi.org/10.1016/j.bej.2012.12.018>.
- [272] Yang T, Fruekilde MB, Xu X. Suppression of acyl migration in enzymatic production of structured lipids through temperature programming. *Food Chem* 2005;92:101–7. <https://doi.org/10.1016/j.foodchem.2004.07.007>.
- [273] SÁ AGA, Meneses AC de, Araújo PHH de, Oliveira D de. A review on enzymatic synthesis of aromatic esters used as flavor ingredients for food, cosmetics and pharmaceuticals industries. *Trends Food Sci Technol* 2017;69:95–105. <https://doi.org/10.1016/j.tifs.2017.09.004>.
- [274] Gao W, Wu K, Chen L, Fan H, Zhao Z, Gao B, et al. A novel esterase from a

- marine mud metagenomic library for biocatalytic synthesis of short-chain flavor esters. *Microb Cell Fact* 2016;15:41–53. <https://doi.org/10.1186/s12934-016-0435-5>.
- [275] Huang S-M, Huang H-Y, Chen Y-M, Kuo C-H, Shieh C-J. Continuous production of 2-phenylethyl acetate in a solvent-free system using a packed-bed reactor with Novozym® 435. *Catalysts* 2020;10:714–27. <https://doi.org/10.3390/catal10060714>.
- [276] Bayout I, Bouzemi N, Guo N, Mao X, Serra S, Riva S, et al. Natural flavor ester synthesis catalyzed by lipases. *Flavour Fragr J* 2020;35:209–18. <https://doi.org/10.1002/ffj.3554>.
- [277] Asmat S, Husain Q. A robust nanobiocatalyst based on high performance lipase immobilized to novel synthesised poly(o-toluidine) functionalized magnetic nanocomposite: sterling stability and application. *Mater Sci Eng C* 2019;99:25–36. <https://doi.org/10.1016/j.msec.2019.01.070>.
- [278] Asmat S, Anwer AH, Husain Q. Immobilization of lipase onto novel constructed polydopamine grafted multiwalled carbon nanotube impregnated with magnetic cobalt and its application in synthesis of fruit flavours. *Int J Biol Macromol* 2019;140:484–95. <https://doi.org/10.1016/j.ijbiomac.2019.08.086>.
- [279] Moreira WC, Elias ALP, Osório WR, Padilha GS. Alternative method to improve the ethyl valerate yield using an immobilised *Burkholderia cepacia* lipase. *J Microencapsul* 2019;36:327–37. <https://doi.org/10.1080/02652048.2019.1626927>.
- [280] Rodriguez-Nogales JM, Roura E, Contreras E. Biosynthesis of ethyl butyrate using

- immobilized lipase: a statistical approach. *Process Biochem* 2005;40:63–8. <https://doi.org/10.1016/j.procbio.2003.11.049>.
- [281] Guillén M, Benaiges MD, Valero F. Biosynthesis of ethyl butyrate by immobilized recombinant *Rhizopus oryzae* lipase expressed in *Pichia pastoris*. *Biochem Eng J* 2012;65:1–9. <https://doi.org/10.1016/j.bej.2012.03.009>.
- [282] Guillén M, Benaiges MD, Valero F. Improved ethyl butyrate synthesis catalyzed by an immobilized recombinant *Rhizopus oryzae* lipase: a comprehensive statistical study by production, reaction rate and yield analysis. *J Mol Catal B Enzym* 2016;133:S371–6. <https://doi.org/10.1016/j.molcatb.2017.02.010>.
- [283] Grosso C, Ferreira-Dias S, Pires-Cabral P. Modelling and optimization of ethyl butyrate production catalysed by *Rhizopus oryzae* lipase. *J Food Eng* 2013;115:475–80. <https://doi.org/10.1016/j.jfoodeng.2012.08.001>.
- [284] Ben Salah R, Ghamghui H, Miled N, Mejdoub H, Gargouri Y. Production of butyl acetate ester by lipase from novel strain of *Rhizopus oryzae*. *J Biosci Bioeng* 2007;103:368–72. <https://doi.org/10.1263/jbb.103.368>.
- [285] Kumari A, Mahapatra P, Garlapati VK, Banerjee R, Dasgupta S. Lipase mediated isoamyl acetate synthesis in solvent-free system using vinyl acetate as acyl donor. *Food Technol Biotechnol* 2009;47:13–8.
- [286] Ghamgui H, Karra-Chaâbouni M, Bezzine S, Miled N, Gargouri Y. Production of isoamyl acetate with immobilized *Staphylococcus simulans* lipase in a solvent-free system. *Enzyme Microb Technol* 2006;38:788–94. <https://doi.org/10.1016/j.enzmictec.2005.08.011>.

- [287] Garlapati VK, Banerjee R. Solvent-free synthesis of flavour esters through immobilized lipase mediated transesterification. *Enzyme Res* 2013;2013:367410. <https://doi.org/10.1155/2013/367410>.
- [288] Dhake KP, Deshmukh KM, Patil YP, Singhal RS, Bhanage BM. Improved activity and stability of *Rhizopus oryzae* lipase via immobilization for citronellol ester synthesis in supercritical carbon dioxide. *J Biotechnol* 2011;156:46–51. <https://doi.org/10.1016/j.jbiotec.2011.08.019>.
- [289] Rios NS, Pinheiro BB, Pinheiro MP, Bezerra RM, dos Santos JCS, Barros Gonçalves LR. Biotechnological potential of lipases from *Pseudomonas*: sources, properties and applications. *Process Biochem* 2018;75:99–120. <https://doi.org/10.1016/j.procbio.2018.09.003>.
- [290] Kirchner G, Scollar MP, Klibanov AM. Resolution of racemic mixtures via lipase catalysis in organic solvents. *J Am Chem Soc* 1985;107:7072–6. <https://doi.org/10.1021/ja00310a052>.
- [291] Palomo JM, Segura RL, Fernandez-Lorente G, Guisán JM, Fernandez-Lafuente R. Enzymatic resolution of ( $\pm$ )-glycidyl butyrate in aqueous media. Strong modulation of the properties of the lipase from *Rhizopus oryzae* via immobilization techniques. *Tetrahedron Asymmetry* 2004;15:1157–61. <https://doi.org/10.1016/j.tetasy.2004.03.003>.
- [292] Songür R, Lurçi B, Bayraktar E, Mehmetoğlu Ü, Demir AS. Enantioselective production of benzoin from benzoin acetate via kinetic resolution and deracemization using *Rhizopus oryzae*. *Artif Cells, Blood Substitutes, Biotechnol* 2011;39:162–8. <https://doi.org/10.3109/10731199.2010.516261>.

- [293] Cabrera Z, Palomo JM. Enantioselective desymmetrization of prochiral diesters catalyzed by immobilized *Rhizopus oryzae* lipase. *Tetrahedron Asymmetry* 2011;22:2080–4. <https://doi.org/10.1016/j.tetasy.2011.11.012>.
- [294] Yousefi M, Mohammadi M, Habibi Z. Enantioselective resolution of racemic ibuprofen esters using different lipases immobilized on octyl sepharose. *J Mol Catal B Enzym* 2014;104:87–94. <https://doi.org/10.1016/j.molcatb.2014.03.005>.
- [295] Matsumoto T, Ito M, Fukuda H, Kondo A. Enantioselective transesterification using lipase-displaying yeast whole-cell biocatalyst. *Appl Microbiol Biotechnol* 2004;64:481–5. <https://doi.org/10.1007/s00253-003-1486-1>.
- [296] Nakamura Y, Matsumoto T, Nomoto F, Ueda M, Fukuda H, Kondo A. Enhancement of activity of lipase-displaying yeast cells and their application to optical resolution of (R,S)-1-benzyloxy-3-chloro-2-propyl monosuccinate. *Biotechnol Prog* 2006;22:998–1002. <https://doi.org/10.1021/bp060136m>.
- [297] Geyer R, Jambeck JR, Law KL. Production, use, and fate of all plastics ever made. *Sci Adv* 2017;3:1700782. <https://doi.org/10.1126/sciadv.1700782>.
- [298] Thakur S, Chaudhary J, Sharma B, Verma A, Tamulevicius S, Thakur VK. Sustainability of bioplastics: opportunities and challenges. *Curr Opin Green Sustain Chem* 2018;13:68–75. <https://doi.org/10.1016/J.COGSC.2018.04.013>.
- [299] Narancic T, O'Connor KE. Microbial biotechnology addressing the plastic waste disaster. *Microb Biotechnol* 2017;10:1232–5. <https://doi.org/10.1111/1751-7915.12775>.
- [300] Scalenghe R. Resource or waste? A perspective of plastics degradation in soil with

- a focus on end-of-life options. *Heliyon* 2018;4:e00941.  
<https://doi.org/10.1016/j.heliyon.2018.e00941>.
- [301] RameshKumar S, Shaiju P, O'Connor KE, P RB. Bio-based and biodegradable polymers - state-of-the-art, challenges and emerging trends. *Curr Opin Green Sustain Chem* 2020;21:75–81. <https://doi.org/10.1016/j.cogsc.2019.12.005>.
- [302] Babu RP, O'Connor K, Seeram R. Current progress on bio-based polymers and their future trends. *Prog Biomater* 2013 21 2013;2:1–16.  
<https://doi.org/10.1186/2194-0517-2-8>.
- [303] European Bioplastics e.V. Bioplastics – European Bioplastics e.V. 2015.  
<https://www.european-bioplastics.org/bioplastics/> (accessed August 19, 2021).
- [304] George A, Sanjay MR, Srisuk R, Parameswaranpillai J, Siengchin S. A comprehensive review on chemical properties and applications of biopolymers and their composites. *Int J Biol Macromol* 2020;154:329–38.  
<https://doi.org/10.1016/J.IJBIOMAC.2020.03.120>.
- [305] Nakajima H, Dijkstra P, Loos K. The recent developments in biobased polymers toward general and engineering applications: polymers that are upgraded from biodegradable polymers, analogous to petroleum-derived polymers, and newly developed. *Polymers* 2017;9:523. <https://doi.org/10.3390/polym9100523>.
- [306] Chuensangjun C, Pechyen C, Chisti Y, Sirisansaneeyakul S. Lipase-catalysed polymerization of lactic acid and the properties of the polymer. *Adv Mater Res* 2012;506:154–7. <https://doi.org/10.4028/www.scientific.net/AMR.506.154>.
- [307] Corneillie S, Smet M. PLA architectures: the role of branching. *Polym Chem*

- 2015;6:850–67. <https://doi.org/10.1039/C4PY01572J>.
- [308] Kobayashi S. Recent developments in lipase-catalyzed synthesis of polyesters. *Macromol Rapid Commun* 2009;30:237–66. <https://doi.org/10.1002/MARC.200800690>.
- [309] Gupta B, Revagade N, Hilborn J. Poly(lactic acid) fiber: an overview. *Prog Polym Sci* 2007;32:455–82. <https://doi.org/10.1016/J.PROGPOLYMSCI.2007.01.005>.
- [310] Lassalle VL, Ferreira ML. Lipase-catalyzed synthesis of polylactic acid: an overview of the experimental aspects. *J Chem Technol Biotechnol* 2008;83:1493–502. <https://doi.org/10.1002/jctb.1994>.
- [311] Cama G, Mogosanu DE, Houben A, Dubruel P. Synthetic biodegradable medical polyesters: poly- $\sigma$ -caprolactone. *Sci. Princ. Biodegrad. Bioresorbable Med. Polym. Mater. Prop.*, Woodhead Publishing; 2017, p. 79–105. <https://doi.org/10.1016/B978-0-08-100372-5.00003-9>.
- [312] Douka A, Vouyiouka S, Papaspyridi LM, Papaspyrides CD. A review on enzymatic polymerization to produce polycondensation polymers: the case of aliphatic polyesters, polyamides and polyesteramides. *Prog Polym Sci* 2018;79:1–25. <https://doi.org/10.1016/J.PROGPOLYMSCI.2017.10.001>.
- [313] Uyama H, Takeya K, Kobayashi S. Enzymatic ring-opening polymerization of lactones to polyesters by lipase catalyst: unusually high reactivity of macrolides. *Bull Chem Soc Jpn* 1995;68:56–61. <https://doi.org/10.1246/bcsj.68.56>.
- [314] Kiran KR, Divakar S. Lipase-catalysed polymerization of lactic acid and its film forming properties. *World J Microbiol Biotechnol* 2003 198 2003;19:859–65.



<https://doi.org/10.1023/A:1026004229239>.

- [315] Omay D, Guvenilir Y. Synthesis and characterization of poly(d,l-lactic acid) via enzymatic ring opening polymerization by using free and immobilized lipase.

<Http://DxDoiOrg/103109/102424222013795148> 2013;31:132–40.

<https://doi.org/10.3109/10242422.2013.795148>.

- [316] Rahmayetty, Whulanza Y, Sukirno, Rahman SF, Suyono EA, Yohda M, et al. Use of *Candida rugosa* lipase as a biocatalyst for L-lactide ring-opening polymerization and polylactic acid production. *Biocatal Agric Biotechnol* 2018;16:683–91. <https://doi.org/10.1016/J.BCAB.2018.09.015>.

# 2

## Objectives



The main objective pursued by the elaboration of this thesis consists of improving *Rhizopus oryzae* lipase (ROL) heterologous production in *Komagataella phaffii* (*Pichia pastoris*) cell factory to obtain a cheaper and more stable biocatalyst capable of being employed in biotransformation of industrial interest. In summary, this objective can be broken down into the following sections:

- Employ immobilized mature sequence ROL (rROL) for biodiesel production:
  - Assess the effect of immobilization support surface groups.
  - Evaluate biodiesel synthesis for second- and third-generation biofuel production.
  - Scale-up biodiesel production to lab-scale reactor (50 mL).
  - In-line monitoring biodiesel synthesis with near infrared spectroscopy (NIR).
- Add the 28 C-terminal amino acids from the native prosequence to mature sequence lipase (proROL) to enhance heterologous production of the enzyme, lower heterologous production bioprocess complexity and, increase enzyme stability:
  - Test proROL heterologous expression in *K. phaffii* under  $P_{AOXI}$  and  $P_{GAP}$ .
  - Biochemically characterize free proROL and evaluate its stability (free and immobilized).
- Assess the synthesis of flavours esters through lipase-based esterification of isoamyl alcohol with butyric acid and acetic acid and scale-up (250 mL reactor) the best performing reaction conditions.
- Use of proROL in polylactic acid biopolymer synthesis through direct lactic acid condensation and ring-opening polymerization of lactides and compare the results with *Candida rugosa* lipase 1.



# 3

## Materials and Methods



### 3. MATERIALS AND METHODS CONTENT

<b>3.1. Materials</b> .....	121
<b>3.2. Lipase heterologous expression</b> .....	122
<b>3.2.1. Plasmids and strains</b> .....	122
<b>3.2.2. Batch cultures</b> .....	123
<b>3.2.3. Fed-batch cultures</b> .....	124
3.2.3.1. Fed-batch cultures: methanol inducible promoter .....	125
3.2.3.2. Fed-batch cultures: constitutive promoter .....	126
3.2.3.3. Biomass determination by dry cell weight (DCW) .....	126
3.2.3.4. Glycerol and methanol determination by HPLC .....	127
3.2.3.5. Fermentation process calculations.....	127
<b>3.2.4. Lipase downstream</b> .....	128
<b>3.3. Lipolytic activity analysis</b> .....	129
<b>3.4. Substrate specificity to <i>p</i>-nitrophenols esters</b> .....	130
<b>3.5. Total protein analysis</b> .....	130
<b>3.6. Electrophoresis techniques</b> .....	131
<b>3.6.1. SDS-PAGE</b> .....	131
<b>3.6.2. Zymogram</b> .....	131
<b>3.6.3. Western blot</b> .....	132
<b>3.7. Proteolytic activity inhibition</b> .....	132
<b>3.8. N-terminal analysis</b> .....	133
<b>3.9. Free enzyme stability analysis</b> .....	133
<b>3.10. Synthesis of MNPs and functionalization with amino groups</b> .....	134
<b>3.11. Functionalization of supports with aldehyde groups</b> .....	134
<b>3.12. Lipase immobilization</b> .....	135
<b>3.13. Immobilized rROL and proROL stability against organic solvents</b> .....	136
<b>3.14. Transesterification reactions: biodiesel production</b> .....	136



<b>3.14.1. Diffusional restriction assessment: transesterification reaction</b> .....	138
<b>3.14.2. Transesterification reaction scale up</b> .....	138
3.14.2.1. Acquisition and processing of near infrared (NIR) spectra .....	139
<b>3.15. Esterification reactions</b> .....	141
<b>3.15.1. Ethyl butyrate production</b> .....	141
<b>3.15.2. Isoamyl esters production</b> .....	141
3.15.2.1. Effect of acid concentration and acid:alcohol molar ratio on reaction parameters during isoamyl esters production .....	142
3.15.2.2. Isoamyl ester esterification reaction scale up .....	143
<b>3.16. Operational stability: half-lives calculations</b> .....	144
<b>3.17. Polymerization reactions</b> .....	145
<b>3.17.1. Direct lactic acid condensation</b> .....	145
<b>3.17.2. Ring-opening polymerization</b> .....	145
<b>3.17.3. Effect of initial lactic acid concentration and total added activity units on lactic acid conversion and total converted amount</b> .....	145
<b>3.18. Gas chromatography analysis of synthesized esters</b> .....	146
<b>3.18.1. FAMEs and FAEEs analysis</b> .....	146
<b>3.18.2. Ethyl butyrate analysis</b> .....	147
<b>3.18.3. Isoamyl esters analysis</b> .....	147
<b>3.19. Oleaginous substrates acidity determination</b> .....	148
<b>3.20. Fatty acid composition determination in WCO</b> .....	148
<b>3.21. Lactic acid conversion assessment</b> .....	148
<b>3.22. NMR spectroscopy</b> .....	149
<b>3.23. References</b> .....	151

### 3.1. Materials

Olive pomace oil (*alperujo oil*) was a gift from Professor Eulogio Castro (University of Jaen, Spain); microbial oil from a modified strain of *Rhodospiridium toruloides* was supplied by Neol Biosolutions (Granada, Spain); jatropha and makauba oils were kindly donated by Professor Denise Freire (Universidade Federal do Rio de Janeiro, Brazil); and WCO was obtained from a local public waste management company. All oils were centrifuged prior to use.

Polymethacrylate matrix supports D6307 (containing epoxide and butyl surface groups, EB), D6308 (containing epoxide and octadecyl surface groups, EO) and D6309 (containing epoxide and divinylbenzene surface groups, EDVB) were kindly supplied by Purolite® (King of Prussia, PA, USA).

The colorimetric kit for enzymatic assay 11821729 was obtained from Roche (Mannheim, Deutschland) and bovine serum albumin standard (Ref. 11811345) was supplied by Thermo Fisher Scientific (Waltham, MA, USA). Butyric acid, isoamyl alcohol, acetic acid, fusel oil and isoamyl butyrate were kindly provided by Hausmann, S.L. (Barcelona, Spain). KOH, heptane, ethanol and methanol were purchased from Panreac (Barcelona, Spain). Cyclohexane, hexane, isooctane, toluene, limonene, anisole, *p*-cymene, pyridine, 2-methylpyridine, chloroform (CDCl<sub>3</sub>), *n*-Butylamine solution, 3-aminopropyltriethoxysilane (APTS), ammonium sulphate, NaBH<sub>4</sub>, FeCl<sub>2</sub>, FeCl<sub>3</sub>, molecular sieves 3Å, L-lactic acid (80% liquid solution), lactide (3,6-Dimethyl-1,4-dioxane-2,5-dione), standards of isoamyl acetate, ethyl butyrate, methyl/ethyl palmitate, methyl/ethyl stearate, methyl/ethyl oleate, methyl/ethyl linoleate, methyl linoleate, 4-Methylumbelliferyl butyrate (MUF-butyrate), *p*-nitrophenyl esters,

phenylmethylsulfonyl fluoride (PMSF), culture media reagents, and all unstated reagents were obtained from Sigma–Aldrich (St. Louis, MO, USA).

## 3.2. Lipase heterologous expression

### 3.2.1. Plasmids and strains

Four different plasmids were used, namely: two pPICZ $\alpha$ A plasmids containing the mature sequence of *Rhizopus oryzae* lipase (rROL P<sub>AOXI</sub>-plasmid), and a derivative thereof containing the 28 C-terminal amino acids of the prosequence of the native lipase in the N-terminal of rROL (proROL P<sub>AOXI</sub>-plasmid), the pair expressed under the inducible promoter of alcohol oxidase 1 (P<sub>AOXI</sub>). The region corresponding to the 28 amino acids was codon-optimized, as it was also done with mature sequence, for *P. pastoris* (GenScript, Piscataway, NJ, USA) and flanked with XhoI and Bts $\alpha$ I restriction sites for subsequent digestion-ligation and cloning. The rROL P<sub>AOXI</sub>-plasmid natively contained both restriction sites, so cloning left no unwanted sequences in it. In both rROL and proROL P<sub>AOXI</sub>-plasmids, P<sub>AOXI</sub> was replaced with the constitutive glyceraldehyde-3-phosphate dehydrogenase promoter (P<sub>GAP</sub>) from pGAPZ $\alpha$ A plasmid. Because exchanged fragments natively contained flanking sequences of BglII and XhoI restrictions sites, no unwanted nucleotides remained in the anew formed plasmids (rROL P<sub>GAP</sub>-plasmid and proROL P<sub>GAP</sub>-plasmid).

*Pichia pastoris* X33 strains were transformed by electroporing 100 ng of the previously linearized corresponding plasmids (e.g. proROL P<sub>AOXI</sub>-plasmid, proROL P<sub>GAP</sub>-plasmid and rROL P<sub>GAP</sub>-plasmid). In P<sub>GAP</sub>-plasmid transformations, a blank consisting of empty pPICZ $\alpha$ A plasmid with the exchanged promoters was additionally

used as a control. In all the cases, the resulting colonies were re-streaked twice on YPD-Zeo plates to avoid population mixing, and five to eight isolated colonies screened as described elsewhere [1], the most representative colony in each run being selected for further study. Single-gene copies were confirmed by digital droplet PCR with the primers 5'-CCCTGTCGTCCAAGAACAAC-3' and 5'-GAGGACCACCAACAGTGAAG-3' for rROL and proROL, and 5'-CCTGAGGCTTTGTTCCACCCATCT-3' and 5'-GGAACATAGTAGTACCACCGGACATAACGA-3' for actin [2].

### 3.2.2. Batch cultures

The inoculum culture was grown for 24 h in a 1 L baffled shake flask at 30 °C and 150 rpm. The flask was filled with 100 mL YPG medium containing 10 g L<sup>-1</sup> yeast extract, 20 g L<sup>-1</sup> peptone, and 20 g L<sup>-1</sup> glycerol and zeocin to a final concentration 100 µg mL<sup>-1</sup> [3]. Then, a sample was centrifuged and resuspended in 100 mL of sterile water. This was followed by the addition of the inoculum to the bioreactor at OD<sub>600</sub> = 2 (for strains transformed with P<sub>AOXI</sub>-plasmid) or OD<sub>600</sub> = 0.1 (for strains transformed with P<sub>GAP</sub>-plasmid) in a culture volume of 1 L. Cells were cultivated in a 2 L bioreactor (Applikon Biotechnology, Delft, Netherlands).

Invitrogen culture medium [26.7 mL 85% H<sub>3</sub>PO<sub>4</sub>, 0.93 g CaSO<sub>4</sub>, 18.2 g K<sub>2</sub>SO<sub>4</sub>, 14.9 g MgSO<sub>4</sub>·7H<sub>2</sub>O, 4.13 g KOH, and 2 mL 200 mg L<sup>-1</sup> biotin], 10 g methanol L<sup>-1</sup>, 5 mL of a trace salts stock solution, and a 0.15 mL L<sup>-1</sup> concentration of antifoaming agent (A6426, Sigma–Aldrich Co.) were used for strains harboring P<sub>AOXI</sub>-plasmid while strains harboring P<sub>GAP</sub>-plasmid were cultured in a medium containing 2.0 g citric acid, 12.4 g (NH<sub>4</sub>)<sub>2</sub>HPO<sub>4</sub>, 0.022 g CaCl<sub>2</sub>·2H<sub>2</sub>O, 0.9 g KCl, 0.5 g MgSO<sub>4</sub>·7H<sub>2</sub>O, 40 g glycerol, 4.6 mL trace salts stock solution and 2 mL 200 mg L<sup>-1</sup> biotin, both of them in a final volume of

1 L culture. The trace salt solution (PTM) contained the following amounts per liter: 6 g  $\text{CuSO}_4 \cdot 5\text{H}_2\text{O}$ , 0.08 g NaI, 3 g  $\text{MnSO}_4 \cdot \text{H}_2\text{O}$ , 0.2 g  $\text{Na}_2\text{MoO}_4 \cdot 2\text{H}_2\text{O}$ , 0.02 g  $\text{H}_3\text{BO}_3$ , 0.5 g  $\text{CoCl}_2$ , 20 g  $\text{ZnCl}_2$ , 65 g  $\text{FeSO}_4 \cdot 7\text{H}_2\text{O}$  and 5 mL concentrated  $\text{H}_2\text{SO}_4$ . The biotin and the trace salt solution were sterilized separately by filtration (SLGV013SL 0.22  $\mu\text{m}$ , Millipore Corporation, Billerica, MA, USA). The growing conditions were adapted from reported recommendations [4]. Cells were grown at 30 °C and at constant pH of 5.5 with rROL harboring strain and pH of 5 with proROL harboring strain by adding 15% (v/v)  $\text{NH}_4\text{OH}$  as required. The oxygen concentration was set at 25% and controlled by cascade stirring between 500 rpm and 1200 rpm with constant aeration at 1 vvm.

Samples were withdrawn at different times from the reactor and analyzed for lipolytic activity, biomass, glycerol and methanol concentration. The end of each batch run was detected by a sudden increase of dissolved oxygen (DO) concentration in the culture broth [4]. All tests were performed in duplicate.

### ***3.2.3. Fed-batch cultures***

The inoculum was grown as described in the previous section and added to the bioreactor at a final  $\text{OD}_{600}$  of 1.5 in 2 L of the same culture medium used in the batch tests for each strain, although methanol was replaced with 40 g  $\text{L}^{-1}$  glycerol in the corresponding strain. Fed-batch cultures were run in a 5 L Biostat B bioreactor from Sartorius (Guxhagen, Germany) and as described for batch cultures, samples were withdrawn at different times and analyzed for lipolytic activity, biomass, glycerol and methanol concentration.

### 3.2.3.1. Fed-batch cultures: methanol inducible promoter

Following to the first stage of batch culture, strains harboring  $P_{AOXI}$ -plasmids were submitted to transition stage to assure a proper shift from growing conditions with glycerol, in which the inducible promoter is repressed, to the final stage, the induction stage, with methanol as substrate and inductor. Thus, in the last stage promoter is required to be derepressed.

Transition stage entails the use of glycerol (50% w/w) and methanol as feeding to gradually, during 5 h, decrease the feeding rates of glycerol while maintaining a constant feeding rate of methanol to ensure a methanol concentration that favors promotor derepression [5].

Induction stage was performed with methanol as the sole carbon source to facilitate protein induction. Two already described strategies were followed for methanol addition, methanol-limited fed-batch cultures (MLFB) and methanol non-limited fed-batch cultures (MNLFB) [6]. Under MLFB strategy, pre-fixed 0.015 and 0.045  $\text{h}^{-1}$  specific growth rates were employed, while for MNLFB, methanol concentration was set at 3  $\text{g L}^{-1}$ , the already published optimum concentration for rROL-strain [6]. Methanol concentration was monitored and controlled with a Raven Biotech (Vancouver, BC, Canada) probe immersed in the culture broth. Oxygen concentration was fixed at 25% and controlled by a cascade stirring first (between 500 to 1200 rpm) and, second, in case of necessity, by enriching gas inlet flow composition with pure oxygen maintaining a constant aeration of 1.5 vvm.

During transition and induction stage, pH set-point was controlled using KOH 5 M due to the interferences that  $\text{NH}_4\text{OH}$  could provoke in the methanol probe signal.

Consequently, nitrogen supplementation was performed with NH<sub>4</sub>Cl solution (200 g NH<sub>4</sub>Cl, 5 mL of trace salts stock and 2 mL of biotin per L of distilled water) with a feeding rate subordinated to methanol one through an estimated ammonium chloride/methanol yield of 0.12 g g<sup>-1</sup>. Further information about the fed-batch bioprocess can be found elsewhere [6,7].

### 3.2.3.2. Fed-batch cultures: constitutive promoter

Batch stage of P<sub>GAP</sub>-plasmid harboring strain was directly followed by the fed-batch stage which was conducted with glucose as sole carbon source, using a carbon-limited feeding strategy and a preset exponential feeding rate intended to maintain a constant specific growth rate of 0.045 h<sup>-1</sup>. The feeding was supplemented by the following composition per liter: 400 g of glucose, 10 g KCl, 6.45 g MgSO<sub>4</sub>·7H<sub>2</sub>O, 0.35 g CaCl<sub>2</sub>·2H<sub>2</sub>O, biotin 0.02% (6 mL), trace salts stock solution (15 mL) and antifoam (0.2 mL).

### 3.2.3.3. Biomass determination by dry cell weight (DCW)

Biomass concentration of the samples was determined as DCW by withdrawing 8 mL samples of the bioreactor; these were then filtered through dried at 105 °C and pre-weighed glass microfibre filters (Whatman GF/F, Maidstone, UK), which were subsequently washed with two volumes of distilled water and dried again at 105 °C to a constant weight. Determinations were performed by triplicate and the relative standard deviation (RSD) was about 4%.

#### 3.2.3.4. Glycerol and methanol determination by high-performance liquid chromatography (HPLC)

The concentration of glycerol and methanol was measured by means of HPLC (Dionex Ultimate 3000, from ThermoFisher) analysis using an anionic exchange column (ICSepICE-COR-EGEL87H3, Transgenomic, NE, USA) as previously described [8]. The mobile phase was 6 mM sulfuric acid, and the sample injection volume was 20  $\mu$ L. Chromeleon software (Dionex) was used for data treatment. Determinations were performed by triplicate and RSD was always less than 2%.

#### 3.2.3.5. Fermentation process calculations

Equations for feeding strategies and fermentation parameters were established following the corresponding balances and already published works [6,9]. Pre-programmed exponential feeding rate for carbon-limited fed-batches (both methanol and glucose) with the objective to control the specific growth rate of the culture at time ( $t$ ) can be obtained from fed-batch substrate balance:

$$\mu(t) = \frac{Y_{X/S}F(t)S_0}{V(t)X(t)} \quad (3.1)$$

By integrating the fed-batch cell mass balance (Eq 3.2) and combining it with the previous equation, the feeding rate  $F(t)$  for a fixed specific growth rate can be expressed by the following equation:

$$X(t)V(t) = X(t_0)V(t_0)\exp[\mu(t - t_0)] \quad (3.2)$$

$$F(t) = \frac{\mu[X(t_0)V(t_0)]}{Y_{X/S}S_0} \exp[\mu(t - t_0)] \quad (3.3)$$



This feeding rate equation can be applied if  $V$  and  $X$  are known at the beginning of the fermentation and if  $Y_{X/S}$  is assumed as constant along the process. Then, feeding can be calculated depending on the value of the first addition with the following equation:

$$F(t + \Delta t) = F(t)\exp(\mu\Delta t) \quad (3.4)$$

For MNLFB feeding strategy, a predictive-PI control was established to maintain the desired concentration of methanol in the culture medium.

$$F(t + \Delta t) = F(t) - \frac{V}{(S_{feed} - S_t)} \cdot \frac{dS}{dt} + K_p \left( \varepsilon_t + \frac{1}{\tau_i} \int_0^t \varepsilon_t dt \right) \quad (3.5)$$

Fermentation procedure rates ( $\mu$  and  $q_p$ ) were obtained by performing mass balances inside the bioreactor for fed-batch operation:

$$\mu = \frac{1}{(XV)} \frac{d(XV)}{dt} \quad (3.6)$$

$$q_p = \left( \frac{dP}{dt} + \frac{FP}{V} \right) \frac{1}{X} \quad (3.7)$$

### 3.2.4. Lipase downstream

rROL and proROL production fed-batch runs were followed by supernatant centrifugation and microfiltration, firstly with 0.7  $\mu\text{m}$  glass fiber prefilters (Merck Millipore Ltd. Tullagreen, Carrigtwohill Co., Cork, Ireland) and secondly with 0.45  $\mu\text{m}$  aqueous nylon membranes (Merck Millipore Ltd.). Then, ultrafiltration and subsequently, diafiltration and concentration in a Tris-HCl 10 mM pH 7 buffer were performed employing a 10 kDa cut-off Centrasette membrane (Pall Filtron, New York, USA). Thus obtained concentrate was lyophilized and stored at  $-20\text{ }^\circ\text{C}$ .

proROL derived lipase (proROLm) was obtained by action of proteases over dissolved proROL [10]. Then, centrifugation and passage through 0.2  $\mu\text{m}$  filters was performed to remove unwanted contaminants.

*Candida rugosa* lipase 1 (CRL1) fed-batch supernatants, kindly donated by the Bioprocess and Applied Biocatalysis group members, were submitted to the same procedure like rROL and proROL so as to obtain lyophilized powder of CRL1. Identical buffer (Tris-HCl 10 mM pH 7) and membrane (10 kDa cut-off Centrasette) were employed.

### 3.3. Lipolytic activity analysis

Lipase activity was determined on a Cary 300 spectrophotometer from Varian (Mulgrave, VIC, Australia), using the 11821792 lipase colorimetric kit from Roche (Mannheim, Germany) in 200 mM Tris-HCl buffer at pH 7.25 at 30 °C. Measurements were made in triplicate with an estimated RSD of 5% following a published procedure [11,12]. Briefly, 300  $\mu\text{L}$  substrate (1,2-O-dilauryl-rac-glycero-3-glutaric-(methylresoru-fin)-ester) was mixed with 500  $\mu\text{L}$  of Tris-HCl buffer and 500  $\mu\text{L}$  of diluted sample in a thermostatically controlled cuvette. The absorbance increase at 580 nm was followed for 7 min and the slope correlated to the lipolytic assay using pH-stat analysis. One unit of lipolytic activity was defined as the amount of lipase required to hydrolyze 1  $\mu\text{mol}$  of ester bond per minute under assay conditions.

As Roche discontinued the colorimetric kit employed for lipolytic activity analysis, a correlation was performed on a Specord 200 Plus spectrophotometer from Analytic Jena (Jena, Germany) using *p*-nitrophenyl butyrate (*p*NPB) by adapting a

procedure described elsewhere [13]. 500  $\mu$ L of the diluted sample was mixed with 800  $\mu$ L of reaction buffer (phosphate buffer, 50 mM pH 7.25) and the activity was monitored at 348 nm and at 30 °C during 7 minutes. Activity units were correlated to those obtained with the Roche colorimetric kit.

### **3.4. Substrate specificity to *p*-nitrophenols esters**

Substrate specificity was assessed by monitoring the hydrolysis of C-4 to C-12 *p*-nitrophenol esters with a Cary Varian 300 spectrophotometer at 30 °C in 50 mM phosphate buffer at pH 7, 0.32% (w/v) Triton X-100, 4% (v/v) acetone and 1mM *p*-nitrophenol ester concentration (for the C12 and C10 2.5% w/v Triton X-100 was used due to the low solubility of these compounds). Activity assay was performed following an already described procedure [14].

### **3.5. Total protein analysis**

Extracellular protein concentration was determined by using the Bradford method with bovine serum albumin as standard and Pierce Coomassie (Bradford) Protein Assay Kit from Thermo Fisher Scientific [15]. Assays were performed in triplicate with an RSD lower than 5%.

## 3.6. Electrophoresis techniques

### 3.6.1. SDS-PAGE

Sodium dodecyl sulphate-polyacrylamide gel electrophoresis (SDS-PAGE) was carried out in a Mini-PROTEAN II apparatus from BioRad (Hercules, CA, USA) with 12% Mini-PROTEAN® TGX™ Precast Protein Gels (Ref. 4561043) and following the recommendations given by the manufacturer and already described procedures [14]. Prestained all blue and unstained Precision Plus Protein™ standards from BioRad were used for molecular weight determination and band quantification, respectively. Colloidal solution of Coomassie G250 (34% v/v ethanol, 2% v/v H<sub>3</sub>PO<sub>4</sub>, 17% w/v NH<sub>4</sub>SO<sub>4</sub> and 0.066% Coomassie G250) was employed for staining gels.

Gel Doc™ EZ Imager and ImageLab v.5.2 software from BioRad were used for image analysis and quantification.

### 3.6.2. Zymogram

Zymograms were performed as previously described [14,16]. Briefly, before staining the SDS-PAGE gel, the SDS was removed by submerging the gel into a 2.5% Triton X-100 solution during 2 h at room temperature. Then, Tris-HCl 20 mM pH 7 buffer was employed for washing the gel twice for 15 mins each time and, afterwards, it was incubated during 30 seconds in a 100 μM MUF-butyrate solution in the same buffer. Finally, the gel was exposed to UV illumination to detect fluorescent bands and stained using G250 colloidal solution to determine the molecular weight of each active protein.

Gel Doc™ EZ Imager and ImageLab v.5.2 software from BioRad were used for image analysis.

### **3.6.3. Western blot**

Western blot tests were done after SDS-PAGE and prior to staining. Proteins were transferred from the gel to a nitrocellulose membrane (Trans-Blot Turbo Midi Nitrocellulose Transfer Pack, BioRad) by using the Trans-Blot® Turbo™ Transfer System (10 min, 2.5 A, 25 V) from BioRad. Then, the membrane was blocked by incubation during 1 h in a solution 5% skim milk and 1 mL Tween 20 and afterwards, incubated with mouse anti-ROL antiserum obtained from the *Servei de Cultius Cel·lulars, Producció d'Anticossos i Citometria (Universitat Autònoma de Barcelona, Bellaterra, Spain)* for lipase immunorecognition. After washing, the HRP-conjugated polyclonal anti-mouse IgG from Sigma Aldrich was employed as secondary antibody. Finally, detection was performed by incubating with Clarify™ Western ECL substrate for 5 minutes [17].

Image analysis and quantification were done with a Molecular Imager® ChemiDoc™ XRS System (BioRad) and the software ImageLab v.5.2. rROL purified samples of known concentration were used for 2-point calibration and sample quantification in western blot.

### **3.7. Proteolytic activity inhibition**

Proteolytic activity inhibition was assessed by using the PMSF inhibitor at a 1.5 mg mL<sup>-1</sup> concentration in ethanol mixed with lipase solution in 5 mM phosphate buffer at pH 7 [18]. Blanks containing no PMSF (C1), or neither alcohol nor PMSF (C2), were also used.

An additional blank (C3) was prepared by sterilizing a sample of lipase solution by filtration with 0.22  $\mu\text{m}$  pore size from Millipore Corporation (Billerica, MA, USA). All samples were kept in a roller at room temperature for 24 h.

### 3.8. N-terminal analysis

The N-terminal sequences of proROL, proROLm (see Section 3.2.4) and rROL were determined by automated Edman's degradation thanks to the group of professor María Jesús Martínez and Alicia Prieto from the *Centro de investigaciones Biológicas (CSIC)*, where the analyses were performed [19]. The resulting sequences were further examined by using the Protein BLAST tool from the National Centre for Biotechnology Information (NCBI).

### 3.9. Free enzyme stability analysis

Temperature and pH stability were examined by dissolving lyophilized lipase powder in 200 mM Tris-HCl buffer under suitable pH and temperature conditions. Samples were withdrawn for analysis after 1 h and 24 h.

Alcohol tolerance of lipases was assessed in 200 mM Tris-HCl buffer at pH 8.12 and 25 °C, containing 0%–30% (v/v) alcohol. Samples were withdrawn for analysis over the first 24 h.

Enzymatic activity was determined by the previously described method (Section 3.3., Roche colorimetric kit), diluting the sample not to alter lipolytic activity assay conditions.

Stability studies were done under sterile conditions by previously passing the samples through a filter of 0.2  $\mu\text{m}$  pore size to avoid unwanted proteases coming from microbial contaminants.

### **3.10. Synthesis of magnetic nanoparticles (MNPs) and functionalization with amino groups**

Nanoparticles of magnetite ( $\text{Fe}_3\text{O}_4$ ) were synthesized and functionalized with amino groups (MNPs- $\text{NH}_2$ ) following an already described protocol [20]. Briefly, magnetite nanoparticles were produced through coprecipitation of an aqueous solution of 0.36 M  $\text{FeCl}_2$  and 0.72 M  $\text{FeCl}_3$  into a 1 M solution of  $\text{NH}_4\text{OH}$ . Thus, obtained black precipitate was separated from the liquid phase using a magnetic field and washed thrice with ultrapure water (MilliQ, Millipore Co.) and twice with PBS (phosphate buffered saline). Obtained nanoparticles contained superficial  $-\text{OH}$ , so an incubation with 2% v/v APTS at 70  $^\circ\text{C}$  under orbital shaking during 24 h was performed. Then, amino functionalized nanoparticles were washed thrice with PBS and kept in the same buffer at 4  $^\circ\text{C}$  until use.

All solutions used for MNPs synthesis and functionalization were prepared in nitrogen-bubbled ultrapure water. The dry weight and concentration of MNPs were determined by using a VR-1/120/240 vacuum concentrator from Heto Lab Equipment (Zealand, Denmark).

### **3.11. Functionalization of supports with aldehyde groups**

Two types of immobilization supports based on polymethacrylate and magnetite were used. The polymethacrylate-based supports (Purolite®) included the support with

epoxide and butyl functional groups (EB); with epoxide and octadecyl groups (EO) and with epoxide and divinylbenzene groups (EDVB). All were conditioned as described elsewhere [21]. Succinctly, epoxide groups were converted firstly into amino groups by incubating 1 g of dried support with 1 M ethylenediamine solution pH 10 at 60 °C during 4 h. Afterwards, solution was vacuum filtered and rinsed with distilled water. Secondly, amino groups were transformed to aldehyde groups by incubating the support with a 2.5% w/v glutaraldehyde solution in phosphate buffer 0.1 M at pH 8 on a roller during 2 h at room temperature. Finally, support was vacuum filtered and rinsed with distilled water.

Previously functionalized MNPs-NH<sub>2</sub> were simply pretreated with glutaraldehyde following the same protocol described for polymethacrylate supports. The resulting aldehyde-functionalized MNPs (MNP-CHO) were further modified by incubation in a 0–1 M butylamine solution in 100 mM phosphate buffer pH 8 at room temperature for 2 h to obtain MNP-But-CHO. MNPs were washed three times with PBS after each step and stored at 4°C until use.

### 3.12. Lipase immobilization

Lipase was immobilized onto the above-described polymethacrylate- and magnetite-based supports by using a modified version of a previously reported method [21]. Unless otherwise stated, 1 g of glutaraldehyde-treated support (dry weight for MNPs) was mixed with a 3500 AU lipase mL<sup>-1</sup> solution at 4°C for 42 h. The polymethacrylate biocatalysts thus obtained (EB-rROL/proROL, EO-rROL/proROL, EDVB-rROL) were vacuum-filtered and dried on silica gel, whereas the magnetite-based biocatalysts were recovered by application of a magnetic field, washed three times with PBS and concentrated to 2 mg mL<sup>-1</sup>.



When indicated, Schiff bases and unreacted aldehyde groups were reduced by incubating the supports with a 1 mg mL<sup>-1</sup> NaBH<sub>4</sub> solution in 100 mM phosphate buffer at pH 8 at room temperature for 2 h [20].

The specific activity of the biocatalysts (immobilized AU mg support<sup>-1</sup>) was calculated as the difference between those of the blank and supernatant solutions divided by the final weight (MNP dry weight) of biocatalyst. The immobilization yield (IY) for the polymethacrylate supports was estimated by exposing them to lipase solutions at concentrations from 55 to 1000 AU mg support<sup>-1</sup>:

$$IY (\%) = \frac{\text{Biocatalyst specific activity}}{\text{offered activity units}} \times 100 \quad (3.8)$$

### 3.13. Immobilized rROL and proROL stability against organic solvents

The stability of EB-proROL and EB-rROL against organic solvents was assessed by using closed vials of 10 mL. Thus, a total amount of 5000 AU of each biocatalyst was incubated with 5 mL of the corresponding solvent at 25 °C under stirring at 350 rpm in the IKA KS 400 incubator (IKA, Staufen, Germany) for 24 h. Then, the biocatalysts were washed with heptane twice and the initial rate of ethyl butyrate production was determined as described in Section 3.15.1. All data given are relative to the initial reaction rate of the same amount of non-incubated biocatalyst for each lipase.

### 3.14. Transesterification reactions: biodiesel production

Reaction runs were conducted in 10 mL closed vials containing 8 g of the corresponding oil and a total amount of biocatalyst of 32000 AU at 30 °C that were placed in the IKA KS 400 incubator under orbital stirring at 350 rpm. Ethanol or methanol was added in 1,

5 or 10 pulses by splitting the stoichiometric volume of alcohol (2:1 alcohol/oil) into 1, 5 or 10 portions, respectively, that were added during the reaction to reach the theoretical maximum yield (66% considering the 1,3-regiospecificity of ROL) following an already described procedure [22].

Olive pomace oil was used as model to investigate diffusional restrictions, the initial reaction rate and the operational stability when assessing different biocatalysts performance. The best performing biocatalyst (amongst the biocatalysts obtained by employing different immobilization supports) was used for further evaluation of the initial reaction rate and operational stability with alternative substrates including jatropha oil, WCO, makauba oil and microbial oil. All reactions components were pre-equilibrated for water activity, using saturated KOH ( $a_w = 0.093$ ) overnight (a minimum of 16 h) [22].

In general, the initial transesterification rate was calculated by adding 0.16 mL of methanol to 8 g of oil (viz., the stoichiometric amount needed to obtain a yield of ca. 14%) and a total amount of biocatalyst of 32000 AU [23]. An identical procedure was followed to assess diffusional restrictions but using an identical mass of biocatalyst (200 mg) with variable immobilized lipase activity.

Operational stability was assessed by causing the biocatalyst to deposit in the vial bottom by decantation (Purolite®) or application of a magnetic field (magnetite) and removing the medium after each reaction run [22].

The optimum butylamine concentration for MNP-CHO functionalization was established by assessing the operational stability of the modified biocatalysts (MNP-But-CHO). Tests were conducted as described above but in triplicate, using a scaled-down reaction volume (1.5 mL vials) and only 1 pulse of ethanol.

### 3.14.1. Diffusional restriction assessment: transesterification reaction

The Weisz–Prater criterion, which is a dimensionless number used to assess internal diffusional restrictions [24,25] was calculated by substituting experimental data from the biodiesel reactions into Eq. 3.9:

$$\Phi = \frac{r_{obs} \rho_p}{D_{eff} C_{m,0}} \left( \frac{V_p}{A_p} \right)^2 \quad (3.9)$$

where  $r_{obs}$  denotes transesterification rate ( $\text{mol g}_{\text{particle}}^{-1} \text{s}^{-1}$ ),  $\rho_p$  particle density ( $\text{g cm}^{-3}$ ),  $V_p$  particle volume ( $\text{cm}^3$ ),  $A_p$  particle area ( $\text{cm}^2$ ),  $C_{m,0}$  bulk concentration of methanol ( $\text{mol cm}^{-3}$ ) and  $D_{eff}$  ( $\text{cm}^2 \text{s}^{-1}$ ) the effective diffusivity coefficient as calculated from Eq. 3.10:

$$D_{eff} = \frac{D_{m,a} \varepsilon_p \sigma}{\tau} \quad (3.10)$$

$D_{m,a}$  ( $\text{cm}^2 \text{s}^{-1}$ ) being the molecular diffusivity of methanol in the reaction medium (olive pomace oil) as estimated from the Nakanishi correlation [26],  $\varepsilon_p$  particle porosity,  $\sigma$  the constriction factor and  $\tau$  particle tortuosity.  $\Phi$  values under 0.3 ensure the absence of internal diffusional restrictions since the resulting effectiveness factor is close to unity [25].

### 3.14.2. Transesterification reaction scale up

Transesterification reaction was scaled up to a 50 mL Scharlau HME-R mini-reactor from Scharlab (Sentmenat, Barcelona, Spain) with mechanical stirring. The described procedures in Section 3.14. were proportionally scaled up to a final WCO mass of 40 g and mechanical stirring at 700 rpm.

The minireactor lid and tank were specially designed in collaboration with Scharlab. Thus, the lid was custom-made to include an inlet that allowed the NIR probe to be inserted in the reaction medium, and a second slightly curved inlet for the stirrer, so that both could reach the reaction medium without colliding. Besides, the stirrer was modified by using an additional propeller —the two were “marine propellers”— to facilitate generation of a turbulent regime in the reactor.

Operational stability was assessed as with vials, by allowing the biocatalyst to settle in the bottom of the reactor.

#### 3.14.2.1. Acquisition and processing of near infrared (NIR) spectra

The transesterification reactions were monitored by recording NIR spectra at 5 min intervals in each reaction cycle [27]. Spectra were acquired in the transreflectance mode, using a Model 5000 spectrophotometer from FOSS NIRSystems (Silver Spring, MD, USA) equipped with an immersive optical probe. The spectrophotometer employed was kindly borrowed by Manel Alcalà from Department of Chemistry, Faculty of Sciences, *Universitat Autònoma de Barcelona* who also performed the chemometrics described below.

A reference spectrum for air was obtained before the reaction. The wavelength range scanned was 1100–2498 nm, the spectral resolution was 2 nm and the optical path length was 1 mm. Raw absorbance spectra were exported to NSAS file format by using the software Vision 2.51, then transformed to Matlab file format with The Unscrambler 10.3 (Camo Analytics, Norway) and finally processed for viewing, exploration and multivariate modeling with the software Solo (Eigenvector Research Inc., Wenatchee, WA, USA).

First- and second-derivative spectra were obtained by using the Savitzky–Golay algorithm with a 15-point moving window and a second-order polynomial. Mean-centered data ( $X$ -block for spectra) were subjected to principal component analysis (PCA). Partial least-squares (PLS) calibration models for mean-centered data ( $X$ -block for spectra and  $Y$ -block for reaction yield) were constructed by cross-validation, using the leave-one-out method. Samples for inclusion in the calibration and prediction sets were selected by using the Kennard–Stone method [28]. The quality of the PLS models and their predictive ability were assessed in terms of the root mean square error of calibration (RMSEC) and prediction (RMSEP), defined as:

$$\text{RMSE} = \sqrt{\frac{\sum_{i=1}^n (Y_i^{\text{pred}} - Y_i^{\text{ref}})^2}{n}} \quad (\text{Eq. 3.11})$$

where  $n$  is the number of samples used,  $Y^{\text{ref}}$  the reaction yield provided by the reference method and  $Y^{\text{pred}}$  that estimated by the NIR model.

The number of PLS factors required to define each model was chosen from the minimum of a plot of RMSEP vs number of factors. The predictive ability was also assessed by statistical evaluation of the least-squares regression line between the reference GC reaction yield and the NIR-predicted value.

The aim of quantitative multivariate modeling is reducing prediction errors by using the simplest possible model (i.e., that with the fewest factors). PLS models were evaluated over wide or narrow spectral intervals selected from different calculations, namely: regression coefficients,  $X$ -loadings,  $XY$  correlation vector, variable importance in projection and selectivity ratio. These tools allow simple numerical assessment of the usefulness of each  $X$ -variable in a regression model. The higher were the results obtained with these calculations over the significant threshold, the greater was the usefulness of

the variables for regression and prediction. Selection of the spectral interval was combined with different spectral processing methods, first in the absorbance mode, and then as their first and second derivatives, and also upon standard normal variate SNV-based scaling. The combination of SNV followed by derivatization was also tested.

### **3.15. Esterification reactions**

#### ***3.15.1. Ethyl butyrate production***

Ethyl butyrate production reactions were conducted in 10 mL closed vials that were placed in the IKA KS 400 incubator at 30 °C under orbital stirring at 350 rpm. Samples were periodically taken for reaction performance assessment by gas chromatography. 100 mM butyric acid and an acid:alcohol mole ratio of 1.25:1 were used to a final heptane volume of 8 mL. All substrates and solvents were dried with UOP type 3 molecular sieves from Sigma-Aldrich prior to use. The biocatalysts were also dried, albeit by placing the amounts corresponding to 10000 AU in a dryer containing silica gel. Operational stability tests were performed by removing used reaction medium and rinsing the biocatalysts with heptane twice. Then, immobilized derivatives were allowed to stand in the dryer for 24 h before the next reaction run [29]. Initial esterification rates were determined by withdrawing samples regularly over the first 90 min of reaction.

#### ***3.15.2. Isoamyl esters production***

The acids studied (butyric and acetic) were esterified with isoamyl alcohol in the presence of 2000 AU of EO-proROL in 15 mL tubes at 30 °C under orbital stirring at 1200 rpm in a Digital Heating Shaking Drybath from Thermo Fisher Scientific. All solvents and

substrates were dried with UOP type 3 molecular sieves, and biocatalysts in a drier containing silica gel for 24 h prior to use.

The solvents initially used were cyclohexane and hexane. An acid:alcohol mole ratio of 1:1, a butyric acid concentration of 100 mM and a reaction time of 5 h were used for isoamyl butyrate synthesis, and a ratio of 1:8, an acetic concentration of 50 mM and a reaction time of 24 h for isoamyl acetate synthesis. The final reaction volume was always 1.6 mL and commercial isoamyl alcohol used as alcoholic substrate.

The operational stability of the biocatalyst was evaluated by allowing it to deposit in the tube bottom and removing depleted medium after the reaction. Then, the biocatalyst was washed three times with solvent and prepared for subsequent esterification.

#### 3.15.2.1. Effect of acid concentration and acid:alcohol molar ratio on reaction parameters during isoamyl esters production

The influence of the initial acid concentration and acid:alcohol mole ratio on isoamyl butyrate biosynthesis was assessed by using Response Surface Methodology (RSM) with production in the first reaction batch and cumulative production after 5 cycles, both in micromoles, as Design of Experiment (DoE) responses. An experimental design of the Box-Hunter type was used with  $\alpha = 1.41$  and 3 central points for replication. Single-batch and cumulative production of isoamyl butyrate were examined at butyric acid concentrations from 10 to 750 mM and acid:alcohol mole ratios from 0.5 to 2 [29,30]. All other reaction conditions were set as described in Section 3.15.2.

The results obtained for each response were fitted to the following second-order polynomial equation by least-squares regression:

$$Y = \beta_0 + \beta_1 X_1 + \beta_2 X_2 + \beta_{12} X_1 X_2 + \beta_{11} X_1^2 + \beta_{22} X_2^2 \quad (\text{Eq. 3.12})$$

where  $Y$  is the dependent variable (single-batch or cumulative ester production);  $X_1$  and  $X_2$  are independent variables (initial acid concentration and acid:alcohol mole ratio);  $\beta_0$  is an intercept term;  $\beta_1$  and  $\beta_2$  are linear coefficients;  $\beta_{12}$  is the interaction coefficient; and  $\beta_{11}$ ,  $\beta_{22}$  are quadratic coefficients [30–32].

Experimental data were processed with the software Design Expert v. 6.0.8 (Stat-Ease, Inc., Minneapolis, MN, USA) and analyzed statistically with SigmaPlot v. 14 (Systat Software, Inc., Chicago, IL, USA).

The goodness of fit of the response surfaces to Eq. 3.12 was assessed in terms of  $R^2$ , adjusted- $R^2$  and predicted- $R^2$ . An analysis of variance (ANOVA)  $F$ -test was used to assess the significance of the obtained equations, their individual coefficients being evaluated with a  $t$ -test. The lack of fit (LOF) test was used to assess differences between experimental and pure error in the fitted equations.  $p$ -values  $< 0.05$  were taken to be statistically significant.

#### 3.15.2.2. Isoamyl ester esterification reaction scale up

The previously established optimum experimental conditions (viz., initial acid concentration and acid:alcohol mole ratio) were used to scale up the esterification reaction to a laboratory reactor using a final working volume of 150 mL and mechanical stirring at 500 rpm. The temperature was kept at 30 °C by means of an external jacket. Also, fusel oil was employed as alcoholic substrate, instead of isoamyl alcohol. The same optimum



concentration conditions were employed, after determining the concentration of isoamyl alcohol present in fusel oil by following the procedure described in Section 3.18.3.

The initial reaction rate was determined by withdrawing samples at regular intervals during the first 2 h of reaction. Enzyme operational stability was assessed identically as in 15 mL tubes (see Section 3.15.2). Biocatalyst performance was compared using both commercial isoamyl alcohol and fusel oil as alcoholic substrates.

### **3.16. Operational stability: half-lives calculation of transesterification and esterification reactions**

The relative yields of consecutive transesterification and esterification cycles as calculated relative to the final yield of the first reaction cycle were fitted by using a first-order exponential decay model (Eq. 3.13) and/or two-component first-order exponential decay model (Eq. 3.14):

$$Y(\%)_t = 100e^{-kt}, \quad (3.13)$$

$$Y(\%)_t = 100e^{-k_1 t} + ce^{-k_2 t} \quad (3.14)$$

where  $k$ ,  $k_1$  and  $k_2$  are deactivation coefficients. All computations were done with the software Sigma Plot v. 14 [33,34].

### 3.17. Polymerization reactions

#### 3.17.1. *Direct lactic acid condensation*

Direct polymerization runs were conducted by adapting a previously reported method [35]. Thus, 20 mL closed vials containing 5 mmol of LA and 8 mL of solvent were incubated with 15000 AU of enzyme unless otherwise stated, using the IKA KS 400 incubator at 30 °C under orbital stirring at 350 rpm. Reactions were allowed to develop for 96 h unless otherwise stated. All runs were done in duplicate, using a blank solution containing no enzyme and a control solution without LA under each set of operating conditions.

#### 3.17.2. *Ring-opening polymerization*

The ROP procedure was a modified version of an existing one [36]. The reaction was performed using 10 mL closed vials containing 5 mmol of lactide and 15000 AU of enzyme in addition to 8 mL of toluene or anisole as solvent. Vials were incubated at 30 °C in the IKA KS 400 incubator that was shaken at 350 rpm. The reaction time was 96 h, and a blank without enzyme and a control solution without lactide were used under the different operating conditions.

#### 3.17.3. *Effect of initial lactic acid concentration and total added activity units on lactic acid conversion and total converted amount*

Following the optimization and statistical analyses described in Section 3.15.2.1 for isoamyl ester production, the influence of initial LA concentration and total added AU on

direct condensation of LA were assessed by using Response Surface Methodology with LA conversion (%) and converted LA amount (mmol) as Design of Experiments (DoE) responses. The effect of these variables was studied by means of a Box-Hunter design with  $\alpha = 1.41$  and 3 central points for replication were performed. All the other conditions were fixed as described in Section 3.17.1.

Initial LA concentration was varied in a range from 1000 to 6000 mM. Total AU added to the reaction were established between 1000 and 50000 AU calculated according to Section 3.3, Roche colorimetric kit analysis.

The results obtained for each response were fitted to the equation 3.12 where  $Y$  is the dependent variable (LA conversion or converted LA);  $X_1$  and  $X_2$  are independent variables (initial LA concentration and enzymatic AU, respectively) [30–32].

### **3.18. Gas chromatography analysis of synthesized esters**

#### ***3.18.1. FAMES and FAEEs analysis***

Samples mass – 10 mg per sample approximately – was measured to avoid error during sampling in biodiesel reactions. Samples were lately diluted in HPLC grade *n*-heptane and mixed 50  $\mu$ L of thus obtained dilution with same volume of internal standard – methyl heptadecanoate in *n*-heptane 1.928 mg mL<sup>-1</sup> [21].

Fatty acid methyl esters (FAMES) and fatty acid ethyl esters (FAEEs) were quantified on a model 7890A gas chromatograph from Agilent (Santa Clara, CA, USA) equipped with a 19095 N-123 capillary column (30 m x 0.53 mm x 1  $\mu$ m) and an autosampler. Inlet conditions were set at 300 °C and 6.5 psi. Initial oven temperature was

set at 150 °C and then, with no hold time, a ramp of 24 °C min<sup>-1</sup> until 240 °C with a hold time of 17 min was established. Detector temperature was maintained at 320 °C with H<sub>2</sub> and airflow of 40 mL min<sup>-1</sup> and 400 mL min<sup>-1</sup>, respectively. The RSD for the FAMEs and FAEEs never exceeded 3%.

### **3.18.2. Ethyl butyrate analysis**

An equal volume of reaction sample was mixed with internal standard – 0.4 M acetophenone – and analyzed in the above described model 7890A gas chromatograph from Agilent. Inlet temperature was set at 250 °C and 15 psi. Initial oven temperature was set at 60 °C for 6 min and then a ramp of 30 °C min<sup>-1</sup> until 180 °C with a final hold time of 2 min. Detector temperature was maintained at 370 °C with He employed as a carrier gas [29].

### **3.18.3. Isoamyl esters analysis**

Isoamyl alcohol, isoamyl acetate and isoamyl butyrate were quantified in a GC8860/MS5977E gas chromatograph/mass spectrometer from Agilent equipped with a HP-5MS capillary column (30 m × 250 μm, 0.25 μm film thickness). The column temperature was raised from 60 to 112 °C at 3 °C min<sup>-1</sup> and then further raised to 246 °C at 12 °C min<sup>-1</sup>, the final level being held for 5 min. The injected sample volume was 1 μL and the split ratio 50:1. Helium at a constant flow-rate of 1 mL min<sup>-1</sup> was used as carrier gas. The inlet and mass transfer line temperatures were 230 and 250 °C, respectively, and the ion source and quadrupole temperatures were set at 230 and 150 °C, respectively. Mass spectra were acquired over the *m/z* range 35–350 after 1.6 min of

solvent delay. Because most reported chromatographic methods fail to fully resolve the structural isomers of isoamyl alcohol and active amyl alcohol, they were referred to as “(iso)amyl alcohol” and “(iso)amyl esters” for comparison unless stated otherwise [37].

### **3.19. Oleaginous substrates acidity determination**

Total acidity was determined in accordance with the protocols in Commission Regulation (EEC) No 2568/91 Annex II, amended by Commission Regulation (EC) No 702/2007.

### **3.20. Fatty acid composition determination in WCO**

Fatty acid composition of WCO was assessed by adapting an already published procedure of chemically catalyzed transesterification [38]. Briefly, 40 g of oil were heated in the commercial standard design of HME-R mini reactor from Scharlab – non-modified tank and lid – at 65 °C under mechanical stirring at 350 rpm. KOH (1% w/w) and methanol (6:1 alcohol/oil) were added and the reaction was extended for 6 h. Samples were taken for gas chromatography analysis and relative fatty acid composition calculation.

### **3.21. Lactic acid conversion assessment**

A volume of 10 mL of tetrahydrofuran was added to the medium in the direct LA condensation reaction and the mixture centrifuged at 4 °C at 3000 rpm for 20 min. Then, the enzyme—which remained as an amorphous mass in the pellet—was discarded and the supernatant used to assess LA conversion [39] by titration with a KOH solution. For this purpose, a fixed volume of supernatant was added to 5 mL of (50:50 v/v) ethanol/acetone mixture under stirring and titrated in triplicate with KOH in the presence

of phenolphthalein as end point indicator. The resulting relative standard deviations (RSD) in conversion never exceeded 5 %. Percent conversion was calculated as:

$$\text{Conversion (\%)} = \frac{m_{\text{blank}} - m_{\text{analyzed}}}{m_{\text{blank}}} \times 100 \quad (3.15)$$

where  $m_{\text{blank}}$  denotes the number of milliequivalents of LA relative to the blank (no enzyme) and  $m_{\text{analyzed}}$  that in the supernatant, which was calculated from:

$$m_{\text{analyzed}} = M(V - V^*) \quad (3.16)$$

where  $M$  is the molarity of KOH solution,  $V$  is the volume consumed in the sample titration and  $V^*$  is the volume consumed in corresponding control titration without LA. Thus, calculated conversion values were used for converted LA amount calculation (Section 3.17.3) considering the initial LA concentration and reaction volume.

### 3.22. NMR spectroscopy

For the NMR analysis, samples were analyzed in collaboration with the *Servei de Ressonància Magnètica Nuclear (Universitat Autònoma de Barcelona)* using a Bruker AVANCE 600 spectrometer (600.13 MHz frequency for  $^1\text{H}$ ) equipped with a 5 mm TBI probehead, an autosampler and a control temperature unit (Bruker BioSpin, Rheinstetten, Germany). The probe temperature was maintained at 298 K for all experiments. Dry samples (dried with a VR-1/120/240 vacuum concentrator from Heto Lab Equipment) were dissolved in a  $\text{CDCl}_3$  stock solution containing an internal standard (tetramethylsilane, TMS, 6.0 mM) and transferred to the NMR tube. All samples were analyzed conducting standard quantitative 1D  $^1\text{H}$  NMR experiments. Data were collected into 32k data points during an acquisition time of 1.7 s using a recycle delay of 15 s.

Spectra were recorded in the time domain as interferograms (FID) across a spectral width of 9615 Hz and as the sum of 64 transients. FIDs were automatically Fourier transformed (FT) and the spectra were phased, and baseline corrected. TMS was used as internal reference ( $\delta(^1\text{H})$  at 0.00 ppm).

### 3.23. References

- [1] Barrero JJ, Casler JC, Valero F, Ferrer P, Glick BS. An improved secretion signal enhances the secretion of model proteins from *Pichia pastoris*. *Microb Cell Fact* 2018;17:161–74. <https://doi.org/10.1186/s12934-018-1009-5>.
- [2] Cámara E, Albiol J, Ferrer P. Droplet digital PCR-aided screening and characterization of *Pichia pastoris* multiple gene copy strains. *Biotechnol Bioeng* 2016;113:1542–51. <https://doi.org/10.1002/bit.25916>.
- [3] Maurer M, Kühleitner M, Gasser B, Mattanovich D. Versatile modeling and optimization of fed batch processes for the production of secreted heterologous proteins with *Pichia pastoris*. *Microb Cell Fact* 2006;5:37–47. <https://doi.org/10.1186/1475-2859-5-37>.
- [4] Garcia-Ortega X, Ferrer P, Montesinos JL, Valero F. Fed-batch operational strategies for recombinant Fab production with *Pichia pastoris* using the constitutive GAP promoter. *Biochem Eng J* 2013;79:172–81. <https://doi.org/10.1016/j.bej.2013.07.013>.
- [5] Minning S, Serrano A, Ferrer P, Solá C, Schmid RD, Valero F. Optimization of the high-level production of *Rhizopus oryzae* lipase in *Pichia pastoris*. *J Biotechnol* 2001;86:59–70. [https://doi.org/10.1016/S0168-1656\(00\)00402-8](https://doi.org/10.1016/S0168-1656(00)00402-8).
- [6] Barrigón JM, Montesinos JL, Valero F. Searching the best operational strategies for *Rhizopus oryzae* lipase production in *Pichia pastoris* Mut<sup>+</sup> phenotype: methanol limited or methanol non-limited fed-batch cultures? *Biochem Eng J* 2013;75:47–54. <https://doi.org/10.1016/j.bej.2013.03.018>.



- [7] Ponte X, Montesinos-Seguí JL, Valero F. Bioprocess efficiency in *Rhizopus oryzae* lipase production by *Pichia pastoris* under the control of  $P_{AOX1}$  is oxygen tension dependent. *Process Biochem* 2016;51:1954–63. <https://doi.org/10.1016/j.procbio.2016.08.030>.
- [8] Jordà J, De Jesus SS, Peltier S, Ferrer P, Albiol J. Metabolic flux analysis of recombinant *Pichia pastoris* growing on different glycerol/methanol mixtures by iterative fitting of NMR-derived ( $^{13}\text{C}$ -labelling data from proteinogenic amino acids. *N Biotechnol* 2014;31:120–32. <https://doi.org/10.1016/J.NBT.2013.06.007>.
- [9] Resina D, Cos O, Ferrer P, Valero F. Developing high cell density fed-batch cultivation strategies for heterologous protein production in *Pichia pastoris* using the nitrogen source-regulated FLD1 promoter. *Biotechnol Bioeng* 2005;91:760–7. <https://doi.org/10.1002/bit.20545>.
- [10] López-Fernández J, Barrero JJ, Benaiges MD, Valero F. Truncated prosequence of *Rhizopus oryzae* lipase: key factor for production improvement and biocatalyst stability. *Catalysts* 2019;9:961–77. <https://doi.org/10.3390/catal9110961>.
- [11] Resina D, Serrano A, Valero F, Ferrer P. Expression of a *Rhizopus oryzae* lipase in *Pichia pastoris* under control of the nitrogen source-regulated formaldehyde dehydrogenase promoter. *J Biotechnol* 2004;109:103–13. <https://doi.org/10.1016/j.jbiotec.2003.10.029>.
- [12] Arnau C, Ramon R, Casas C, Valero F. Optimization of the heterologous production of a *Rhizopus oryzae* lipase in *Pichia pastoris* system using mixed substrates on controlled fed-batch bioprocess. *Enzyme Microb Technol* 2010;46:494–500. <https://doi.org/10.1016/j.enzmictec.2010.01.005>.

- [13] Chang SW, Lee GC, Shaw JF. Codon optimization of *Candida rugosa* lip1 gene for improving expression in *Pichia pastoris* and biochemical characterization of the purified recombinant LIP1 lipase. *J Agric Food Chem* 2006;54:815–22. <https://doi.org/10.1175/JAS3661.1>.
- [14] Guillén M, Benaiges MD, Valero F. Comparison of the biochemical properties of a recombinant lipase extract from *Rhizopus oryzae* expressed in *Pichia pastoris* with a native extract. *Biochem Eng J* 2011;54:117–23. <https://doi.org/10.1016/j.bej.2011.02.008>.
- [15] Bradford MM. A rapid and sensitive method for the quantitation of microgram quantities of protein utilizing the principle of protein-dye binding. *Anal Biochem* 1976;72:248–54. [https://doi.org/10.1016/0003-2697\(76\)90527-3](https://doi.org/10.1016/0003-2697(76)90527-3).
- [16] Diaz P, Prim N, Pastor FIJ. Direct fluorescence-based lipase activity assay. *Biotechniques* 1999;27:696–700. <https://doi.org/10.2144/99274bm14>.
- [17] Cámara E, Landes N, Albiol J, Gasser B, Mattanovich D, Ferrer P. Increased dosage of AOX1 promoter-regulated expression cassettes leads to transcription attenuation of the methanol metabolism in *Pichia pastoris*. *Sci Rep* 2017;7:1–16. <https://doi.org/10.1038/srep44302>.
- [18] Kohno M, Kugimiya W, Hashimoto Y, Morita Y. Purification, characterization, and crystallization of two types of lipase from *Rhizopus niveus*. *Biosci Biotechnol Biochem* 1994;58:1007–12. <https://doi.org/10.1271/bbb.58.1007>.
- [19] Romero E, Ferreira P, Martínez ÁT, Martínez MJ. New oxidase from *Bjerkandera arthroconidial* anamorph that oxidizes both phenolic and nonphenolic benzyl alcohols. *Biochim Biophys Acta - Proteins Proteomics* 2009;1794:689–97.

- <https://doi.org/10.1016/j.bbapap.2008.11.013>.
- [20] Cruz-Izquierdo Á, Picó EA, López C, Serra JL, Llama MJ. Magnetic Cross-Linked Enzyme Aggregates (mCLEAs) of *Candida antarctica* lipase: an efficient and stable biocatalyst for biodiesel synthesis. PLoS One 2014;9:1–22. <https://doi.org/10.1371/journal.pone.0115202>.
- [21] Bonet-Ragel K, Canet A, Benaiges MD, Valero F. Synthesis of biodiesel from high FFA *alperujo* oil catalysed by immobilised lipase. Fuel 2015;161:12–7. <https://doi.org/10.1016/j.fuel.2015.08.032>.
- [22] Bonet-Ragel K, Canet A, Benaiges MD, Valero F. Effect of acyl-acceptor stepwise addition strategy using *alperujo* oil as a substrate in enzymatic biodiesel synthesis. J Chem Technol Biotechnol 2018;93:541–7. <https://doi.org/10.1002/jctb.5399>.
- [23] Bonet-Ragel K. Enzymatic synthesis of biodiesel from high free fatty acid feedstock using a recombinant *Rhizopus oryzae* lipase. Universitat Autònoma de Barcelona, 2018.
- [24] Weisz PB, Prater CD. Interpretation of measurements in experimental catalysis. Adv Catal 1954;6:143–96. [https://doi.org/10.1016/S0360-0564\(08\)60390-9](https://doi.org/10.1016/S0360-0564(08)60390-9).
- [25] Harvey W. Blanch DSC. Biochemical Engineering, Second Edition - Douglas S. Clark, Harvey W. Blanch. 1997.
- [26] Poling BE, Prausnitz JM, O’Connell JP. The Properties of Gases & Liquids - Fifth Edition. 2001. [https://doi.org/10.1016/0894-1777\(88\)90021-0](https://doi.org/10.1016/0894-1777(88)90021-0).
- [27] Blanco M, Alcalá M, González JM, Torras E. A process analytical technology approach based on near infrared spectroscopy: tablet hardness, content uniformity,

- and dissolution test measurements of intact tablets. *J Pharm Sci* 2006;95:2137–44. <https://doi.org/10.1002/jps.20653>.
- [28] Ng W, Minasny B, Malone B, Filippi P. In search of an optimum sampling algorithm for prediction of soil properties from infrared spectra. *PeerJ* 2018;2018. <https://doi.org/10.7717/peerj.5722>.
- [29] Guillén M, Benaiges MD, Valero F. Biosynthesis of ethyl butyrate by immobilized recombinant *Rhizopus oryzae* lipase expressed in *Pichia pastoris*. *Biochem Eng J* 2012;65:1–9. <https://doi.org/10.1016/j.bej.2012.03.009>.
- [30] Guillén M, Benaiges MD, Valero F. Improved ethyl butyrate synthesis catalyzed by an immobilized recombinant *Rhizopus oryzae* lipase: a comprehensive statistical study by production, reaction rate and yield analysis. *J Mol Catal B Enzym* 2016;133:S371–6. <https://doi.org/10.1016/j.molcatb.2017.02.010>.
- [31] Grosso C, Ferreira-Dias S, Pires-Cabral P. Modelling and optimization of ethyl butyrate production catalysed by *Rhizopus oryzae* lipase. *J Food Eng* 2013;115:475–80. <https://doi.org/10.1016/j.jfoodeng.2012.08.001>.
- [32] Salihu A, Alam MZ, AbdulKarim MI, Salleh HM. Esterification for butyl butyrate formation using *Candida cylindracea* lipase produced from palm oil mill effluent supplemented medium. *Arab J Chem* 2014;7:1159–65. <https://doi.org/10.1016/J.ARABJC.2013.08.012>.
- [33] Rodrigues J, Canet A, Rivera I, Osório NM, Sandoval G, Valero F, et al. Biodiesel production from crude *Jatropha* oil catalyzed by non-commercial immobilized heterologous *Rhizopus oryzae* and *Carica papaya* lipases. *Bioresour Technol* 2016;213:88–95. <https://doi.org/10.1016/j.biortech.2016.03.011>.

- [34] Aymard C, Belarbi A. Kinetics of thermal deactivation of enzymes: a simple three parameters phenomenological model can describe the decay of enzyme activity, irrespectively of the mechanism. *Enzyme Microb Technol* 2000;27:612–8. [https://doi.org/10.1016/S0141-0229\(00\)00258-1](https://doi.org/10.1016/S0141-0229(00)00258-1).
- [35] Lassalle VL, Ferreira ML. Lipase-catalyzed synthesis of polylactic acid: An overview of the experimental aspects. *J Chem Technol Biotechnol* 2008;83:1493–502. <https://doi.org/10.1002/jctb.1994>.
- [36] Zhao H, Nathaniel GA, Merenini PC. Enzymatic ring-opening polymerization (ROP) of lactides and lactone in ionic liquids and organic solvents: digging the controlling factors. *RSC Adv* 2017;7:48639–48. <https://doi.org/10.1039/C7RA09038B>.
- [37] Sun J, Yu B, Curran P, Liu SQ. Lipase-catalysed ester synthesis in solvent-free oil system: Is it esterification or transesterification? *Food Chem* 2013;141:2828–32. <https://doi.org/10.1016/j.foodchem.2013.05.109>.
- [38] Vicente G, Martínez M, Aracil J. Integrated biodiesel production: a comparison of different homogeneous catalysts systems. *Bioresour Technol* 2004;92:297–305. <https://doi.org/10.1016/j.biortech.2003.08.014>.
- [39] V L, GB G, ML F. Lipase-catalyzed copolymerization of lactic and glycolic acid with potential as drug delivery devices. *Bioprocess Biosyst Eng* 2008;31:499–508. <https://doi.org/10.1007/S00449-007-0188-Y>

# 4

## Results I: Biodiesel production

### 4.1. Second- and third-generation biodiesel production with immobilized recombinant *Rhizopus oryzae* lipase: influence of the support, substrate acidity and bioprocess scale up

---

Chapter published as research article in **Bioresource Technology**

López-Fernández J, Benaiges MD, Valero F.

Second- and third-generation biodiesel production with immobilised recombinant *Rhizopus oryzae* lipase: influence of the support, substrate acidity and bioprocess scale-up. *Bioresour Technol* 2021;334:125233. <https://doi.org/10.1016/j.biortech.2021.125233>



## **4. RESULTS (I)**

### **4.1. Second- and third-generation biodiesel production with immobilized recombinant *Rhizopus oryzae* lipase: influence of the support, substrate acidity and bioprocess scale up.**

<b>4.1.1. Introduction</b> .....	161
<b>4.1.2. Results and discussion</b> .....	163
4.1.2.1. Lipase immobilization and diffusional restrictions.....	163
4.1.2.2. Polymethacrylate supports .....	165
4.1.2.3. Lipase immobilization onto magnetite-based supports.....	169
4.1.2.4. Biocatalyst performance .....	171
4.1.2.5. Alternative substrates .....	172
4.1.2.6. Transesterification scale-up .....	175
<b>4.1.3. Conclusions</b> .....	176
<b>4.1.4. References</b> .....	178





### ***4.1.1. Introduction***

Global warming is an unavoidable process that requires a change of paradigm to enable a climate-neutral society and avoid environmental collapse. In this scenario, a wide variety of clean energy sources have the potential to jointly replace polluting fossil fuels. One such source is biodiesel, which is likely to play a major role in the process [1–3]. Biodiesel, as described in Section 1.6.1, is a mixture of mono-alkyl esters of long-chain fatty acids obtained by transesterification of a wide range of oily substrates and classified as first-, second- or third-generation biodiesel depending on the source of such oils. Production of the last two generation biofuels, as they avoid severe ethical problems of using food for fuels, is being boosted by public institutions (European Union, 2015/1513) as they are obtained from non-edible oils (e.g., waste cooking oil, WCO), oils from plants growing in agriculturally unsuitable land (e.g., jatropha, makauba) [4] or microbial oils respectively [5,6]. Nevertheless, as stated in the Introduction, the high content in free fatty acids (FFA) of second- and third-generation biodiesel substrates makes basic transesterification a more complex approach and promotes enzymatic transesterification with lipases as an effective choice for biodiesel production. However, lipases for use as biocatalysts by the biodiesel industry are expensive and unstable (especially in the presence of alcohols such as methanol, which diminishes enzyme reusability and compromises economic feasibility of enzymatic biodiesel production) [7]. Immobilizing enzymes provides an effective way of circumventing the shortcomings of biocatalysts by improving their stability against deactivation and enabling their reuse [8,9]. In addition, depending on the surface groups of the immobilization support, they might have an effect on enzyme performance or on the microenvironment of the immobilized enzyme, which might have an impact in enzyme activity and stability as well. The enzyme activity is

influenced by enzyme orientation during immobilization, depending on the involved amino acids in the process, and by the number of binding points of the protein to the support. In fact, it has been reported that the highest enzymatic activity level is achieved when the active center amino acids are not involved in the linkage with the support and the increased stability when unlimited covalent binding between the enzyme and the support are achieved. However, in some cases, having several binding points between the enzyme and the support can become counterproductive as it increases the rigidity of the enzyme and might provoke negative steric effects. Regarding the microenvironment of the biocatalysts, the presence of functional groups of different nature in the support surface might provoke alterations in the substrate/product concentration, pH, etc. in the liquid milieu in which immobilized enzyme operate [10–14]. For instance, the presence of hydrophobic surface groups on the support of a biocatalysts used for biodiesel synthesis might lower the alcohol (hydrophilic molecule) concentration in the microenvironment around the enzyme and, this way, favor enzyme stability.

In this chapter, mature sequence of *Rhizopus oryzae* lipase (rROL) expressed in the methylotrophic yeast *Komagataella phaffii*, which has been claimed as the most suitable cell factory for rROL expression (see Introduction, section 1.5.1.), was used for enzymatic second- and third-generation biodiesel production. Transesterification reaction catalyzed by rROL gives the corresponding mono-alkyl esters and, provided acyl-migration is controlled [15], 2-monoacylglyceride as well, thereby avoiding glycerol formation and giving a product with a high added value for the cosmetics and food industries [16]. The lipase was covalently immobilized onto three glutaraldehyde-treated polymethacrylate-based supports containing both epoxide and hydrophobic functional groups. The effects of functional groups on lipase immobilization and diffusional

restrictions, and also on the initial reaction rate and operational stability of the catalyst, were assessed. Glutaraldehyde-treated superparamagnetic nanoparticles containing hydrophobic functional groups at variable densities were also used for covalent immobilization of lipase and evaluation of biodiesel production. Tests were conducted by using *alperujo* oil (non-edible olive pomace oil with a high FFA content obtained in the olive extraction process [17]) as a model substrate for transesterification. Subsequently, the best biocatalyst was used for production of second- and third-generation biodiesel from alternative substrates of potential industrial use, including jatropha, makauba, WCO, and microbial oils. Finally, transesterification with WCO was scaled-up to a 50 mL mini-laboratory reactor.

#### **4.1.2. Results and discussion**

##### 4.1.2.1. Lipase immobilization onto polymethacrylate-based supports and diffusional restrictions

Recombinant *Rhizopus oryzae* lipase was covalently immobilized following the procedure described in Section 3.12 onto three glutaraldehyde-treated polymethacrylate-based Purolite® supports containing both epoxide and hydrophobic functional groups, namely: EB-rROL (epoxide and butyl), EO-rROL (epoxide and octadecyl) and EDVB-rROL (epoxide and divinylbenzene). Lipase solutions with an activity ranging from 55 to 1000 AU per mg support were used to evaluate the immobilization yield and maximum lipase activity loading. All supports studied were identical in these parameters irrespective of their characteristics (Figure 4.1.1A). Considering lipase immobilization trend, offered activity values lower than 55 AU mg<sup>-1</sup> support resulted in immobilization

yields (Eq. 3.8, Section 3.12) of 100% and less than 90 AU mg<sup>-1</sup> support in greater than 80%. As expected, increasing offered lipase activity decreased the immobilization yield. Also, biocatalysts activity increased in proportion to a maximum lipase activity loading of approximately 200 immobilized AU mg<sup>-1</sup> support with all supports. Immobilized activity was maximal with lipase solutions of 400 AU mg<sup>-1</sup> support, above which no further improvement was observed.

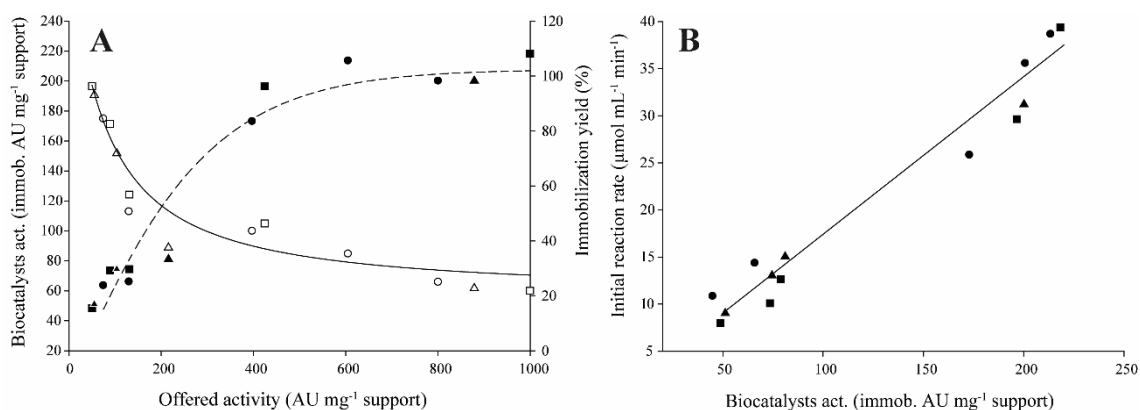


**Figure 4.1.1.** (A) Biocatalyst activity (black symbols) and immobilization yield (white symbols) at a variable offered activity. (B) Initial transesterification rate for each biocatalyst: EB-rROL (circles), EO-rROL (squares) and EDVB-rROL (triangles).

Mass transfer limitations in immobilized enzymes usually reflect in diffusional restrictions, whether external or internal. The latter are usually more severe with enzymes embedded in a solid porous matrix such as Purolite® supports [18]. Diffusional restrictions were experimentally evaluated following the procedure described in Sections 3.14 and 3.14.1 by examining the initial transesterification rate with methanol of biocatalysts containing variable amounts of immobilized enzyme (Figure 4.1.1B). The proportional relationship observed suggested the absence of internal diffusional restrictions under the conditions studied. However, because mass transfer limitations may be an artefact on enzyme stability assessment [19,20], the absence of restrictions was

confirmed by calculating the Weisz–Prater Criterion ( $\Phi$ ). Table 4.1.1 shows the results for the three Purolite® biocatalysts with the highest immobilized activity (further calculations can be found in Annexes).  $\Phi$  was  $< 0.3$  in all cases, which supports the previous conclusion.

**Table 4.1.1.** Weisz–Prater criterion for pomace oil transesterification with methanol in the presence of various biocatalysts immobilized onto a polymethacrylate matrix.  $\Phi$  and  $D_{\text{eff}}$  were calculated from Eq. 3.9 and 3.10, respectively, using  $\sigma = 1$  and  $\tau = 1.41$  in the latter. Porosity ( $\epsilon_p$ ) and specific volume of the supports were 0.6 and  $1.4 \text{ cm}^3 \text{ g}^{-1}$  support.

Parameters	Biocatalyst		
	EB-rROL	EO-rROL	EDVB-rROL
$r_{\text{obs}} (\text{mol s}^{-1} \text{ cm}^{-3}) \times 10^7$	$6.44 \pm 0.05$	$6.57 \pm 0.02$	$5.20 \pm 0.1$
Biocatalyst weight (g)	$0.2 \pm 0.05$	$0.2 \pm 0.03$	$0.2 \pm 0.01$
$\rho_p (\text{g cm}^{-3})^1$	0.72	0.72	0.72
Specific area ( $\text{m}^2 \text{ g}^{-1}$ ) <sup>1</sup>	152	139	59
$r_{\text{obs}} (\text{mol g}_{\text{particle}}^{-1} \text{ s}^{-1}) \times 10^5$	$2.89 \pm 0.02$	$2.95 \pm 0.01$	$2.33 \pm 0.07$
$C_{\text{m},0} (\text{mol cm}^{-3}) \times 10^4$	4.41	4.41	4.41
$D_{\text{m},a} (\text{cm}^2 \text{ s}^{-1}) \times 10^6$	1.18	1.18	1.18
$D_{\text{eff}} (\text{cm}^2 \text{ s}^{-1}) \times 10^7$	5.04	5.04	5.04
$\Phi \times 10^7$	$0.78 \pm 0.05$	$0.95 \pm 0.03$	$4.19 \pm 0.08$

<sup>1</sup> Data kindly provided by Purolite®

#### 4.1.2.2. Polymethacrylate supports. Initial transesterification rate and operational stability

The catalytic performance of immobilized enzymes and the physico–chemical conditions of their microenvironment are strongly influenced by functional groups in the supports [11]. This led us to compare the initial reaction rate with methanol and operational stability, with both ethanol and methanol as acyl-acceptors, of the biocatalysts obtained by covalently immobilizing rROL onto Purolite® supports containing both epoxide and hydrophobic functional groups (viz., EB-rROL, EO-rROL and EDVB-rROL) with those of rROL covalently immobilized onto a polymethacrylate-based support containing epoxide groups only (EX-rROL) [21]. The methods employed for initial

transesterification and operational stability assessment are thoroughly described in Section 3.14.

The initial transesterification rate was similar with all polymethacrylate-based biocatalysts irrespective of the particular functional group —EB-rROL  $24.9 \pm 0.9$ , EO-rROL  $25.1 \pm 0.51$ , EDVB-rROL  $24.4 \pm 0.33$  and EX-rROL  $24.6 \pm 0.78$   $\mu\text{mol FAME min}^{-1} \text{cm}^{-3}$ . Contrary to the expectations, these results showed that chemical differences in surface composition among supports had no effect on the initial reaction rate under the conditions studied.

On the other hand, the operational stability of the biocatalysts was dramatically influenced by the functional groups of the supports. Figures 4.1.2A–2C shows the relative yield obtained by exposing each biocatalyst to 1 and 5 pulses of the different alcohols in consecutive reaction cycles. Operational stability with 1 pulse of methanol was not assessed owing to the low yield of the first reaction cycle by effect of deactivation of the enzyme (Figure 4.1.2D) [21]. Because rROL is a 1,3-regiospecific enzyme, the maximum expected yield was 66%. Using a stoichiometric amount of alcohol (viz., a 2:1 alcohol-to-oil mole ratio) avoided the presence of too high alcohol concentration in the reaction medium —and hence potentially adverse effects on the operational stability of the biocatalysts.

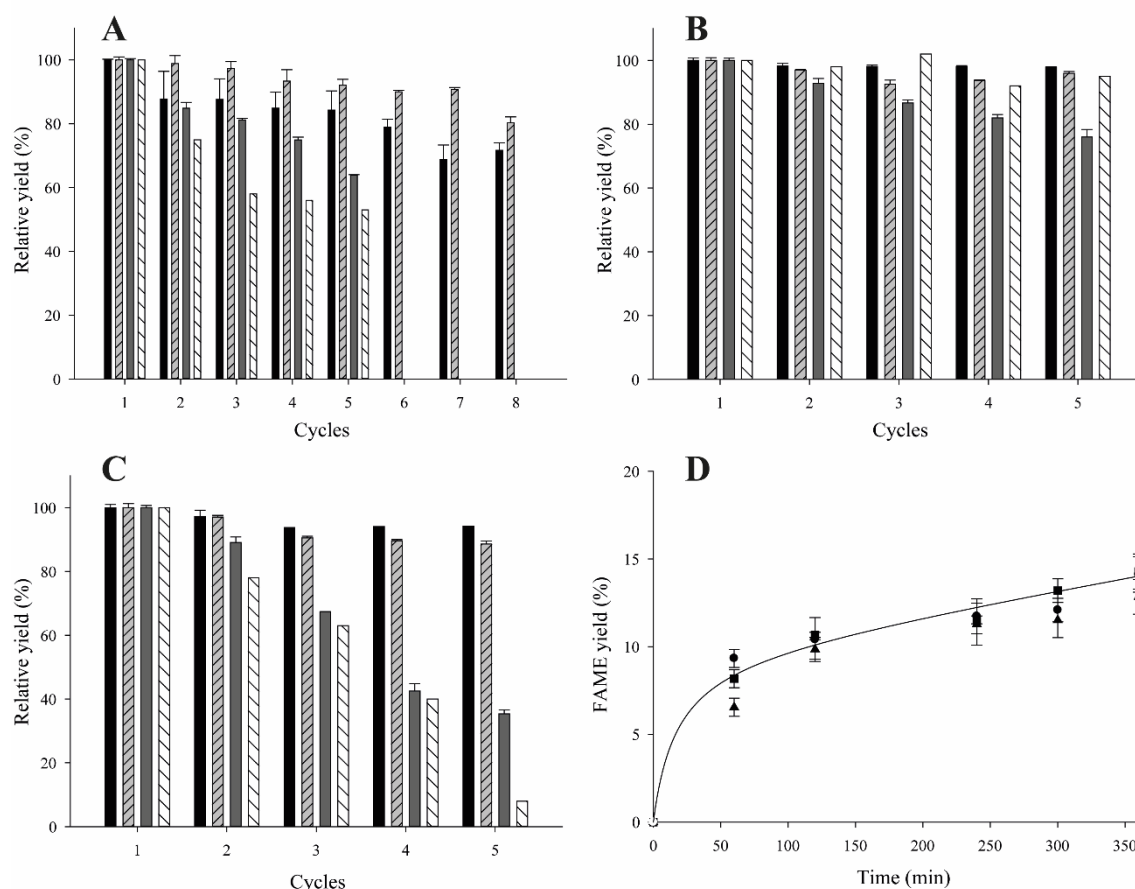


**Figure 4.1.2.** Relative yield (%) in consecutive transesterification runs with biocatalysts immobilized on polymethacrylate-based supports upon exposure to (A) 1 pulse of ethanol, (B) 5 pulses of ethanol and (C) 5 pulses of methanol. The respective first reactions yields were taken to represent 100% yield. EB-rROL (black), EO-rROL (up-striped grey), EDVB-rROL (dark grey) and EX-rROL (down-striped white) [21]. (D) First transesterification run with 1 pulse of methanol. The solid line represents the average FAME yield for the biocatalysts as a whole. EB-rROL (circles), EO-rROL (squares) and EDVB-rROL (triangles)

The joint presence of epoxide/butyl and epoxide/octadecyl groups in supports EB and EO, respectively, substantially increased the operational stability of the biocatalysts relative to EX-rROL upon exposure to 1 pulse of ethanol and 5 of methanol addition strategies. By way of example, Figure 4.1.2C shows the most extreme case, in which EB-rROL and EO-rROL were roughly 9 times more stable than EX-rROL after 5 reaction



cycles with 5 pulses of methanol. In contrast to EB-rROL and EO-rROL, EDVB-rROL exhibited no increase in stability—which was similar to that of EX-rROL. These results suggested that the increased stability of EB-rROL and EO-rROL was not a consequence of microenvironmental changes due the presence of hydrophobic functional groups—in fact, EDVB-rROL did not follow this trend—, but rather to that of surface hydrocarbon chains in the support possibly enhancing catalytic performance of the enzyme [22]. In addition, EO-rROL was 20% more stable than EB-rROL against 1 pulse of ethanol (Figure 4.1.2A), which testified to the positive effect of the hydrocarbon chain length on the operational stability of the biocatalysts.

The increased operational stability of EO-rROL and EB-rROL additionally made them resistant to 5 pulses of methanol. In fact, unlike EX-rROL and EDVB-rROL, both biocatalysts exhibited an identical relative yield close to 100% after 5 reaction cycles irrespective of the alcohol used (Figures 4.1.2B and 4.1.2C)—being methanol a more powerful lipase inactivator than ethanol in this reaction [21]. However, neither EO-rROL nor EB-rROL resisted deactivation by 1 pulse of methanol, the final FAME yield being around 15% rather than the expected theoretical maximum: 66% (Figure 4.1.2D).

Covalent lipase immobilization causes the formation of Schiff bases through condensation of amino groups in lysines with aldehyde groups in the supports [23]. Unless they have been properly reduced, formation of these bases is reversible in presence of water and might provoke enzyme leakage. However, EB-rROL performed identically in terms of initial reaction rate and operational stability with ethanol with reduced and unreduced Schiff bases (Figure 4.1.3). Consequently, there was no enzyme leakage, i.e., formation of Schiff bases was not reversed owing to the low water concentration in the transesterification medium and the well-known high complexity of the interaction

between aldehyde groups in glutaraldehyde-treated supports and immobilized enzymes [23].

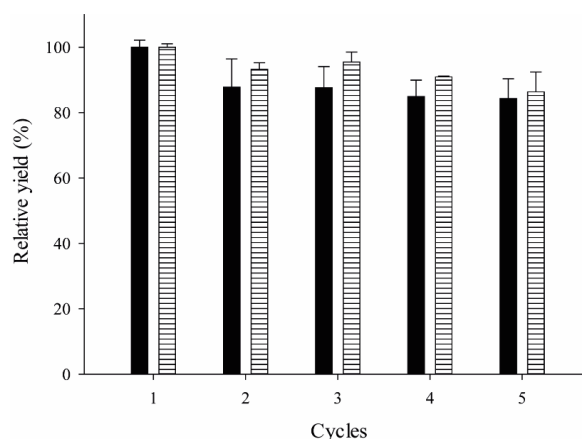


**Figure 4.1.3.** Relative yield (%) of EB-rROL in consecutive transesterification runs with non-reduced (black) and reduced (stranded white) Schiff bases upon exposure to 1 pulse of ethanol. The respective initial reactions yields were taken to be 100%.

#### 4.1.2.3. Lipase immobilization onto magnetite-based supports

Superparamagnetic nanoparticles (MNPs) have been widely used as supports for immobilized enzymes by virtue of their easy recovery by application of a magnetic field. The MNP matrix is non-porous, spherical-like solid magnetite ( $\text{Fe}_3\text{O}_4$ ) that can be functionalized with a broad variety of chemicals for immobilization purposes [24]. In this work, MNPs containing aldehyde groups (MNP-CHO) were synthesized and further functionalized with butylamine to obtain particles with both aldehyde and butyl groups following the methodology described in Sections 3.10 and 3.11. The particles were treated with butylamine solutions of eight different concentrations to obtain functionalized derivatives from MNP-CHO (the blank control, with no butyl groups) to MNP-1MBut-CHO (functionalized with the most concentrated butylamine solution, 1 M). Functionalized nanoparticles were then used to immobilize rROL and the

biocatalysts thus obtained were assessed for the influence of surface butyl groups in the support on biocatalyst performance.

Figure 4.1.4A shows the results of the operational stability screening with ethanol as acyl-acceptor for the optimum butylamine concentration for use in 1.5 mL vials (see Section 3.14). As can be seen, MNPs functionalized with solutions containing a butylamine concentration above 10  $\mu\text{M}$  provided biocatalysts more than twice as stable as those immobilized on MNPs treated with lower butylamine concentrations or no amine (blank). Also, no differences in operational stability were observed with butylamine concentrations above 10  $\mu\text{M}$ . Therefore, a concentration of 1 mM was chosen to assess the influence on the initial transesterification rate and operational stability in 10 mL vials following the same procedure as with Purolite®-based biocatalysts (Section 3.14).

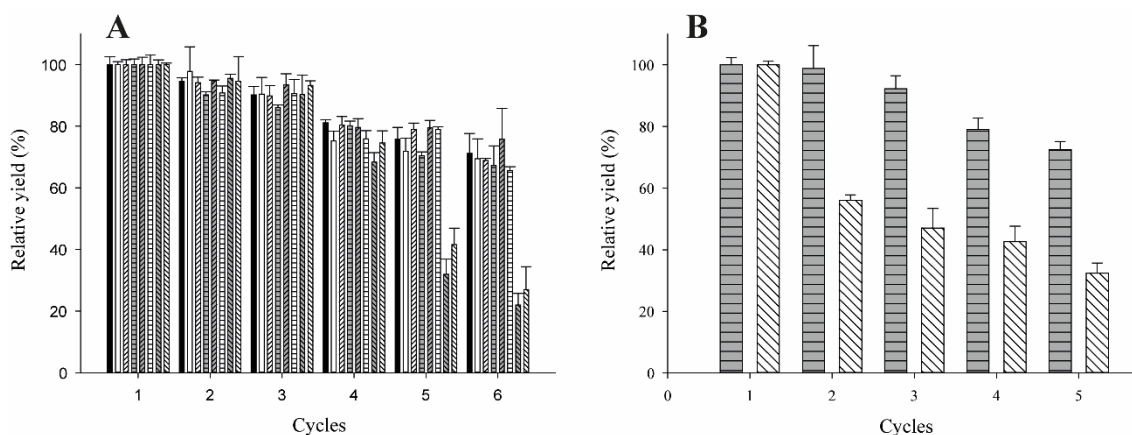


**Figure 4.1.4.** (A) Relative yield (%) of consecutive transesterification runs (1 pulse of ethanol) in the presence of rROL immobilized on MNP-based supports functionalized with solutions ranging from 0 (blank control) to 1 M butylamine in 1.5 mL vials. The bars correspond to the functionalized MNPs obtained by using a butylamine concentration of 1 M (MNP-1MBut-rROL, black,  $\blacksquare$ ), 100 mM (MNP-100mMBut-rROL, white,  $\square$ ), 10 mM (MNP-10mMBut-rROL, up-striped white,  $\text{▨}$ ), 1 mM (MNP-1mMBut-rROL, horizontally striped grey,  $\text{▧}$ ), 100  $\mu\text{M}$  (MNP-100 $\mu\text{M}$ But-rROL, up-striped grey,  $\text{▩}$ ), 10  $\mu\text{M}$  (MNP-10 $\mu\text{M}$ But-rROL, horizontally striped grey,  $\text{▨}$ ), 1  $\mu\text{M}$  (MNP-1 $\mu\text{M}$ But-rROL, down-striped grey,  $\text{▩}$ ) and 0 M (MNP-rROL, blank, down-striped white,  $\text{▩}$ ). (B) Relative yield (%) of consecutive transesterification runs (1 pulse of ethanol) with MNP-1mMBut-rROL (horizontally striped grey,  $\text{▧}$ ) and MNP-rROL (white, down-striped white,  $\text{▩}$ ) in 10 mL vials. The respective first reactions yields were taken to represent 100% yield.

MNP-rROL and MNP-1mMBut-rROL exhibited a similar initial transesterification rate in 10 mL vials. As with the Purolite®-based biocatalysts, the presence of surface hydrocarbon chains on the support had no effect on the initial rate. However, the initial reaction rate with the MNP-based biocatalysts was roughly one-half that obtained with the Purolite®-based counterparts —MNP-rROL  $10.3 \pm 0.25$  and MNP-1mMBut-rROL  $12.2 \pm 0.85$   $\mu\text{mol FAME min}^{-1} \text{cm}^{-3}$ . Operational stability (Figure 4.1.4B) followed the same trend as in the screening tests (Figure 4.1.4A), MNP-1mMBut-rROL being twice more stable than MNP-rROL after 5 consecutive reaction cycles. Whereas MNP-rROL and EX-rROL (i.e., two catalysts with homologous supports as regards functional groups) were similar in operational stability, MNP-1mMBut-rROL was 20% less stable than EO-rROL and 15% less than EB-rROL against 1 pulse of ethanol addition strategy. Therefore, as MNP-based biocatalysts exhibited lower initial reaction rate and operational stability, no further research was performed with them.

#### 4.1.2.4. Biocatalyst performance

In addition to initial reaction rate and operational stability, the biocatalysts were assessed in terms of productivity ( $\mu\text{mol FAEE/FAME min}^{-1}$ ) in 5 consecutive reaction cycles. As can clearly be seen from Table 4.1.2, the biocatalysts immobilized onto supports functionalized with hydrocarbon chains performed better than those onto supports containing none, irrespective of matrix type (polymethacrylate or magnetite nanoparticles). Besides, Purolite®-based biocatalysts with surface hydrocarbon chains exhibited better productivity than MNP-based biocatalysts also containing surface chains (e.g., 20% higher with EO-rROL than with MNP-1mMBut-rROL). Also, productivity among Purolite®-based biocatalysts was 1.5–2 times greater in EO and EB-rROL than in

EX-rROL with 1 pulse of ethanol and 5 of methanol, respectively —differences were smaller with 5 pulses of ethanol as a result of the weaker adverse effect of this acyl-acceptor and of its application being split over several pulses [21]. In addition, adding ethanol in 5 pulses resulted in roughly twice better productivity than using a single pulse with any biocatalyst. Further research splitting the amount of alcohol in more pulses was not performed as it would reduce biodiesel productivity [21].

**Table 4.1.2.** Productivity and volumetric productivity of polymethacrylate- and magnetite-based biocatalysts exposed to a variable number of pulses of methanol or ethanol.

Biocatalyst	Productivity ( $\mu\text{mol min}^{-1}$ )		
	Ethanol 1 pulse	Ethanol 5 pulses	Methanol 5 pulses
EB-rROL	38.27 $\pm$ 1.96	74.89 $\pm$ 0.36	48.76 $\pm$ 0.30
EO-rROL	41.56 $\pm$ 0.91	73.43 $\pm$ 0.42	48.04 $\pm$ 0.35
EDVB-rROL	34.83 $\pm$ 0.28	67.07 $\pm$ 0.39	34.25 $\pm$ 0.38
EX-rROL	23.00 $\pm$ 0.33	60.36 $\pm$ 0.40	19.62 $\pm$ 0.33
MNP-rROL	22.16 $\pm$ 0.66		
MNP-1mMBut-rROL	35.36 $\pm$ 1.50		

Consequently, the productivity and operational stability results led us to choose EO-rROL and 5 pulses of either alcohol for further testing.

#### 4.1.2.5. Alternative substrates: second- and third-generation biodiesel

Although oil pomace was used as a model substrate to assess biocatalysts performance, the potential usefulness of this substrate for the food industry could still stir the ethical debate between food and fuels. We therefore chose to investigate alternative oily substrates such as non-edible vegetable oils from makauba and jatropha, microbial oil from *Rhodospiridium toruloides* and WCO.

Table 4.1.3 shows the acidity of each alternative substrate found following the procedure described in Section 3.19. The values for vegetable oils from makauba [25] and jatropha [26] are consistent within previous reports. However, the acidity of these oils depends markedly on factors such as the harvest and storage conditions [27]. The acidity of microbial oil from *R. toruloides* is also similar to previously reported values [28]. Although the acidity of WCO falls within the typical ranges (less than 0.5% for refined oils and 0.5–15% for used oils; [29]), its low value suggests that it was not extensively cooked—the presence of FFAs in waste oil is mainly a result of oxidative, hydrolytic and thermolytic reactions during frying [30].

**Table 4.1.3.** Percent acidity of alternative oily substrates and initial transesterification rate with EO-rROL.

Substrate	Acidity (%)	Initial reaction rate ( $\mu\text{mol FAME min}^{-1} \text{cm}^{-3}$ )
Makauba oil	$12.16 \pm 0.85$	$21.4 \pm 0.15$
Jatropha oil	$7.85 \pm 0.22$	$24.5 \pm 0.22$
Microbial oil	$2.47 \pm 0.19$	$22.06 \pm 0.34$
WCO	$0.77 \pm 0.13$	$22.8 \pm 0.68$
Olive pomace oil	$18.93 \pm 0.8$	$24.4 \pm 0.33$

The presence of FFAs has been reported to have a favorable effect on the initial reaction rate and the operational stability of enzymes during transesterification [17]. Although EO-rROL exhibited a similar initial rate irrespective of substrate acidity (Table 4.1.3)—what might be explained because not only the initial FFA content is crucial, but also the immediately generated FFAs [31]—this property had a marked effect on its operational stability. With ethanol as acyl-acceptor in the transesterification reaction, oil acidity had no appreciable effect (Figure 4.1.5A) because this alcohol is known to scarcely inactivate lipase. With methanol, a more powerful lipase inactivator [21], FFAs did influence the results (Figure 4.1.5B). Thus, with the least acidic substrate (WCO), the

operational stability of the biocatalyst was rather poor —more than 95% of the initial relative yield was lost after only 5 reaction cycles. Meanwhile, substrates with acidity > 2% maintained at least 60% of the initial value —roughly 30 times more than the relative yield obtained with WCO.

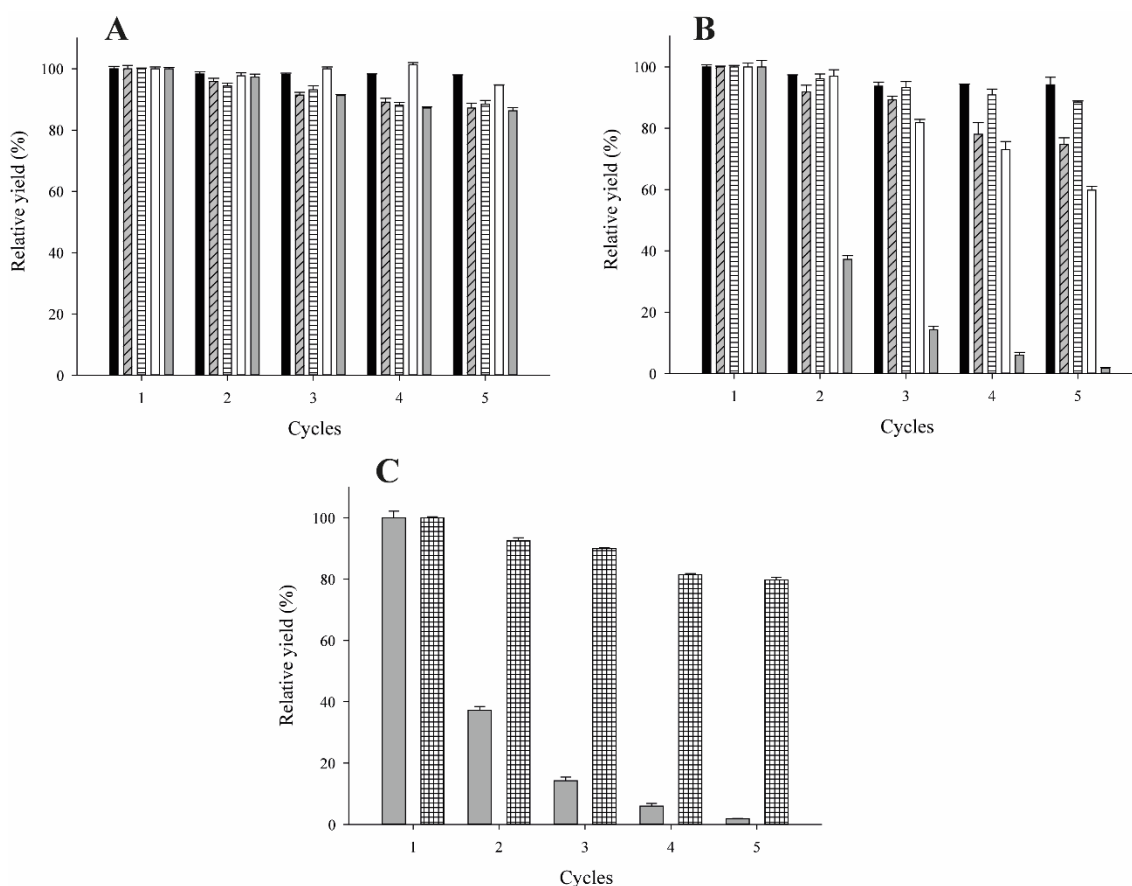


**Figure 4.1.5.** Relative yield (%) of consecutive transesterification cycles of various types of oil with 5 pulses of ethanol (A) or 5 of methanol (B) in the presence of biocatalyst EO-rROL. The bars correspond to pomace (black), makauba (up-striped grey), jatropa (striped white), microbial (white) and WCO (grey). (C) Comparison of the relative yield (%) obtained with 5 (grey) and 10 pulses of methanol (squared white) and WCO as substrate. The initial reactions yields were taken to be 100%.

Therefore, substrate acidity strongly influenced the operational stability of the biocatalyst. Also, the results are suggestive of a synergistic effect of the alcohol and substrate acidity on deactivation of the biocatalysts. This hypothesis was checked by using a reduced concentration of methanol in the reaction medium (specifically, by

splitting the amount of alcohol used in 10 pulses instead of 5) with WCO as substrate. As can be seen from Figure 4.1.5C, the operational stability of the biocatalyst was 20 times greater under these conditions. Therefore, the origin of the synergistic effect was confirmed to be the increased polarity of the reaction medium in the presence of FFAs, which acted as a buffering agent for the high polarity of methanol—and hence for its also high deactivation capacity [32].

#### 4.1.2.6. Transesterification scale-up

Once WCO was found to be the most suitable substrate on the grounds of its low cost, high production and potential for use in accordance with the principles of circular economy [30,33], it was used to scale up the enzymatic production of biodiesel to a 50 mL mini-reactor for industrial proof of concept (Figure 4.1.6A).

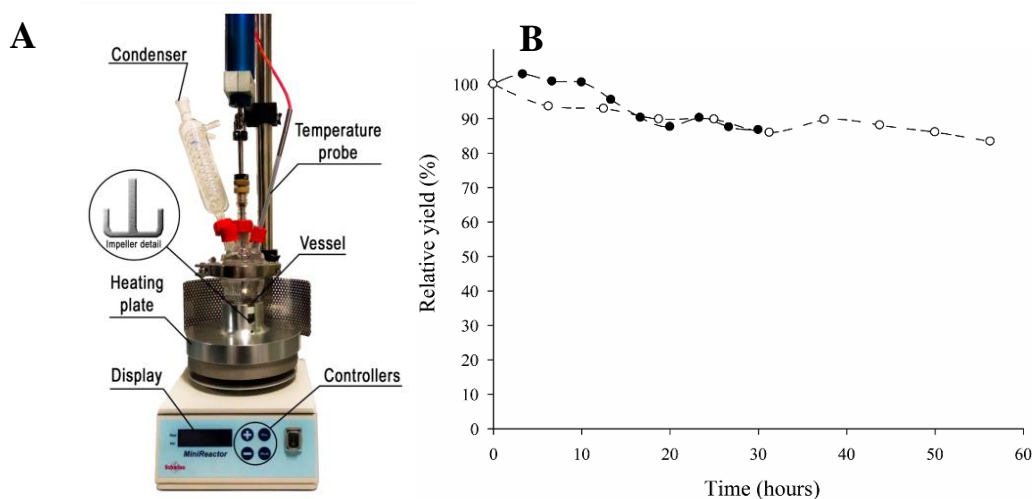


**Figure 4.1.6.** (A) 50 mL Scharlau HME-R mini-reactor from Scharlab. (B) Relative yield (%) of consecutive transesterification cycles of WCO with 5 pulses of ethanol (black circles) and 10 of methanol (white circles) in the presence of biocatalyst EO-rROL. The times on the x-axis are those at which each cycle was started. The initial reactions yield for first cycles were taken to be 100%.



Transesterification runs in 10 mL vials under orbital stirring were successfully scaled up to a stirred tank reactor under mechanical stirring [34]. As can be seen from Figure 4.1.6B, the relative yields obtained in consecutive cycles using 5 pulses of ethanol and 10 of methanol with the laboratory-scale mini-reactor were similar to those obtained in 10 mL vials (Figure 4.1.5). Therefore, the proposed enzymatic biodiesel production method can be easily implemented on an industrial proof of concept scale. Also, around 85% of the initial relative yield was maintained after 10 consecutive reaction cycles with either acyl-acceptor.

Although few studies on the use of WCO in combination with *Rhizopus oryzae* lipase have been reported [35], similar operational stabilities have been obtained with other substrates [36,37]. Also, there was virtually no difference between using 5 pulses of ethanol and 10 pulses of methanol, in order to minimize the negative synergistic effect of the alcohol concentration and substrate acidity on biocatalyst activity at the expense of longer reaction times, reduced productivity and increased operational costs for a potential biodiesel plant.

### **4.1.3. Conclusions**

*Rhizopus oryzae* lipase proved a suitable biocatalyst for biodiesel production from various oily substrates. The hydrocarbon chain length was found to play a key role in increasing the operational stability of rROL immobilized onto polymethacrylate- and magnetite-based supports. Despite their easy recovery, magnetite-based biocatalysts were outperformed by Purolite®-based biocatalysts in terms of initial reaction rate (Purolite® supports showed twice more initial transesterification rate) and operational stability (20% higher operational stability of EO-rROL rather than MNP-1mMBut-rROL).

Regarding the use of alternative substrates to the model olive pomace oil (*alperujo* oil), the factors oil acidity and acyl-acceptor concentration proved crucial and synergistically influential on biocatalyst performance. Concretely, this influence was tested with WCO (the substrate with lower acidity). By minimizing the alcohol concentration in the reaction media by splitting the alcohol in 10 rather than 5 pulses, the operational stability increased in 20 times.

Finally, the fact that the enzymatic transesterification of WCO with EO-rROL was successfully scaled up to a 50 mL mini-reactor for industrial proof of concept validated its potential for implementation to enable enzymatic biodiesel production from an inexpensive substrate and management of the waste under the circular economy principles.

#### 4.1.4. References

- [1] Connolly D, Lund H, Mathiesen B V. Smart Energy Europe: The technical and economic impact of one potential 100% renewable energy scenario for the European Union. *Renew Sustain Energy Rev* 2016;60:1634–53. <https://doi.org/10.1016/j.rser.2016.02.025>.
- [2] Ranganathan SV, Narasimhan SL, Muthukumar K. An overview of enzymatic production of biodiesel. *Bioresour Technol* 2008;99:3975–81. <https://doi.org/10.1016/j.biortech.2007.04.060>.
- [3] Rodrigues J, Perrier V, Lecomte J, Dubreucq E, Ferreira-Dias S. Biodiesel production from crude jatropha oil catalyzed by immobilized lipase/acyltransferase from *Candida parapsilosis* in aqueous medium. *Bioresour Technol* 2016;218:1224–9. <https://doi.org/10.1016/j.biortech.2016.07.090>.
- [4] Hama S, Kondo A. Enzymatic biodiesel production: an overview of potential feedstocks and process development. *Bioresour Technol* 2013;135:386–95. <https://doi.org/10.1016/j.biortech.2012.08.014>.
- [5] Ma Y, Gao Z, Wang Q, Liu Y. Biodiesels from microbial oils: opportunity and challenges. *Bioresour Technol* 2018;263:631–41. <https://doi.org/10.1016/j.biortech.2018.05.028>.
- [6] Navarro López E, Robles Medina A, González Moreno PA, Esteban Cerdán L, Martín Valverde L, Molina Grima E. Biodiesel production from *Nannochloropsis gaditana* lipids through transesterification catalyzed by *Rhizopus oryzae* lipase. *Bioresour Technol* 2016;203:233–44.

- <https://doi.org/10.1016/j.biortech.2015.12.036>.
- [7] López-Fernández J, Barrero JJ, Benaiges MD, Valero F. Truncated prosequence of *Rhizopus oryzae* lipase: key factor for production improvement and biocatalyst stability. *Catalysts* 2019;9:961–77. <https://doi.org/10.3390/catal9110961>.
- [8] Madhavan A, Sindhu R, Binod P, Sukumaran RK, Pandey A. Strategies for design of improved biocatalysts for industrial applications. *Bioresour Technol* 2017;245 Part B:1304–13. <https://doi.org/10.1016/j.biortech.2017.05.031>.
- [9] Ariaeenejad S, Motamedi E, Hosseini Salekdeh G. Application of the immobilized enzyme on magnetic graphene oxide nano-carrier as a versatile bi-functional tool for efficient removal of dye from water. *Bioresour Technol* 2021;319:124228. <https://doi.org/10.1016/j.biortech.2020.124228>.
- [10] Mohamad NR, Marzuki NHC, Buang NA, Huyop F, Wahab RA. An overview of technologies for immobilization of enzymes and surface analysis techniques for immobilized enzymes. *Biotechnol Biotechnol Equip* 2015;29:205–20. <https://doi.org/10.1080/13102818.2015.1008192>.
- [11] Bolivar JM, Nidetzky B. The microenvironment in immobilized enzymes: methods of characterization and its role in determining enzyme performance. *Molecules* 2019;24:3460–84. <https://doi.org/10.3390/molecules24193460>.
- [12] Homaei AA, Sariri R, Vianello F, Stevanato R. Enzyme immobilization: an update. *J Chem Biol* 2013;6:185. <https://doi.org/10.1007/S12154-013-0102-9>.
- [13] Smith S, Goodge K, Delaney M, Struzyk A, Tansey N, Frey M. A Comprehensive review of the covalent immobilization of biomolecules onto electrospun

- nanofibers. *Nanomater* 2020;10:1–39. <https://doi.org/10.3390/NANO10112142>.
- [14] Rodrigues RC, Berenguer-Murcia Á, Carballares D, Morellon-Sterling R, Fernandez-Lafuente R. Stabilization of enzymes via immobilization: multipoint covalent attachment and other stabilization strategies. *Biotechnol Adv* 2021;52:107821. <https://doi.org/10.1016/J.BIOTECHADV.2021.107821>.
- [15] Canet A, Benaiges MD, Valero F, Adlercreutz P. Exploring substrate specificities of a recombinant *Rhizopus oryzae* lipase in biodiesel synthesis. *N Biotechnol* 2017;39:59–67. <https://doi.org/10.1016/j.nbt.2017.07.003>.
- [16] Luo X, Ge X, Cui S, Li Y. Value-added processing of crude glycerol into chemicals and polymers. *Bioresour Technol* 2016;215:144–54. <https://doi.org/10.1016/j.biortech.2016.03.042>.
- [17] Bonet-Ragel K, Canet A, Benaiges MD, Valero F. Synthesis of biodiesel from high FFA *alperujo* oil catalysed by immobilised lipase. *Fuel* 2015;161:12–7. <https://doi.org/10.1016/j.fuel.2015.08.032>.
- [18] Illanes A. Enzyme biocatalysis: principles and applications. *Enzym. Biocatal. Princ. Appl.*, 2008, p. 172–3. <https://doi.org/10.1007/978-1-4020-8361-7>.
- [19] Klibanov AM. Stabilization of enzymes against thermal inactivation. *Adv Appl Microbiol* 1983;29:1–28. [https://doi.org/10.1016/S0065-2164\(08\)70352-6](https://doi.org/10.1016/S0065-2164(08)70352-6).
- [20] Ollis DF. Diffusion influences in denaturable insolubilized enzyme catalysis. *Biotechnol Bioeng* 1972;14:871–84. <https://doi.org/10.1002/bit.260140603>.
- [21] Bonet-Ragel K, Canet A, Benaiges MD, Valero F. Effect of acyl-acceptor stepwise addition strategy using *alperujo* oil as a substrate in enzymatic biodiesel synthesis.

- J Chem Technol Biotechnol 2018;93:541–7. <https://doi.org/10.1002/jctb.5399>.
- [22] Urrutia P, Arrieta R, Alvarez L, Cardenas C, Mesa M, Wilson L. Immobilization of lipases in hydrophobic chitosan for selective hydrolysis of fish oil: the impact of support functionalization on lipase activity, selectivity and stability. *Int J Biol Macromol* 2018;108:674–86. <https://doi.org/10.1016/j.ijbiomac.2017.12.062>.
- [23] Sheldon RA, van Pelt S. Enzyme immobilisation in biocatalysis: why, what and how. *Chem Soc Rev* 2013;42:6223–35. <https://doi.org/10.1039/C3CS60075K>.
- [24] Del Arco J, Alcántara AR, Fernández-Lafuente R, Fernández-Lucas J. Magnetic micro-macro biocatalysts applied to industrial bioprocesses. *Bioresour Technol* 2021;322:124547. <https://doi.org/10.1016/j.biortech.2020.124547>.
- [25] Agueiras ECG, Cavalcanti-Oliveira ED, De Castro AM, Langone MAP, Freire DMG. Biodiesel production from *Acrocomia aculeata* acid oil by (enzyme/enzyme) hydroesterification process: use of vegetable lipase and fermented solid as low-cost biocatalysts. *Fuel* 2014;135:315–21. <https://doi.org/10.1016/j.fuel.2014.06.069>.
- [26] Jain S, Sharma MP. Kinetics of acid base catalyzed transesterification of *Jatropha curcas* oil. *Bioresour Technol* 2010;101:7701–6. <https://doi.org/10.1016/j.biortech.2010.05.034>.
- [27] Souza GK, Scheufele FB, Pasa TLB, Arroyo PA, Pereira NC. Synthesis of ethyl esters from crude macauba oil (*Acrocomia aculeata*) for biodiesel production. *Fuel* 2016;165:360–6. <https://doi.org/10.1016/j.fuel.2015.10.068>.
- [28] Singh G, Jeyaseelan C, Bandyopadhyay KK, Paul D. Comparative analysis of

- biodiesel produced by acidic transesterification of lipid extracted from oleaginous yeast *Rhodospiridium toruloides*. 3 Biotech 2018;8:434. <https://doi.org/10.1007/s13205-018-1467-9>.
- [29] Lam MK, Lee KT, Mohamed AR. Homogeneous, heterogeneous and enzymatic catalysis for transesterification of high free fatty acid oil (waste cooking oil) to biodiesel: a review. Biotechnol Adv 2010;28:500–18. <https://doi.org/10.1016/j.biotechadv.2010.03.002>.
- [30] Hama S, Yoshida A, Tamadani N, Noda H, Kondo A. Enzymatic production of biodiesel from waste cooking oil in a packed-bed reactor: an engineering approach to separation of hydrophilic impurities. Bioresour Technol 2013;135:417–21. <https://doi.org/10.1016/j.biortech.2012.06.059>.
- [31] Lin YH, Luo JJ, John Hwang SC, Liao PR, Lu WJ, Lee HT. The influence of free fatty acid intermediate on biodiesel production from soybean oil by whole cell biocatalyst. Biomass and Bioenergy 2011;35:2217–23. <https://doi.org/10.1016/j.biombioe.2011.02.039>.
- [32] Canet A, Bonet-Ragel K, Benaiges MD, Valero F. Lipase-catalysed transesterification: viewpoint of the mechanism and influence of free fatty acids. Biomass and Bioenergy 2016;85:94–9. <https://doi.org/10.1016/j.biombioe.2015.11.021>.
- [33] Olkiewicz M, Torres CM, Jiménez L, Font J, Bengoa C. Scale-up and economic analysis of biodiesel production from municipal primary sewage sludge. Bioresour Technol 2016;214:122–31. <https://doi.org/10.1016/j.biortech.2016.04.098>.
- [34] Bonet-Ragel K. Enzymatic synthesis of biodiesel from high free fatty acid

- feedstock using a recombinant *Rhizopus oryzae* lipase. Universitat Autònoma de Barcelona, 2018.
- [35] López-Fernández J, Benaiges MD, Valero F. *Rhizopus oryzae* lipase, a promising industrial enzyme: biochemical characteristics, production and biocatalytic applications. *Catalysts* 2020;10:1277. <https://doi.org/10.3390/catal10111277>.
- [36] Duarte SH, del Peso Hernández GL, Canet A, Benaiges MD, Maugeri F, Valero F. Enzymatic biodiesel synthesis from yeast oil using immobilized recombinant *Rhizopus oryzae* lipase. *Bioresour Technol* 2015;183:175–80. <https://doi.org/10.1016/j.biortech.2015.01.133>.
- [37] Su F, Li G, Zhang H, Yan Y. Enhanced performance of *Rhizopus oryzae* lipase immobilized on hydrophobic carriers and its application in biorefinery of rapeseed oil deodorizer distillate. *Bioenergy Res* 2014;7:935–45. <https://doi.org/10.1007/s12155-014-9415-y>.





# 4

## Results I: Biodiesel production

### 4.2. Industrial enzymatic synthesis of biodiesel from waste cooking oil: Near Infrared Spectroscopy, a useful technique for inline monitoring of the biosynthesis

---

Chapter accepted as research article in Fuel  
Research performed in collaboration with Manel Alcalà Bernàrdez,  
from the Research Group of Applied Chemometric  
López-Fernández J, Moya D, Benaiges MD, Valero F, Alcalà M.  
Near Infrared Spectroscopy: a useful technique for inline monitoring of the  
enzyme catalyzed biosynthesis of third-generation biodiesel from waste cooking oil  
Fuel (accepted)



## **4. RESULTS I**

### **4.2. Industrial enzymatic synthesis of biodiesel from waste cooking oil: Near Infrared Spectroscopy, a useful technique for inline monitoring of the biosynthesis.**

<i>4.2.1. Introduction</i> .....	189
<i>4.2.2. Results and discussion</i> .....	191
4.2.2.1. Fatty acid composition of the waste cooking oil.....	191
4.2.2.2. Transesterification reaction.....	192
4.2.2.3. Near infrared (NIR) spectra.....	195
<i>4.2.3. Conclusions</i> .....	205
<i>4.2.4. References</i> .....	207



### 4.2.1. Introduction

During chemically or enzymatically catalyzed transesterification for biodiesel production, the reaction medium contains a mixture of fatty acid methyl and ethyl esters (FAM/EE), FFA and tri-, di- and monoacylglycerols. Production performance is usually assessed by gas chromatography (GC), using an offline and sluggish analytical procedure [1]. Moreover, low volatile substances can damage capillary columns and other elements of the chromatographic system, so a number of alternative techniques including high-performance liquid chromatography (HPLC) [2] and proton nuclear magnetic resonance ( $^1\text{H-NMR}$ ) spectroscopy [3] are being increasingly used instead. Chromatographic techniques, however, are expensive and time-consuming; also, they cannot operate inline, which prevents timely decision-making during the process and can increase production costs by requiring stops —or even batch reprocessing if the target quality is not achieved [4]. The principles of Continued Process Verification (CPV) have made bioprocess automatization and Process Analytical Technology (PAT) increasingly attractive; also, they have promoted the use of analytical methods allowing real-time quality assessment, adoption of corrective measures and a better understanding of bioprocesses [5,6]. Such methods require in- or online monitoring of the process, and hence using, for instance, spectroscopic techniques (Raman, fluorescence, UV-Vis, IR, NIR) in combination with multivariate calibration [7].

NIR spectroscopy is an extensively studied analytical technique based on the interaction of matter and light radiation in the wavelength region from 780 to 2500 nm that affords multicomponent, fast, reliable, inexpensive and non-destructive analysis [1]. Besides, it avoids the need for sample withdrawal when used inline, waste production, and the need for complex pre-treatments of samples with solvents or other chemicals, all

of which makes it a safe, clean, energy-saving choice fully compliant with the principles of green chemistry [8]. NIR spectra are complex and possess broad overlapping bands that require special mathematical procedures to accurately interpret spectra and understand the results, such as principal component analysis (PCA) or partial least-squares (PLS) regression [9]. NIR spectroscopy has so far been successfully used by the biodiesel industry to assess the quality or properties of biofuel/diesel blends [9,10], and also for inline monitoring of chemically catalyzed transesterification reactions [1,11,12].

In this chapter, the mature sequence of ROL (rROL) was immobilized onto a suitable support (Purolite® with surface epoxide and octadecyl groups) in order to catalyze the transesterification of waste cooking oil (WCO) in a solvent-free system with ethanol or methanol as acyl-acceptor. Due to the already indicated importance of WCO in Section 4.1.2.6 for the principles of circular economy and to avoid the generation of a waste with a high potential to contaminate the water in case it is not handled properly, this substrate was selected for further research related to industrial implementation and control of the biosynthesis of biodiesel from this oleaginous waste. The main novelty of this work is the use of near infrared spectroscopy for inline monitoring of an enzyme catalyzed transesterification reaction in a laboratory-scale reactor specially designed for use of a NIR probe. The results were compared with those obtained by gas chromatography (GC) as reference in order to confirm the suitability of the NIR technique for accurate real-time monitoring of transesterification under the principles of CPV and PAT while avoiding the environmental and economic costs of withdrawing samples during the process. Unlike previous works on the NIR based monitoring of biodiesel production, the fact of performing a stepwise addition of alcohol and the employment of immobilized enzyme might generate background noise in the spectra, making the NIR

monitoring more challenging. Besides, the biocatalyst operational stability and mechanical strength were evaluated and compared with previously reported data.

All the chemometrics analyses of this chapter were performed by Manel Alcalà Bernàrdez, from the Research Group of Applied Chemometric, under a collaboration that aimed to apply this field of research in the monitoring of enzymatic transesterification of biodiesel.

### 4.2.2. Results and discussion

#### 4.2.2.1. Fatty acid composition of the waste cooking oil

Local public waste management companies typically collect large amounts of WCO from different sources and must manage it properly. As a result, WCO composition can vary widely depending on consumption patterns and regional or local cooking traditions. In Spain, most cooking is done with olive or sunflower oil, which leave vast amounts of oleaginous waste [13].

Because it was obtained from a public waste management company not implementing traceability, the oil used here was of unknown origin. Analysis of its fatty acid composition were performed as described in Section 3.20 to compare it with published profile of olive and sunflower oil and results exhibited that the fatty acid profile for the WCO was similar to that for olive oil (Table 4.2.1) [14].

**Table 4.2.1.** Percent fatty acid composition profile for sunflower, olive and waste cooking oil (WCO).

Acid	Sunflower oil	Olive oil	WCO
Stearic	2.8	2.3	2.46 ± 0.04
Oleic	28.0	66.4	70.78 ± 0.38
Linoleic	62.2	16.4	10.21 ± 0.01
Linolenic	0.16	1.6	2.45 ± 0.02



#### 4.2.2.2. Transesterification reaction: scale up, productivity and half-life

The transesterification reactions initially conducted in 10 mL vials were successfully scaled up to a 50 mL laboratory reactor specially designed for use with a NIR following the methodology described in Section 3.14.2. Already optimized conditions, regarding the biocatalyst and the alcohol addition strategy for biodiesel production from WCO (Section 4.1) were employed and as can be seen from Figures 4.2.1A and 4.2.1B, the yield profiles for the first reaction batch were almost identical with ethanol and methanol in both the vial and the reactor —because of the 1,3-regioespecificity of ROL, the theoretical maximum yield in the absence of acyl-migration phenomena is 66%, resulting in the formation of the corresponding alkyl esters and 2-monoacylglycerol [15]. The results therefore suggest that mass transfer and reaction performance in the vials and the reactor were essentially identical under the employed conditions, and also that the presence of the NIR probe did not detract from homogeneity in the reaction medium. Thus, the 50 mL reactor with a customized lid and tank, and a second stirrer (Figure 4.2.2A), reproducibly echoed the results obtained with 10 mL vials. In fact, both systems led to similar relative yields after 5 consecutive cycles (Figures 4.2.1C-1D).

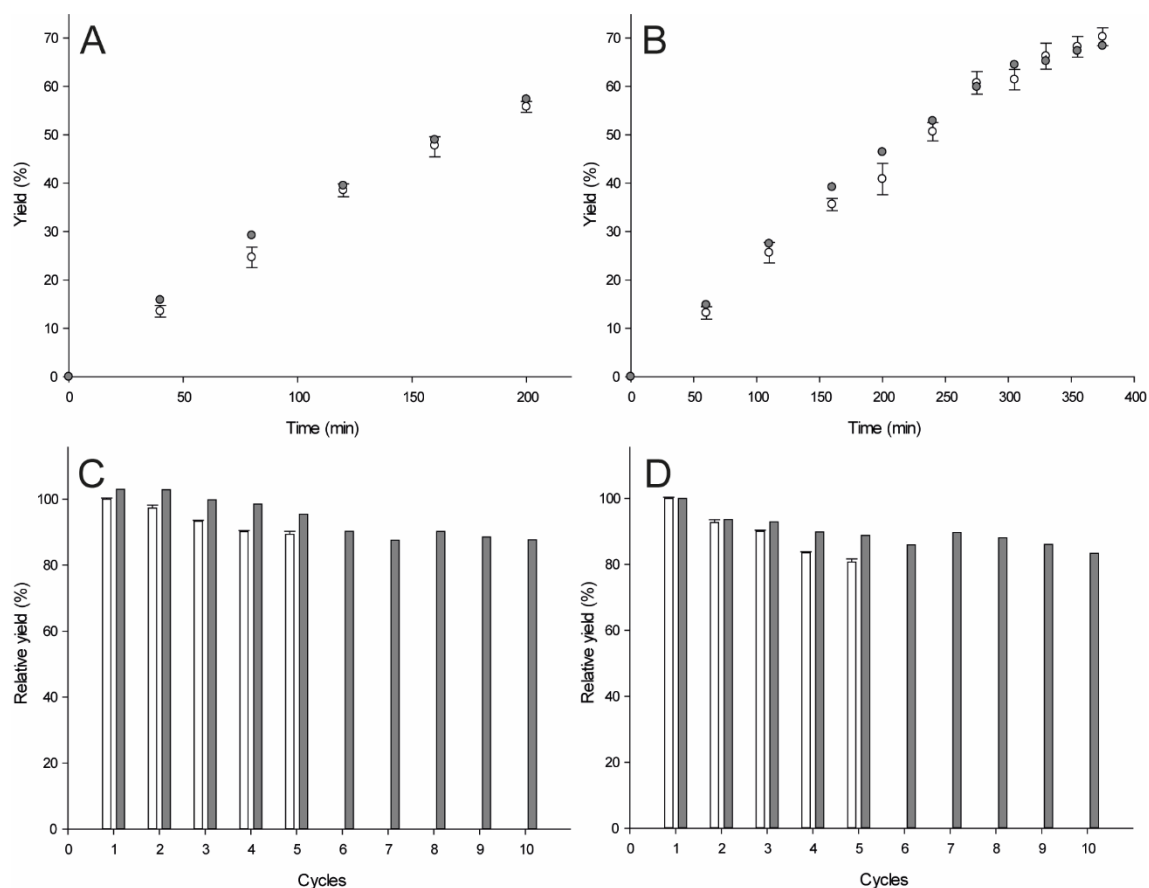


**Figure 4.2.1.** Yield profile for WCO transesterification with 5 pulses of ethanol (A) and 10 of methanol (B) in the presence of EO-rROL. Relative yield of consecutive transesterification cycles with 5 pulses of ethanol (C) and 10 of methanol (D). White bars and points correspond to the reaction in 10 mL vials and grey bars and points to that in the laboratory minireactor. Relative yields were calculated against that of the first cycle (100 %).

Biodiesel productivity with each alcohol was calculated as the combined figure for all 10 cycles performed in the laboratory-scale reactor. As expected, FAEE productivity (ethanol as acyl-acceptor) was 1.5 times higher than FAME productivity (methanol as acyl-acceptor) as a result of the longer reaction times required for transesterification with the latter alcohol (Table 4.2.2), even though, the final transesterification yields with methanol were slightly higher than those obtained with ethanol (Figures 4.2.1A-1B). In fact, splitting the amount of alcohol used into 10 pulses is unproductive with alcohols such as ethanol—it has scarce negative impact on the

operational stability of the biocatalyst— but can be useful with others such as methanol with severe influence on enzyme stability [16,17]. Thus, the biocatalyst half-life in hours with methanol as acyl-acceptor was about 1.5–2.5 times higher than it was with ethanol as a result of the amount of methanol used being split into more pulses than that of ethanol (Table 4.2.2). However, when reaction cycles corresponding to these hours were compared, half-lives ( $t_{1/2}$  values into square brackets in Table 4.2.2) tended to be similar with both alcohols as a consequence of the reaction times differing between the two.

**Table 4.2.2** – EO-rROL productivity and half-life in biodiesel production with ethanol and methanol as calculated by fitting to a first-order exponential decay (Eq. 1) and two-component first-order exponential decay (Eq. 2) deactivation model.

Acyl acceptor	Model equation	$R^2$	Half-life (h) <sup>1</sup>	Productivity ( $\mu\text{mol min}^{-1}$ )
Ethanol	1	0.8696	170 [51]	327
	2	0.9578	146.7 [44]	
Methanol	1	0.8682	225 [36]	219
	2	0.9534	337.5 [54]	

<sup>1</sup> The numbers in square brackets represent the number of cycles for those of reaction hours

ROL has exhibited widely variable operational stability in biodiesel production from various substrates. For instance, ROL covalently immobilized onto Relizyme™ OD403 was used to transesterify olive pomace oil with methanol and the relative yield found to decrease to 60% after 26.7 h reaction (7 batches) [18]. In another study with soybean oil, the transesterification yield with glutaraldehyde cross-linked whole-cell biocatalysts decreased from 84 to 65% after 2520 h reaction (35 batches) [19]. By contrast, the ROL catalyzed transesterification of WCO has been the subject of little study, so comparison with previous results is challenging [20]. Therefore, although a number of half-life values for ROL based biocatalysts used in biodiesel transesterification reactions have been reported with several substrates, comparison with WCO would be

more accurate since this substrate may deactivate the enzyme more markedly as the likely result of its containing detrimental components such as phenolics or varying widely in acidity [21–23].



**Figure 4.2.2.** (A) Customized reactor for use of the NIR probe. (B) The EO-rROL biocatalyst after 10 consecutive reaction cycles as seen under a binocular loupe.

The biocatalysts were imaged with a binocular loupe after the whole sequence of reaction with each acyl-acceptors in order to check whether they had retained their structure without fracturing by effect of mechanical stress under agitation (Figure 4.2.2B). No substantial breaks were detected after the ten cycles, which confirms the strength of the support and its suitability for industrial use.

#### 4.2.2.3. Near infrared (NIR) spectra: a useful tool for the biodiesel industry

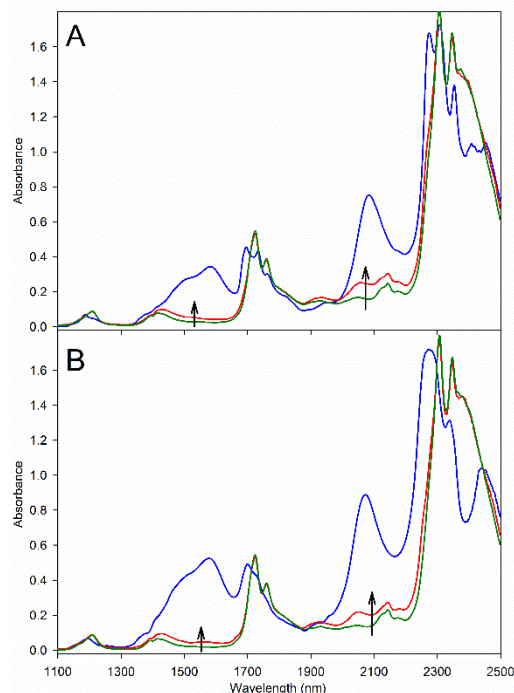
Once the biocatalyst suitability for biodiesel production under conditions mimicking industrial work was confirmed, development of a system enabling compliance with CPV and PAT principles during monitoring of the reaction was sought by using an inline monitoring technique instead of gas chromatography—the most common choice for offline monitoring of biodiesel production. NIR spectroscopy was chosen on the grounds of its allowing immediate detection of potential deviations in the process that might detract from biodiesel quality, modification of the alcohol feeding pattern and renewal of

the biocatalyst when required to avoid deactivation and its adverse impact on productivity. A NIR probe inserted in a customized reactor was used in combination with two different calibration models to monitor the transesterification reaction. The results obtained in these subsections were performed in collaboration with Manel Alcalà Bernàrdez PhD., from the Research Group of Applied Chemometrics, who carried out all the chemometrics analyses.

#### 4.2.2.3.1. Spectral data

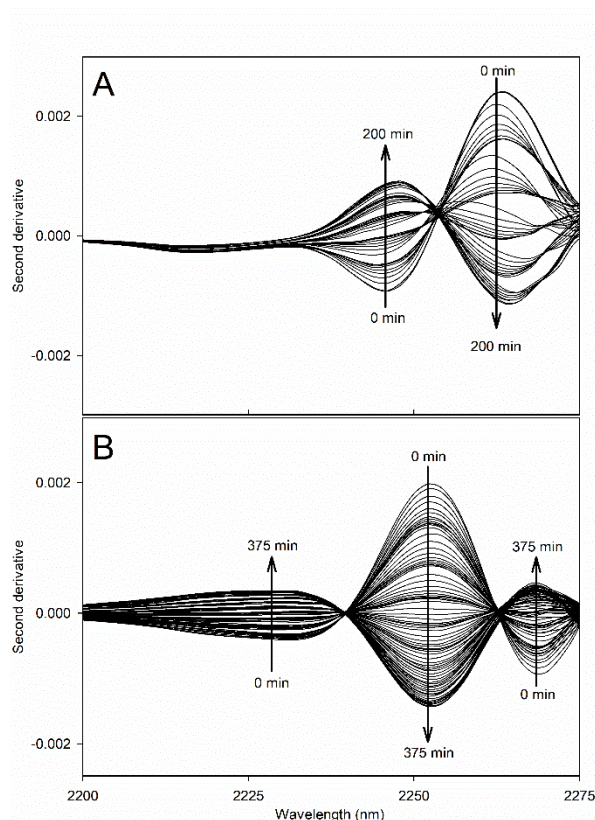
Absorbance spectra acquired across the NIR spectral range (1100–2498 nm) were visually inspected to identify gross outliers and noisy spectral regions. The range from 2352 to 2498 nm exhibited little variability and considerable noise typical of fiber optic probes, so only that from 1100 to 2350 nm was used. Figure 4.2.3 shows the first and last spectra obtained in a reaction run with ethanol and methanol as compared with those for the pure alcohols. Ethanol and methanol (Figure 4.2.3, blue plots) exhibited the following major spectral bands: 1425–1475 nm (OH first overtone), 1650–1750 nm (CH first overtone), 2000–2100 nm (OH combinations) and 2200–2450 nm (CH+CH combinations and CC+CH combinations). Expectedly, methanol spectra presented less bands than that of ethanol at 1650–1750 nm and 2200–2450 nm due to the absence of CH<sub>2</sub>; the bands corresponding with CH first overtone, CH+CH and CH+CC combinations are only related with the CH<sub>3</sub> group from methanol. The spectra at the start of the reaction (Figure 4.2.3, green plots) exhibited the following spectral bands: high absorbance at 1650–1750 nm (CH first overtone), very low absorbance at 1875–1950 nm (CO second overtone), low absorbance at 2000–2100 nm (OH combinations) and very high absorbance at 2200–2450 nm (CH+CH and CC+CH combinations). The spectra at the end of the reaction

(Figure 4.2.3, red plots) showed higher absorbance than that of the starting point almost throughout the whole studied spectral range (1100-2400 nm). The final yield after the two batches of Figure 4.2.3 was 61.0% with ethanol and 65.9% with methanol.



**Figure 4.2.3.** NIR absorbance spectra recorded at the start (green) and end (red) of the reaction as compared with those for each pure alcohol (blue): ethanol (A) and methanol (B). The arrows represent evolution of the reactions.

The typically extensive overlap of bands and fairly low resolution of the NIR technique required increasing resolution by using a spectral derivative treatment. The spectral ranges 1400–1700 nm and 1900–2300 nm were adequate to visualize the spectral changes during the reaction because of the low absorbance of the WCO and high absorbance of the alcohols. Figure 4.2.4 shows the second derivative spectra of the first cycle with ethanol (Figure 4.2.4A) and with methanol (Figure 4.2.4B), in the wavelength range between 2200 and 2275 nm. As can be seen, the bands were highly ordered in terms of yield and reaction time. This result is also observed throughout the entire wavelength range of 1100–2350nm.



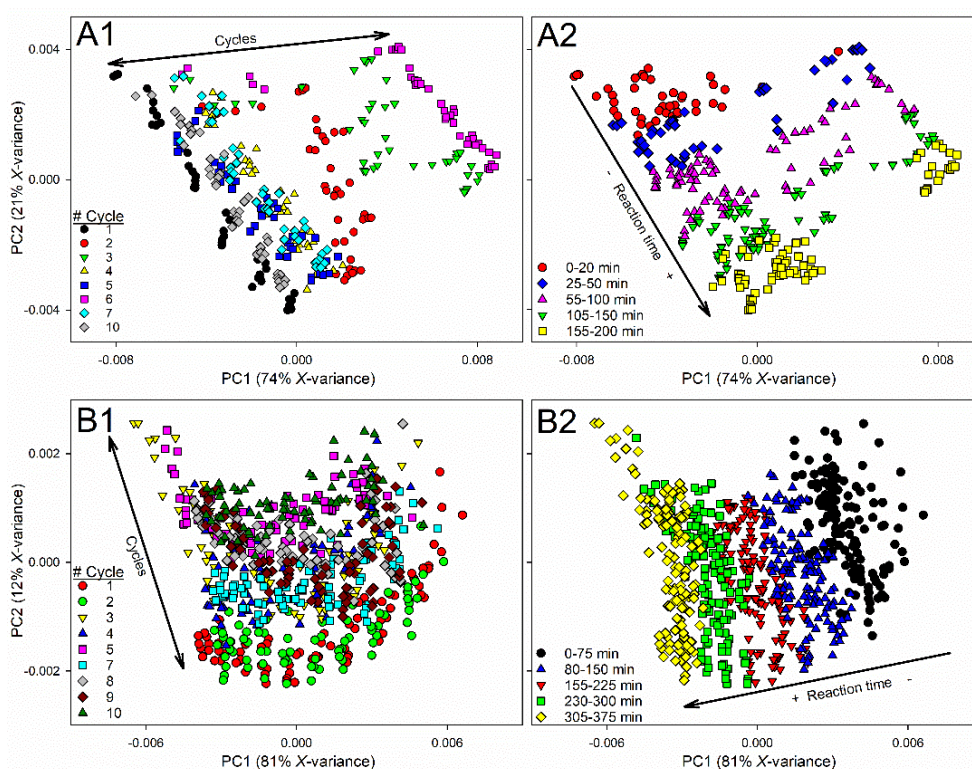
**Figure 4.2.4.** Second-derivative NIR spectra obtained in the first reaction batch with (A) ethanol and (B) methanol as acyl-acceptor. The arrows represent reaction time.

Table 4.2.3 summarizes the dimensions of the *X*- and *Y*-datasets. The number of rows coincided with that of measured spectra and the number of columns with that of variables (wavelengths and reaction yield). The reaction with methanol took almost twice as long as that with ethanol (375 min vs 200 min). Since the spectrum acquisition frequency was identical with both alcohols (1 spectrum every 5 min), the available *X*-matrix for the reaction with methanol contained many more rows than that for ethanol (684 vs 322). The sampling frequency for gas chromatography analysis was approximately 1 sample every 15 min. As a result, the number of rows in the *Y*-matrix for which a yield value was available was roughly one-third of all (viz., 123 out of 322 for ethanol and 243 out of 684 for methanol).

**Table 4.2.3.** Dimensions of the X-dataset and Y-dataset.

	Reaction with ethanol	Reaction with methanol
Reaction time (min)	200	375
X-matrix (1100–2350 nm)	322 rows and 626 columns	684 rows and 626 columns
Y-matrix (Reaction yield %)	123 rows and 1 column	243 rows and 1 column

Data from second-derivative spectra spanning the range 1100–2350 nm were initially explored through PCA method. One PCA for each alcohol was calculated by using the whole X-matrix. The scores plot of the second principal component against the first (PC2 vs PC1) explained approximately 95% of the variance in X (Figure 4.2.5).



**Figure 4.2.5.** PCA scores plot constructed from second-derivative spectra over the range 1100–2350 nm obtained with ethanol (A1-A2) and methanol as acyl-acceptor (B1-B2). The 1 and 2 subplots stand for different symbol related to cycles and reaction time, respectively.



Figures 4.2.5A were calculated from the reactions with ethanol, and 4.2.5B with methanol. There were two main sources of spectral variability, namely: reaction time and reaction cycle. For the reaction with ethanol (4.2.5A1-A2), the reaction cycle is mostly explained by the PC1, accounting for 81% of the *X*-variance, and the reaction time by the PC2 (21%). For the reaction with methanol (4.2.5B1-B2), the reaction time is mostly explained by the PC1 (74%) and the reaction cycle by the PC2 (12%). Neither standard normal variate (SNV) scaling nor first-derivative treatment, whether individually or in combination, provided better results for the reaction with ethanol—at least not on a par with the scores plots for methanol.

#### 4.2.3.3.2. Calibration

The Kennard–Stone method selects a subset of calibration samples which provide a very uniformly distributed network of selected points over the dataset and includes samples on its boundary. Table 4.2.4 shows the number of spectra used for calibration and prediction. The calibration set for the ethanol reaction included 24 samples from reaction cycles 1, 2, 3 and 6, which spanned a FAEE yield range of 0.0–61.0%, while the set for methanol comprised 27 samples from reaction cycles 2, 3 and 10, with a FAME yield of 6.2–68.9%. No spectrum for a near-zero yield was available for methanol owing to instrumental issues arising at the beginning of the reaction. All other spectra were included in the prediction set.

**Table 4.2.4.** Number of spectra used to construct the calibration and prediction sets, figures of merit of the calibration models and predictive ability.

	<b>Reaction with ethanol</b>	<b>Reaction with methanol</b>
<b>Calibration</b>		
Number of spectra	24 (4 cycles)	27 (3 cycles)
PLS factors	2	2
Yield range (%)	0.0–61.0	6.2–68.9
Cumulative <i>Y</i> -variance explained		
Factor 1	66.9	91.4
Factor 2	98.1	99.6
NIR vs GC regression		
Slope	0.98 ± 0.06	0.99 ± 0.03
Intercept	0.6 ± 2.1	0.2 ± 1.2
Correlation coefficient ( <i>r</i> )	0.990	0.998
RMSEC (%)	2.4	1.3
<b>Prediction</b>		
Number of spectra (total)	298 (8 cycles)	657 (9 cycles)
Number of spectra (with GC reaction yield value)	99	203
Number of spectra (without GC reaction yield value)	199	454
Yield range (%)	0.0-59.4	6.3-68.8
NIR vs GC regression		
Slope	0.98 ± 0.03	0.99 ± 0.01
Intercept	1.0 ± 1.1	-0.3 ± 0.6
Correlation coefficient ( <i>r</i> )	0.989	0.996
RMSEP (%)	2.1	2.0

Reaction yields were quantified by using PLS calibration models constructed from independent calibration and prediction sets of NIR spectra. Models spanning a narrow spectral range failed to reduce calibration or prediction errors relative to the whole spectral range. Also, narrow ranges failed to reduce the number of factors required by each model. Second-derivative spectra proved the best choice in any case.

Table 4.2.4 summarizes the calibration and prediction results obtained with the PLS model for each alcohol. Both were constructed with two factors and explained a cumulative *Y*-variance (yield) higher than 98%. The only difference between the two was the *Y*-variance captured by the first factor, which was 66.9% with ethanol and 91.4% with

methanol. This was a result of the distribution of PCA scores and the two sources of variability observed (reaction time and reaction cycle; Figure 4.2.5). The *Y*-variable was explained mainly by PC1 in the reaction with methanol, and by both PC1 and PC2 in the reaction with ethanol. The model using PC1 alone was more robust for methanol than it was for ethanol. With PC1 and PC2 jointly, however, the two models captured almost the same *Y*-variance (98.1% for ethanol and 99.6% for methanol). The upper range of biodiesel yield for the reaction with methanol (68.9%) was higher by effect of the increased experimental reaction yield. Calibration errors (RMSEC), expressed in the same units as yield, were 2.4% for ethanol and 1.3% for methanol and the correlation coefficients were higher than 0.99.

The prediction results of Table 4.2.4 were obtained from pure independent sets which were not employed during calibration. Regression lines for NIR yield versus GC yield plots were evaluated through different tests and analysis. In this sense, the correlation coefficients were high (viz., 0.989 and 0.996 for ethanol and methanol, respectively). The residuals were randomly distributed around 0 and their normal distribution was demonstrated with the Anderson-Darling, Ryan-Joiner and Kolmogorov-Smirnov tests (95% of significance). The Mandel test for linearity was calculated for the two regressions and the F-tests (95% of significance) concluded that quadratic models do not perform better than linear ones. The absence of significant differences between the two techniques was demonstrated through the t-tests (95% of significance) of the slope and intercept of the NIR versus GC regressions. In fact, the slopes and intercepts were not significantly different from 1 and 0, respectively, which highlights the accuracy of the NIR method. Finally, the satisfactory predictive ability was also assessed with the low RMSEP prediction errors (2.1% for ethanol and 2.0% for methanol). As can be seen in

Table 4.2.5, RMSEP for the individual reaction cycles ranged from 1.0 to 2.7%. Although RMSEC for the methanol model was lower than for the ethanol model (1.3% vs 2.4%), there were virtually no differences in predictive ability between the two on an individual batch basis.

**Table 4.2.5.** RMSEP (%) value for each reaction cycle.

RMSEP	Cycle										Overall
	1	2	3	4	5	6	7	8	9	10	
<b>Reaction with ethanol</b>	2.4	2.0	2.7	2.1	1.9	2.1	1.6	NA	NA	1.6	2.1
<b>Reaction with methanol</b>	2.0	1.0	1.9	2.1	2.1	N/A	2.5	1.9	2.0	2.3	2.0

N/A: not available

#### 4.2.3.3.3. Validation

Figures 4.2.6 and 4.2.7 show the NIR profiles of yield vs time used to validate the results of the reaction cycles with the two alcohols. The figures represent the NIR predictions from the whole set of prediction spectra (with or without a matching reaction yield obtained by GC), namely: 298 spectra for ethanol and 657 for methanol. These spectra were distributed among the 8 reaction cycles examined for ethanol and the 9 for methanol.

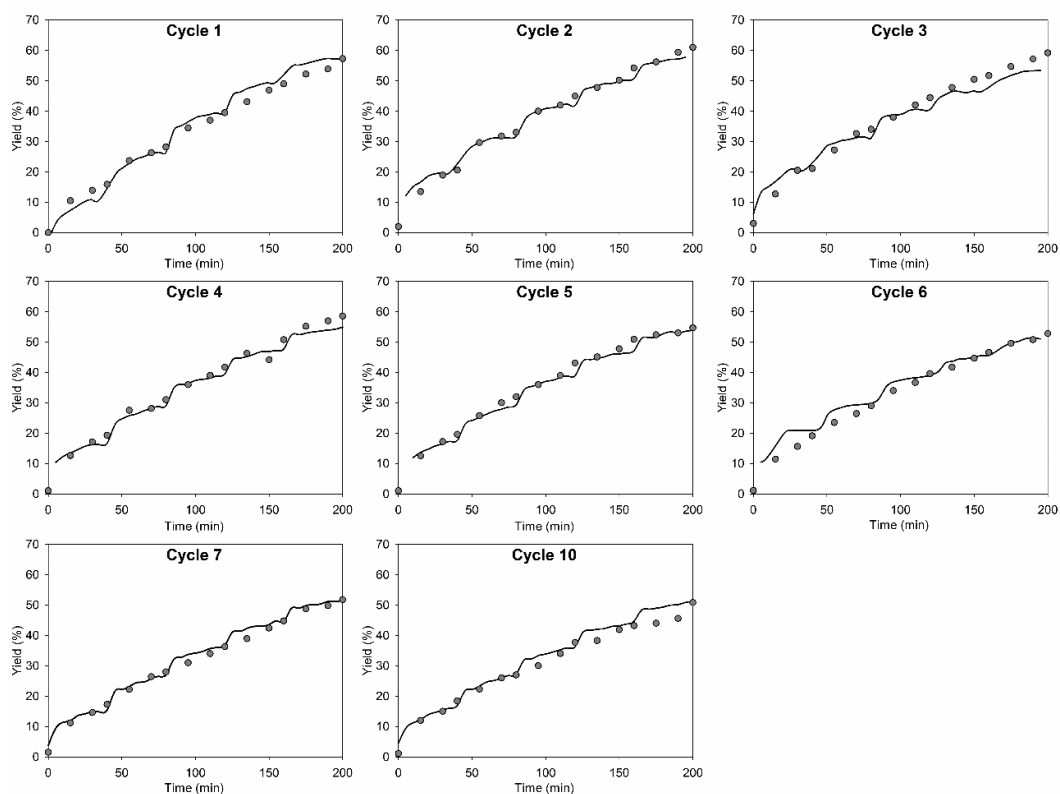


**Figure 4.2.6.** NIR prediction of reaction yields (solid line) with ethanol as acyl-acceptor. Dots represent reference GC yield values.

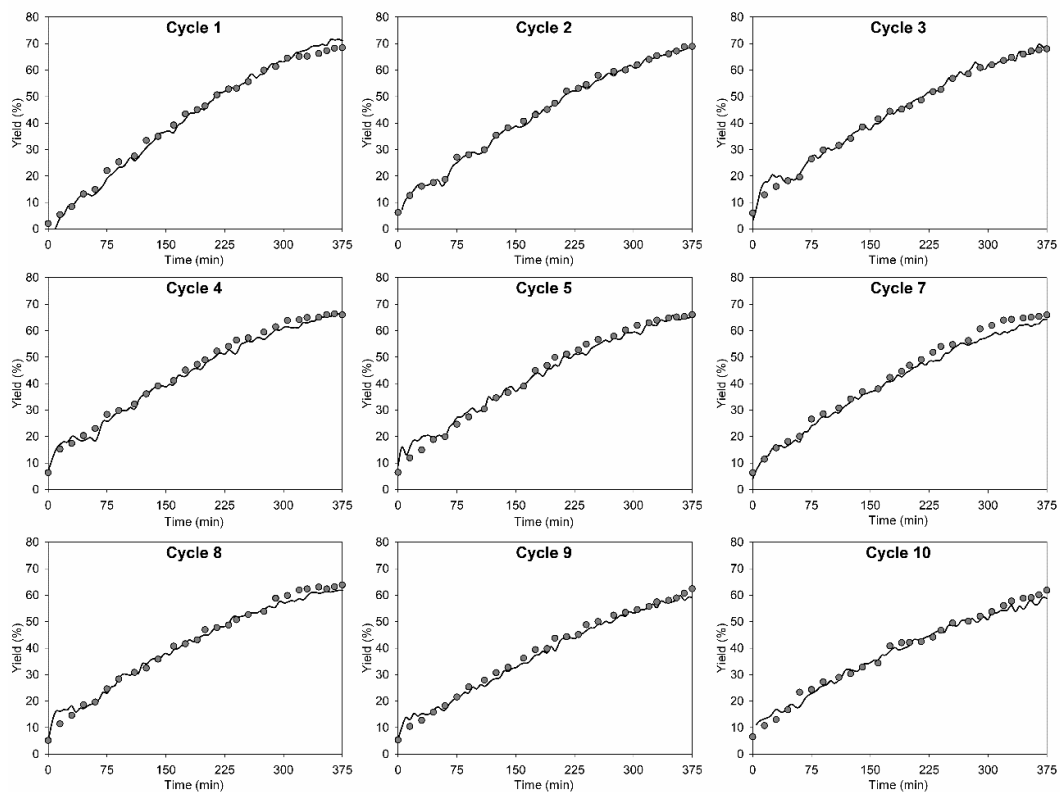


**Figure 4.2.7.** NIR prediction of reaction yields (solid line) with methanol as acyl-acceptor. Dots represent GC yield values.

As can be seen, there was high correlation between the NIR and GC results. Uncertainty in the prediction of each spectrum was assessed via the estimated error, which is a measure of goodness of prediction and calibration error, and was expressed in reaction yield units. This error measure is software specific (Solo) and it uses equation 9 of a previously described procedure [24]. The 298 NIR predictions of the reaction with ethanol were subject to an estimated average error of 2.94% (min = 2.84, max = 3.13), while the 657 NIR predictions of the reaction with methanol had an estimated average error of 1.51% (min = 1.47, max = 1.65). The magnitude of the error was not constant throughout the reaction, however; rather, it was smallest in the middle of each batch, and peaked at the beginning and end. This result is consistent with the typical distribution of interpolation errors observed with least-squares regression. The PCA scores plot (Figure 4.2.5) affected the larger estimated error for the reaction with ethanol compared with the reaction with methanol. The *Y*-variable (yield) in the reaction with ethanol was explained by both PC1 and PC2. This led to a PLS model for the reaction of ethanol with a *Y*-explained variance of the first factor of 66.9% (Table 4). The yield in the reaction with methanol was explained mostly by PC1 and the *Y*-explained variance of the PLS model was 91.4%. The PLS for both reactions used two factors, achieving 98.1% and 99.6% of the *Y*-explained variance. The previous results testify to the robustness of NIR spectroscopy for monitoring biodiesel production by enzymatic transesterification with ethanol or methanol as acyl-acceptor.

### **4.2.3. Conclusions**

Waste cooking oil (WCO), which based on its fatty acid composition was probably of olive oil origin, was used to obtain third-generation biodiesel with immobilized *Rhizopus*

*oryzae* lipase in 10 mL vials and in a 50 mL laboratory reactor as an industrial proof of concept. Because reaction yields and enzyme operational stability were similar in the two systems (vial and reactor), mass transfer was assumed to be identical in both of them. Thus, the transesterification reaction was easily scaled up from orbitally stirred vials to a mechanically stirred reactor mimicking industrial conditions. Besides, in the reactor, EO-rROL biocatalyst exhibited a high operational stability in terms of half-life ( $t_{1/2}$ ), over 35 reaction batches with both methanol and ethanol. However, methanol-based reaction showed decreased productivity as a result of the increased reaction times (219 vs 327  $\mu\text{mol min}^{-1}$ ).

Regarding the inline monitoring of the enzymatic transesterification of WCO with NIR spectroscopy, the fact of using effective prediction models allowed the reaction in the 50 mL reactor to be accurately monitored with both acyl-acceptors, ethanol and methanol. The GC and NIR results were highly correlated, with a prediction error (RMSEP) of 2.0% for methanol and 2.1% for ethanol. Based on these results, using immobilized enzymes and adding the alcohol stepwise, which might have increased background noise in spectral measurements, was no issue here. Consequently, NIR spectroscopy stands as a robust tool for monitoring industrial biodiesel production in compliance with CPV and PAT principles. Moreover, inline monitoring of the reaction can help identify the most suitable time for addition of alcohol pulses and renewal of the biocatalyst for optimal performance.

#### 4.2.4. References

- [1] Pinzi S, Alonso F, García Olmo J, Dorado MP. Near infrared reflectance spectroscopy and multivariate analysis to monitor reaction products during biodiesel production. *Fuel* 2012;92:354–9. <https://doi.org/10.1016/j.fuel.2011.07.006>.
- [2] Syed MB. Analysis of biodiesel by high performance liquid chromatography using refractive index detector. *MethodsX* 2017;4:256–9. <https://doi.org/10.1016/J.MEX.2017.07.002>.
- [3] Morgenstern M, Cline J, Meyer S, Cataldo S. Determination of the kinetics of biodiesel production using proton nuclear magnetic resonance spectroscopy ( $^1\text{H}$  NMR). *Energy and Fuels* 2006;20:1350–3. <https://doi.org/10.1021/ef0503764>.
- [4] de Lima Furtado W, Corgozinho CNC, Tauler R, Sena MM. Monitoring biodiesel and its intermediates in transesterification reactions with multivariate curve resolution alternating least squares calibration models. *Fuel* 2021;283:119275. <https://doi.org/10.1016/j.fuel.2020.119275>.
- [5] Rosas JG, Blanco M, González JM, Alcalà M. Real-time determination of critical quality attributes using near-infrared spectroscopy: a contribution for Process Analytical Technology (PAT). *Talanta* 2012;97:163–70. <https://doi.org/10.1016/j.talanta.2012.04.012>.
- [6] Gorsky I. Process Validation Stage 3: Continued Process Verification. *Princ Parenter Solut Valid A Pract Lifecycle Approach* 2020:209–32. <https://doi.org/10.1016/B978-0-12-809412-9.00008-3>.



- [7] De Lima SM, Silva BFA, Pontes DV, Pereira CF, Stragevitch L, Pimentel MF. In-line monitoring of the transesterification reactions for biodiesel production using NIR spectroscopy. *Fuel* 2014;115:46–53. <https://doi.org/10.1016/j.fuel.2013.06.057>.
- [8] Blanco M, Alcalá M, González JM, Torras E. A process analytical technology approach based on near infrared spectroscopy: tablet hardness, content uniformity, and dissolution test measurements of intact tablets. *J Pharm Sci* 2006;95:2137–44. <https://doi.org/10.1002/jps.20653>.
- [9] Palou A, Miró A, Blanco M, Larraz R, Gómez JF, Martínez T, et al. Calibration sets selection strategy for the construction of robust PLS models for prediction of biodiesel/diesel blends physico-chemical properties using NIR spectroscopy. *Spectrochim Acta - Part A Mol Biomol Spectrosc* 2017;180:119–26. <https://doi.org/10.1016/j.saa.2017.03.008>.
- [10] Rocha WF de C, Sheen DA. Determination of physicochemical properties of petroleum derivatives and biodiesel using GC/MS and chemometric methods with uncertainty estimation. *Fuel* 2019;243:413–22. <https://doi.org/10.1016/j.fuel.2018.12.126>.
- [11] Richard R, Dubreuil B, Thiebaud-Roux S, Prat L. On-line monitoring of the transesterification reaction carried out in microreactors using near infrared spectroscopy. *Fuel* 2013;104:318–25. <https://doi.org/10.1016/j.fuel.2012.07.054>.
- [12] Sales R, da Silva NC, da Silva JP, França HH, Pimentel MF, Stragevitch L. Handheld near-infrared spectrometer for on-line monitoring of biodiesel production in a continuous process. *Fuel* 2019;254:115680.

- <https://doi.org/10.1016/J.FUEL.2019.115680>.
- [13] Consumo en España | Anierac n.d. <https://anierac.org/consumo-en-espana/?lang=en> (accessed September 17, 2021).
- [14] Orsavova J, Misurcova L, Vavra Ambrozova J, Vicha R, Mlcek J. Fatty acids composition of vegetable oils and its contribution to dietary energy intake and dependence of cardiovascular mortality on dietary intake of fatty acids. *Int J Mol Sci* 2015;16:12871–90. <https://doi.org/10.3390/ijms160612871>.
- [15] Canet A, Benaiges MD, Valero F, Adlercreutz P. Exploring substrate specificities of a recombinant *Rhizopus oryzae* lipase in biodiesel synthesis. *N Biotechnol* 2017;39:59–67. <https://doi.org/10.1016/j.nbt.2017.07.003>.
- [16] Bonet-Ragel K, Canet A, Benaiges MD, Valero F. Effect of acyl-acceptor stepwise addition strategy using *alperujo* oil as a substrate in enzymatic biodiesel synthesis. *J Chem Technol Biotechnol* 2018;93:541–7. <https://doi.org/10.1002/jctb.5399>.
- [17] Lotti M, Pleiss J, Valero F, Ferrer P. Effects of methanol on lipases: molecular, kinetic and process issues in the production of biodiesel. *Biotechnol J* 2015;10:22–30. <https://doi.org/10.1002/biot.201400158>.
- [18] Bonet-Ragel K, López-Pou L, Tutusaus G, Benaiges MD, Valero F. Rice husk ash as a potential carrier for the immobilization of lipases applied in the enzymatic production of biodiesel. *Biocatal Biotransformation* 2018;36:151–8. <https://doi.org/10.1080/10242422.2017.1308498>.
- [19] Sun T, Du W, Liu D. Comparative study on stability of whole cells during biodiesel production in solvent-free system. *Process Biochem* 2011;46:661–4.

- <https://doi.org/10.1016/j.procbio.2010.11.006>.
- [20] López-Fernández J, Benaiges MD, Valero F. *Rhizopus oryzae* lipase, a promising industrial enzyme: biochemical characteristics, production and biocatalytic applications. *Catalysts* 2020;10:1277. <https://doi.org/10.3390/catal10111277>.
- [21] Bonet-Ragel K, Canet A, Benaiges MD, Valero F. Synthesis of biodiesel from high FFA *alperujo* oil catalysed by immobilised lipase. *Fuel* 2015;161:12–7. <https://doi.org/10.1016/j.fuel.2015.08.032>.
- [22] Lin YH, Luo JJ, John Hwang SC, Liao PR, Lu WJ, Lee HT. The influence of free fatty acid intermediate on biodiesel production from soybean oil by whole cell biocatalyst. *Biomass and Bioenergy* 2011;35:2217–23. <https://doi.org/10.1016/j.biombioe.2011.02.039>.
- [23] Tan Y, Chang SKC, Zhang Y. Comparison of  $\alpha$ -amylase,  $\alpha$ -glucosidase and lipase inhibitory activity of the phenolic substances in two black legumes of different genera. *Food Chem* 2017;214:259–68. <https://doi.org/10.1016/j.foodchem.2016.06.100>.
- [24] Faber NM, Bro R. Standard error of prediction for multiway PLS: 1. Background and a simulation study. *Chemom Intell Lab Syst* 2002;61:133–49. [https://doi.org/10.1016/S0169-7439\(01\)00204-0](https://doi.org/10.1016/S0169-7439(01)00204-0).

# 5

## Results II: *Rhizopus oryzae* lipase production improvement and biocatalysts stability

### 5.1. Truncated prosequence of *Rhizopus oryzae* lipase: key factor for production improvement and biocatalyst stability

---

Chapter accepted as research article in *Catalysts*  
López-Fernández J, Barrero JJ, Benaiges MD, Valero F.

Truncated prosequence of *Rhizopus oryzae* lipase: Key factor for production improvement and biocatalyst stability. *Catalysts* 2019;9:961. <https://doi.org/10.3390/catal9110961>



## **5. RESULTS (II)**

### **5.1. Truncated prosequence of *Rhizopus oryzae* lipase: key factor for production improvement and biocatalyst stability**

<b>5.1.1. Introduction</b> .....	215
<b>5.1.2 Results and discussion</b> .....	216
5.1.2.1. Batch and Fed-Batch production of proROL and rROL.....	216
5.1.2.2 Electrophoretic studies .....	220
5.1.2.3. Influence of ionic strength, temperature, and pH on enzyme activity .....	222
5.1.2.4. Substrate specificity .....	224
5.1.2.5. proROL <i>N</i> -terminal proteolysis.....	225
5.1.2.6. Free enzymes stability studies.....	227
<b>5.1.3. Conclusions</b> .....	229
<b>5.1.4. References</b> .....	231



### 5.1.1. Introduction

As described in Section 1.2, lipases are widely known for carrying out synthesis reactions including interesterification and transesterification reactions in organic media. However, two of the most significant restrictions to the industrial use of lipases as biocatalysts are their costs and their poor stability, which limits their reusability and compromises the economic feasibility of the bioprocesses [1]. In this sense, several approaches have been employed for improving enzyme stability. For instance, protein engineering is a common target employed to improve biocatalysts features [2]. Some methods, such as directed mutagenesis, have provided promising results in this respect [3]. In addition, immobilization methods have also allowed adverse effects on enzyme stability in industrial reactions to be minimized [4–6] —as it was already addressed in Section 4.1. Furthermore, other authors have successfully prevented lipase inactivation by improving the bioprocess, for instance, by adding alcohol stepwise during biodiesel synthesis [7].

On the other hand, regarding biocatalyst price, which is a significant part of the economic cost of bioprocesses [8], heterologous expression of enzymes becomes essential to lower its economic cost and increase and ease enzyme production. In this sense, ROL has been already produced both in the native organism and in various cell factories (see Section 1.4). For instance, the production and function of its prosequence have been examined in *Saccharomyces cerevisiae* [9–11]. Nevertheless, *Komagataella phaffii* has proved to be one of the most suitable cell factories for synthesizing ROL, due to the already described advantages that this yeast provides.

Recently, the role of prosequences of various enzymes has been deepened [12]. These sequences are mainly found at the *N*-terminal and *C*-terminal of proteins and act



as intramolecular chaperones participating in the folding of enzymes both *in vivo* and *in vitro*, improving enzymes stability and lowering their deleterious effects during production [13–15]. Thus, the proper use of prosequences might enable biocatalysts operational stability enhancement and an easier and cheaper production of enzymes, as they minimize the noxious effect of their production. In this sense, the prosequence of ROL has been deeply studied (Section 1.3) and seemingly, the last 28 C-terminal amino acids of the prosequence—which are secreted jointly with the mature sequence by the native microorganism— alongside the mature sequence are enough for some of the presumed advantages of the whole prosequence to occur [16–19].

This chapter aimed to elucidate whether the truncated prosequence suffices to obtain a biocatalyst with improved industrially relevant features, e.g., enzyme stability and increased heterologous production. Therefore, 28 C-terminal amino acids of the prosequence were fused to the N-terminal of recombinant mature sequence of *Rhizopus oryzae* lipase (rROL), forming truncated prosequence plus rROL (proROL), and expressed in *K. phaffii*. To the best of our knowledge, it is the first time that a joint expression of the truncated prosequence of *Rhizopus oryzae* lipase and the mature sequence was carried out in *Komagataella phaffii*, performing a study of the heterologous production, enzyme stability, and biochemical features.

## **5.1.2 Results and discussion**

### **5.1.2.1. Batch and Fed-Batch production of proROL and rROL**

The proROL producing strain (proROL P<sub>AOX1</sub>-strain) used in the tests was selected from a pool of previously screened colonies according to the procedure described in Section

3.2.1. A single plasmid integration was confirmed by droplet digital PCR (ddPCR), and a batch culture was run by using an initial methanol concentration of  $10 \text{ g L}^{-1}$  for comparison with the rROL producing single-copy strain (rROL  $P_{AOXI}$ -strain). All batches were run in duplicate (see Section 3.2.2). Initially, all were performed at a controlled pH of 5.5, the standard value for rROL  $P_{AOXI}$ -strain. However, with proROL  $P_{AOXI}$ -strain, the medium was highly cloudy by the end of the fermentation process. This result is likely to be due to the closeness of the pH to the isoelectric point of proROL—6.08, calculated by bioinformatics tool ExPASy—so the fermentation pH was reduced to 5 in order to avoid this unwanted effect.

Table 5.1.1 compares the main batch fermentation parameters between proROL  $P_{AOXI}$ -strain and rROL  $P_{AOXI}$ -strain. Although final proROL activity was slightly higher than rROL activity, the greatest difference between the two strains was that in  $\mu_{\max}$ , which was 1.6 times greater in the former, although smaller than the value for wild-type *K. phaffii* (ca.  $0.1 \text{ h}^{-1}$ ). Apparently, *K. phaffii* growth was less markedly affected by proROL than by rROL heterologous protein expression, as it was also previously described for *E. coli* strains producing ROL [18]. In this sense,  $Y_{P/X}$  was also higher in proROL  $P_{AOXI}$ -strain than in rROL  $P_{AOXI}$ -strain.

**Table 5.1.1.** Results of the batch with  $10 \text{ g methanol L}^{-1}$ .

Parameter	rROL	proROL
$\mu_{\max} (\text{h}^{-1})$	$0.045 \pm 0.002$	$0.073 \pm 0.004$
Final activity ( $\text{AU mL}^{-1}$ )	$10.51 \pm 1.15$	$12.38 \pm 1.05$
$Y_{X/S} (\text{g}_X \text{g}_{\text{MeOH}}^{-1})$	$0.28 \pm 0.02$	$0.335 \pm 0.005$
$Y_{P/X} (\text{AU g}_X^{-1})$	$3753 \pm 240$	$5017 \pm 320$

Regarding fed-batch cultures, both methanol non-limiting fed-batch (MNLFB) and methanol limiting fed-bath (MLFB) strategies were employed to compare rROL- and

proROL  $P_{AOXI}$ -strain performance (see Section 3.2.3.1). In the former strategy, a methanol concentration of  $3 \text{ g L}^{-1}$  was maintained—the reported optimum level for rROL  $P_{AOXI}$ -strain [20]—while for the latter, two different methanol feeding rates resulting in two different growth rates were used. Table 5.1.2 shows the parameter values obtained for both strains. Feeding rates and parameter values were calculated according to the equations described in Section 3.2.3.5.

**Table 5.1.2.** Results of the fed-batch with rROL and proROL  $P_{AOXI}$ -strain under two methanol addition strategies. Methanol limiting fed-batch (MLFB) under two pre-fixed specific growth rates ( $0.015$  and  $0.045 \text{ h}^{-1}$ ). Methanol non-limiting fed-batch (MNLFB), maintaining a constant methanol concentration at  $3 \text{ g L}^{-1}$ .

Parameter	MLFB				MNLFB	
	proROL $0.015 \text{ h}^{-1}$	rROL $0.015 \text{ h}^{-1}$	proROL $0.045 \text{ h}^{-1}$	rROL $0.045 \text{ h}^{-1}$	proROL $3 \text{ g L}^{-1}$	rROL $3 \text{ g L}^{-1}$
Final activity (AU $\text{mL}^{-1}$ )	219	135	147	27	358	280
$Y_{P/X}$ (total AU total $\text{gX}^{-1}$ )	5264	2644	1908	479	4972	5282
$\mu$ ( $\text{h}^{-1}$ )	0.011	0.014	0.038	0.043	0.065	0.046
$q_p$ (AU $\text{gX}^{-1} \text{ h}^{-1}$ )	57	46	68.5	18	308	322
Specific productivity* (AU $\text{gX}^{-1} \text{ h}^{-1}$ )	49	36	44	11	99	102
Volumetric productivity* (AU $\text{L}^{-1} \text{ h}^{-1}$ )	2763	1857	2782	623	7160	5406

\* Specific and volumetric productivity were estimated throughout the fermentation run.

As in the batch cultures, in MNLFB, the mean specific growth rate of proROL  $P_{AOXI}$ -strain exceeded that of rROL  $P_{AOXI}$ -strain. The total fermentation time was quite similar for both (about 52 h). The volumetric productivity of proROL  $P_{AOXI}$ -strain was 1.3 times higher than this of rROL  $P_{AOXI}$ -strain. However,  $Y_{(P/X)}$ ,  $q_p$ , and specific productivity were quite similar. Interestingly, the specific growth rate of rROL  $P_{AOXI}$ -strain in the batch and fed-batch MNLFB tests was the same, although lower in the fed-batch tests than in batch cultures for proROL  $P_{AOXI}$ -strain. These results suggested that

the optimum methanol set-point for maximal efficiency during MNLFB might differ between rROL  $P_{AOXI}$ -strain and proROL  $P_{AOXI}$ -strain, and consequently, be the reason of proROL  $P_{AOXI}$ -strain lower growth rate.

When MLFB strategy was employed for comparing both strains, the differences were more appreciated. After the transition phase, the rROL production was practically negligible for all the  $\mu$  set-point tested, except for the lowest  $\mu$  in which a sharp increase of lipolytic activity was observed at the end of the fed-batch culture [20]. Instead, when the MLFB strategy was studied with proROL  $P_{AOXI}$ -strain, a different behavior was observed (Figure 5.1.1). In fact, even if proROL  $P_{AOXI}$ -strain production parameters were lower in MLFB strategy than in MNLFB one, they were higher for the two  $\mu$  set-points tested when compared with rROL  $P_{AOXI}$ -strain—4.4 times greater in the most extreme case—as can be seen in Figure 5.1.1 and Table 5.1.2. Besides, as it was described for rROL  $P_{AOXI}$ -strain, MLFB cultures at the lowest  $\mu$  improved the proROL  $P_{AOXI}$ -strain titer [20].

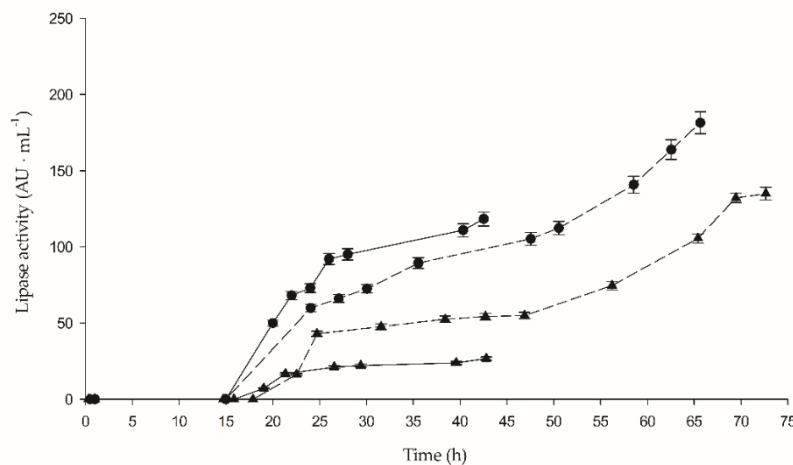


**Figure 5.1.1.** Lipase activity evolution in MLFB (methanol limiting fed-batch) cultures of proROL  $P_{AOXI}$ -strain and rROL  $P_{AOXI}$ -strain at two pre-fixed specific growth rates, 0.015 and 0.045 h<sup>-1</sup>. pre-fixed  $\mu$  of 0.015 h<sup>-1</sup> (discontinuous line) and 0.045 h<sup>-1</sup> (continuous line). proROL  $P_{AOXI}$ -strain (circles) and rROL  $P_{AOXI}$ -strain (triangles).

Thus, the better growth of proROL P<sub>AOXI</sub>-strain combined with the better productivities observed in both studied strategies, MLFB and MNLFB, suggested a stress reduction during recombinant protein expression caused by the presence of the 28 amino acids of the prosequence. As a result, an unfolded protein response (UPR) phenomena might not be triggered to the same extent as in the rROL P<sub>AOXI</sub>-strain [21].

#### 5.1.2.2 Electrophoretic studies

The electrophoretic techniques (methods were described in Section 3.6) were used to identify differences between proROL and rROL free enzymes and also to examine some properties of lyophilized powders of each lipase. First, the band corresponding to proROL in the SDS-PAGE gel was identified by using 4-Methylumbelliferyl butyrate (MUF-butyrate) as a substrate, and then the molecular weight of the lipase was determined. As can be seen in Figure 5.1.2C, the zymogram contained only one active band. This result, which was also obtained with rROL lyophilized powder (Figure 5.1.2D), suggested that *K. phaffii* secretome contained no additional esterases or lipases [22]. After the zymograms were recorded, the gel was dyed with Coomassie Blue to determine the molecular weight of the enzymes. The band corresponding to proROL fell at 33 kDa (Figure 5.1.2B), which is similar to the value reported elsewhere [23] and also to that for naturally secreted lipase from *Rhizopus oryzae* [24] (Section 1.4 for further information). As can also be seen (Figure 5.1.2E), the band for rROL was around 29 kDa, 4 kDa lower than proROL, which agreed to the lack of the 28 amino acids of the prosequence [25].

Furthermore, as can be seen in Figure 5.1.2F-2G, the western blot analysis provided faint bands with similar but higher molecular weights to the main bands observed for rROL and proROL, suggesting that there are different conformations of the

lipases. These results are consistent with previously published work, in which some attempts to explain these findings were done, including *N*-terminal and glycosylation studies, although no relevant conclusions were obtained [22].

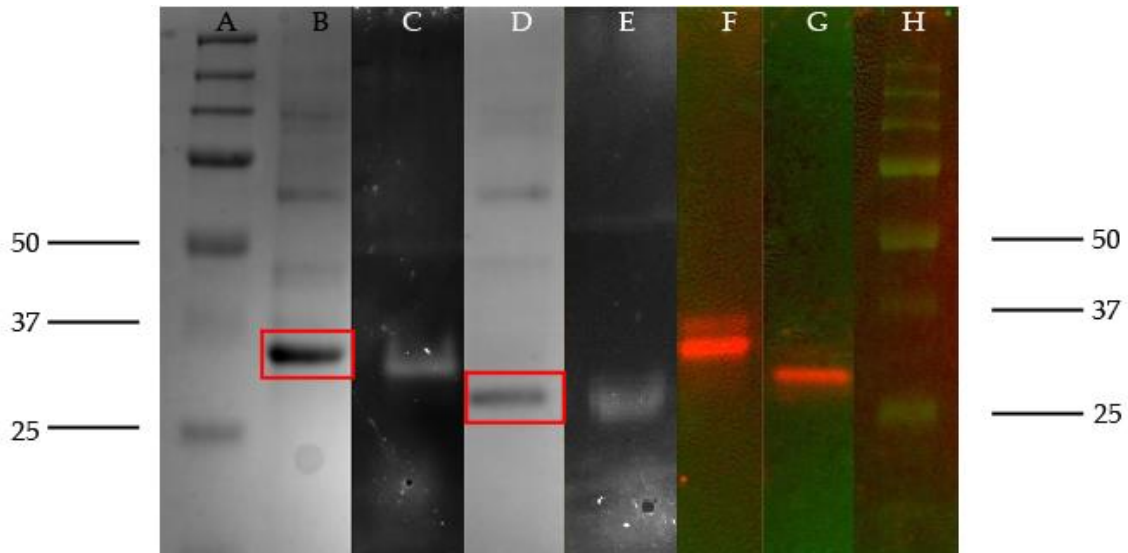


**Figure 5.1.2.** (A) Prestained all blue Precision Plus Protein™ standards molecular weight marker. (B) SDS-PAGE results for proROL (square). (C) Zymogram for proROL lipase. (D) SDS-PAGE results for rROL lipase (square). (E) Zymogram for rROL lipase. (F) Western blot results for proROL lipase. (G) Western blot results for rROL lipase. (H) Precision Plus™ all blue standards molecular weight marker.

The western blot results allowed the amount of lipase present in each lyophilized powder (rROL and proROL) to be quantified and the two enzymes to be compared in terms of specific activity. For this purpose, two samples of purified rROL of known concentration were used as lipase standards. As can be seen from Table 5.1.3, the presence of the 28 *C*-terminal amino acids of the prosequence in proROL had no adverse effect on the specific activity of the enzyme with the employed lipolytic activity test (Roche substrate test, see Section 3.2.6). The table also shows the protein/lyophilized powder and lipase/total protein percentage ratios. Approximately 8% of the lyophilized powder was protein and 25%–30% of all protein was the recombinant protein, confirming *K. phaffii* to be an effective cell factory for heterologous protein production.

**Table 5.1.3.** Specific activity, mass/mass % of total protein/lyophilized powder, and ratio lipase/protein of proROL and rROL calculated with the Western blot test.

Enzyme	Specific Activity (AU g <sub>enzyme</sub> <sup>-1</sup> )	%Protein/Lyophilized Powder	% Lipase/Protein
rROL	17.8 ± 0.6	7.2	28.5
proROL	16.1 ± 0.3	8.5	25.2

Finally, the samples were also subjected to densitometry analysis by using SDS-PAGE gels and a protein standard marker (Precision Plus Protein™ unstained) of known concentration from Bio-Rad. The results were similar to those of the western blot test. This suggested that *K. phaffii* secreted no other proteins similar to the lipases in molecular weight and potentially interfering with densitometric analyses.

#### 5.1.2.3. Influence of ionic strength, temperature, and pH on enzyme activity

proROL was characterized in biochemical terms to examine the influence of ionic strength, temperature, and pH on enzyme activity, as well as to compare the results with those previously reported for rROL [22]. As shown by reported evidence, ionic strength has a marked effect on enzyme activity. In this work, its influence was examined by using 50–400 mM concentrations of Tris-HCl buffer at pH 7.25. As expected, lipolytic activity (Figure 5.1.3) was strongly influenced by ionic strength because the activity dropped dramatically at 400 mM and 50 mM. Both enzymes behaved similarly in this respect, suggesting that the presence of the prosequence had no appreciable effect on this parameter.

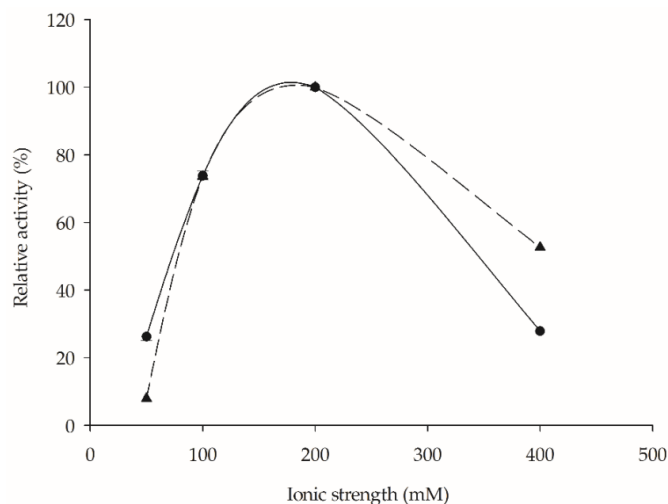


**Figure 5.1.3.** Influence of ionic strength on lipolytic activity relative to the maximum value for proROL (circles) and rROL (triangles) in Tris-HCl buffer at pH 7.25 at 30 °C that was taken to be 100% in each case.

Due to the significance of the ionic strength in enzyme activity, the temperature and pH assays were done at 200 mM and 400 mM, considering the different behavior observed for rROL [22]. The influence of temperature is illustrated in Figure 5.1.4A. As can be seen, the optimum temperature for proROL at both ionic strength levels was 40 °C; by contrast, that for rROL shifted from 40 °C to 30 °C at the higher value. Similar optimum temperatures were previously reported (e.g., 40 °C and 35 °C for native ROL [24,26], and 30 °C for lipase formed by the mature sequence produced in *K. phaffii* [27]). Regarding pH, as can be seen from Figure 5.1.4B, the influence was similar to that of temperature; thus, proROL exhibited an identical optimum pH at both ionic strength levels, whereas rROL had an optimum pH of 7.25 at the higher ionic strength value and 8 at the lower. An optimum pH of 8 was previously reported for native ROL [26,27] and one of 7.5 for purified native lipase [24].



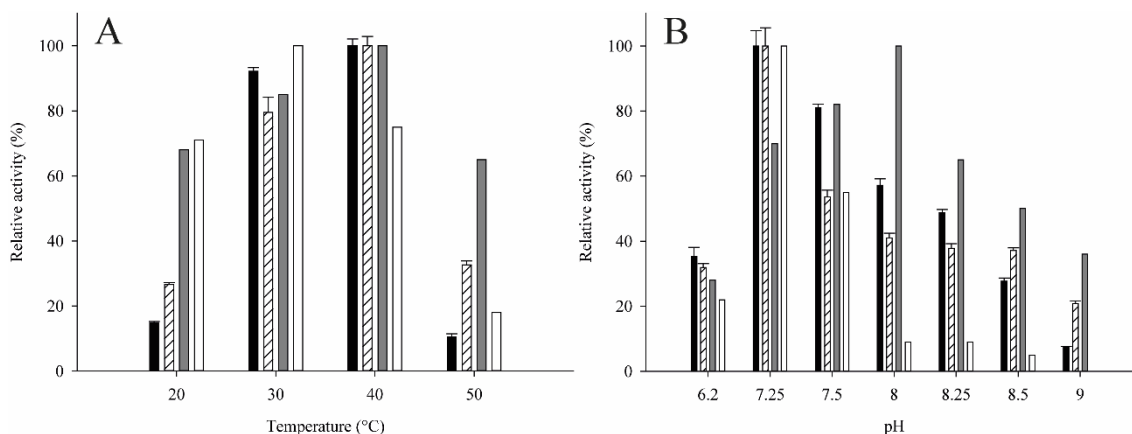


**Figure 5.1.4.** (A) Effect of temperature on lipolytic activity relative to the maximum value for proROL and rROL in Tris-HCl buffer at pH 7.25 at two different ionic strengths (200 and 400 Mm) that were taken to be 100% in each case. (B) Effect of pH on lipolytic activity relative to the maximum value for proROL and rROL in Tris-HCl buffer at 30 °C at two different ionic strengths (200 and 400 mM) that were taken to be 100% in each case. (black) 200 mM proROL. (striped-white) 400 mM proROL. (grey) 200 mM rROL. (white) 400 mM rROL.

Nevertheless, for both pH and temperature optimum values, several different results can be found in the literature for *Rhizopus oryzae* lipase (see Section 1.3). Besides, the presence of the 28 amino acids of the prosequence might be the reason of such variability. These amino acids have been described to act as an intramolecular chaperone [18], increasing protein stability and, consequently, proROL enzyme activity might be less markedly influenced by changes in medium ionic strength, temperature or pH than those of rROL. Thus, the 28 amino acids might be the reason why proROL maintains identical temperature and pH optimums at both assayed medium ionic strength.

#### 5.1.2.4. Substrate specificity

The presence of the 28 amino acids in the *N*-terminal of *Rhizopus oryzae* lipase has been associated with changes in substrate specificity [17]. This led us to examine proROL specificity by using commercial *p*-nitrophenol esters of variable carbon chain length and

compare the results with those of previous studies on the specificity of rROL and commercial native lipase from *R. oryzae* (nROL) [22]. As can be seen in Figure 5.1.5, the profile for proROL was similar to that for nROL, with a peak at C8. However, consistent with previous results [10], it was different from that for rROL, which peaked at a greater chain length (C12). The presence of the 28 amino acids of the prosequence, therefore, had a clear-cut effect on lipase specificity. In fact, previous studies have reported the significance of the 28 amino acids in *Rhizopus oryzae* lipase substrate specificity by using bioinformatic prediction tools to build 3D models [17]. According to this work, the 28 amino acids of the prosequence are located near to the lid region, and as they contain 50% of hydrophobic residues, they are supposed to play a relevant role in the interaction with substrates.

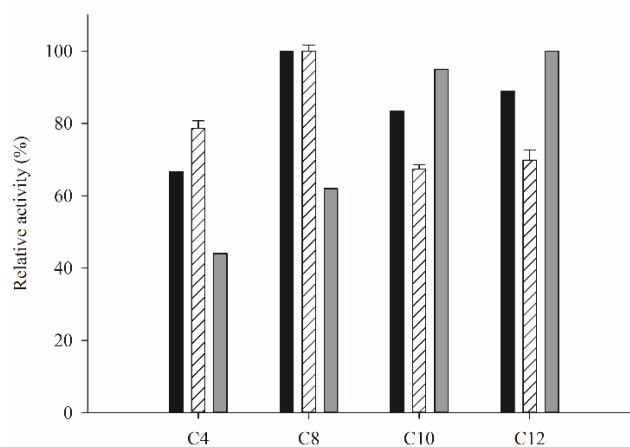


**Figure 5.1.5.** C4 to C12 *p*-nitrophenol ester specificity for nROL (black), proROL (striped-white), and rROL (grey). The maximum activity at 30 °C in 50 mM phosphate buffer at pH 7 in each run was taken to be 100%.

#### 5.1.2.5. proROL *N*-terminal proteolysis

Previous studies confirmed the proteolysis of the *N*-terminal in purified *Rhizopus niveus* lipase [25], whose *N*-terminal is identical with that in *R. oryzae* lipase [28]—seemingly,

proteolysis was the result of the presence of a serine protease in the purified lipase solution. Taking this into account, the proROL enzyme was left in solution for 24 h at room temperature to evaluate, by SDS-PAGE, possible proteolysis and compare it with the controls described in Section 3.7. As can be seen from Figure 5.1.6, proROL (C2) lost a molecular weight of approximately 4 kDa, exactly the weight corresponding to the 28 amino acids of the prosequence. However, no proteolysis was observed in the presence of the protease inhibitor (I) and under sterile conditions (C3). Moreover, proteolysis was less marked with C1 as the likely result of the antiseptic effect of ethanol added to the proROL solution.

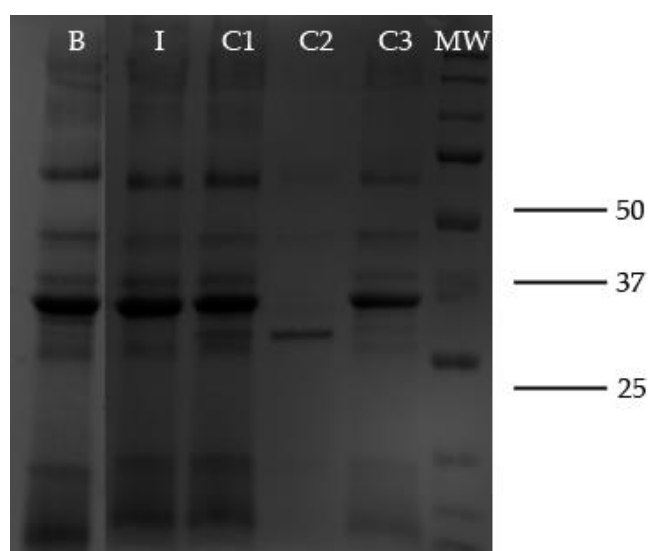


**Figure 5.1.6.** SDS-PAGE analysis of the samples from the proteolysis study. (B) The initial solution of proROL lipase. (I) proROL solution after 24 h in the presence of inhibitor. (C1) proROL solution after 24 h in the presence of ethanol. (C2) proROL solution in 5 mM phosphate buffer after 24 h. (C3) Sterilized proROL solution in 5 mM phosphate buffer after 24 h. (MW) Molecular weight marker.

Thus, as revealed by the blanks, proteolysis might have been caused by proteases produced by external microbial contaminants present in the lipase solution. Seemingly, the 28 amino acids were preferentially lost since no other bands suggesting non-specific proteolysis were observed upon lipase hydrolysis. This may have been a result of the 28

amino acids of the prosequence being naturally designed for removal to obtain a lipase exclusively containing the mature sequence.

#### 5.1.2.6. Free enzymes stability studies

Because proROL has been deemed more stable than the enzyme consisting of the mature sequence only [15], proROL stability was compared to rROL stability following the procedure described in Section 3.9 and under three different conditions selected from a previously done design of experiment (DoE) for rROL characterization [29]. Such conditions were chosen on the grounds that they previously led to a variable loss of activity. As can be seen from Figure 5.1.7A, proROL was more stable than rROL after 1 h of incubation irrespective of the particular pH and temperature conditions. For example, proROL was up to 7 times more stable than rROL at 35 °C and pH 8.12.

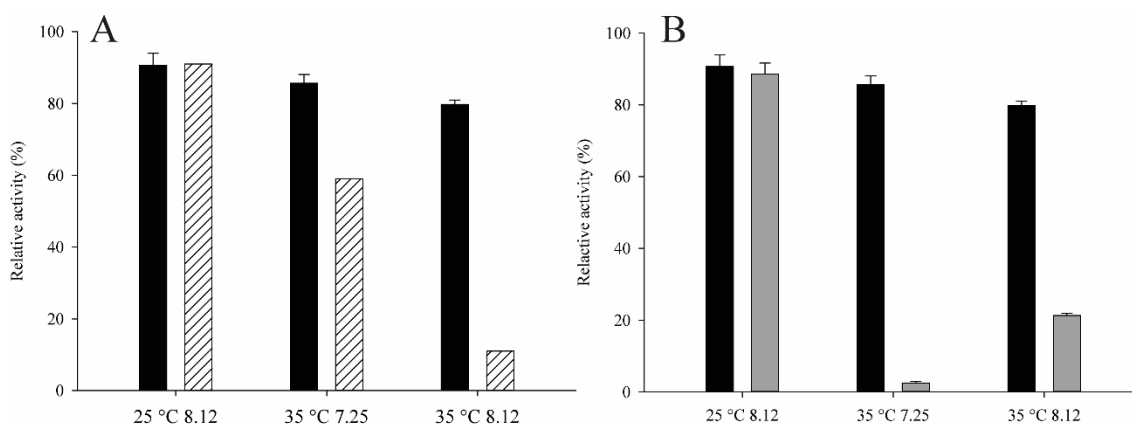


**Figure 5.1.7.** (A) Influence of pH and temperature on lipase stability. Results obtained after incubation for 1 h of proROL (black) and rROL (striped-white) lipase in 200 mM Tris-HCl buffer under different temperature and pH conditions. (B) proROL stability after 1 h (black) and 24 h (grey) of incubation under different temperature and pH conditions in 200 mM Tris-HCl buffer. Activity values relative to  $t = 0$ .

These results led us to examine proROL further than rROL by extending the incubation time to 24 h under sterile conditions to avoid the unwanted proteolysis

described in Section 5.1.4. As can be seen in Figure 5.1.7B, proROL lost only 10% of its activity after 24 h of incubation at 25 °C and pH 8.12. Therefore, the temperature had a stronger effect than pH on proROL stability, which is consistent with the results of previous studies on rROL stability [29].

The stability of both lipases during 24 h under sterile conditions in the presence of ethanol or methanol at four different concentrations was also studied (see Section 3.9). As can be seen from Figure 5.1.8, proROL was more stable than rROL irrespective of the conditions. For instance, proROL retained 17 times more activity than rROL after 24 h in the presence of 15% methanol. Also, consistent with previous results [30], both lipases were more strongly affected by ethanol than they were by methanol. However, this result conflicts with those for rROL in biodiesel synthesis reactions, where methanol proved to be more detrimental (see Results Section 4.1.2.2). This contradiction can be ascribed to the alcohol interacting with the active site of the enzyme during biodiesel reactions, which is unlikely in a lipase-alcohol solution because the enzyme lid is closed.

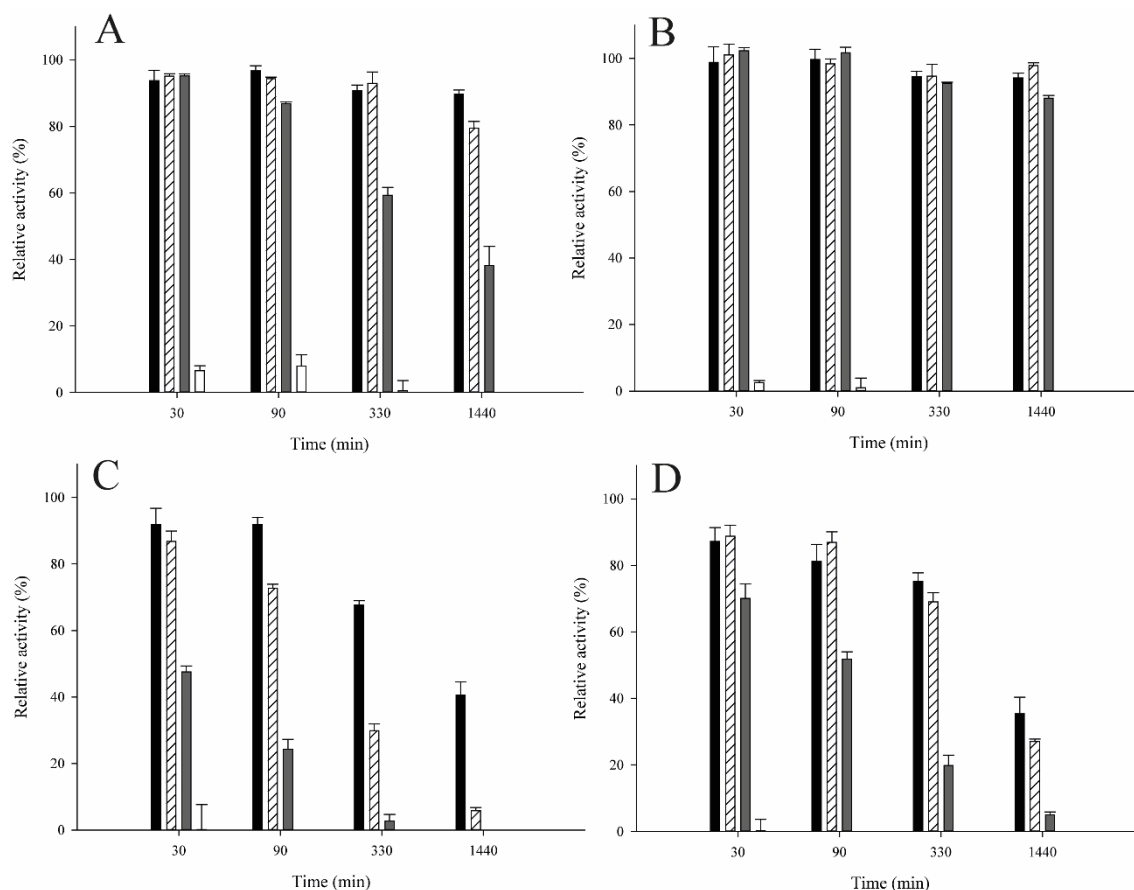


**Figure 5.1.8.** Stability of proROL and rROL in solution in the presence of ethanol and methanol at four different concentrations. (A) proROL in ethanol, (B) proROL in methanol, (C) rROL in ethanol, and (D) rROL in methanol. Activity values relative to  $t = 0$ . Alcohol concentration: 0% (black), 5% (striped-white), 15% (grey), and 30% (white).

In summary, the 28 amino acids of the prosequence in the *N*-terminal of lipase improved protein stability, not only under different conditions of pH and temperature but also in the presence of variable concentrations of alcohol.

### 5.1.3. Conclusions

Two of the main drawbacks of lipase-catalyzed transesterification for the biodiesel industry are lipase production economic cost and its stability, which are directly related to the economic feasibility of the whole bioprocess. The presence of only 28 *C*-terminal amino acids of the prosequence in proROL resulted in significant improvements in

comparison to the mature sequence lipase (rROL). In terms of bioprocess engineering, the maximum specific growth rate value for proROL producing strain in batch cultures,  $0.073 \text{ h}^{-1}$ , was 1.6 times greater than that for rROL  $P_{AOXI}$ -strain but still much smaller than the value for wild-type *K. phaffii* (about  $0.1 \text{ h}^{-1}$ ). In addition, lipase production and volumetric productivity of proROL  $P_{AOXI}$ -strain in fed-batch cultures were also greater in both methanol-addition strategies. All these results suggested a stress reduction caused by recombinant protein expression during proROL production and a potential decrease in the economic cost of the biocatalyst due to higher productivity.

Although proROL and rROL free lipases showed similar specific activity and patterns during biochemical characterization, the presence of the 28 amino acids in the former resulted in some differences. Thus, proROL differed not only in molecular weight but also in the optimum pH and temperature at each ionic strength. Substrate specificity also differed between the two lipases, and selective proteolysis of the 28 amino acids of the prosequence was observed. However, the most significant difference was the increased stability of proROL relative to rROL under all the stability tests carried out at different pH and temperature conditions in the presence or absence of alcohols (methanol and ethanol). Thus, advantageous traits of this lipase may open up new avenues for its application in industry.

#### 5.1.4. References

- [1] Lotti M, Pleiss J, Valero F, Ferrer P. Effects of methanol on lipases: molecular, kinetic and process issues in the production of biodiesel. *Biotechnol J* 2015;10:22–30. <https://doi.org/10.1002/biot.201400158>.
- [2] Singh RK, Tiwari MK, Singh R, Lee JK. From protein engineering to immobilization: promising strategies for the upgrade of industrial enzymes. *Int J Mol Sci* 2013;14:1232–77. <https://doi.org/10.3390/ijms14011232>.
- [3] Korman TP, Sahachartsiri B, Charbonneau DM, Huang GL, Beauregard M, Bowie JU. Dieselzymes: development of a stable and methanol tolerant lipase for biodiesel production by directed evolution. *Biotechnol Biofuels* 2013;6:1–13. <https://doi.org/10.1186/1754-6834-6-70>.
- [4] Canet A, Bonet-Ragel K, Benaiges MD, Valero F. Lipase-catalysed transesterification: viewpoint of the mechanism and influence of free fatty acids. *Biomass and Bioenergy* 2016;85:94–9. <https://doi.org/10.1016/j.biombioe.2015.11.021>.
- [5] Bonet-Ragel K, Canet A, Benaiges MD, Valero F. Synthesis of biodiesel from high FFA *alperujo* oil catalysed by immobilised lipase. *Fuel* 2015;161:12–7. <https://doi.org/10.1016/j.fuel.2015.08.032>.
- [6] Picó EA, López C, Cruz-Izquierdo Á, Munarriz M, Iruretagoyena FJ, Serra JL, et al. Easy reuse of magnetic cross-linked enzyme aggregates of lipase B from *Candida antarctica* to obtain biodiesel from *Chlorella vulgaris* lipids. *J Biosci Bioeng* 2018;126:451–7. <https://doi.org/10.1016/j.jbiosc.2018.04.009>.



- [7] Bonet-Ragel K, Canet A, Benaiges MD, Valero F. Effect of acyl-acceptor stepwise addition strategy using *alperujo* oil as a substrate in enzymatic biodiesel synthesis. *J Chem Technol Biotechnol* 2018;93:541–7. <https://doi.org/10.1002/jctb.5399>.
- [8] Guldhe A, Singh B, Mutanda T, Permaul K, Bux F. Advances in synthesis of biodiesel via enzyme catalysis: novel and sustainable approaches. *Renew Sustain Energy Rev* 2015. <https://doi.org/10.1016/j.rser.2014.09.035>.
- [9] Ueda M, Takahashi S, Washida M, Shiraga S, Tanaka A. Expression of *Rhizopus oryzae* lipase gene in *Saccharomyces cerevisiae*. *J Mol Catal - B Enzym* 2002;17:113–24. [https://doi.org/10.1016/S1381-1177\(02\)00018-8](https://doi.org/10.1016/S1381-1177(02)00018-8).
- [10] Takahashi S, Ueda M, Tanaka A. Independent production of two molecular forms of a recombinant *Rhizopus oryzae* lipase by KEX2-engineered strains of *Saccharomyces cerevisiae*. *Appl Microbiol Biotechnol* 1999;52:534–40. <https://doi.org/10.1007/s002530051556>.
- [11] Takahashi S, Ueda M, Tanaka A. Function of the prosequence for in vivo folding and secretion of active *Rhizopus oryzae* lipase in *Saccharomyces cerevisiae*. *Appl Microbiol Biotechnol* 2001;55:454–62. <https://doi.org/10.1007/s002530000537>.
- [12] Chen YJ, Inouye M. The intramolecular chaperone-mediated protein folding. *Curr Opin Struct Biol* 2008;18:765–70. <https://doi.org/10.1016/j.sbi.2008.10.005>.
- [13] Wang Z, Lv P, Luo W, Yuan Z, He D. Expression in *Pichia pastoris* and characterization of *Rhizomucor miehei* lipases containing a new propeptide region. *J Gen Appl Microbiol* 2016;62:25–30. <https://doi.org/10.2323/jgam.62.25>.
- [14] Takahashi S, Ueda M, Atomi H, Beer HD, Bornscheuer UT, Schmid RD, et al.

- Extracellular production of active *Rhizopus oryzae* lipase by *Saccharomyces cerevisiae*. *J Ferment Bioeng* 1998;86:164–8. [https://doi.org/10.1016/S0922-338X\(98\)80055-X](https://doi.org/10.1016/S0922-338X(98)80055-X).
- [15] Satomura A, Kuroda K, Ueda M. Generation of a functionally distinct *Rhizopus oryzae* lipase through protein folding memory. *PLoS One* 2015;10:1–13. <https://doi.org/10.1371/journal.pone.0124545>.
- [16] Hama S, Tamalampudi S, Shindo N, Numata T, Yamaji H, Fukuda H, et al. Role of *N*-terminal 28-amino-acid region of *Rhizopus oryzae* lipase in directing proteins to secretory pathway of *Aspergillus oryzae*. *Appl Microbiol Biotechnol* 2008;79:1009–18. <https://doi.org/10.1007/s00253-008-1502-6>.
- [17] Sayari A, Frikha F, Miled N, Mtibaa H, Ali Y Ben, Verger R, et al. *N*-terminal peptide of *Rhizopus oryzae* lipase is important for its catalytic properties. *FEBS Lett* 2005;579:976–82. <https://doi.org/10.1016/j.febslet.2004.12.068>.
- [18] Beer HD, Wohlfahrt G, Schmid RD, McCarthy JE. The folding and activity of the extracellular lipase of *Rhizopus oryzae* are modulated by a prosequence. *Biochem J* 1996;319:351–9. <https://doi.org/10.1042/bj3190351>.
- [19] Beer HD, McCarthy JEG, Bornscheuer UT, Schmid RD. Cloning, expression, characterization and role of the leader sequence of a lipase from *Rhizopus oryzae*. *Biochim Biophys Acta - Gene Struct Expr* 1998;1399:173–80. [https://doi.org/10.1016/S0167-4781\(98\)00104-3](https://doi.org/10.1016/S0167-4781(98)00104-3).
- [20] Barrigón JM, Montesinos JL, Valero F. Searching the best operational strategies for *Rhizopus oryzae* lipase production in *Pichia pastoris* Mut<sup>+</sup> phenotype: methanol limited or methanol non-limited fed-batch cultures? *Biochem Eng J* 2013;75:47–

54. <https://doi.org/10.1016/j.bej.2013.03.018>.
- [21] Valkonen M, Penttilä M, Saloheimo M. Effects of inactivation and constitutive expression of the unfolded-protein response pathway on protein production in the yeast *Saccharomyces cerevisiae*. *Appl Environ Microbiol* 2003;69:2065–72. <https://doi.org/10.1128/AEM.69.4.2065-2072.2003>.
- [22] Guillén M, Benaiges MD, Valero F. Comparison of the biochemical properties of a recombinant lipase extract from *Rhizopus oryzae* expressed in *Pichia pastoris* with a native extract. *Biochem Eng J* 2011;54:117–23. <https://doi.org/10.1016/j.bej.2011.02.008>.
- [23] Niu W, Li Z, Tan T. Secretion of pro- and mature *Rhizopus arrhizus* lipases by *Pichia pastoris* and properties of the proteins. *Mol Biotechnol* 2006;32:73–81. <https://doi.org/10.1385/MB:32:1:073>.
- [24] Hiol A, Jonzo MD, Rugani N, Druet D, Sarda L, Comeau LC. Purification and characterization of an extracellular lipase from a thermophilic *Rhizopus oryzae* strain isolated from palm fruit. *Enzyme Microb Technol* 2000;26:421–30. [https://doi.org/10.1016/S0141-0229\(99\)00173-8](https://doi.org/10.1016/S0141-0229(99)00173-8).
- [25] Kohno M, Kugimiya W, Hashimoto Y, Morita Y. Purification, characterization, and crystallization of two types of lipase from *Rhizopus niveus*. *Biosci Biotechnol Biochem* 1994;58:1007–12. <https://doi.org/10.1271/bbb.58.1007>.
- [26] Pashangeh K, Akhond M, Karbalaeei-Heidari HR, Absalan G. Biochemical characterization and stability assessment of *Rhizopus oryzae* lipase covalently immobilized on amino-functionalized magnetic nanoparticles. *Int J Biol Macromol* 2017;105:300–7. <https://doi.org/10.1016/j.ijbiomac.2017.07.035>.

- [27] Minning S, Schmidt-Dannert C, Schmid RD. Functional expression of *Rhizopus oryzae* lipase in *Pichia pastoris*: high-level production and some properties. *J Biotechnol* 1998;66:147–56. [https://doi.org/10.1016/S0168-1656\(98\)00142-4](https://doi.org/10.1016/S0168-1656(98)00142-4).
- [28] Ben Salah A, Sayari A, Verger R, Gargouri Y. Kinetic studies of *Rhizopus oryzae* lipase using monomolecular film technique. *Biochimie* 2001;83:463–9. [https://doi.org/10.1016/S0300-9084\(01\)01283-4](https://doi.org/10.1016/S0300-9084(01)01283-4).
- [29] Guillén M, Benaiges MD, Valero F. Immobilization and stability of a *Rhizopus oryzae* lipase expressed in *Pichia pastoris*: comparison between native and recombinant variants. *Biotechnol Prog* 2011;27:1232–41. <https://doi.org/10.1002/btpr.654>.
- [30] Wang JR, Li YY, Xu S De, Li P, Liu JS, Liu DN. High-level expression of pro-form lipase from *Rhizopus oryzae* in *Pichia pastoris* and its purification and characterization. *Int J Mol Sci* 2014;15:203–17. <https://doi.org/10.3390/ijms15010203>.



# 5

## Results II: *Rhizopus oryzae* lipase production improvement and biocatalysts stability

### 5.2. Mature *Rhizopus oryzae* lipase jointly with its truncated prosequence allows methanol independent heterologous production in *Komagataella phaffii* and improves biocatalyst operational stability

---

Chapter accepted as research article in *Catalysts*  
López-Fernández J., Benaiges MD, Valero F.

Constitutive expression in *Komagataella phaffii* of mature *Rhizopus oryzae* lipase jointly with its truncated prosequence improves production and the biocatalyst operational stability. *Catalysts* 2021;11:1192. <https://doi.org/10.3390/catal11101192>



## **5. RESULTS (II)**

### **5.2. Mature *Rhizopus oryzae* lipase jointly with its truncated prosequence allows methanol independent heterologous production in *Komagataella phaffii* and improves biocatalyst operational stability**

<b>5.2.1. Introduction</b> .....	241
<b>5.2.2. Results and discussion</b> .....	242
5.2.2.1. Batch and fed-batch bioprocess strategies .....	242
5.2.2.2. N-terminal amino acids sequence analysis.....	246
5.2.2.3. Immobilized enzymes stability .....	248
5.2.2.4. Transesterification and esterification reactions.....	250
5.2.2.4.1. Biodiesel production .....	250
5.2.2.4.2. Ethyl butyrate production.....	252
<b>5.2.3. Conclusions</b> .....	254
<b>5.2.4. References</b> .....	256





### 5.2.1. Introduction

The alcohol oxidase 1 promoter ( $P_{AOXI}$ ) has been extensively used to express *Rhizopus oryzae* lipase in *Komagataella phaffii*, whose suitability has been already described in Sections 1.5.1 and 5.1. This promoter is strongly induced by methanol but repressed by glucose and glycerol. Although  $P_{AOXI}$  allows large amounts of protein to be obtained, the use of methanol increases oxygen requirements and heat production—and raises production costs through the need to store and handle methanol properly [1,2]. These drawbacks have prompted the use of methanol-independent promoters such as the formaldehyde dehydrogenase 1 promoter ( $P_{FLDI}$ ), which is inducible by both methanol as sole carbon and energy source and methylamine as nitrogen source [3,4], and the constitutive glyceraldehyde-3-phosphate dehydrogenase promoter ( $P_{GAP}$ ) from central carbon metabolism [5]. Regarding the latter, despite the constitutive nature of  $P_{GAP}$ , its strong expression capacity depends on the carbon source and growth rate of the particular culture [6,7]. In addition, although the expression of ROL has been already reported under this constitutive promoter, proROL-gene, which encodes both the prosequence and the mature sequence is needed to alleviate the adverse effects of producing the mature sequence of ROL under  $P_{GAP}$  [8], as this lipase form is harmful to the host cell [9]. In fact, rROL-gene expression has only been accomplished under the inducible  $P_{AOXI}$  [10,11]—inducible promoters are less troublesome than constitutive promoters in this respect [12].

In this sense, the primary aim of this chapter was to express ROL under the constitutive promoter  $P_{GAP}$  by using the 28 amino acids of its prosequence fused to the mature sequence to alleviate the adverse effects of mature sequence expression and to enable a methanol-independent and more environmentally friendly bioprocess. The

alleged positive traits of the 28 C-terminal amino acids of the prosequence were assessed. In addition, besides the reduce in the negative impact on host strain growth, bioprocess productivity was evaluated and a deeper study of the role of the 28 amino acids in increasing the stability of the immobilized biocatalyst against organic solvents and in boosting its operational stability during the model reactions of biodiesel and ethyl butyrate (pineapple flavor) production was performed.

## **5.2.2. Results and discussion**

### 5.2.2.1. Batch and fed-batch bioprocess strategies under GAP promoter

The fact that some of the positive traits of the whole prosequence have also been identified with truncated sequences [13,14], led us to transform *K. phaffii* with 28proROL P<sub>GAP</sub>-plasmid, rROL P<sub>GAP</sub>-plasmid and the empty plasmid —blank— to investigate the role of the C-terminal 28 amino acids of the prosequence following the procedure described in Section 3.2.1.

Three transformation runs with each plasmid produced 252 colonies with the blank and 21 with 28proROL P<sub>GAP</sub>-plasmid but none with rROL P<sub>GAP</sub>-plasmid. Based on this outcome, the ROL mature sequence must somehow hinder constitutive expression in *K. phaffii*. In fact, these results are consistent with those of previous work where production of the ROL mature sequence caused cell lysis in *E.coli* owing to its phospholipase activity but no lysis when 28 C-terminal amino acids in the prosequence were expressed together with the mature sequence [9]. Consequently, the truncated prosequence of ROL (28 C-terminal amino acids) can be assumed to alleviate the

deleterious effects of the lipase and enable production of viable clones of *K. phaffii* as a result.

Viable clones expressing proROL were identified by colony PCR and a pool of positive colonies was selected, the most productive clone being chosen for further testing. Single plasmid integration in the proROL  $P_{GAP}$ -strain clone was confirmed by ddPCR and duplicate batch cultures were run with glycerol as carbon source as described in Section 3.2.2. Key production and growth parameters of batch cultures (described in Section 3.2.3.5) were compared with reported values for proROL  $P_{AOXI}$ -strain and rROL  $P_{AOXI}$ -strain grown in methanol extracted from previous Section 5.1.2.1 (Table 5.2.1).

**Table 5.2.1** – Results obtained in batch tests involving proROL  $P_{AOXI}$ -strain and rROL  $P_{AOXI}$ -strain in 10 g MeOH L<sup>-1</sup>, and proROL  $P_{GAP}$ -strain in 40 g glycerol L<sup>-1</sup>.

Parameter	proROL $P_{AOXI}$ <sup>1</sup>	proROL $P_{GAP}$	rROL $P_{AOXI}$ <sup>1</sup>
Final activity (AU mL <sup>-1</sup> )	12.38	74.71	10.51
$Y_{P/X}$ (total AU total gX <sup>-1</sup> )	5017	4273	3753
$\mu$ (h <sup>-1</sup> )	0.073	0.22	0.045
$q_p$ (AU gX <sup>-1</sup> h <sup>-1</sup> )	391	874	168
Specific productivity (AU gX <sup>-1</sup> h <sup>-1</sup> )	195	192	139
Volumetric productivity (AU L <sup>-1</sup> h <sup>-1</sup> )	462	3367	389

<sup>1</sup> Data obtained from section 5.1.2.1.

The greatest differences between proROL  $P_{AOXI}$ -strain and proROL  $P_{GAP}$ -strain were those in final activity and volumetric productivity, which were 6.5 times higher in the latter. Also,  $q_p$  was 2.2 times higher with proROL  $P_{GAP}$ -strain than it was with proROL  $P_{AOXI}$ -strain. However,  $Y_{P/X}$  was greater with the latter than it was with the former. In line with these results, specific productivities were very similar with both strains. In fact, the increased  $Y_{P/X}$  value obtained with proROL  $P_{AOXI}$ -strain was offset by

the increased specific growth rate of proROL P<sub>GAP</sub>-strain, which reduced bioprocess operation time.

Furthermore, the truncated prosequence minimized the harmful effects of mature ROL production on *K. phaffii* growth, no matter the promoter employed (Table 5.2.1). In fact, growth rates with proROL producing strains were similar to those of wild-type strain under both glycerol (0.22 h<sup>-1</sup> with proROL P<sub>GAP</sub>-strain and 0.25 h<sup>-1</sup> with the wild-type strain) and methanol (0.073 h<sup>-1</sup> with proROL P<sub>AOXI</sub>-strain and 0.09 h<sup>-1</sup> with the wild-type strain). By contrast, the growth rate of rROL P<sub>AOXI</sub>-strain in methanol was markedly lower (0.045 h<sup>-1</sup>). These results suggest that *K. phaffii* is an effective cell factory for ROL production; as unlike with *E. coli*, in which proROL expression inhibits cell growth [9].

proROL P<sub>GAP</sub>-strain was also grown in fed-batch cultures, using a pre-programmed exponential glucose feeding rate to maintain a constant specific growth rate of 0.045 h<sup>-1</sup> according to the procedure described in Section 3.2.3.2. Various key bioprocess parameters for proROL P<sub>GAP</sub>-strain (Table 5.2.2) were determined for comparison with previously reported results in Section 5.1.2.1 of proROL P<sub>AOXI</sub>-strain using methanol limited fed-batch (MLFB) strategy at a constant specific growth rate, and the methanol non-limited fed-batch (MNLFB) strategy at a constant methanol concentration of 3 g L<sup>-1</sup> in the culture broth throughout the induction stage (see calculations in Section 3.2.3.5). Based on previously obtained evidence, the latter is the most suitable strategy with this production system.

**Table 5.2.2** – Results obtained with proROL P<sub>GAP</sub>-strain under carbon-limited fed-batch conditions, and also with proROL P<sub>AOXI</sub>-strain under either methanol-limited fed-batch (MLFB) conditions at a preset specific growth rate of 0.045 h<sup>-1</sup> or methanol non-limited fed-batch (MNLFB) conditions at a constant methanol concentration of 3 g L<sup>-1</sup>.

Parameter	Carbon-limited fed-batch $\mu_{\text{set-point}} = 0.045 \text{ h}^{-1}$		MNLFB 3 g L <sup>-1</sup>
	proROL P <sub>AOXI</sub> <sup>1</sup>	proROL P <sub>GAP</sub>	proROL P <sub>AOXI</sub> <sup>1</sup>
	Final activity (AU mL <sup>-1</sup> )	147	341
$Y_{PX}$ (total AU total g <sub>X</sub> <sup>-1</sup> )	1908	6789	4972
Estimated $\mu$ (h <sup>-1</sup> )	0.038	0.045	0.065
$q_p$ (AU g <sub>X</sub> <sup>-1</sup> h <sup>-1</sup> )	68.5	479	308
Specific productivity (AU g <sub>X</sub> <sup>-1</sup> h <sup>-1</sup> )	44	156	99
Volumetric productivity (AU L <sup>-1</sup> h <sup>-1</sup> )	2782	7881	7160

<sup>1</sup> Data obtained from section 5.1.2.1.

As in the batch cultures, final activity (Figure 5.2.1) and volumetric productivity (Table 5.2.2) with proROL P<sub>GAP</sub>-strain were higher in the fed-batch cultures than with proROL P<sub>AOXI</sub>-strain grown under carbon-limited fed-batch conditions at a similar specific growth rate (Section 5.1.2.1). However,  $Y_{PX}$  was greater with proROL P<sub>GAP</sub>-strain than it was with proROL P<sub>AOXI</sub>-strain, contrary to what was observed during batch cultures. This outcome is consistent with the results of previous work where the MLFB strategy was reported to perform poorly [15].

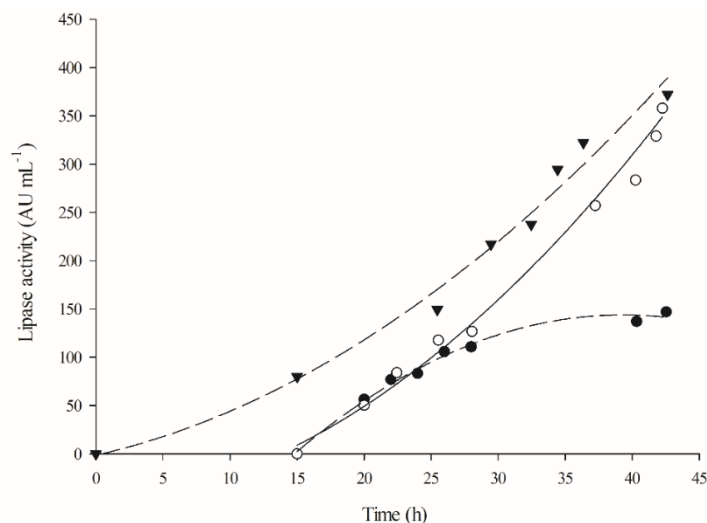


**Figure 5.2.1.** Time course of lipase activity in carbon limited fed-batch cultures of proROL P<sub>GAP</sub>-strain and proROL P<sub>AOXI</sub>-strain at a preset specific growth rate of 0.045 h<sup>-1</sup> (dashed line) and with MNLFB (solid line). proROL P<sub>AOXI</sub>-strain (circles) and proROL P<sub>GAP</sub>-strain (triangles).

Interestingly,  $Y_{P/X}$  was 1.5 times higher with proROL P<sub>GAP</sub>-strain than it was with proROL P<sub>AOXI</sub>-strain under MNLFB. However, final activity and volumetric productivity were similar with both strains. Thus, the bioprocess parameters for proROL P<sub>GAP</sub>-strain grown at specific rate of 0.045h<sup>-1</sup> on glucose were similar to those provided by proROL P<sub>AOXI</sub>-strain with the best strategy devised so far (MNLFB at a constant methanol concentration of 3 g L<sup>-1</sup>). Therefore, this strategy not only enables methanol-free proROL production but also lends itself readily to bioprocess optimization with proROL P<sub>GAP</sub>-strain.

#### 5.2.2.2. N-terminal amino acids sequence analysis

Previous results obtained by SDS-PAGE molecular weight analysis suggested selective proteolysis of the N-terminal 28 amino acids in the truncated prosequence of proROL by effect of proteases (Section 5.1.2.5). Similar results were also obtained with *R. niveus*

lipase, whose *N*-terminal is identical with that of ROL [16]. Therefore, these 28 amino acids seem to be naturally designed for removal to obtain the lipase mature sequence (rROL). proROL behaved identically here. The qualitative information of proteolysis obtained by SDS-PAGE technique was confirmed by performing the *N*-terminal sequence analysis described in Section 3.8, which involved automated Edman's degradation of proROLm (proteolyzed proROL, see Section 3.2.4), proROL and rROL *N*-terminal (Table 5.2.3). The 28 amino acids in the prosequence were confirmed to be primarily hydrolyzed by proteases in order to convert proROL into the lipase mature sequence (rROL). However, the expected proROLm sequence, which should have been identical with that of rROL, did not materialize because the first serine was removed. Based on studies done with the bioinformatic tool ExPASy, the digestion pattern could be ascribed to AspN and AspGluN endoproteases.

**Table 5.2.3** – Expected sequence for the *N*-terminal based on the cloned sequence and actual sequence as determined by Edman's degradation analysis.

Enzyme	Expected sequence	Actual sequence
proROL	DDNLVG	EADDNL
proROLm	SDGGKVV	DGGKVV
rROL <sup>1</sup>	SDGGKVV	EAEFSDGGKVVA

<sup>1</sup> Data obtained from [17]

Regarding proROL *N*-terminal, as previously reported for rROL [17], the plasmid used for heterologous production of the lipase in *K. phaffii* left the last two amino acids of the alpha-factor sequence of *S. cerevisiae* (EA) in the resulting protein. The presence of these amino acids is important because the theoretical isoelectric point (pI) for proROL as calculated with ExPASy bioinformatic tool switches from 6.32 to 6.08, which explains previously encountered turbidity issues in proROL strain fermentations at pH 5.5 —a



value near the pI level leading to enzyme denaturation (see Section 5.1.2.1). Besides, unlike in rROL [17], the following two amino acids, EF—an unwanted sequence coming from the restriction site—, were not found because plasmid restriction sites were upgraded in proROL plasmids. Then, besides the EA amino acids, proROL *N*-terminal showed the same sequence as native lipase from *Rhizopus oryzae* (indicated in Table 5.2.3 as the expected sequence) [18]. This outcome might explain that in the previous section 5.1.2.4, proROL and the native ROL showed similar substrate specificity towards *p*-nitrophenol esters of different chain length.

#### 5.2.2.3. Immobilized enzymes stability

For industrial use, biocatalysts must be stable enough in the organic solvents typically used [19]. ROL has been deemed tolerant to non-aqueous solvents [20]. However, because proROL is a more stable enzyme than rROL by virtue of its truncated prosequence (Section 5.1.2.6), in this work we wanted to compare the stability of both lipases covalently immobilized onto a support containing epoxide and butyl functional groups (EB) in solvents spanning a wide range of Log *P* values (Figure 5.2.2).

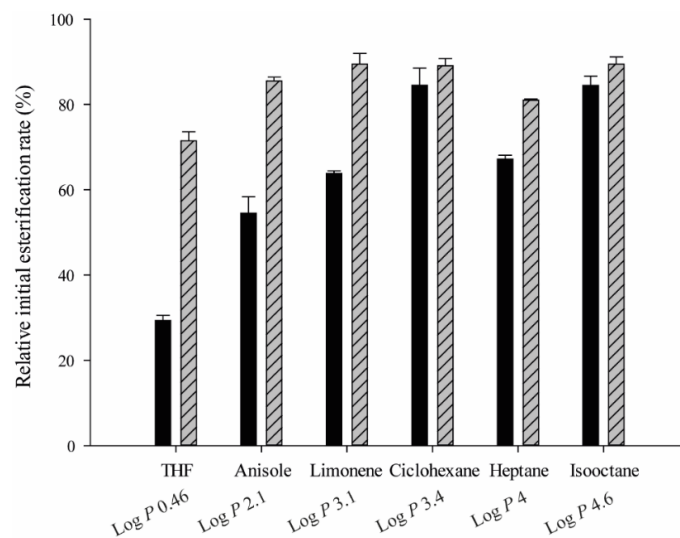


**Figure 5.2.2** – Relative initial reaction rate (%) of ethyl butyrate synthesis after incubation of the biocatalysts for 24 h in the following solvents: tetrahydrofuran (THF), anisole, limonene, cyclohexane, heptane and isooctane. The Log *P* values for each solvent are shown under its name. EB-rROL (black). EB-proROL (striped grey). The initial reaction rate for each non-incubated biocatalyst was taken to be 100%.

The presence of the truncated prosequence had a positive effect on EB-proROL stability, which exceeded that of EB-rROL in all cases. In fact, EB-proROL was 2.5 times more stable than EB-rROL in tetrahydrofuran (THF), the most extreme case. In anisole and limonene, two solvents with a high potential for use in green chemistry [21] and medium Log *P* values, EB-proROL was about 30% more stable than EB-rROL. Log *P* had a marked effect on biocatalyst stability, decreasing values leading to reduce stability due to the removal of structural water from the enzymes [22]. Obviously, the adverse effects of low Log *P* values on proROL were less marked than those on rROL.

The results for EB-rROL in heptane and isooctane were compared with previously reported values for rROL immobilized onto various supports (EP100, Eupergit® CM and octadecyl-Sepabeads) [23]. This way, immobilization onto the EB support obtained from Purolite® was found to also increase the stability of rROL.

#### 5.2.2.4. Transesterification and esterification reactions.

rROL and proROL free lipases were covalently immobilized onto a Purolite® D6307 support containing epoxide and butyl functional groups (EB) to elucidate the effect of the 28 amino acids of the lipase on the initial reaction rate and operational stability of the biocatalyst during biodiesel and ethyl butyrate production. The employed reaction procedures for both transesterification and esterification reactions can be found in Sections 3.14 and 3.15.1, respectively.

##### *5.2.2.4.1. Biodiesel production*

The enzymatic production of biodiesel has several advantages in terms of process sustainability over its chemical production. However, only exceptionally stable biocatalysts allow cost-effective production [24,25]. This led us to assess the potential of the truncated prosequence of ROL for increasing the operational stability of the resulting biocatalyst under enzymatic biodiesel production conditions and its influence on the initial transesterification rate.

No differences in initial reaction rate were observed between the two biocatalysts studied: EB-rROL and EB-proROL (Table 5.2.4). Therefore, the presence of the 28 amino acids in proROL had no influence on this parameter even though previous results suggested that its being close to the “lid region” in the 3D structure might interfere with interfacial activation and substrate–enzyme interaction processes [26,27]. In fact, specificity results found in the comparison of proROL and rROL free enzymes (see Section 5.1.2.4) showed a clear effect of these 28 amino acids.

**Table 5.2.4** – EB-rROL and EB-proROL initial transesterification rate, productivity and half-lives as calculated by using the best-fitting deactivation model (see Section 3.16).

Reaction	Biocatalyst	Initial rate ( $\mu\text{mol product mL}^{-1} \text{min}^{-1}$ )	Productivity ( $\mu\text{mol product min}^{-1}$ )	Half-life (h)
Transesterification	EB-proROL	27.2	39.43	498
	EB-rROL	25.1	34.17	102

As regards operational stability, Figure 5.2.3 shows the relative yield obtained in consecutive transesterification reaction cycles with each immobilized lipase. After 8 cycles, EB-proROL exhibited the greatest operational stability, with a relative yield exceeding 90% of the initial value and that of EB-rROL (70%) by 25%. These results testify to the influence of biocatalyst stability on productivity and obviously, on half-life (Table 5.2.4). In fact, after 8 reaction cycles EB-proROL exhibited 15% higher productivity than EB-rROL. Half-lives were calculated by fitting the experimental relative yields with the deactivation models described in Section 3.16. The results obtained with EB-proROL fitted equation 3.14 (Eq. 3.14, a two-component first-order exponential decay model) more closely than they fitted equation 3.13 (Eq. 3.13, a first-order exponential decay model); thus,  $R^2$  was 0.844 with Eq. 3.14 and 0.7389 with Eq. 3.13. On the other hand, the results for EB-rROL fitted both models almost identically well,  $R^2$  being 0.977 with Eq. 3.13 and 0.991 with Eq. 3.14. The best model for each biocatalyst (Eq. 3.14) was used to calculate the corresponding half-life. As can be seen from Table 5.2.4,  $t_{1/2}$  was almost 5 times greater with EB-proROL than it was with EB-rROL. Thus, EB-proROL is clearly a more stable biocatalyst.

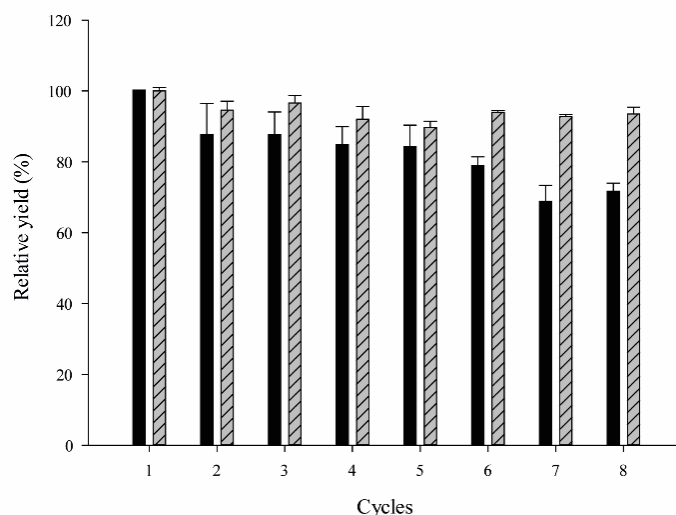


**Figure 5.2.3** – Relative yield of consecutive transesterification runs with each biocatalyst as obtained by following the 1-pulse ethanol addition procedure. EB-rROL (black) and EB-proROL (striped grey). The final yield of the first run was taken to be 100%.

Similar half-life results in biodiesel production were previously obtained with a whole-cell ROL biocatalyst (456 h) [28], rROL immobilized onto Purolite® Lifetech™ ECR1030M (579 h) and IRA-96 (381 h) [29]. By contrast, rROL immobilized onto AP1090M and Lewatit VP OC 1600 had a markedly shorter half-life (270 and 113 h, respectively). Interestingly, rROL immobilized onto Lifetech™ ECR8285M —a biocatalyst identical with EB-rROL— had a much shorter half-life: 16 h [29]. Since the only difference was that in reaction conditions, these results testify to the importance of reaction conditions in biocatalyst operational stability [30].

#### 5.2.2.4.2. Ethyl butyrate production

Short-chain esters are arousing increasing interest in sectors such as agri-food and cosmetic production by virtue of their pleasant sensory attributes [31]. One such ester is ethyl butyrate, which possesses a characteristic strong pineapple flavor and can be obtained by esterifying butyric acid with ethanol. Although ROL has been successfully

used to synthesize ethyl butyrate, previous work showed that a more stable lipase is needed to prevent deactivation by both the acid and the alcohol [32]. This led us to test immobilized proROL here for comparison with rROL in order to assess the significance of the truncated prosequence with a view to improving the operational stability of the biocatalyst in this bioprocess and examining its influence on the initial reaction rate. As in biodiesel production, the truncated prosequence had no effect on the initial esterification rate. In fact, both biocatalysts led to an identical value in the first reaction cycle (Table 5.2.5, Figure 5.2.4).

**Table 5.2.5** – EB-rROL and EB-proROL initial esterification rate, productivity and half-lives as calculated by using the best-fitting deactivation model (see Section 3.16).

Reaction	Biocatalyst	Initial rate ( $\mu\text{mol product mL}^{-1} \text{min}^{-1}$ )	Productivity ( $\mu\text{mol product min}^{-1}$ )	Half-life (h)
Esterification	EB-proROL	308	4.74	70
	EB-rROL	294	3.10	30

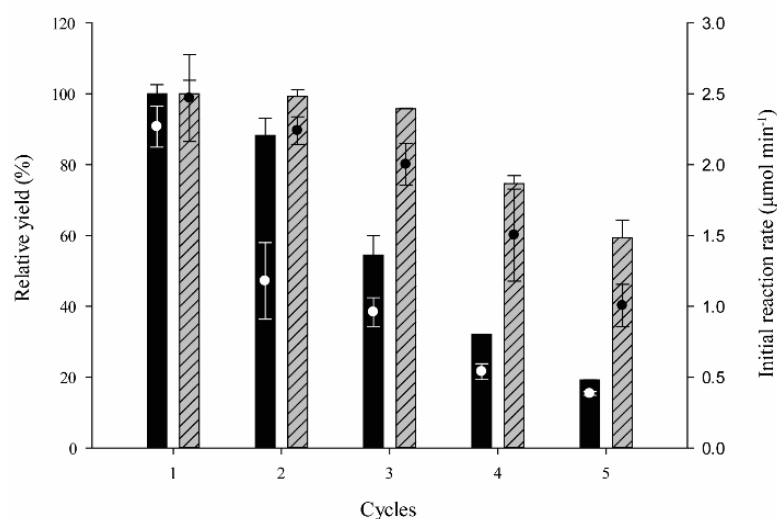


**Figure 5.2.4** –Relative yield of consecutive esterification reactions of each biocatalyst as obtained with butyric acid and ethanol as substrates. EB-rROL (black) and EB-proROL (striped grey). The final yield of the first run was taken to be 100%.

On the other hand, the truncated prosequence strongly affected the operational stability of the biocatalyst during ethyl butyrate synthesis —even to a greater extent than in biodiesel production. Thus, after 5 reaction cycles, EB-proROL led to a 3 times higher relative yield than did EB-rROL (Figure 5.2.4). As a result, productivity with EB-proROL was 35% higher than it was with EB-rROL. The half-lives of the two biocatalysts were calculated by fitting the relative yield results to Eqs 3.13 and 3.14. Both fitted Eq. 3.14 better than they fitted Eq. 3.13 (EB-rROL  $R^2 = 0.9004$  and EB-proROL  $R^2 = 0.9694$ ). Besides, EB-proROL proved more stable (Table 5.2.5): its half-life was 2.5 times greater. Therefore, EB-proROL stands as a promising biocatalyst to avoid deactivation by the alcohol or the acid during esterification.

### 5.2.3. Conclusions

The truncated prosequence of *Rhizopus oryzae* lipase was confirmed to suffice in order to alleviate the adverse effects on ROL and enable its expression in *K. phaffii* under the constitutive promoter  $P_{GAP}$  with glucose and glycerol as substrates —and hence to avoid the need for methanol. A more environmentally friendly bioprocess for proROL production afforded final activity and productivity values similar to those obtained with the best existing methanol feeding strategy (MNLFB, 3 g L<sup>-1</sup>).

Besides, the preferential hydrolysis of the 28 amino acids in the truncated prosequence was demonstrated by *N*-terminal analysis (that is, the 28 amino acids were confirmed to be naturally designed for removal). Also, the truncated prosequence increased the tolerance of organic solvents, and the operational stability in biodiesel and ethyl butyrate production, of EB-proROL relative to EB-rROL. However, no influence on initial reaction rates was observed, which suggests that EB-proROL and EB-rROL

interact identically with the substrates under the studied conditions no matter the results obtained for free proROL and rROL specificity with *p*-nitrophenyl esters of different chain length.



### 5.2.4. References

- [1] Garrigós-Martínez J, Nieto-Taype MA, Gasset-Franch A, Montesinos-Seguí JL, Garcia-Ortega X, Valero F. Specific growth rate governs AOX1 gene expression, affecting the production kinetics of *Pichia pastoris* (*Komagataella phaffii*) P<sub>AOX1</sub> - driven recombinant producer strains with different target gene dosage. *Microb Cell Fact* 2019;18:187. <https://doi.org/10.1186/s12934-019-1240-8>.
- [2] Garrigós-Martínez J, Vuoristo K, Nieto-Taype MA, Tähtiharju J, Uusitalo J, Tukiainen P, et al. Bioprocess performance analysis of novel methanol-independent promoters for recombinant protein production with *Pichia pastoris*. *Microb Cell Fact* 2021;20. <https://doi.org/10.1186/s12934-021-01564-9>.
- [3] Resina D, Serrano A, Valero F, Ferrer P. Expression of a *Rhizopus oryzae* lipase in *Pichia pastoris* under control of the nitrogen source-regulated formaldehyde dehydrogenase promoter. *J Biotechnol* 2004;109:103–13. <https://doi.org/10.1016/j.jbiotec.2003.10.029>.
- [4] Cos O, Resina D, Ferrer P, Montesinos JL, Valero F. Heterologous production of *Rhizopus oryzae* lipase in *Pichia pastoris* using the alcohol oxidase and formaldehyde dehydrogenase promoters in batch and fed-batch cultures. *Biochem Eng J* 2005;26:86–94. <https://doi.org/10.1016/j.bej.2005.04.005>.
- [5] García-Ortega X, Cámara E, Ferrer P, Albiol J, Montesinos-Seguí JL, Valero F. Rational development of bioprocess engineering strategies for recombinant protein production in *Pichia pastoris* (*Komagataella phaffii*) using the methanol-free GAP promoter. Where do we stand? *N Biotechnol* 2019;53:24–34.

- <https://doi.org/10.1016/j.nbt.2019.06.002>.
- [6] Müller JM, Bruhn S, Flaschel E, Friehs K, Risse JM. GAP promoter-based fed-batch production of highly bioactive core streptavidin by *Pichia pastoris*. *Biotechnol Prog* 2016;32:855–64. <https://doi.org/10.1002/btpr.2283>.
- [7] Nieto-Taype MA, Garrigós-Martínez J, Sánchez-Farrando M, Valero F, Garcia-Ortega X, Montesinos-Seguí JL. Rationale-based selection of optimal operating strategies and gene dosage impact on recombinant protein production in *Komagataella phaffii* (*Pichia pastoris*). *Microb Biotechnol* 2020;13:315–27. <https://doi.org/10.1111/1751-7915.13498>.
- [8] Yu XW, Yang M, Jiang C, Zhang X, Xu Y. *N*-glycosylation engineering to improve the constitutive expression of *Rhizopus oryzae* lipase in *Komagataella phaffii*. *J Agric Food Chem* 2017;65:6009–15. <https://doi.org/10.1021/acs.jafc.7b01884>.
- [9] Beer HD, Wohlfahrt G, Schmid RD, McCarthy JE. The folding and activity of the extracellular lipase of *Rhizopus oryzae* are modulated by a prosequence. *Biochem J* 1996;319:351–9. <https://doi.org/10.1042/bj3190351>.
- [10] López-Fernández J, Barrero JJ, Benaiges MD, Valero F. Truncated prosequence of *Rhizopus oryzae* lipase: key factor for production improvement and biocatalyst stability. *Catalysts* 2019;9:961–77. <https://doi.org/10.3390/catal9110961>.
- [11] Ponte X, Barrigón JM, Maurer M, Mattanovich D, Valero F, Montesinos-Seguí JL. Towards optimal substrate feeding for heterologous protein production in *Pichia pastoris* (*Komagataella* spp) fed-batch processes under P<sub>AOX1</sub> control: a modeling aided approach. *J Chem Technol Biotechnol* 2018;93:3208–18.

- <https://doi.org/10.1002/jctb.5677>.
- [12] Kluge J, Terfehr D, Kück U. Inducible promoters and functional genomic approaches for the genetic engineering of filamentous fungi. *Appl Microbiol Biotechnol* 2018;102:6357–72. <https://doi.org/10.1007/s00253-018-9115-1>.
- [13] Hama S, Tamalampudi S, Shindo N, Numata T, Yamaji H, Fukuda H, et al. Role of N-terminal 28-amino-acid region of *Rhizopus oryzae* lipase in directing proteins to secretory pathway of *Aspergillus oryzae*. *Appl Microbiol Biotechnol* 2008;79:1009–18. <https://doi.org/10.1007/s00253-008-1502-6>.
- [14] Beer HD, McCarthy JEG, Bornscheuer UT, Schmid RD. Cloning, expression, characterization and role of the leader sequence of a lipase from *Rhizopus oryzae*. *Biochim Biophys Acta - Gene Struct Expr* 1998;1399:173–80. [https://doi.org/10.1016/S0167-4781\(98\)00104-3](https://doi.org/10.1016/S0167-4781(98)00104-3).
- [15] Barrigón JM, Montesinos JL, Valero F. Searching the best operational strategies for *Rhizopus oryzae* lipase production in *Pichia pastoris* Mut<sup>+</sup> phenotype: methanol limited or methanol non-limited fed-batch cultures? *Biochem Eng J* 2013;75:47–54. <https://doi.org/10.1016/j.bej.2013.03.018>.
- [16] Kohno M, Kugimiya W, Hashimoto Y, Morita Y. Purification, characterization, and crystallization of two types of lipase from *Rhizopus niveus*. *Biosci Biotechnol Biochem* 1994;58:1007–12. <https://doi.org/10.1271/bbb.58.1007>.
- [17] Guillén M, Benaiges MD, Valero F. Comparison of the biochemical properties of a recombinant lipase extract from *Rhizopus oryzae* expressed in *Pichia pastoris* with a native extract. *Biochem Eng J* 2011;54:117–23. <https://doi.org/10.1016/j.bej.2011.02.008>.

- [18] Takahashi S, Ueda M, Tanaka A. Independent production of two molecular forms of a recombinant *Rhizopus oryzae* lipase by KEX2-engineered strains of *Saccharomyces cerevisiae*. *Appl Microbiol Biotechnol* 1999;52:534–40. <https://doi.org/10.1007/s002530051556>.
- [19] Kumar A, Dhar K, Kanwar SS, Arora PK. Lipase catalysis in organic solvents: advantages and applications. *Biol Proced Online* 2016;18:1–11. <https://doi.org/10.1186/s12575-016-0033-2>.
- [20] Hiol A, Jonzo MD, Rugani N, Druet D, Sarda L, Comeau LC. Purification and characterization of an extracellular lipase from a thermophilic *Rhizopus oryzae* strain isolated from palm fruit. *Enzyme Microb Technol* 2000;26:421–30. [https://doi.org/10.1016/S0141-0229\(99\)00173-8](https://doi.org/10.1016/S0141-0229(99)00173-8).
- [21] McDowell C, Bazan GC. Organic solar cells processed from green solvents. *Curr Opin Green Sustain Chem* 2017;5:49–54. <https://doi.org/10.1016/J.COGSC.2017.03.007>.
- [22] Wang S, Meng X, Zhou H, Liu Y, Secundo F, Liu Y. Enzyme stability and activity in non-aqueous reaction systems: a mini review. *Catalysts* 2016;6:32. <https://doi.org/10.3390/catal6020032>.
- [23] Guillén M, Benaiges MD, Valero F. Biosynthesis of ethyl butyrate by immobilized recombinant *Rhizopus oryzae* lipase expressed in *Pichia pastoris*. *Biochem Eng J* 2012;65:1–9. <https://doi.org/10.1016/j.bej.2012.03.009>.
- [24] Zhong L, Feng Y, Wang G, Wang Z, Bilal M, Lv H, et al. Production and use of immobilized lipases in/on nanomaterials: a review from the waste to biodiesel production. *Int J Biol Macromol* 2020;152:207–22.

- <https://doi.org/10.1016/J.IJBIOMAC.2020.02.258>.
- [25] López-Fernández J, Dolors Benaiges M, Valero F. Second- and third-generation biodiesel production with immobilised recombinant *Rhizopus oryzae* lipase: influence of the support, substrate acidity and bioprocess scale-up. *Bioresour Technol* 2021;334:125233. <https://doi.org/10.1016/j.biortech.2021.125233>.
- [26] Sayari A, Frikha F, Miled N, Mtibaa H, Ali Y Ben, Verger R, et al. N-terminal peptide of *Rhizopus oryzae* lipase is important for its catalytic properties. *FEBS Lett* 2005;579:976–82. <https://doi.org/10.1016/j.febslet.2004.12.068>.
- [27] Cheng C, Jiang T, Wu Y, Cui L, Qin S, He B. Elucidation of lid open and orientation of lipase activated in interfacial activation by amphiphilic environment. *Int J Biol Macromol* 2018;119:1211–7. <https://doi.org/10.1016/J.IJBIOMAC.2018.07.158>.
- [28] He Q, Shi H, Gu H, Naka G, Ding H, Li X, et al. Immobilization of *Rhizopus oryzae* ly6 onto loofah sponge as a whole-cell biocatalyst for biodiesel production. *BioResources* 2016;11:850–60. <https://doi.org/10.15376/biores.11.1.850-860>.
- [29] Rodrigues J, Canet A, Rivera I, Osório NM, Sandoval G, Valero F, et al. Biodiesel production from crude *Jatropha* oil catalyzed by non-commercial immobilized heterologous *Rhizopus oryzae* and *Carica papaya* lipases. *Bioresour Technol* 2016;213:88–95. <https://doi.org/10.1016/j.biortech.2016.03.011>.
- [30] Bonet-Ragel K, Canet A, Benaiges MD, Valero F. Effect of acyl-acceptor stepwise addition strategy using *alperujo* oil as a substrate in enzymatic biodiesel synthesis. *J Chem Technol Biotechnol* 2018;93:541–7. <https://doi.org/10.1002/jctb.5399>.

- [31] Asmat S, Anwer AH, Husain Q. Immobilization of lipase onto novel constructed polydopamine grafted multiwalled carbon nanotube impregnated with magnetic cobalt and its application in synthesis of fruit flavours. *Int J Biol Macromol* 2019;140:484–95. <https://doi.org/10.1016/j.ijbiomac.2019.08.086>.
- [32] Guillén M, Benaiges MD, Valero F. Improved ethyl butyrate synthesis catalyzed by an immobilized recombinant *Rhizopus oryzae* lipase: a comprehensive statistical study by production, reaction rate and yield analysis. *J Mol Catal B Enzym* 2016;133:S371–6. <https://doi.org/10.1016/j.molcatb.2017.02.010>.



# 6

## Results III: Biotransformations catalyzed with improved proROL biocatalyst

### 6.1. Natural flavors production with proROL from isoamyl alcohol and fusel oil

---

Chapter submitted as research article to *J. of Agricultural and Food Chemistry*  
López-Fernández J, Benaiges MD, Sebastián X, Bueno JM, Valero F.  
Research performed in collaboration with Hausmann S.L.  
Producing natural flavors from isoamyl alcohol and  
fusel oil by using immobilized *Rhizopus oryzae* lipase.  
Submitted to *Journal of Agricultural and Food Chemistry*





## **6. RESULTS (III)**

### **6.1. Natural flavors production with proROL from isoamyl alcohol and fusel oil**

<i>6.1.1. Introduction</i> .....	267
<i>6.1.2. Results and discussion</i> .....	269
6.1.2.1. Reaction solvent studies: isoamyl esters production .....	269
6.1.2.2. Experimental design: optimization of isoamyl butyrate single-batch and cumulative production .....	271
6.1.2.3. Isoamyl butyrate synthesis reaction scale up and fusel oil employment .....	275
6.1.2.4. Structural isomers: 3-methylbutanol and 2-methylbutanol...	278
<i>6.1.3. Conclusions</i> .....	279
<i>6.1.4 References</i> .....	281



### **6.1.1. Introduction**

Flavor esters are short-chain esters commonly found in various fruits and plants that possess favorable sensory attributes (floral, spicy, fruity) and are used by the food, beverage, cosmetics and pharmaceutical industry [1]. The flavor and fragrance market was valued at \$28 billion in 2019 and is expected to expand at a compound annual growth rate (CAGR) of 4.7% to \$35 billion from 2021 to 2027 [2]. Thus, the large demand of these esters has boosted the need of greener production routes and food safety aspects for human consumption making enzymatic synthesis a great alternative to chemical catalysts route (see Section 1.6.3) [3,4].

Amongst the extremely important aroma compounds that are produced through esterification of short-chain alcohols and short-chain fatty acids, isoamyl alcohol esters, such as isoamyl butyrate and acetate can be found. These esters serve as flavoring agents in numerous industries due to their characteristic fruity banana and intense banana flavor, respectively [5,6]. However, the use of short-chain fatty acids, being more hydrophilic, lower the pH of the microenvironment and might lead to enzyme inactivation, while the use of short-chain alcohols tends to strip the essential water from the enzyme and act as a dead-end inhibitor, making enzymatic synthesis of esters challenging. Moreover, the use of isoamyl alcohol, as it presents branching in its structure, has been suggested to exert higher steric hindrance on enzyme activity. Therefore, isoamyl alcohol might serve as an interest model to understand esterification with such acids and alcohols [7,8].

In addition to using biocatalysis as an environmentally friendly approach for esters production, the use of by-products as substrates for flavor esters production has emerged as a relevant way to support circular economy principles and reduce waste

generation. During great scale bioethanol synthesis for fuel or food production, fusel oil is generated, which is a by-product obtained in fermentation and distillation steps and removed during alcohol rectification—this by-product accounts for approximately 0.25% by volume of bioethanol [9]. The quality and amount of generated fusel oil are affected by the processing parameters such as mash preparation, fermentation conditions, and the distillation process. Higher alcohols (e.g. isoamyl alcohol, isobutanol, butanol), water, aldehyde, and esters are the main compounds found in fusel oil samples [10,11]. Owing to its intense odor, the use of fusel oil as solvent is limited although it has been used as foam coating or added into diesel or gasoline to increase cetane index and octane number. Nevertheless, due to its high alcohol content (specifically isoamyl alcohol) it results attractive as low-cost substrate for esterification and production of a wide variety of aromatic esters [12].

In this chapter, proROL was covalently immobilized onto the optimized biocatalyst through the previous chapters (polymethacrylate supports from Purolite® containing surface epoxide and octadecyl groups, EO-proROL). The biocatalyst was used to obtain isoamyl butyrate and isoamyl acetate by esterification. The influence of the solvent was evaluated, and single-batch and cumulative production of isoamyl butyrate were maximized by optimizing the initial acid concentration and acid:alcohol mole ratio with a central composite design in combination with response surface methodology. The optimum conditions thus found were used to scale up the reaction and the results thus obtained were compared with those of esterifying butyric acid with waste from alcoholic fermentation (fusel oil). The specificity of the biocatalyst for structural isomers of the alcohol was also assessed. All reported results in this chapter were performed in the facilities of Hausmann S.L. under a scientific collaboration for the doctoral stay.

## **6.1.2. Results and discussion**

### 6.1.2.1. Reaction solvent studies: isoamyl esters production

The solvents initially used as reaction media in the esterification of butyric and acetic acid with isoamyl alcohol were cyclohexane and hexane, both of which are allowed for the production of foodstuffs and food ingredients by European legislation (2009/32/EC). Other allowed solvents were avoided because they have a strong odor, low concentrations are allowed after purification or might have interfered with the reaction.

The two solvents chosen were assessed by performing esterification reactions as described in Section 3.15.2. Higher acid and isoamyl alcohol concentrations were avoided in this first step not to inactivate the biocatalyst [13]. Under the established conditions, butyric acid esterification with isoamyl alcohol reached yields close to 100% and approximately 1.8 times higher than acetic acid esterification (Figure 6.1.1), despite the longer reaction time used in the latter (24 h for isoamyl acetate and 5 h for isoamyl butyrate). In fact, acetic acid is believed to be a more potent enzyme inhibitor than other acids such as propionic or butyric because it causes more severe dead-end inhibition through preferential reaction with the serine residue at the active site of the lipase [14].

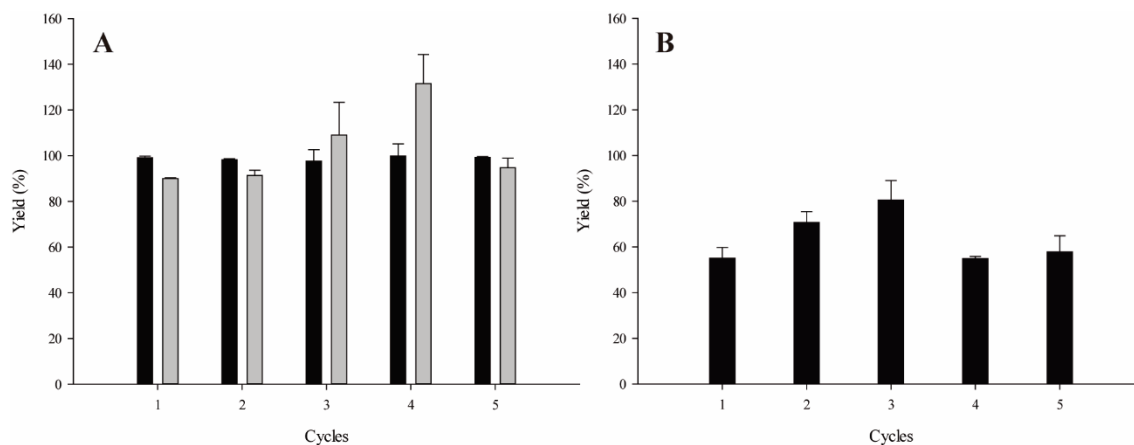


**Figure 6.1.1.** Esterification yield (%) of butyric acid (A) and acetic acid (B) with isoamyl alcohol in cyclohexane (black) and hexane (grey).

Interestingly, EO-proROL showed excellent esterification performance with isoamyl alcohol, even though esterification of  $\beta$ - and  $\gamma$ -branched alcohols is thought to sterically hinder enzyme activity [7]. Although whether a linear or branched alcohol is used is seemingly not a crucial factor according to some reports [15], some authors have suggested that whether it is primary or secondary does influence reaction performance [16].

As can be seen from Figure 6.1.1, EO-proROL exhibited a high operational stability. Thus, no loss of enzyme activity was detected after 5 reaction cycles of isoamyl butyrate synthesis with either cyclohexane or hexane as solvent—the yield was ca. 100%. The increased yield variability observed with hexane (more than 20%) was probably due to evaporation, especially over the long reaction time used to synthesize isoamyl acetate. This led us to choose cyclohexane for further testing in order not to increase the acid concentration through evaporation and hinder biocatalyst activity, and also to discard isoamyl acetate biosynthesis owing to the low reaction yields obtained and the need for longer reaction times.

### 6.1.2.2. Experimental design: optimization of isoamyl butyrate single-batch and cumulative production

DoE methodology is extensively used to assess the individual and combined effects of operational variables on one or several responses [17] in processes such as flavor ester biosynthesis [18]. In this work, we used it to understand the effect of, and relationship between, two major variables (viz., acid concentration and acid:alcohol mole ratio) in order to maximize single-batch and cumulative production of isoamyl butyrate in cyclohexane with a Box-Hunter design (see Section 3.15.2.1). The resulting matrix (Figure 6.1.2) consisted of 11 experiments whose data were fitted to Eq. 3.12; the fitted data being used to construct the response surfaces of Figure 6.1.3 for easier understanding. The values of the coefficients are listed in Table 6.1.1. The statistical significance of the different functions and their respective coefficients were assessed via ANOVA (Table 6.1.1).

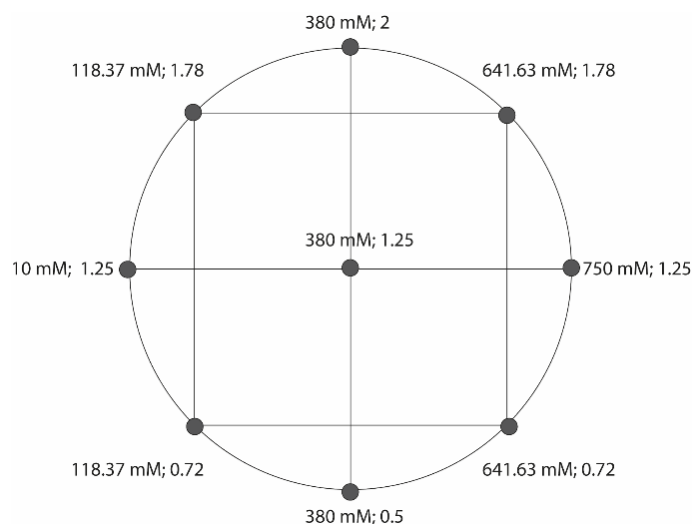


**Figure 6.1.2.** Box-Hunter design matrix representing the butyric acid concentration and acid:alcohol mole ratio used to maximize single-batch and cumulative production.



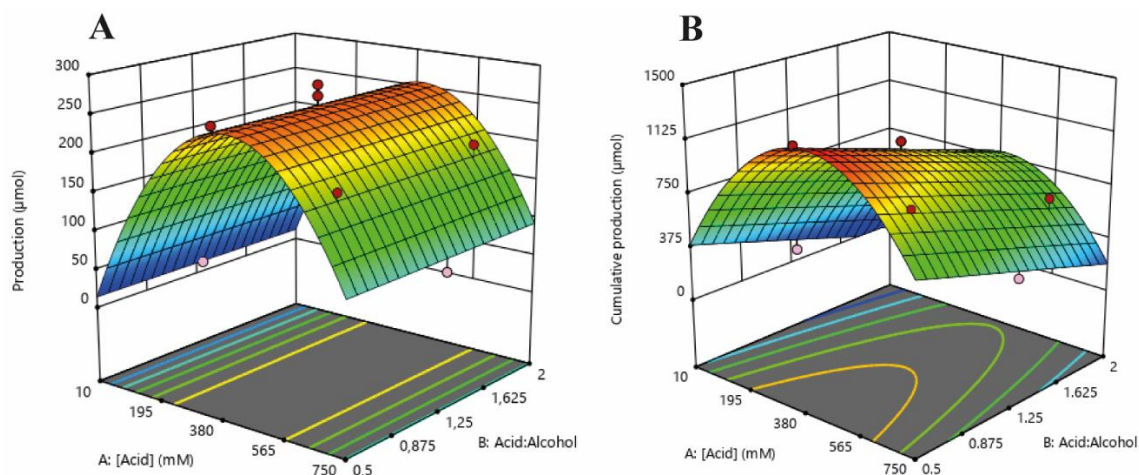


**Figure 6.1.3.** Experimental response surfaces for single-batch (A) and cumulative production (B) of isoamyl butyrate at different initial butyric acid concentrations and acid:alcohol mole ratios. The red dots correspond to the design points listed in Table 6.1.1. Measured values greater and smaller than the predictions are shown in dark red and light red, respectively.

The experimental data for the first cycle of isoamyl butyrate production were fitted to Eq. 3.12 and the coefficients of the terms  $\beta_2$ ,  $\beta_{12}$  and  $\beta_{22}$  were found not to be statistically significant ( $p$ -value > 0.05), resulting in the Eq. 6.1.4, a quadratic function of the acid concentration alone.  $R^2$  for the function exceeded 0.9 and the difference between adjusted- $R^2$  and predicted- $R^2$  was less than 0.2, so the goodness of fit was acceptable.

$$Production (\mu\text{mol}) = 260 + 28 * [\text{acid}] - 104 * [\text{acid}]^2 \quad (6.1.4)$$

Interestingly, the acid:alcohol mole ratio was scarcely influential on ester production. This result is similar to that of a previous study [11] but contradicts one where the influence of the initial acid concentration on isoamyl butyrate yield was not considered as a DoE variable [19]. Therefore, only the initial acid concentration influenced production of the ester in this work, production peaking with a concentration around 400 mM (Figure 6.1.3A, Table 6.1.1) and declining above that concentration.

**Table 6.1.1.** Box-Hunter design, independent variables, responses values obtained and results of the ANOVA analysis.

<b>Box-Hunter Design</b>					
Experimental run	Variables			Production response	
	[Butyrate] (mM)	Acid:alcohol mole ratio	[Isoamyl alcohol] <sup>1</sup> (mM)	Single-batch (μmol)	Cumulative (μmol)
1	118.37	1.78	66.49	105.2	537.14
2	10	1.25	8	12.7	78.74
3	641.63	0.72	891.56	194.6	968.8
4	380	1.25	304	241.2	1092.4
5	380	2	190	200.6	686.9
6	380	0.5	760	263.2	1293.2
7	750	1.25	600	75.8	383.7
8	118.37	0.72	164.48	153.9	742.7
9	380	1.25	304	263.1	972.9
10	641.63	1.78	360.40	199.6	672
11	380	1.25	304	281.4	1006.14
<b>Statistical Analysis</b>					
Production	<i>F</i> test <i>p</i> -value	LOF test <i>p</i> -value	R <sup>2</sup>	Adjusted-R <sup>2</sup>	Predicted-R <sup>2</sup>
Single-batch	<0.01	0.3593	0.9193	0.8991	0.8566
Cumulative	<0.01	0.3085	0.9541	0.9345	0.8620
Model	Single-batch production		Cumulative production		
Parameters	Coefficient	<i>p</i> -value	Coefficient	<i>p</i> -value	
β <sub>0</sub>	260	< 0.05	1036	< 0.05	
β <sub>1</sub>	28	0.02	99	0.016	
β <sub>2</sub>	NS	> 0.05	-170	< 0.01	
β <sub>12</sub>	NS	> 0.05	NS	> 0.05	
β <sub>11</sub>	104	< 0.01	-370	< 0.01	
β <sub>22</sub>	NS	> 0.05	NS	>0.05	

<sup>1</sup> As calculated from the butyric acid concentration and acid:alcohol mole ratio  
NS: not statistically significant

Similarly, previous studies with ROL found butyrate concentrations of 54.6 mM [20] and 225 mM [21] to result in optimal esterification and production of ethyl butyrate. The fact that production decreased above 400 mM butyric acid can be caused by deactivation or inhibition of the enzyme. In fact, high acid concentrations were previously found to promote denaturation of immobilized enzymes and to render them inactive as a result [22]. Also, as previously noted for acetic acid, butyric acid can, to a lesser extent,

bind to the acyl–enzyme complex unproductively and give a dead-end intermediate unable to form an ester [23]. In addition, esterification reactions have been shown to follow the ping-pong kinetic model and may thus be subject to acid-mediated inhibition [24]. However, some studies have shown esterification to be hindered by alcohols and also by both alcohols and acids [25].

Evaluating cumulative production allowed us not only to identify the most productive conditions after 5 reaction cycles, but also to assess, indirectly, the best conditions for retaining biocatalyst activity—operational stability. Experimental data for cumulative production fitted Eq. 3.12, coefficients  $\beta_{12}$  and  $\beta_{22}$  had  $p$ -value  $> 0.05$  and were thus deemed non-significant, so Eq. 6.1.5 was obtained with  $R^2 > 0.95$ , and adjusted- $R^2$  and predicted- $R^2$  values differing by less than 0.2.

$$\text{Cum.prod. } (\mu\text{mol}) = 1036 + 99 \times [\text{acid}] - 170 \times \text{acid:alcohol} - 370.2 \times [\text{acid}]^2 \quad (6.1.5)$$

As expected, increasing the initial acid concentration to about 400 mM resulted in increasing cumulative production while higher acid levels lead to a decline (Figure 6.1.3B, Table 6.1.1). This was a result of increased acid concentrations detracting from operational stability in the biocatalyst for the above-described reasons. Raising the proportion of alcohol (i.e., lowering the acid:alcohol mole ratio) increased cumulative production, in line with previous results and consistent with the protective role of the alcohol [26]. Although a high alcohol concentration in the reaction medium can also have a negative impact on enzyme performance, none of the concentrations used in this study fell above that theoretical threshold (Figure 6.1.3B). The negative impact of short-chain alcohols on esterification has been ascribed to their sequestering water molecules needed to maintain the 3D conformation and activity of the lipase [27].

Based on the previous results, an initial butyric acid concentration of 410 mM and an acid:alcohol mole ratio of 0.5 were chosen as optimal to maximize single-batch and cumulative ester production. The predicted maximum values (256.28 and 1282.78  $\mu\text{mol}$ , respectively) were experimentally validated—the highest deviation was only about 2.5%.

#### 6.1.2.3. Isoamyl butyrate synthesis reaction scale up and fusel oil employment

The previously established optimum butyric acid concentration and acid:alcohol mole ratio were used to scale up the esterification reaction to a laboratory bioreactor as described in Section 3.15.2.2. Commercial isoamyl alcohol and fusel oil were used as substrates to assess single-batch yield, initial esterification rate, productivity and enzyme operational stability, and finally to compare the results obtained between both substrates. The high moisture content of fusel oil required drying over 3 Å molecular sieves for 48 h [28] and centrifugation to remove any solid residue prior to use. The proportion of isoamyl alcohol concentration in dry fusel oil as assessed by GC/MS (see Section 3.18.3 for further information about chromatographic analysis) was 92%, other alcohols such as ethanol and pentanol were also found [29].

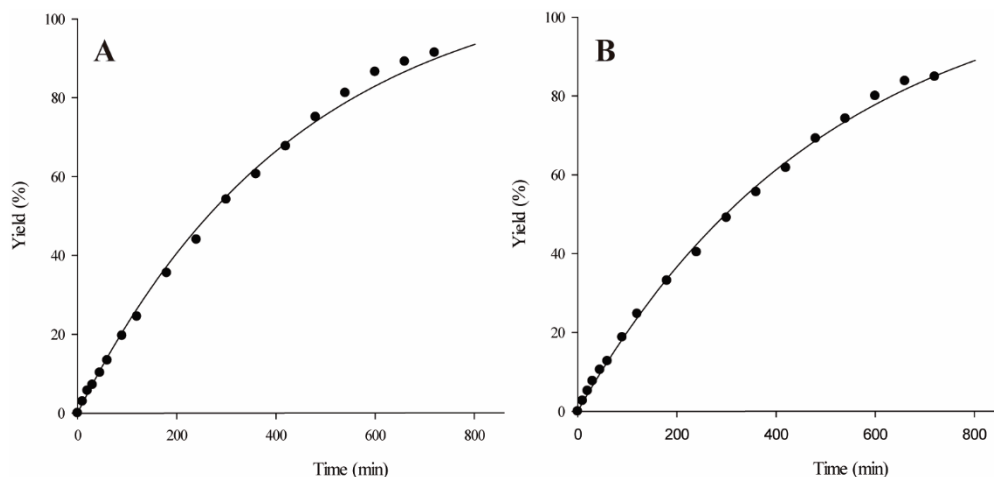


**Figure 6.1.4.** Isoamyl butyrate esterification yield profile with butyric acid and commercial isoamyl alcohol (A) or fusel oil (B) as substrate. The solid line corresponds to the quadratic fitting of the experimental data.

Figure 6.1.4A shows the esterification yield obtained with commercial isoamyl alcohol as substrate, which reached 91% after 720 min. The fact that the yield obtained after 5 h was similar to that previously found in 15 mL tubes confirmed that the reaction was successfully scaled up. As can be seen from Figure 6.1.4B, the esterification yield with fusel oil was similar to that obtained with commercial isoamyl alcohol. As expected, fusel oil gave a lower yield after 720 min reaction (84% instead of 91%) owing to the presence of other alcohols also acting as substrates and hence using some butyric acid. Productivity in the first reaction batch was similar with commercial isoamyl alcohol and fusel oil (31.09 vs 28.7 mM h<sup>-1</sup>). These productivities are only slightly lower than those previously obtained with Lipozyme TL IM (55 mM h<sup>-1</sup>) [11] and *Rhizopus sp.* lipase (78 mM h<sup>-1</sup>) [19], and could be improved by increasing the reaction temperature or the amount of biocatalyst used. However, a deeper economic analysis would be needed to confirm whether increasing productivity at the expense of altering some variables might compromise the feasibility of the bioprocess. In any case, these results show that EO-

proROL stands as a promising biocatalyst for industrial production of natural isoamyl butyrate.

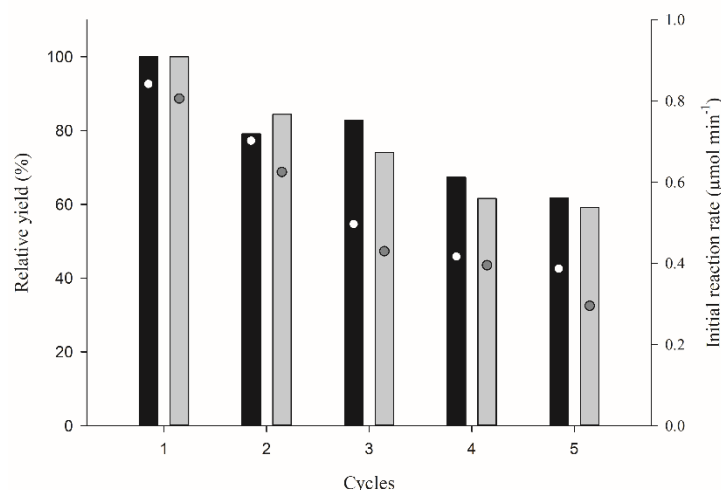


**Figure 6.1.5.** Relative yield (%) of consecutive isoamyl butyrate esterification cycles with butyric acid and commercial isoamyl alcohol (black) or fusel oil (grey) as substrate. The yield for the first cycle was taken to be 100%. Initial esterification rate of butyric acid by commercial isoamyl alcohol (white circles) or fusel oil (grey circles).

The initial esterification rates were close to  $0.8 \mu\text{mol min}^{-1}$  with both alcohols (Figure 6.1.5), which suggests that the biocatalyst reacted identically with the isoamyl alcohol present in both substrates. Operational stability was also identical with both substrates (Figure 6.1.5). Thus, the relative yield decreased by about 40% after 5 reaction cycles with both. Similar operational stability results have been reported in ethyl butyrate [30] and butyl acetate production [24]. The half-life ( $t_{1/2}$ ) of the biocatalyst during esterification was calculated by fitting the relative yields to Eq. 3.14 (Table 6.1.2).

**Table 6.1.2.** Parameter values for Eq. 3.14 and correlation ( $R^2$ ) upon fitting of relative yields with commercial isoamyl alcohol and fusel oil.

Alcohol	$k_1$	$k_2$	$c$	$R^2$
<b>Commercial isoamyl alcohol</b>	2.498	0.0926	99.986	0.9571
<b>Fusel oil</b>	0.1122	0.9124	26.629	0.9944

Although relative yields were similar with both substrates (Figure 6.1.5), the biocatalyst exhibited a slightly higher operational stability with commercial isoamyl alcohol. As a result, the biocatalyst half-life with the latter (7 batches, equivalent to 84 h reaction) was only slightly greater than that with fusel oil (6 batches or 72 h reaction). This result can be ascribed to the presence of detrimental compounds (e.g., acids, esters, remaining moisture after water separation or other impurities) in fusel oil [31].

#### 6.1.2.4. Structural isomers: 3-methylbutanol and 2-methylbutanol

As stated in Section 3.18.3, isoamyl alcohol (3-methylbutanol) and active amyl alcohol (2-methylbutanol) are structural isomers that cannot be fully resolved by ordinary GC [28]. However, using GC/MS in this work allowed the two to be successfully resolved, thereby allowing us to assess the specificity of EO-proROL for each isomer in the esterification reaction (Figure 6.1.6).

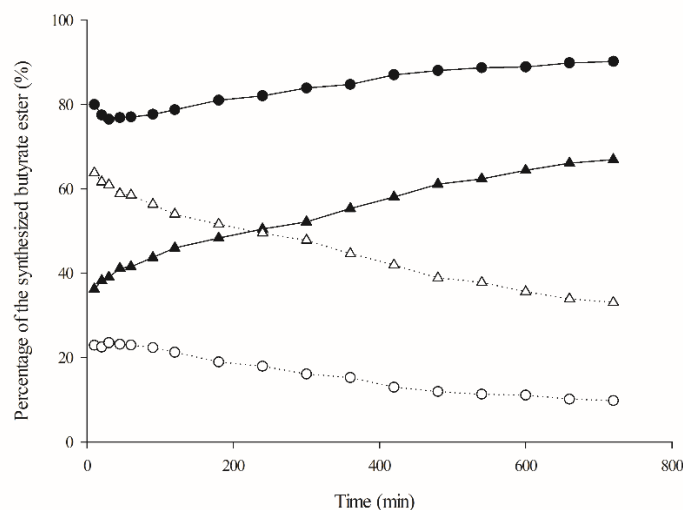


**Figure 6.1.6.** Percent composition of the butyrate esters obtained from 3-methylbutanol (solid line, black symbols) and 2-methylbutanol (dotted line, white symbols) in commercial isoamyl alcohol (circles) and fusel oil (triangles).

Commercial isoamyl alcohol was found to consist of 94% 3-methylbutanol and 6% 2-methylbutanol, whereas fusel oil contained 70% 3-methylbutanol and 30% 2-methylbutanol. Therefore, 2-methylbutanol was the minor isomer in both substrates, albeit in a different proportion. As a result, if EO-proROL had been identically specific for both structural isomers the esterification products should have retained the same isomer composition of the initial alcohols. However, the proportion of 2-methylbutanol ester exceeded the expected value (Figure 6.1.6) from the very beginning of the reaction (especially with fusel oil, which gave 2-methylbutyl butyrate as the major ester). Therefore, EO-proROL was clearly more specific to 2-methylbutanol than it was to 3-methylbutanol, which contradicts the results of previous studies suggesting that enzyme activity was adversely affected by proximity of the methyl group to the hydroxyl group [7].

### **6.1.3. Conclusions**

Immobilized *Rhizopus oryzae* lipase (EO-proROL) proved a suitable biocatalyst for producing natural isoamyl esters of acetic and butyric acid, especially the latter, in cyclohexane. A central composite rotatable Box-Hunter design predicted a 410 mM initial butyric acid concentration and an acid:alcohol mole ratio of 0.5 to be the optimum values for maximizing single-batch and cumulative production of isoamyl butyrate, which peaked at 256.28 and 1282.78  $\mu\text{mol}$ , respectively. These predictions were validated by deviations less than 2.5% from the experimental results and proved at some extent the potential protective role of alcohol for enzyme activity. The reaction was successfully scaled up from 15 mL tubes with orbital stirring to a laboratory bioreactor with a final volume of 150 mL and mechanical stirring. The results obtained by using commercial



isoamyl alcohol in the bioreactor were compared with those provided by fusel oil. Both substrates gave similar yields (91% with commercial alcohol vs 84% with fusel oil), initial reaction rate ( $0.8 \mu\text{mol min}^{-1}$  with both substrates), operational stability (40% activity loss after 5 runs with both) and productivity ( $31.09$  vs  $28.7 \text{ mM h}^{-1}$ ). Besides, the enzyme was proved to be more specific to 2-methylbutanol than it was to 3-methylbutanol notwithstanding previous results suggesting the activity to be hindered by the proximity of the methyl group to the hydroxyl group.

Based on the results, EO-proROL stands as a suitable biocatalyst for industrial production of natural isoamyl butyrate, even from an inexpensive substrate such as fusel oil to comply with the principles of circular economy.

#### 6.1.4 References

- [1] Cong S, Tian K, Zhang X, Lu F, Singh S, Prior B, et al. Synthesis of flavor esters by a novel lipase from *Aspergillus niger* in a soybean-solvent system. *3 Biotech* 2019;9:244. <https://doi.org/10.1007/s13205-019-1778-5>.
- [2] Flavors and Fragrance Market Size, Share & Trends | Forecast by 2027 <https://www.alliedmarketresearch.com/flavors-and-fragrances-market> (accessed August 11, 2021).
- [3] Bansode SR, Rathod VK. Enzymatic synthesis of Isoamyl butyrate under microwave irradiation. *Chem Eng Process - Process Intensif* 2018;129:71–6. <https://doi.org/10.1016/J.CEP.2018.04.015>.
- [4] Bansode SR, Hardikar MA, Rathod VK. Evaluation of reaction parameters and kinetic modelling for Novozym 435 catalysed synthesis of isoamyl butyrate. *J Chem Technol Biotechnol* 2017;92:1306–14. <https://doi.org/10.1002/JCTB.5125>.
- [5] Zare M, Golmakani MT, Niakousari M. Lipase synthesis of isoamyl acetate using different acyl donors: comparison of novel esterification techniques. *LWT* 2019;101:214–9. <https://doi.org/10.1016/j.lwt.2018.10.098>.
- [6] Taghizadeh T, Ameri A, Talebian-Kiakalaieh A, Mojtabavi S, Ameri A, Forootanfar H, et al. Lipase@zeolitic imidazolate framework ZIF-90: A highly stable and recyclable biocatalyst for the synthesis of fruity banana flavour. *Int J Biol Macromol* 2021;166:1301–11. <https://doi.org/10.1016/J.IJBIOMAC.2020.11.011>.
- [7] Hari Krishna S, Prapulla SG, Karanth NG. Enzymatic synthesis of isoamyl

- butyrate using immobilized *Rhizomucor miehei* lipase in non-aqueous media. *J Ind Microbiol Biotechnol* 2000;25:147–54. <https://doi.org/10.1038/SJ.JIM.7000045>.
- [8] Bansode SR, Rathod VK. Ultrasound assisted lipase catalysed synthesis of isoamyl butyrate. *Process Biochem* 2014;49:1297–303. <https://doi.org/10.1016/J.PROCBIO.2014.04.018>.
- [9] Tran TTV, Kongparakul S, Karnjanakom S, Reubroycharoen P, Guan G, Chanlek N, et al. *Selective production of green solvent (isoamyl acetate) from fusel oil using a sulfonic acid-functionalized KIT-6 catalyst*. *Mol Catal* 2020;484:110724. <https://doi.org/10.1016/J.MCAT.2019.110724>.
- [10] Dias ALB, Hatami T, Martínez J, Ciftci ON. Biocatalytic production of isoamyl acetate from fusel oil in supercritical CO<sub>2</sub>. *J Supercrit Fluids* 2020;164:104917. <https://doi.org/10.1016/J.SUPFLU.2020.104917>.
- [11] Anschau A, Aragão VC, Porciuncula BDA, Kalil SJ, Burkert CAV, Burkert JFM. Enzymatic synthesis optimization of isoamyl butyrate. *J Braz Chem Soc* 2011;22:2148–56. <https://doi.org/10.1590/S0103-50532011001100018>.
- [12] Romero MD, Calvo L, Alba C, Daneshfar A, Ghaziaskar HS. Enzymatic synthesis of isoamyl acetate with immobilized *Candida antarctica* lipase in n-hexane. *Enzyme Microb Technol* 2005;37:42–8. <https://doi.org/10.1016/J.ENZMICTEC.2004.12.033>.
- [13] Gomes Almeida SÁ A, de Meneses AC, Hermes de Araújo PH, de Oliveira D. A review on enzymatic synthesis of aromatic esters used as flavor ingredients for food, cosmetics and pharmaceuticals industries. *Trends Food Sci Technol* 2017;69:95–105. <https://doi.org/10.1016/j.tifs.2017.09.004>.

- [14] Hari Krishna S, Divakar S, Prapulla SG, Karanth NG. Enzymatic synthesis of isoamyl acetate using immobilized lipase from *Rhizomucor miehei*. *J Biotechnol* 2001;87:193–201. [https://doi.org/10.1016/S0168-1656\(00\)00432-6](https://doi.org/10.1016/S0168-1656(00)00432-6).
- [15] Larios A, García HS, Oliart RM, Valerio-Alfaro G. Synthesis of flavor and fragrance esters using *Candida antarctica* lipase. *Appl Microbiol Biotechnol* 2004 654 2004;65:373–6. <https://doi.org/10.1007/S00253-004-1602-X>.
- [16] Cha H-J, Park J-B, Park S. Esterification of secondary alcohols and multi-hydroxyl compounds by *Candida antarctica* lipase B and subtilisin. *Biotechnol Bioprocess Eng* 2019 241 2019;24:41–7. <https://doi.org/10.1007/S12257-018-0379-1>.
- [17] Djoudi W, Aissani-Benissad F, Bourouina-Bacha S. Optimization of copper cementation process by iron using central composite design experiments. *Chem Eng J* 2007;133:1–6. <https://doi.org/10.1016/j.cej.2007.01.033>.
- [18] Fabbri F, Bertolini FA, Guebitz GM, Pellis A. Biocatalyzed synthesis of flavor esters and polyesters: a Design of Experiments (DoE) approach. *Int J Mol Sci* 2021;22:8493. <https://doi.org/10.3390/IJMS22168493>.
- [19] Macedo GA, Pastore GM, Rodrigues MI. Optimising the synthesis of isoamyl butyrate using *Rhizopus* sp. lipase with a central composite rotatable design. *Process Biochem* 2004;39:687–93. [https://doi.org/10.1016/S0032-9592\(03\)00153-5](https://doi.org/10.1016/S0032-9592(03)00153-5).
- [20] Guillén M, Benaiges MD, Valero F. Improved ethyl butyrate synthesis catalyzed by an immobilized recombinant *Rhizopus oryzae* lipase: a comprehensive statistical study by production, reaction rate and yield analysis. *J Mol Catal B Enzym* 2016;133:S371–6. <https://doi.org/10.1016/j.molcatb.2017.02.010>.

- [21] Grosso C, Ferreira-Dias S, Pires-Cabral P. Modelling and optimization of ethyl butyrate production catalysed by *Rhizopus oryzae* lipase. *J Food Eng* 2013;115:475–80. <https://doi.org/10.1016/j.jfoodeng.2012.08.001>.
- [22] Bolivar JM, Nidetzky B. The microenvironment in immobilized enzymes: methods of characterization and its role in determining enzyme performance. *Molecules* 2019;24:3460–84. <https://doi.org/10.3390/molecules24193460>.
- [23] Hari Krishna S, Karanth NG. Lipase-catalyzed synthesis of isoamyl butyrate: a kinetic study. *Biochim Biophys Acta - Protein Struct Mol Enzymol* 2001;1547:262–7. [https://doi.org/10.1016/S0167-4838\(01\)00194-7](https://doi.org/10.1016/S0167-4838(01)00194-7).
- [24] Ben Salah R, Ghamghui H, Miled N, Mejdoub H, Gargouri Y. Production of butyl acetate ester by lipase from novel strain of *Rhizopus oryzae*. *J Biosci Bioeng* 2007;103:368–72. <https://doi.org/10.1263/jbb.103.368>.
- [25] Lopresto CG, Calabrò V, Woodley JM, Tufvesson P. Kinetic study on the enzymatic esterification of octanoic acid and hexanol by immobilized *Candida antarctica* lipase B. *J Mol Catal B Enzym* 2014;110:64–71. <https://doi.org/10.1016/J.MOLCATB.2014.09.011>.
- [26] Matte CR, Bordinhaõ C, Poppe JK, Rodrigues RC, Hertz PF, Ayub MAZ. Synthesis of butyl butyrate in batch and continuous enzymatic reactors using *Thermomyces lanuginosus* lipase immobilized in Immobead 150. *J Mol Catal B Enzym* 2016;127:67–75. <https://doi.org/10.1016/J.MOLCATB.2016.02.016>.
- [27] Pires-Cabral P, da Fonseca MMR, Ferreira-Dias S. Synthesis of ethyl butyrate in organic media catalyzed by *Candida rugosa* lipase immobilized in polyurethane foams: a kinetic study. *Biochem Eng J* 2009;43:327–32.

- <https://doi.org/10.1016/J.BEJ.2008.11.002>.
- [28] Sun J, Yu B, Curran P, Liu SQ. Lipase-catalysed ester synthesis in solvent-free oil system: is it esterification or transesterification? *Food Chem* 2013;141:2828–32. <https://doi.org/10.1016/j.foodchem.2013.05.109>.
- [29] Ferreira MC, Meirelles AJA, Batista EAC. Study of the fusel oil distillation Process. *Ind Eng Chem Res* 2013;52:2336–51. <https://doi.org/10.1021/IE300665Z>.
- [30] Guillén M, Benaiges MD, Valero F. Biosynthesis of ethyl butyrate by immobilized recombinant *Rhizopus oryzae* lipase expressed in *Pichia pastoris*. *Biochem Eng J* 2012;65:1–9. <https://doi.org/10.1016/j.bej.2012.03.009>.
- [31] Webb AD, Kepner RE, Ikeda RM. Composition of typical grape brandy fusel oil. *Anal Chem* 2002;24:1944–9. <https://doi.org/10.1021/AC60072A020>.



# 6

## Results III: Biotransformations catalyzed with improved proROL biocatalyst

### 6.2. Polylactic acid production: direct condensation and ring-opening polymerization





## **6. RESULTS (III)**

### **6.2. Polylactic acid production: Direct condensation and ring-opening polymerization**

<i>6.2.1. Introduction</i> .....	291
<i>6.2.2. Results and discussion</i> .....	293
6.2.2.1. Direct lactic acid condensation: lipase source .....	293
6.2.2.2. Direct lactic acid condensation: reaction solvent .....	294
6.2.2.3. Direct lactic acid condensation: toward the use of green solvents .....	295
6.2.2.4. Direct lactic acid condensation: immobilized and free proROL .....	297
6.2.2.5. Ring-opening polymerization (ROP) .....	302
<i>6.2.3. Conclusions</i> .....	303
<i>6.2.4. References</i> .....	305



### 6.2.1. Introduction

Poly(lactic acid) (PLA) is a biodegradable polymer commonly used to manufacture packaging materials, containers and stationery items on the grounds of its high transparency and processability [1]. Because it is biodegradable and biocompatible, PLA has aroused much interest for medical and agricultural uses. Thus, the USA FDA and European Medicine Agency (EMA) have approved its use in various food and surgical applications such as drug-releasing systems. Thanks to these salient advantages, the PLA global market is expected to amount to USD 6 billion by 2025 [2].

PLA is a polyester typically obtained by polymerization of 2-hydroxypropionic acid, more commonly known as “lactic acid” (LA), which is a chiral molecule occurring as two different enantiomers (viz., *L*- and *D*-lactic acid; Figure 6.2.1). Lactic acid forms primarily through bacterial fermentation of corn starch, which gives the *L* enantiomer mainly (yield > 99.5 %) [3]. The significance of LA chirality lies in the ability to modulate some properties of PLA by using appropriate proportions of each enantiomer [4,5].

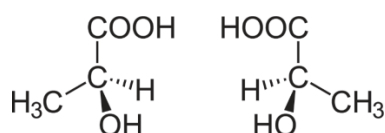


**Figure 6.2.1.** Lactic acid enantiomers: *L*-lactic acid (left) and *D*-lactic acid (right).

Lactic acid monomer is an  $\alpha$ -hydroxyacid bearing a hydroxyl group close to a carboxyl group. This makes it especially suitable for self-polymerization by esterification. As stated in Section 1.6.5, there are two main ways of synthesizing PLA, namely: ring-opening polymerization (ROP) and direct LA condensation. Although both are usually conducted in the presence of a chemical catalyst, lipases have lately emerged as

advantageous alternatives for compliance with the principles of “Green Polymer Chemistry”. For instance, lipases avoid the need for chemical catalysts such as Zn and Sn oxides, which can contaminate the end product with unwanted hazardous residues—a source of special concern for medical applications. Besides, enzymes possess an increased catalytic activity that results in greater turnover; also, they can be used under milder operating conditions, as regards temperature and pressure, reduce energy use as a result and avoid the need for toxic or hazardous solvents [6–9]. As stated in previous chapters, using lipases in immobilized form can provide additional advantages such as facilitating separation of the resulting polymer from the enzyme in order to avoid the presence of unwanted residues in the end product, enabling recovery and reuse of the enzyme, increasing its stability and leading to a more cost-effective overall bioprocess [10].

The results of this chapter are part of the BIOCON-CO<sub>2</sub> European Project that seeks to fix the CO<sub>2</sub> emitted into the atmosphere by steel companies and to transform it into chemical products with greater added value. Besides, the carbon neutrality of these great gas emitters is sought. Amongst these chemicals, the lactic acid employed as substrate for PLA synthesis can be found. In this sense, the methylotrophic yeast *Komagataella phaffii* (*Pichia pastoris*) was used for heterologous production of *Rhizopus oryzae* lipase (proROL) and *Candida rugosa* lipase 1 (CRL1). The two enzymes in free form, and proROL additionally immobilized onto polymethacrylate based supports from Purolite® (EO-proROL), were assessed for PLA production by direct LA condensation and ring-opening polymerization (ROP). The former pathway was examined for the influence of the reaction solvent in order to maximize LA conversion and converted LA amount. The operating conditions were optimized in terms of initial LA concentration

and total amount of enzyme used, in activity units (AU), by using a central composite design in combination with response surface methodology. ROP was conducted in two different solvents, toluene and anisole, in which lactide was soluble, using the same reaction conditions as in direct LA condensation and proROL.

### **6.2.2. Results and discussion**

#### 6.2.2.1. Direct lactic acid condensation: lipase source

Various lipases have previously been used for LA direct condensation and resulted in variable reaction yields, which highlights the importance of choosing an effective biocatalyst [7,11]. In this work, the performance of CRL1 and proROL in LA polymerization, following the reaction procedure described in Section 3.17.1, was assessed by comparing the resulting LA conversions, analyzed through titration (Section 3.21). First, identical amounts (AU) of each lipase (see Section 3.3) were added to a reaction medium containing toluene—an extensively used organic solvent for polymerization reactions [7,12]. Under these conditions, proROL outperformed CRL1 in conversion by a factor exceeding 12 (Table 6.2.1). However, the specificity of the lipases for *p*NPB—the substrate used in the lipolytic activity test—may have differed and led to an inaccurate comparison.

**Table 6.2.1.** Percent lactic acid conversion with proROL and CRL1 in toluene. The amount of lipase added to reaction medium was normalized in terms of AU or lipase mass.

<b>Variable</b>	<b>proROL</b>	<b>CRL1</b>
Conversion (added lipase normalized by AU)	82.22 ± 1.29	6.67 ± 0.23
Conversion (added lipase normalized by mass)	83.01 ± 1.02	38.64 ± 1.02
AU mg <sup>-1</sup> lyophilized powder	148 ± 5.20	2132 ± 23.44
AU mg <sup>-1</sup> protein	3008 ± 3.45	52520 ± 128
% Lipase/protein in lyophilized powder	32.3 ± 0.23	35.1 ± 0.29

The effects of this potential bias were circumvented by densitometric analysis (SDS-PAGE, Section 3.6.1) of the two enzymes in lyophilized powder form. As can be seen in Table 6.2.1, both contained a similar proportion of enzyme. Using an identical amount of lipase for direct LA condensation increased conversion with CRL1 by a factor of 5.8 but still failed to bring it close enough to the levels obtained with proROL, which were about 2.20 times higher. Therefore, proROL proved a more efficient biocatalyst for polymerizing LA in terms of conversion and was thus chosen for further testing.

#### 6.2.2.2. Direct lactic acid condensation: reaction solvent

The use of organic solvents in biocatalytic processes is continuously spreading by effect of their enabling the use of hydrophobic substrates, suppressing unwanted side reactions such as hydrolysis, minimizing contamination and, especially with lipases, shifting thermodynamic equilibrium toward synthesis [13,14]. However, there is no way of predicting how a biocatalyst will behave in a given reaction conducted in a certain organic solvent [15].

In this work, identical amounts (AU) of proROL were used to catalyze LA polymerization in various solvents spanning a wide range of Log *P* values (Table 6.2.2);

Log  $P$ , however, is not the only reaction variable influencing lipase performance, which can be in fact also affected by others factors such as denaturation capacity of the solvent [13].

**Table 6.2.2.** Percent lactic acid conversion with proROL in different solvents spanning a wide range of Log  $P$ .

Solvent	Conversion (%)	log $P$
Isooctane	26.67 ± 0.67	4.6
Heptane	25.58 ± 0.55	4
Cyclohexane	76.27 ± 0.29	3.4
Toluene	82.22 ± 1.29	2.5
2-Methylpyridine	19.52 ± 0.58	1.1
Pyridine	24.13 ± 0.21	0.7
THF	7.5 ± 0.36	0.46

Clearly, solvents with low Log  $P$  values can be expected to have a strongly adverse impact by stripping structural water from the enzyme [16]. The best result (conversion slightly over 80%) was obtained with toluene (Log  $P$  = 2.5). According to some authors, water plays a central role in direct condensation reactions. However, adding a proportion of water of 1.5% to the medium [8] made no difference here, probably because the substrate itself contained a large amount of moisture that could not be removed with classical choices such as silica gel, because it masks enzymatic LA polymerization—the sole usage of silica gel has been described to promote LA self-polymerization and even its use in conjunction with lipases has shown worse results [17].

#### 6.2.2.3. Direct lactic acid condensation: toward the use of green solvents

Green chemistry is promoting a shift from polluting to more environmentally friendly industrial processes by boosting efficient use of renewable materials while avoiding waste



production, and the need for toxic or hazardous reagents and catalysts, in producing chemicals [6,18].

Using toluene as solvent here gave the best conversion results in the direct condensation of LA with proROL as catalyst. Although this organic solvent can be bioremediated by using some fungi and bacteria, its toxicity makes its use rather controversial [19]. The LA polymerization reaction should thus be conducted in an alternative, green solvent [20]—preferably one obtained by processing agricultural crops or natural products— of similar Log *P* and/or structure—or, alternatively, no solvent (i.e., by solvent-free reaction) [21]. Three different green solvents were tested here, namely: limonene, anisole and *p*-cymene. As can be seen from Table 6.2.3, conversion peaked with limonene (83.12 %), which even outperformed toluene in this respect.

**Table 6.2.3.** Percent lactic acid conversion with proROL in green solvents of different Log *P* values and chemical structures.

<b>Solvent</b>	<b>Conversion (%)</b>	<b>Log <i>P</i></b>
<i>p</i> -Cymene	65.25 ± 0.38	4.1
Limonene	83.12 ± 0.89	3.4
Toluene	82.22 ± 1.29	2.5
Anisole	71.51 ± 0.96	2.1

On the other hand, conversion in the solvent-free reaction was zero, probably because the enzyme was inactivated by LA. In fact, high acid concentrations were previously found to denature enzymes and render them inactive as a result [22,23] (see Section 6.1.2). Also, moisture in the reaction medium may have thermodynamically promoted hydrolysis over esterification—the reaction substrate contained 80% LA in water. Based on the results, limonene was chosen as alternative reaction solvent for further testing.

#### 6.2.2.4. Direct lactic acid condensation: immobilized and free proROL

Enzyme immobilization enables more environmentally friendly reactions as it allows enzymes to be reused, downstream reactions eased, and —usually— enzyme stability and cost-effectiveness increased [24]. In this work, proROL was covalently immobilized onto glutaraldehyde-treated polymethacrylate supports containing epoxide and octadecyl surface groups (EO-proROL). The resulting biocatalyst was used with limonene as solvent for LA polymerization as described in Section 3.17.1. However, conversion was 2.44 times lower than that with free enzyme (34% vs 83.12%). In addition, reused EO-proROL resulted in no conversion. This unforeseen outcome for an immobilized biocatalyst can be ascribed to denaturation of the enzyme or to steric problems of immobilized lipase in producing a polymer. The latter hypothesis was discarded as the biocatalyst was repeatedly washed with chloroform to remove all polymer potentially adsorbed onto the biocatalyst prior to reuse. On the other hand, the former hypothesis was confirmed by subjecting recovered immobilized proROL to lipolytic qualitative activity testing with *p*NPB, both before and after washing with chloroform. The test confirmed the absence of enzyme activity after the first LA polymerization batch. Therefore, no further research was performed with immobilized biocatalyst.

The optimum reaction time for direct LA condensation was established by using the enzyme in free form in limonene as solvent and analyzing duplicates of independent vials under identical conditions for different times up to 336 h (Figure 6.2.3). Based on the resulting profile, the polymerization reaction was catalyzed largely within the first 24 h; also, no increase in conversion was observed after 96 h, probably because the enzyme was inactivated or equilibrium reached by then. This led us to assess activity in

recovered lipase (specifically, in a sample of amorphous mass in the pellet; Section 3.21). The sample was subjected to the *p*NPB lipolytic test and found to have no activity. Therefore, the enzyme was completely inactivated within 96 h. These results are consistent with previous reports on EO-proROL inactivation.

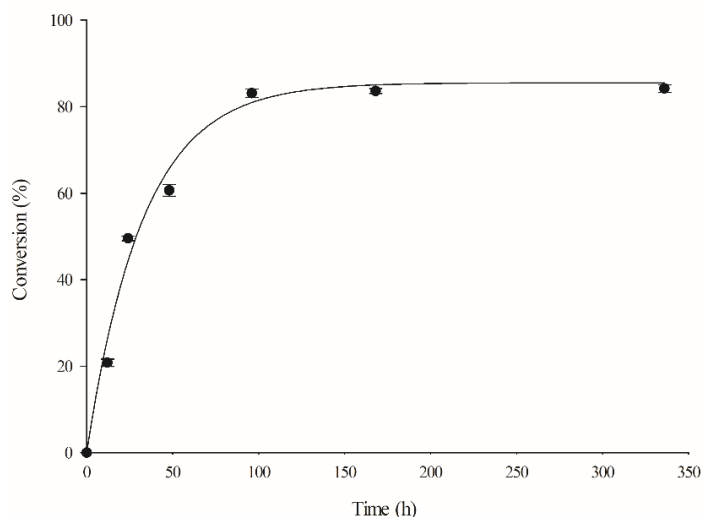


**Figure 6.2.3.** Conversion profile for LA polymerization with proROL in free form and limonene as solvent.

A design of experiments (DoE) approach was used to optimize especially relevant variables influencing direct LA condensation [8]. For this purpose, variable initial LA concentrations and amounts (AU) of lipase following a Box-Hunter design (Figure 6.2.4) were used to assess their effect on LA conversion and LA converted. The latter response allowed us to identify reaction conditions that resulted in very high conversion but catalyzed small total amounts of LA by effect of conversion being a relative value dependent on the initial LA concentration. The resulting matrix (Figure 6.2.4) comprised 11 experiments whose data were fitted to Eq. 3.12 and used to construct the response surfaces of Figure 6.2.5 for easier interpretation. Table 6.2.4 shows the coefficients and statistical significance of the different functions as established by ANOVA.

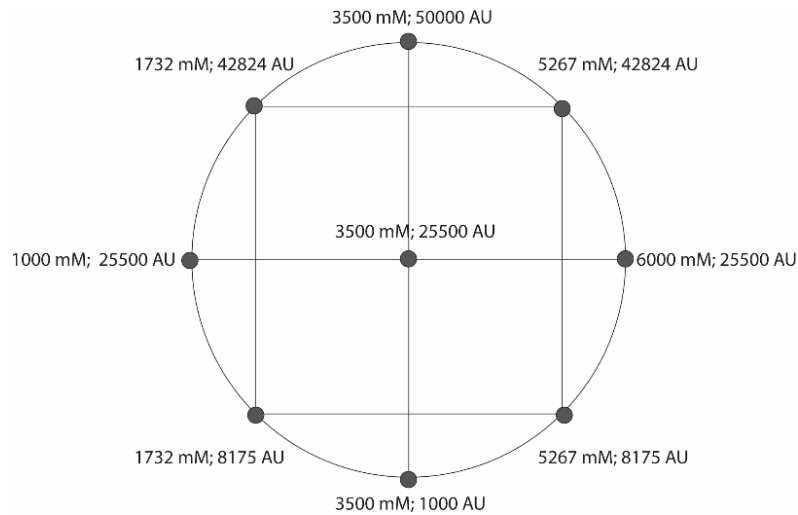


**Figure 6.2.4.** Box-Hunter design matrix representing the LA concentration and AU used to maximize LA conversion and LA converted in the direct condensation reaction.

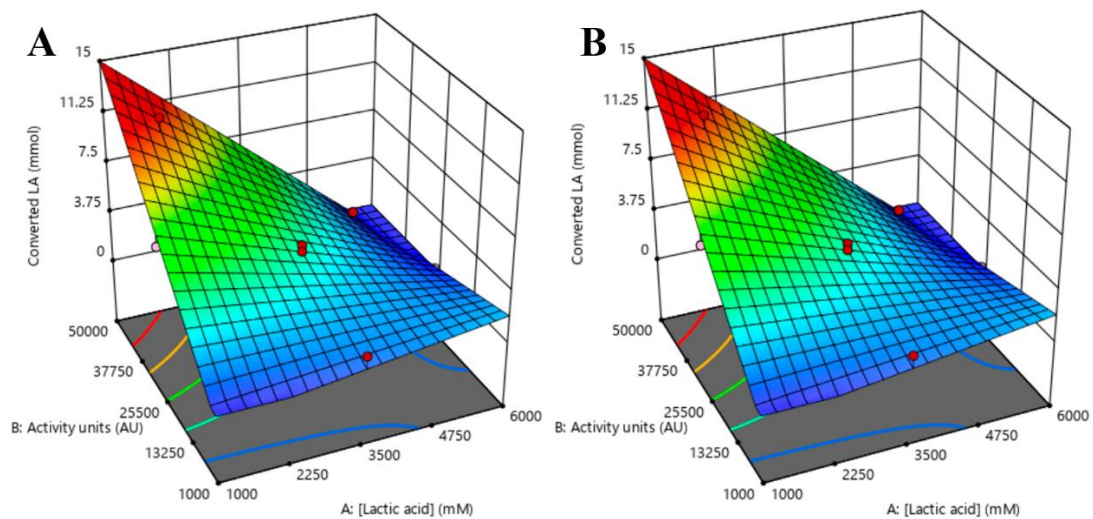


**Figure 6.2.5.** Experimental response surfaces for conversion (A) and converted LA (B) at different initial lactic acid concentrations and amounts of enzyme (AU). The red dots correspond to the design points listed in Table 6.2.4. Measured values greater and smaller than the predictions are shown in dark and light red, respectively

**Table 6.2.4.** Box-Hunter design, independent variables, responses values obtained and results of the ANOVA analysis.

<b>Box-Hunter Design</b>				
Experimental run	Variables		Responses	
	[LA] (mM)	Activity units (AU)	Conversion (%)	Converted LA (mmol)
1	3500	25500	10.03	2.81
2	3500	25500	14.91	4.16
3	5267	8175	2.38	1.00
4	5267	42824	3.57	1.50
5	1732	42824	84.12	11.66
6	3500	1000	5.69	1.59
7	6000	25500	0	0
8	1000	25500	79.77	6.38
9	3500	25500	13.20	3.69
10	1732	8175	11.11	1.54
11	3500	50000	22	6.16

<b>Statistical Analysis</b>					
Responses	<i>F</i> test <i>p</i> -value	LOF test <i>p</i> -value	<i>R</i> <sup>2</sup>	Adjusted- <i>R</i> <sup>2</sup>	Predicted- <i>R</i> <sup>2</sup>
Conversion	<0.01	0.06	0.95	0.92	0.77
Converted LA	<0.01	0.47	0.96	0.94	0.87

Model	Conversion		Converted LA	
	Coefficient	<i>p</i> -value	Coefficient	<i>p</i> -value
$\beta_0$	12.88	< 0.01	3.68	< 0.01
$\beta_1$	-25.26	< 0.01	-2.46	< 0.01
$\beta_2$	12.16	< 0.01	2.13	< 0.01
$\beta_{12}$	-17.96	< 0.01	-2.40	< 0.01
$\beta_{11}$	13.15	< 0.01	NS	> 0.05
$\beta_{22}$	NS	> 0.05	NS	> 0.05

NS: not statistically significant

The coefficient  $\beta_{22}$  for LA conversion in Eq. 6.2.1 (obtained model for LA conversion response) was not statistically significant ( $p > 0.05$ ). Also,  $R^2$  for the reduced quadratic model exceeded 0.95 and the difference between adjusted- $R^2$  and predicted- $R^2$  was less than 0.2, so the goodness of fit was acceptable.

$$\text{Conv. (\%)} = 12.88 - 25.26[\text{LA}] + 12.16\text{AU} - 17.96[\text{LA}]\text{AU} + 13.14[\text{LA}]^2 \quad (6.2.1)$$

Interestingly, the initial LA concentration had a crucial influence, with a quadratic effect on conversion. On the other hand, the amount of enzyme added, in AU, only had a linear influence on conversion in addition to its joint influence with the LA concentration. As expected, the greater the amount of enzyme used was, the higher was conversion. Although similar results have previously been reported [7,8], some authors found conversion to peak and then decline above a given amount of enzyme [25].

Regarding LA converted, as with conversion, the data provided by the Box-Hunter tests were fitted to Eq. 3.12 resulting in Eq. 6.2.2 (model for LA converted).

$$\text{Conv. LA } (\mu\text{mol}) = 3.68 - 2.46[\text{LA}] + 2.13\text{AU} - 2.40[\text{LA}]\text{AU} \quad (6.2.2)$$

Interestingly, Eq. 6.2.2 exhibited a similar trend to Eq. 6.2.1 except that the quadratic effect of LA was not significant. However, as can be seen from the respective response surfaces in Figure 6.2.5, high LA concentrations led to decreased conversion and converted LA. This outcome may have resulted from the above-mentioned ability of acids to inactivate enzymes. Besides, esterification reactions—the basis for direct LA condensation—have been shown to fit the ping-pong kinetic model, so they may undergo substrate inhibition [26].

Consequently, an initial LA concentration of 1482 mM and an amount of enzyme of 42600 AU were chosen as optimal to maximize conversion and converted LA. The predicted conversion (89.18%) and amount of converted LA (12.6 mmol) were experimentally confirmed with a deviation never exceeding 3.94%.

Based on the results of the 11 Box-Hunter tests, a correlation between reaction conversion and the molecular weight of PLA was sought in the NMR spectra (Section 3.22). However, no PLA was found in several samples obtained at variable conversion

levels. Lassalle et al. [8] encountered a similar discrepancy between conversion and gravimetric tests but found no satisfactory explanation. In our experience, the problem may be related to using samples downstream for NMR analysis, due to the differential solubility of LA, its oligomers and PLA in the solvents [27]. Consequently, further experiments should focus on the improvement of the downstream process.

#### 6.2.2.5. Ring-opening polymerization (ROP)

Ring-opening polymerization has been widely reported to yield PLA with a higher molecular weight than direct LA condensation. However, its using a lactide rather than LA makes the reaction challenging as it requires harsh conditions to obtain cyclic diesters despite fairly successful attempts at alleviating them [28–30].

Various lipases including porcine pancreatic lipase and *Candida antarctica* lipase B have enabled enzymatically catalyzed ROP processes [8,31,32]. In this work, ROP was conducted with the same biocatalysts used for direct LA condensation, namely: immobilized proROL (EO-proROL), free proROL and free CRL1, which were assessed for performance in toluene and anisole as solvents (solvents in which lactide was soluble). Reaction runs were done as described in Section 3.17.2 and the resulting homopolymers analyzed by NMR spectroscopy (Section 3.22).

Free CRL1 resulted in no polymerization, even though other authors previously succeeded with it [33,34]. On the other hand, free and immobilized proROL enabled polymerization in both solvents. There were no differences in outcome between solvents, so anisole stands as a more suitable option as it is the greener —less environmentally adverse— of the two. Interestingly, free and immobilized proROL provided LA dimers

(Figure 6.2.5) and hence PLA polymers of very small molecular weight relative to previous reports, around 3-5 kDa [25,31,33].

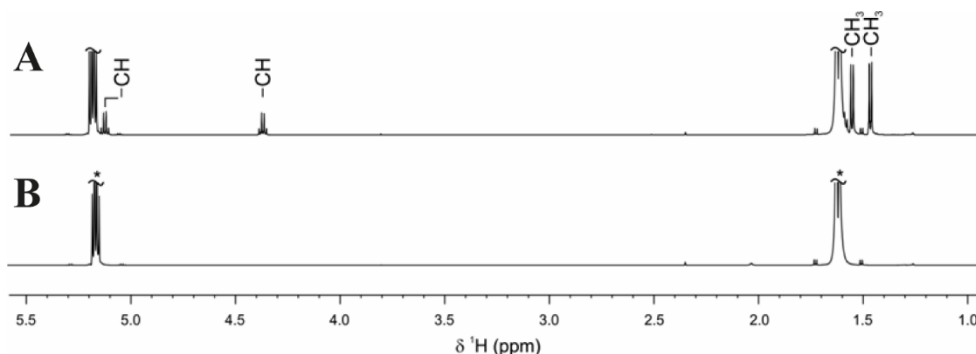


**Figure 5.**  $^1\text{H}$  NMR spectra for samples of the products obtained with EO-proROL (A) and a blank (B). The asterisks in B denote signals for residual lactide.

This outcome may have resulted from the low temperature used, which was the same as that for direct LA condensation in order to enable comparison of the ability to obtain PLA through two different pathways under identical mild conditions. Nevertheless, ROP stands as a more promising choice for lipase-based polymerization, but direct LA condensation warrants further research on the grounds of its potential as an environmentally friendly route for PLA production. Especially considering that this reaction is part of a European project based on the fixation of atmospheric  $\text{CO}_2$  for the production of various compounds, including lactic acid, to carry out this polymerization.

### 6.2.3. Conclusions

*Rhizopus oryzae* lipase (proROL) and *Candida rugosa* lipase 1 (CRL1) efficiently catalyzed direct LA condensation. Under the best operating conditions, the former exhibited 2.20 higher conversion and proved a more suitable biocatalyst for this pathway. Using various reaction solvents for direct LA condensation with free proROL showed



low Log *P* values to detract from reaction performance as the likely result of the solvents stripping essential water from the enzyme. Limonene, a green solvent, resulted in the highest conversion values (up to 83.12%). Alternative approaches intended to make the reaction more cost-effective and environmentally friendly such as using the enzymes in immobilized form or solvent-free reactions failed as they led to lower conversion or no conversion at all. The reaction conditions used inactivated both free and immobilized proROL after 96 h of direct LA condensation. Conversion and converted LA were successfully maximized by using a Box-Hunter design, the former peaking at 89.18% and the latter at 12.6 mmol with an initial LA concentration of 1482 mM and an amount of enzyme of 42600 AU. Irrespective of conversion, no PLA was apparent in the NMR spectra, which suggests that further research is needed to detect PLA potentially formed through this pathway.

Free and immobilized proROL were also more effective than was CRL1 in synthesizing PLA (in dimeric form) by ring-opening polymerization. No difference in biocatalyst performance was observed with toluene and anisole as solvents, so the latter was chosen for further work on the grounds of its being a greener choice. Based on the foregoing, ring-opening polymerization (ROP) is a more suitable pathway for enzyme-based synthesis of PLA than is direct LA condensation. However, further research into the former is needed with a view to alleviating the harsh operating conditions required to obtain lactides. Also, the results can open up new prospects for the chemoenzymatic synthesis of PLA by performing ROP in a chemically catalyzed step to obtain the lactide and a subsequent enzyme-based step for its polymerization.

#### 6.2.4. References

- [1] Auras RA, Lim LT, Selke SEM, Tsuji H. Poly(Lactic Acid): synthesis, structures, properties, processing and applications. Wiley. 2010.
- [2] Singhvi MS, Zinjarde SS, Gokhale D V. Polylactic acid: synthesis and biomedical applications. *J Appl Microbiol* 2019;127:1612–26. <https://doi.org/10.1111/JAM.14290>.
- [3] Gupta B, Revagade N, Hilborn J. Poly(lactic acid) fiber: an overview. *Prog Polym Sci* 2007;32:455–82. <https://doi.org/10.1016/J.PROGPOLYMSCI.2007.01.005>.
- [4] Cicero JA, Dorgan JR, Janzen J, Garrett J, Runt J, Lin JS. Supramolecular morphology of two-step, melt-spun poly(lactic acid) fibers. *J Appl Polym Sci* 2002;86:2828–38. <https://doi.org/10.1002/APP.11267>.
- [5] Cicero JA, Dorgan JR. Physical properties and fiber morphology of poly(lactic acid) obtained from continuous two-step melt spinning. *J Polym Environ* 2001 91 2001;9:1–10. <https://doi.org/10.1023/A:1016012818800>.
- [6] van Schie MMCH, Spöring JD, Bocola M, Domínguez de María P, Rother D. Applied biocatalysis beyond just buffers - from aqueous to unconventional media. Options and guidelines. *Green Chem* 2021;23:3191–206. <https://doi.org/10.1039/d1gc00561h>.
- [7] Chuensangjun C, Pechyen C, Chisti Y, Sirisansaneeyakul S. Lipase-catalysed polymerization of lactic acid and the properties of the polymer. *Adv Mater Res* 2012;506:154–7. <https://doi.org/10.4028/www.scientific.net/AMR.506.154>.
- [8] Lassalle VL, Ferreira ML. Lipase-catalyzed synthesis of polylactic acid: an

- overview of the experimental aspects. *J Chem Technol Biotechnol* 2008;83:1493–502. <https://doi.org/10.1002/jctb.1994>.
- [9] Omay D, Guvenilir Y. Synthesis and characterization of poly(d,l-lactic acid) via enzymatic ring opening polymerization by using free and immobilized lipase. *Biocatal. Biotransformation* 2013;31:132–40. <https://doi.org/10.3109/10242422.2013.795148>.
- [10] Ismail AR, Baek KH. Lipase immobilization with support materials, preparation techniques, and applications: present and future aspects. *Int J Biol Macromol* 2020;163:1624–39. <https://doi.org/10.1016/j.ijbiomac.2020.09.021>.
- [11] Kobayashi S. Recent developments in lipase-catalyzed synthesis of polyesters. *Macromol Rapid Commun* 2009;30:237–66. <https://doi.org/10.1002/MARC.200800690>.
- [12] Hans M, Keul H, Moeller M. Ring-opening polymerization of DD-lactide catalyzed by Novozyme 435. *Macromol Biosci* 2009;9:239–47. <https://doi.org/10.1002/mabi.200800236>.
- [13] Kumar A, Dhar K, Kanwar SS, Arora PK. Lipase catalysis in organic solvents: advantages and applications. *Biol Proced Online* 2016;18:1–11. <https://doi.org/10.1186/s12575-016-0033-2>.
- [14] López-Fernández J, Benaiges MD, Valero F. *Rhizopus oryzae* lipase, a promising industrial enzyme: biochemical characteristics, production and biocatalytic applications. *Catalysts* 2020;10:1277. <https://doi.org/10.3390/catal10111277>.
- [15] Castro GR, Knubovets T. Homogeneous biocatalysis in organic solvents and

- water-organic mixtures. *Crit* 2003;23:195-231.  
<https://doi.org/10.1080/BTY.23.3.195>.
- [16] Zitian Wang, Dai L, Liu D, Liu H, Du W. Kinetics and mechanism of solvent influence on the lipase-catalyzed 1,3-diolein synthesis. *ACS Omega* 2020;5:24708–16. <https://doi.org/10.1021/ACSOMEGA.0C03284>.
- [17] Sonwalkar RD, Chen C, Ju LK. Roles of silica gel in polycondensation of lactic acid in organic solvent. *Bioresour Technol* 2003;87:69–73.  
[https://doi.org/10.1016/S0960-8524\(02\)00197-9](https://doi.org/10.1016/S0960-8524(02)00197-9).
- [18] Sheldon RA. Metrics of green chemistry and sustainability: past, present, and future. *ACS Sustain Chem Eng* 2017;6:32–48.  
<https://doi.org/10.1021/ACSSUSCHEMENG.7B03505>.
- [19] Prenafeta-Boldú FX, Kuhn A, Luykx DMAM, Anke H, Van Groenestijn JW, De Bont JAM. Isolation and characterisation of fungi growing on volatile aromatic hydrocarbons as their sole carbon and energy source. *Mycol Res* 2001;105:477–84. <https://doi.org/10.1017/S0953756201003719>.
- [20] Clarke CJ, Tu WC, Levers O, Bröhl A, Hallett JP. Green and sustainable solvents in chemical processes. *Chem Rev* 2018;118:747–800.  
<https://doi.org/10.1021/acs.chemrev.7b00571>.
- [21] Sahoo BM, Banik BK. Solvent-less reactions: green and sustainable approaches in medicinal chemistry. *Green Approaches Med. Chem. Sustain. Drug Des.*, Elsevier; 2020, p. 523–48. <https://doi.org/10.1016/b978-0-12-817592-7.00014-9>.
- [22] Bolivar JM, Nidetzky B. The microenvironment in immobilized enzymes: methods

- of characterization and its role in determining enzyme performance. *Molecules* 2019;24:3460–84. <https://doi.org/10.3390/molecules24193460>.
- [23] Pirozzi D, Greco G. Activity and stability of lipases in the synthesis of butyl lactate. *Enzyme Microb Technol* 2004;34:94–100. <https://doi.org/10.1016/J.ENZMICTEC.2003.01.002>.
- [24] Zdarta J, Meyer AS, Jesionowski T, Pinelo M. A general overview of support materials for enzyme immobilization: characteristics, properties, practical utility. *Catalysts* 2018;8:92–119. <https://doi.org/10.3390/catal8020092>.
- [25] Kiran KR, Divakar S. Lipase-catalysed polymerization of lactic acid and its film forming properties. *World J Microbiol Biotechnol* 2003 198 2003;19:859–65. <https://doi.org/10.1023/A:1026004229239>.
- [26] Ben Salah R, Ghamghui H, Miled N, Mejdoub H, Gargouri Y. Production of butyl acetate ester by lipase from novel strain of *Rhizopus oryzae*. *J Biosci Bioeng* 2007;103:368–72. <https://doi.org/10.1263/jbb.103.368>.
- [27] Glotova VN, Bikmullina TN, Lukianov AE, Novikov VT, Poharukova YE. Lactide and lactic acid oligomer solubility in certain solvents. *Pet Coal* 2016;58:585–9.
- [28] Ghadamyari M, Chaemchuen S, Zhou K, Dusselier M, Sels BF, Mousavi B, et al. One-step synthesis of stereo-pure L,L-lactide from L-lactic acid. *Catal Commun* 2018;114:33–6. <https://doi.org/10.1016/J.CATCOM.2018.06.003>.
- [29] Zhao H, Nathaniel GA, Merenini PC. Enzymatic ring-opening polymerization (ROP) of lactides and lactone in ionic liquids and organic solvents: digging the controlling factors. *RSC Adv* 2017;7:48639–48.

- <https://doi.org/10.1039/C7RA09038B>.
- [30] Douka A, Vouyiouka S, Papaspyridi LM, Papaspyrides CD. A review on enzymatic polymerization to produce polycondensation polymers: the case of aliphatic polyesters, polyamides and polyesteramides. *Prog Polym Sci* 2018;79:1–25. <https://doi.org/10.1016/J.PROGPOLYMSCI.2017.10.001>.
- [31] Divakar S. Porcine pancreas lipase catalyzed ring-opening polymerization of  $\epsilon$ -Caprolactone. <https://doi.org/10.1081/MA-120030923> 2007;41 A:537–46. <https://doi.org/10.1081/MA-120030923>.
- [32] Kundys A, Białocka-Florjańczyk E, Fabiszewska A, Małajowicz J. *Candida antarctica* lipase B as catalyst for cyclic esters synthesis, their polymerization and degradation of aliphatic polyesters. *J Polym Environ* 2017 261 2017;26:396–407. <https://doi.org/10.1007/S10924-017-0945-1>.
- [33] Rahmayetty, Whulanza Y, Sukirno, Rahman SF, Suyono EA, Yohda M, et al. Use of *Candida rugosa* lipase as a biocatalyst for L-lactide ring-opening polymerization and polylactic acid production. *Biocatal Agric Biotechnol* 2018;16:683–91. <https://doi.org/10.1016/J.BCAB.2018.09.015>.
- [34] Barrera-Rivera KA, Marcos-Fernández Á, Vera-Graziano R, Martínez-Richa A. Enzymatic ring-opening polymerization of  $\epsilon$ -caprolactone by *Yarrowia lipolytica* lipase in ionic liquids. *J Polym Sci Part A Polym Chem* 2009;47:5792–805. <https://doi.org/10.1002/pola.23623>.



# 7

## General conclusions





## 7. General conclusions

This thesis has attempted to improve *Rhizopus oryzae* lipase (ROL) features as biocatalyst to use it in various reactions of industrial interest, including biodiesel, natural flavors and biopolymers production. Correspondingly, the thesis has focused on improving ROL heterologous production in the methylotrophic yeast *Komagataella phaffii* (*Pichia pastoris*).

Firstly, by using the production of biodiesel from *alperujo* oil (olive pomace oil) as a model reaction with rROL (mature sequence ROL), the effect of immobilization support on the obtained biocatalyst was assessed and optimized. The presence of hydrocarbon chains functional groups in the immobilization supports (both onto polymethacrylate- and magnetite-based supports) promoted the operational stability of the biocatalyst. However, these groups had no effect on initial reaction rate although magnetite-based biocatalysts were doubled by Purolite®-based biocatalysts in this parameter and the best performing magnetite-based biocatalyst was 20% less stable than EO-rROL —the biocatalyst with highest operational stability, formed by rROL immobilization onto polymethacrylate-based support with epoxide and octadecyl surface groups. Therefore, further studies were only carried out with EO-rROL.

EO-rROL was used to evaluate the production of second- and third-generation biodiesel with alternative substrates to olive pomace oil. The initial transesterification rate with all the substrates assessed was identical, notwithstanding the different free fatty acid (FFA) content in each oil. However, this parameter and acyl-acceptor concentration proved crucial and synergistically influential in operational stability as FFAs increase the polarity of the reaction medium and therefore act as buffering agents for the high polarity of the acyl-acceptor and also its deactivating capacity.

EO-rROL based synthesis of biodiesel was successfully scaled up to a 50 mL mini-reactor for industrial proof of concept by using waste cooking oil as substrate making enzymatic biodiesel feasible and complying with the principles of circular economy. Besides, the biocatalyst showed a remarkable half-life, over 35 batches, notwithstanding the acyl-acceptor employed, ethanol or methanol.

Given the importance in industry of inline monitoring of reactions, in compliance with CPV and PAT principles, a NIR spectroscopy probe was inserted in the reactor during biodiesel synthesis with WCO, using gas chromatography as the reference technique. The models obtained from the NIR spectra for both employed acyl-acceptors correlated remarkably well with the results of gas chromatography with a prediction error (RMSEP) of 2.0% for methanol and 2.1% for ethanol. Therefore, regardless of the acyl-acceptor, the adding strategy or the use of immobilized biocatalyst, which could generate background noise in the measurement, it was possible to accurately monitor inline enzymatic biodiesel synthesis by NIR spectroscopy.

Once immobilization support was optimized, rROL was modified by adding the 28 C-terminal amino acids of the native prosequence of ROL—which have been described to act as intramolecular chaperone—to the N-terminal of the mature sequence (proROL). The positive effects of this truncated prosequence were evaluated at different levels. First, in terms of bioprocess engineering, the presence of the truncated prosequence proved to decrease lipase harmful effects during its heterologous production in *K. phaffii* under methanol-inducible promoter ( $P_{AOXI}$ ). In fact, the maximum specific growth rate value for proROL producing strain, as well as the lipase production and volumetric productivity were higher than these with rROL-producing strain, supporting the stress reduction hypothesis and enabling a more efficient and cost-effective bioprocess. Moreover, it was also tested that the truncated prosequence of ROL can be

assumed to alleviate the deleterious effects of the lipase and enable its constitutive production in *K. phaffii*, unlike with rROL, whose constitutive expression must be hindered due to its phospholipase activity. Therefore, truncated prosequence enabled a methanol independent proROL production achieving a more environmentally friendly bioprocess with final lipase activity and productivities similar to the best strategy reported so far for proROL production (proROL P<sub>AOXI</sub>-strain under methanol non-limited fed-batch at 3 g L<sup>-1</sup>).

Second, in terms of biochemical characterization, proROL showed similar patterns to these from rROL, although some differences were detected. Besides the higher molecular weight, proROL was found to have a more stable conformation as optimum pH and temperature values did not show any change regardless the ionic strength of the medium, unlike it was observed for rROL. In terms of substrate specificity with ester of *p*-nitrophenol, proROL exhibited a similar trend to native ROL and different from rROL supporting the importance of these 28 amino acids in lipase catalysis since they have been described to be close to the active center. However, the most significant difference was the increased stability of free proROL in comparison to free rROL under all the stability tests performed at different pH, temperature and presence or absence of alcohols (methanol and ethanol). Even when immobilized, proROL showed higher stability than rROL in presence of different organic solvents. Furthermore, after incubation of the free enzyme under non-sterile conditions, selective hydrolysis of the 28 amino acids was observed, as with other similar lipases such as that of *Rhizopus niveus*, due to the presence of contaminating proteases in the medium. These results were demonstrated by N-terminal analysis suggesting that these 28 amino acids are naturally designed to be removed.

Similarly, the truncated prosequence increased operational stability of immobilized proROL in biodiesel and ethyl butyrate production, although no influence on initial reaction rate was observed, which suggests that EB-proROL and EB-rROL interact identically with the substrates under the studied conditions, no matter the results obtained for free proROL and rROL specificity analysis. Thus, in general, 28 C-terminal amino acids of the native prosequence have proved to affect different aspects of the enzyme, including increased stability and decreased deleterious effects during its synthesis, likely due to the influence of the 28 amino acids in enzyme folding, as they act as intramolecular chaperone. After optimizing immobilization support and lipase sequence, immobilized proROL onto polymethacrylate-based support containing epoxide and octadecyl (EO) surface groups was used for further research on isoamyl esters (natural flavors) and biopolymers (polylactic acid, PLA) production.

EO-proROL proved to be efficient in the esterification reaction of isoamyl acetate and butyrate in cyclohexane, being the production of the latter the one that showed better results and whose synthesis was optimized through a Design of Experiments (DoE) following a Box-Hunter design. The optimal conditions found through DoE were successfully validated and then scaled up to a laboratory reactor, for industrial proof of concept. Commercial isoamyl alcohol and fusel oil were used exhibiting similar results. Therefore, EO-proROL stands as a suitable biocatalyst for industrial production of natural isoamyl butyrate, even from an inexpensive substrate such as fusel oil to comply with the principles of circular economy. Besides, it was found that EO-proROL is more specific to 2-methylbutanol than it is to 3-methylbutanol, notwithstanding previous results suggesting the activity to be hindered by the proximity of the methyl group to the hydroxyl group.

proROL was tested for direct lactic acid condensation to produce PLA. Under all the studied conditions, regarding amount of lipase and reaction solvent, free proROL outperformed the conversion obtained with free *Candida rugosa* lipase 1 (CRL1), also tested in this section. Green solvents and immobilization of proROL (EO-proROL) were assessed to achieve a more environmentally friendly biotransformation, and although the latter attempt failed, free proROL achieved the highest lactic acid conversion reported so far in this work with limonene as green solvent. Direct LA condensation reaction was optimized by means of a DoE with a Box-Hunter design and although high conversions were achieved (89.18%), no PLA was detected in any samples through nuclear magnetic resonance (NMR) analysis. Besides, an alternative route for PLA synthesis was tested, the ring-opening polymerization of lactide. Through this route, lactic acid dimers detectable by NMR were obtained and proROL (both free and immobilized) outperformed free CRL1 performance under the studied conditions. Therefore, this data opens up a new research line to carry out the chemoenzymatic synthesis of PLA through ring-opening polymerization by performing a first chemically catalyzed step (lactide formation) with the consecutive enzyme-based polymerization of lactides.

In summary, *Rhizopus oryzae* lipase has proved to be a suitable biocatalyst to perform industrially relevant biotransformations. Furthermore, the thorough study carried out in this thesis, including the evaluation of the joint expression of the truncated prosequence of the native lipase plus the mature sequence, the use of different immobilization supports and the scale up of the most promising reactions together with new approaches focused on the use of inline monitoring techniques, such as NIR spectroscopy, have brought proROL to a “ready to use” state at the industrial scale.



# 8

## Abbreviations





## 8. Abbreviations

28proROL-gene	Gene encoding a truncated prosequence of <i>Rhizopus oryzae</i> lipase 28 C-terminal amino acids fused to the N-terminal of the mature lipase region
28proROL P <sub>AOXI</sub> -plasmid	Plasmid containing the sequence of proROL under P <sub>AOXI</sub>
28proROL P <sub>GAP</sub> -plasmid	Plasmid containing the sequence of proROL under P <sub>GAP</sub>
proROL P <sub>AOXI</sub> -strain	Genetically modified <i>Komagataella phaffii</i> strain used to produce proROL under P <sub>AOXI</sub>
proROL P <sub>GAP</sub> -strain	Genetically modified <i>Komagataella phaffii</i> strain used to produce proROL under P <sub>GAP</sub>
2-MAG	2-monoacylglycerol
Ac	Acids
Al	Alcohols
ALO/OP	<i>Alperujo</i> oil (olive pomace oil)
AOX	Alcohol oxidase
AU	Activity units
BR	Batch reactor
C	Conversion (%)
CA	Capric acid
CBE	Cocoa butter equivalents
CI	Covalently immobilized or stabilized biocatalyst through crosslinking
CO	Canola oil
CRA	Caprylic acid
CRL	<i>Candida rugosa</i> lipase
DAG	Diacylglycerol
DCW	Dry cell weight
ddPCR	Droplet digital PCR
D <sub>eff</sub>	Effective diffusivity
DO	Dissolved oxygen
DoE	Design of experiments
EB	Purolite® polymethacrylate matrix support containing Epoxide and butyl functional surface groups
EB-rROL	rROL covalently immobilized onto EB support
EB-proROL	proROL covalently immobilized onto EB support
EDTA	Ethylenediaminetetraacetic acid
EDVB	Purolite® polymethacrylate matrix support containing epoxide and divinylbenzene functional surface groups
EDVB-rROL	rROL covalently immobilized onto EDVB support
EDVB-proROL	proROL covalently immobilized onto EDVB support
ee	Enantiomeric excess
entire-proROL	<i>Rhizopus oryzae</i> lipase including the whole prosequence and mature sequence
EO	Purolite® polymethacrylate matrix support containing epoxide and octadecyl functional surface groups

EO-rROL	rROL covalently immobilized onto EO support
EO-proROL	proROL covalently immobilized onto EO support
EPAX 1050TG	TAG rich in omega-3 PUFAs
Es	Esters
EtOH	Ethanol
FAME	Fatty acid methyl esters
FFA	Free fatty acid
FLD	Formaldehyde dehydrogenase
GAP	Glyceraldehyde-3-phosphate dehydrogenase
His	Histidine
HMFS	Human milk fat substitutes
HPLC	High-performance liquid chromatography
IA	Immobilization through adsorption
ICL	Isocitrate lyase
ID	Incorporation degree (%)
IE	Immobilization through physical entrapment
JO	Jatropha oil
KO	Karanja oil
L	Long-chain fatty acid
LA	Lactic acid
M	Medium-chain fatty acid
MAG	Monoacylglycerol
MeOH	Methanol
MLFB	Methanol limited fed-batch
MNLFB	Methanol non-limited fed-batch
MSFBR	Magnetically-stabilised fluidized bed reactor
MUF	4-Methylumbelliferone
Mut <sup>+</sup>	Methanol utilization plus phenotype
Mut <sup>s</sup>	Methanol utilization slow phenotype
MW	Molecular weight (kDa)
NBS	<i>N</i> -bromosuccinimide
NIR	Near infrared
nROL	native lipase secreted by <i>Rhizopus oryzae</i>
OA	Oleic acid
OO	Olive oil
OP/ALO	Olive pomace oil
OPO	TAG with oleic acid in <i>sn</i> -1,3 positions and palmitic acid in <i>sn</i> -2 position
OS	Operational stability
PA	Palmitic acid
P <sub>AOX1</sub>	Inducible alcohol oxidase 1 promoter
PBR	Packed bed reactor
PCA	Principal component analysis
PFL	<i>Pseudomonas fluorescens</i> lipase
P <sub>FLD1</sub>	Inducible formaldehyde dehydrogenase 1 promoter
P <sub>GAP</sub>	Constitutive glyceraldehyde-3-phosphate dehydrogenase promoter
pI	Isoelectric point

PLA	Polylactic acid
PLS	Partial least-squares
PMSF	Phenylmethylsulfonyl fluoride
<i>p</i> NPB	<i>p</i> -nitrophenyl butyrate
PPL	Porcine pancreatic lipase
proROL	<i>R. oryzae</i> lipase containing the <i>N</i> -terminal of mature sequence attached to 28 <i>C</i> -terminal amino acids of the prosequence
proROL-gene	Gene encoding the prosequence of 97 amino acids fused to the <i>N</i> -terminal of the mature lipase region of 269 amino acids
proROLm	proROL modified by the activity of proteases
PUFA	Polyunsaturated fatty acids
PVA	Polyvinyl alcohol
$q_p$	Specific production rate (AU gX <sup>-1</sup> h <sup>-1</sup> )
RMSEC	Root mean square error of calibration
RMSEP	Root mean square error of prediction
RO	Rapeseed oil
ROL	<i>Rhizopus oryzae</i> lipase
ROP	Ring-opening polymerization
rROL	<i>Rhizopus oryzae</i> lipase containing mature sequence of <i>R. oryzae</i> lipase
rROL-gene	Gene encoding the sequence of rROL
rROL P <sub>AOXI</sub> -plasmid	Plasmid containing the sequence of rROL under P <sub>AOXI</sub>
rROL P <sub>GAP</sub> -plasmid	Plasmid containing the sequence of rROL under P <sub>GAP</sub>
rROL P <sub>AOXI</sub> -strain	Genetically modified <i>Komagataella phaffii</i> strain used to produce rROL under P <sub>AOXI</sub>
rROL P <sub>GAP</sub> -strain	Genetically modified <i>Komagataella phaffii</i> strain used to produce rROL under P <sub>GAP</sub>
RSM	Response surface methodology
S	Short-chain fatty acid
SA	Stearic acid
SCG	Spent coffee ground
SDS-PAGE	Sodium dodecyl sulfate polyacrylamide gel electrophoresis
SGLB	Solid gas liquid bioreactor
SL	Structured lipids
SLLB	Solid liquid liquid bioreactor
SO	Sunflower oil
STR	Stirred tank reactor
SYO	Soybean oil
TAG	Triacylglycerol
TGA40	Commercial oil
TGA55E	Hydrolyzed TGA40 oil
TGA58F	<i>Mortierella alpina</i> single-cell oil
TPB	Three phase bioreactor
UPR	Unfolding protein response
WCB	Whole cells biocatalyst

WCO	Waste cooking oil
X	Biomass (gX)
Y	Yield (%)
$Y_{P/X}$	Product-biomass yield (AU gX <sup>-1</sup> )
$Y_{X/S}$	Biomass-substrate yield (gX g substrate <sup>-1</sup> )
$\epsilon_p$	Porosity of the particle
$\rho_p$	Density of the particle
$\Phi$	Weisz–Prater Criterion
$\mu$	Specific growth rate (h <sup>-1</sup> )

# 9

## Scientific contributions



## 9. Scientific contributions

- López-Fernández J, Barrero JJ, Benaiges MD, Valero F. Truncated prosequence of *Rhizopus oryzae* lipase: Key factor for production improvement and biocatalyst stability. *Catalysts* 2019;9:961. <https://doi.org/10.3390/catal9110961>.
- López-Fernández J, Benaiges MD, Valero F. *Rhizopus oryzae* lipase, a promising industrial enzyme: Biochemical characteristics, production and biocatalytic applications. *Catalysts* 2020;10:1277. <https://doi.org/10.3390/catal10111277>
- López-Fernández J, Benaiges MD, Valero F. Second- and third-generation biodiesel production with immobilised recombinant *Rhizopus oryzae* lipase: influence of the support, substrate acidity and bioprocess scale-up. *Bioresour Technol* 2021;334:125233. <https://doi.org/10.1016/j.biortech.2021.125233>
- López-Fernández J, Benaiges MD, Valero F. Constitutive expression in *Komagataella phaffii* of mature *Rhizopus oryzae* lipase jointly with its truncated prosequence improves production and the biocatalyst operational stability. *Catalysts* 2021;11:1192. <https://doi.org/10.3390/catal11101192>
- López-Fernández J, Moya D, Benaiges MD, Valero F, Alcalà M. Near Infrared Spectroscopy: a useful technique for inline monitoring of the enzyme catalyzed biosynthesis of third-generation biodiesel from waste cooking oil. *Fuel*. 2022. (accepted)





# 10

**Annexes**



## 10. Annexes

**Table 10.1.** Weisz–Prater criterion for pomace oil transesterification with methanol in the presence of various biocatalysts immobilized onto a polymethacrylate matrix.  $\Phi$  and  $D_{\text{eff}}$  were calculated from Eq. 3.9 and 3.10, respectively, using  $\sigma = 1$  and  $\tau = 1.41$  in the latter. Porosity ( $\varepsilon_p$ ) and specific volume of the supports were 0.6 and  $1.4 \text{ cm}^3 \text{ g}^{-1}$  support.

Biocatalyst	$r_{\text{obs}}$ (mol $\text{s}^{-1} \text{ cm}^{-3}$ )	Biocatalyst weight (g)	$\rho_p$ (g $\text{cm}^{-3}$ )	Specific area ( $\text{m}^2 \text{ g}^{-1}$ )	$r_{\text{obs}}$ (mol $\text{g}_{\text{particle}}^{-1} \text{ s}^{-1}$ )	$C_{\text{m},0}$ (mol $\text{cm}^{-3}$ )	$D_{\text{m},a}$ ( $\text{cm}^2 \text{ s}^{-1}$ )	$D_{\text{eff}}$ ( $\text{cm}^2 \text{ s}^{-1}$ )	$\Phi$
<b>EB-rROL 1</b>	$1.81 \cdot 10^{-07}$	0.2	0.72	152	$8.11 \cdot 10^{-06}$	$4.41 \cdot 10^{-04}$	$1.18 \cdot 10^{-06}$	$5.04 \cdot 10^{-07}$	$2.20 \cdot 10^{-08}$
<b>EB-rROL 2</b>	$2.39 \cdot 10^{-07}$	0.2	0.72	152	$1.07 \cdot 10^{-05}$	$4.41 \cdot 10^{-04}$	$1.18 \cdot 10^{-06}$	$5.04 \cdot 10^{-07}$	$2.91 \cdot 10^{-08}$
<b>EB-rROL 3</b>	$4.31 \cdot 10^{-07}$	0.2	0.72	152	$1.93 \cdot 10^{-05}$	$4.41 \cdot 10^{-04}$	$1.18 \cdot 10^{-06}$	$5.04 \cdot 10^{-07}$	$5.23 \cdot 10^{-08}$
<b>EB-rROL 4</b>	$5.93 \cdot 10^{-07}$	0.2	0.72	152	$2.66 \cdot 10^{-05}$	$4.41 \cdot 10^{-04}$	$1.18 \cdot 10^{-06}$	$5.04 \cdot 10^{-07}$	$7.20 \cdot 10^{-08}$
<b>EB-rROL 5</b>	$6.44 \cdot 10^{-07}$	0.2	0.72	152	$2.89 \cdot 10^{-05}$	$4.41 \cdot 10^{-04}$	$1.18 \cdot 10^{-06}$	$5.04 \cdot 10^{-07}$	$7.83 \cdot 10^{-08}$
<b>EO-rROL 1</b>	$1.34 \cdot 10^{-07}$	0.2	0.72	139	$5.99 \cdot 10^{-06}$	$4.41 \cdot 10^{-04}$	$1.18 \cdot 10^{-06}$	$5.04 \cdot 10^{-07}$	$1.94 \cdot 10^{-08}$
<b>EO-rROL 2</b>	$1.68 \cdot 10^{-07}$	0.2	0.72	139	$7.55 \cdot 10^{-06}$	$4.41 \cdot 10^{-04}$	$1.18 \cdot 10^{-06}$	$5.04 \cdot 10^{-07}$	$2.45 \cdot 10^{-08}$
<b>EO-rROL 3</b>	$2.11 \cdot 10^{-07}$	0.2	0.72	139	$9.44 \cdot 10^{-06}$	$4.41 \cdot 10^{-04}$	$1.18 \cdot 10^{-06}$	$5.04 \cdot 10^{-07}$	$3.06 \cdot 10^{-08}$
<b>EO-rROL 4</b>	$4.94 \cdot 10^{-07}$	0.2	0.72	139	$2.22 \cdot 10^{-05}$	$4.41 \cdot 10^{-04}$	$1.18 \cdot 10^{-06}$	$5.04 \cdot 10^{-07}$	$7.18 \cdot 10^{-08}$
<b>EO-rROL 5</b>	$6.57 \cdot 10^{-07}$	0.2	0.72	139	$2.95 \cdot 10^{-05}$	$4.41 \cdot 10^{-04}$	$1.18 \cdot 10^{-06}$	$5.04 \cdot 10^{-07}$	$9.54 \cdot 10^{-08}$
<b>EDVB-rROL 1</b>	$1.51 \cdot 10^{-07}$	0.2	0.72	59	$6.77 \cdot 10^{-06}$	$4.41 \cdot 10^{-04}$	$1.18 \cdot 10^{-06}$	$5.04 \cdot 10^{-07}$	$1.22 \cdot 10^{-07}$
<b>EDVB-rROL 2</b>	$2.18 \cdot 10^{-07}$	0.2	0.72	59	$9.76 \cdot 10^{-06}$	$4.41 \cdot 10^{-04}$	$1.18 \cdot 10^{-06}$	$5.04 \cdot 10^{-07}$	$1.75 \cdot 10^{-07}$
<b>EDVB-rROL 3</b>	$2.51 \cdot 10^{-07}$	0.2	0.72	59	$1.13 \cdot 10^{-05}$	$4.41 \cdot 10^{-04}$	$1.18 \cdot 10^{-06}$	$5.04 \cdot 10^{-07}$	$2.02 \cdot 10^{-07}$

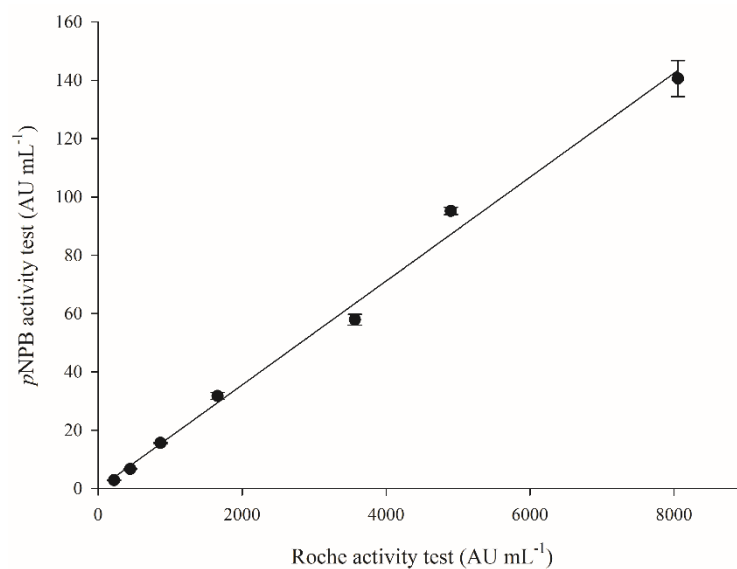


**Figure 10.1.** Correlation between the two employed activity tests in the present thesis. Activity conditions described in Section 3.3.  $R^2 = 0.99$ .

## Notes

